Spring 1-1-2011

Assessment of Steady-State Infiltration Heat Recovery Models and Their Impact on Predicted Home Energy Consumption

Mikel Solupe
University of Colorado at Boulder, misolupe@aol.com

ASSESSMENT OF STEADY-STATE INFILTRATION HEAT RECOVERY MODELS AND THEIR IMPACT ON PREDICTED HOME ENERGY CONSUMPTION

by

MIKEL SOLUPE

B.S., University of Miami - Coral Gables, 2008

A thesis submitted to the

Faculty of the Graduate School of the

University of Colorado in partial fulfillment

of the requirement for the degree of

Master of Science

Department of Civil, Environmental, and Architectural Engineering

2011

This thesis entitled:

Assessment of Steady-State Infiltration Heat Recovery Models and their Impact on Predicted Home Energy Consumption
written by Mikel Solupe

has been approved for the Department of Civil, Environmental, and Architectural Engineering

_____

Moncef Krarti, Committee Chair

_____

Marcus Bianchi

_____

John Zhai

Date _____

The final copy of this thesis has been examined by the signatories, and we find that both the content and the form meet acceptable presentation standards of scholarly work in the above mentioned discipline.

ABSTRACT

Solupe, Mikel (M.S., Department of Civil, Environmental, and Architectural Engineering)

Assessment of Steady-State Infiltration Heat Recovery Models and their Impact on Predicted Home Energy Consumption

Thesis directed by Associate Professor Moncef Krarti

Infiltration is a major contributor to the energy consumption of buildings, particularly in homes where it accounts for one-third of the heating and cooling loads. Traditionally, infiltration is calculated independent of the building envelope performance, however, research has found a coupling exists between the infiltration and conduction heat transfer of the building envelope. This effect is known as infiltration heat recovery (IHR). Experiments have shown infiltration heat recovery can reduce the infiltration load by ten to twenty percent.

Currently, energy simulation tools do not account for infiltration heat recovery. Over the years, five steady-state IHR models have been developed to account for the interaction between infiltration and the building envelope. The effects of each model have been quantified against traditional calculations but a lack of testing has been found in literature. In this study, inter-model and experimental comparisons are done to assess the models' performance. This is a beneficial and necessary step to accurately model IHR. Sensitivity analysis will help determine which model parameters impact IHR the most. Using a sample case study of homes in Colorado, an evaluation of measured infiltration heat recovery is compared to the IHR models. In addition, results from the EnergyPlus simulation engine implemented with infiltration heat recovery are compared.

Comparative model analysis verifies each model provides the same solution when using a reference method. The models deviate in their results once their parameters are considered. A sensitivity study of IHR models reveals the most important consideration to characterize infiltration heat recovery is diffuse air fraction and wall participation factor. Experimental comparison of the IHR models reveal the models predict within 2% in a 1D flow case with the use of a wall participation factor, but within 10%

and greater when comparing to 2D flow cases. When applying IHR to EnergyPlus simulation, a significant reduction in heating consumption is found for the case study of homes in Boulder, ranging from 5-40%, but minimum of 5-14% reduction. The Claridge IHR model is found to provide the best comparison to the sample data set in this study.

ACKNOWLEDGEMENTS

I am very grateful for my time and education in the Building Systems Program at the University of Colorado at Boulder, University of Miami at Coral Gables, and to have been given the opportunity for a research assistant position in the Residential Buildings Group at the National Renewable Energy Laboratory (NREL). Thanks to Marcus Bianchi (NREL), Sean Casey (NREL), and Moncef Krarti (University of Colorado) for providing me with this opportunity. During my thesis work, I would like to express my appreciation again to Moncef Krarti (CU) and Marcus Bianchi, as well as Craig Christensen, David Roberts, and Ben Polly (NREL) for their terrific guidance and technical support. Additional recognition goes out to Neal Kruis (NREL) and El Hadddan Rissouane (NREL) for their support. To all my friends and classmates throughout my time in school, I appreciate your support and kind friendship. Lastly, I would like a special mention to my family; their unwavering support and tremendous motivation has helped me achieve so much throughout this endeavor.

TABLE OF CONTENTS

LIST OF TABLES

LIST OF FIGURES

NOMENCLATURE

a	Heating slope
A_{wall}	Wall area
$A_{conditioned}$	Conditioned floor area
A_{panel}	Experimental test panel wall area
ACH	Air changes per hour
BES	Building energy simulation
BLC	Building loss coefficient
$BLC_{conduction}$	Conduction loss coefficient
$BLC_{infiltration}$	Infiltration loss coefficient
$BLC_{measured}$	Building loss coefficient derived from utility bills
$BLC_{predicted}$	Building loss coefficient predicted from envelope description
Bi_i	Biot number on the interior surface
Bi_o	Biot number on the exterior surface
c_p	Specific heat capacity of air
d	Wall thickness
ELA	Estimated leakage area
f	Infiltration heat recovery factor
h_i	Interior surface convection coefficient
h_o	Exterior surface convection coefficient
hr	Hour
IHR	Infiltration heat recovery
j	Wall participation factor (Buchanan)
k	Thermal conductivity of insulation
$\dot{m}$	Air mass flow rate, per unit area
$A * \dot{m}c_p$	Infiltration heat loss coefficient
n	Blower door test flow exponent
Pe	Peclet number
Pr	Prandtl number
Re	Reynolds number
SLA	Specific leakage area
t	Home operation adjustment factor
T_i	Indoor temperature
T_o	Outdoor temperature
T_{si}	Indoor surface temperature
T_{so}	Outdoor surface temperature
$T_{air\ exit}$	Experimental air temperature exiting test panel
$T_{ambient}$	Experimental cold air temperature
T_{gypsum}	Experimental gypsum surface temperature
T_{room}	Experimental warm air temperature (ASHRAE)
$T_{x=0}$	Temperature at inside surface
$T_{x=d}$	Temperature at outside surface
U	Thermal transmittance of insulation
U_{eff}	Overall thermal transmittance of wall
U_{gypsum}	Thermal transmittance of gypsum board
UA	Conductive heat loss coefficientg
V	Air velocity

$Q_{classical}$	Classical total heat transfer
$Q_{conduction}$	Classical conduction heat transfer
$Q_{infiltration}$	Classical infiltration heat transfer
$Q_{recovery}$	Conduction-infiltration coupled total heat transfer
$Q_{new\ infiltration}$	Infiltration heat transfer with heat recovery
r	Ratio of heat loss; recovery vs. no recovery
x	Position coordinate
$X_{diffuse}$	Fraction of diffuse air flow (Claridge)
$X_{concentrated}$	Fraction of concentrated air flow (Claridge)
Z_1, Z_2	Constants
θ	Normalized temperature
ξ	Normalized coordinate
ρ	Air pressure
μ	Viscosity
ω	Experimental uncertainty
η	Heating system efficiency

1. INTRODUCTION

Building energy simulation (BES) tools are becoming increasingly critical in the assessment of residential building energy performance. Since the 1980s, the development of BES tools has provided capabilities to capture the energy performance of new technologies and construction methods used in homes. Recently, with the increasing need to reduce energy consumption from existing homes, the focus of BES model development has shifted to simulate the performance of older, poorly insulated, leaky homes using the latest developments in residential energy modeling. There are concerns that the current simulation tools do not capture important phenomena properly.

The many causes that can impact energy predictions can be placed into three general groups:

- Building description – The dimensions, areas, and material properties of the home construction, in addition to system efficiencies, are needed to analyze the proper size and thermal performance of the home.
- Occupant behavior – Times of occupancy, use of systems (lights, water, space-conditioning, etc.), and frequency of system use are necessary to capture the life of the occupant(s) and their impact on the energy consumption and performance of a home.
- Building physics – All forms of heat transfer phenomena in a home are captured by the calculations and algorithms used in simulation.

Building description and occupant behavior are important to properly characterize a home energy model. However, quantifying them can be subjective without an extremely large data set, which has not yet been identified. On the other hand, the building physics of energy simulation engines is well documented, and any changes and improvements made to building physics can be well quantified for future comparison. Thus, the present study only focuses on the building physics of energy models.

The building physics algorithms in BES are of considerable importance because it is typically the foundation for providing energy predictions. Improvements in this field can be helpful across all future

simulation work. Through sensitivity analyses of potential building physics modeling issues, an understanding of important issues can be found to determine the best path in impacting building energy predictions. In terms of addressing simulation discrepancy, focusing on building physics may imply other information used in simulation is accurate, but this can be misleading. To provide good quality analysis, inputs used in each sensitivity studies will be given extra consideration to isolate and test the effects in building physics.

1.1 Motivation

In the United States, residential buildings account for 21% of the nation's entire energy consumption (U.S. DOE, 2011). Major steps can be taken to reduce the nation's energy consumption through the development and implementation of home energy efficiency methods and technologies. Building energy simulation (BES) tools provide the analysis needed to predict energy consumption. About 91% of homes in the United States were built before the year 2000 (U.S. EIA, 2008). Discrepancies between prediction and measured energy consumption can have significant financial implications in design and retrofit projects. Providing additional capabilities in state of the art simulation engines can potentially provide more accurate energy analysis to account for the building behavior and physics phenomena of existing homes.

2. LITERATURE REVIEW

An extensive literature search in simulation accuracy is needed for an understanding of the development in residential BES tools. The scope of interest is limited to residential tools currently used in industry. Although research and development of simulation engines has been ongoing for over three decades, only state of the art residential energy modeling tools are considered of relevance to this study. While past BES tools are important, they may not reflect the current capabilities from present energy analysis software. An additional literature search of potential home energy modeling issues will help provide indications of what issues are likely to be the most important in energy modeling.

2.1 Home Energy Simulation Performance Studies

The majority of the research on home energy modeling discrepancy looks only at the capabilities to predict retrofit energy savings from a sample of homes. A number of different home energy simulation tools have been studied by different authors. Each published report provides a comparison between annual predicted and measured energy consumption in their findings. The measured energy is gathered either through metering methods or from the occupants' utility bills. This information provides an outline over the simulation discrepancy currently found in residential energy simulation.

The majority of the tools shown in the literature were reviewed by national research laboratories and state organizations. Several studies were done to compare results of multiple simulation tools; others were interested in the performance of retrofit savings predictions. An overview of the findings in the literature is shown in Figure 1. Each point on the graph represents a software performance evaluation, comparing measured heating energy consumption to the tools' heating energy prediction of either a single home or multiple homes. The line of perfect agreement determines how close predicted energy consumption matches actual energy consumption. Points shown above the line are considered over prediction, and points below the line are under prediction in BES. Published findings are plotted on the graph to provide an overall assessment of energy simulation accuracy in a number of tools. From the

results of Figure 1, there is strong evidence of discrepancy found between predicted and actual energy use, with the predictions usually larger than the actual energy use. A detailed summary of each simulation performance study in Figure 1 is provided in the Appendix.

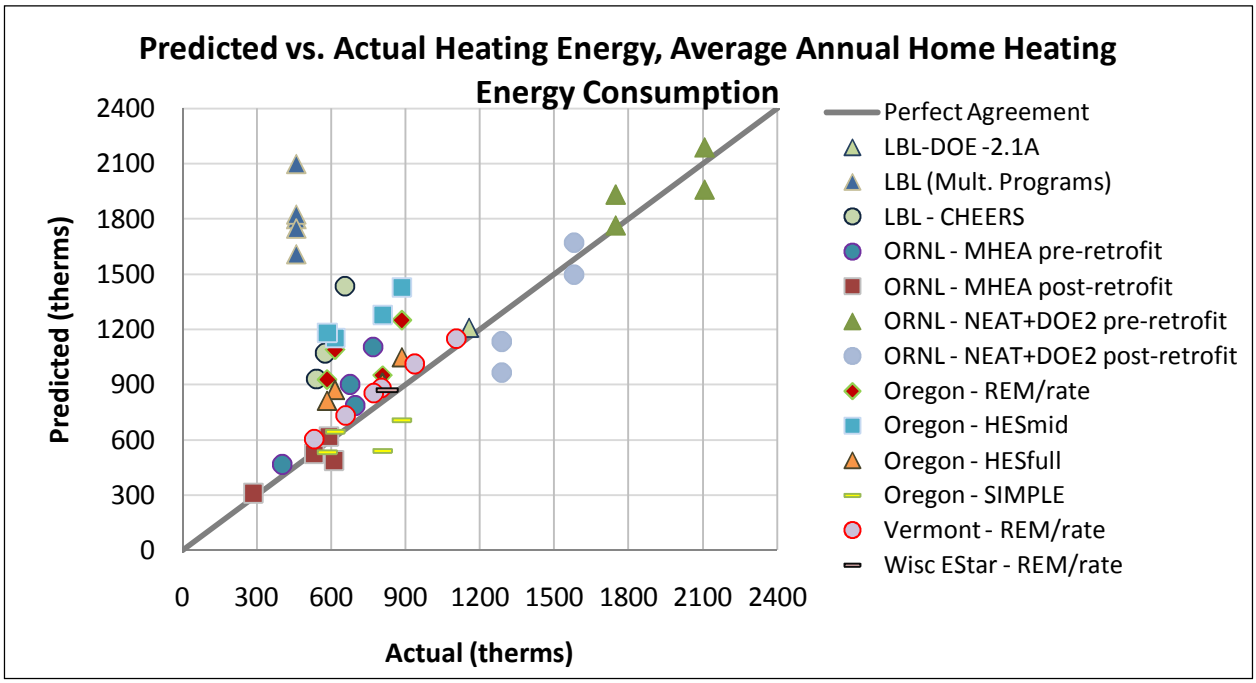

Figure 1: Summary of simulation performance studies - Actual vs. predicted heating energy consumption

Figure 1 gauges the amount of discrepancy found between models and measured data. It is not intended to show which tool performs the best. A ranking or assessment of each simulation tool is not possible because the differences in the analyses methods for each report prevent a fair comparison. Normalization over a number of variables would be needed to provide valid comparisons of each report. This would require a considerable amount of additional information and time, impractical in the scope of this research. Despite the lack of a common analysis method, Figure 1 shows there is a trend of over-prediction. There can be many reasons for this, but as previously mentioned, this study is focused on addressing issues related to the building physics in simulation.

In Figure 1 some of the studies appear to agree fairly well due to their proximity to the line of perfect agreement. However, at higher energy consumption this metric can become misleading, because

any changes in energy are not weighted as heavily. To provide a better statistical assessment, Figure 2 reformats the published findings to compare actual energy consumption against percentage discrepancy to provide a better understanding of simulation discrepancy when accounting for the size of the home.

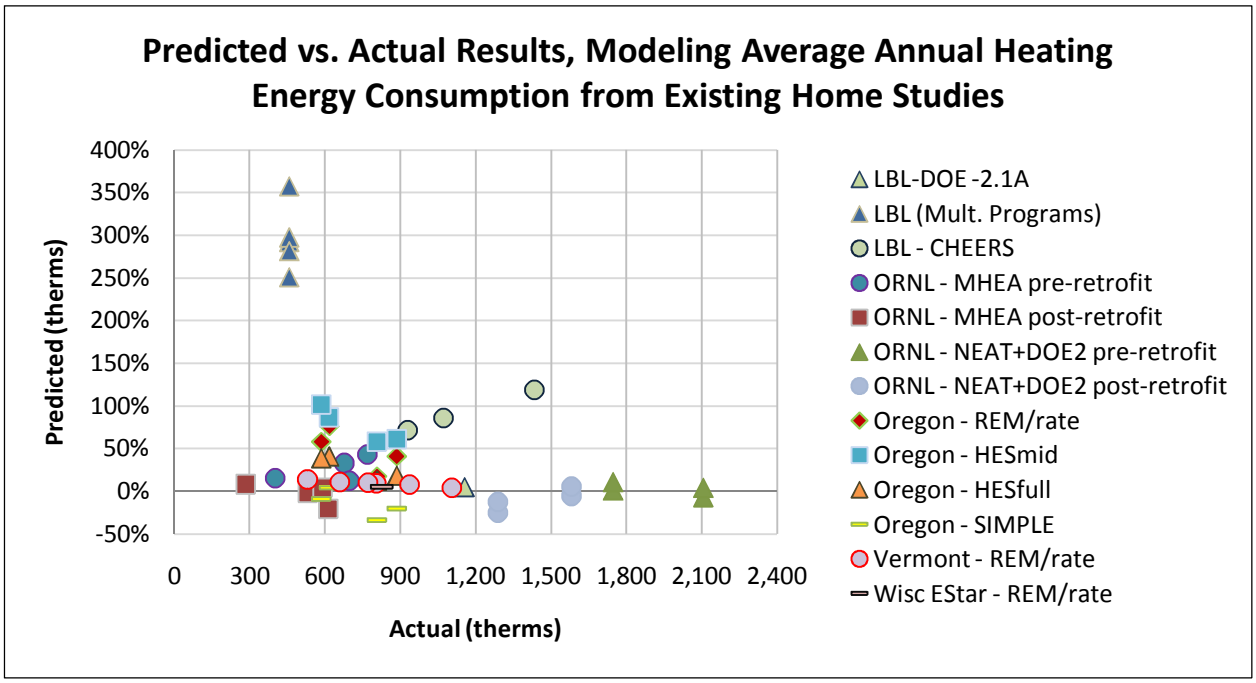

Figure 2: Summary of simulation performance studies - Percent discrepancy vs. actual heating energy consumption

In Figure 2, one study shows a very large discrepancy relative to the other studies. An assessment of simulation accuracy is performed for a small set of simulation tools, selected from over one hundred tools (Mills, 2002). When each tool is tested against a measured home, over prediction of at least two times greater than the home heating energy consumption was found. Limited information of the analysis was provided in the report, giving little confidence in the results. In the report the author notes each simulation tool was tested by a separate experienced modeler. There is also no description of the home or if model calibration was performed, casting uncertainty of what information and how much of it was initially provided to building the home energy model in each tool. Additional sources of discrepancy are possible if limited information was provided about the home. Due to the lack of information about their modeling methods, along with the very high over-prediction, there is very low confidence in these results

and are removed from the comparison. Figure 3 provide a summary of the remaining studies in much greater detail when these points are removed.

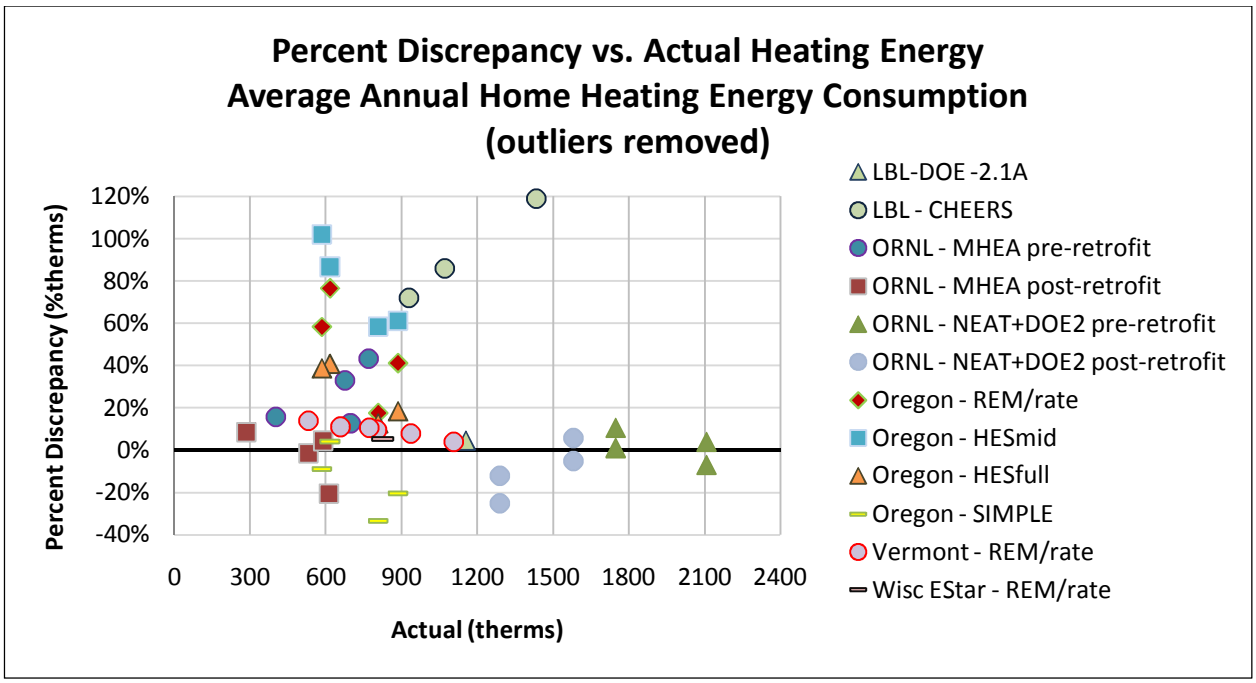

Figure 3: Summary of simulation performance studies - Percent discrepancy vs. actual heating energy (outliers removed)

After establishing a trend based on results from literature, further investigation is needed to explain reasons for any discrepancy. Evidence in the literature is useful to determine any improvements that can be made. However, from the research found, very little is suggested to explain possible causes of discrepancy. The lack of evidence is a key point for the need to address issues causing modeling discrepancy. Two case studies are discussed to highlight the major findings found. Results from both case studies find there is much more discrepancy when modeling older homes or pre-retrofit homes. One reason for this is the uncertainty is a lack of documentation providing details of the home's construction and specifications. In addition, over time changes in the thermal performance of the home can occur due to degradation of the existing materials. This creates a higher potential for errors in energy modeling. An investigation of issues in modeling will look into causes of modeling discrepancy. Further discussion of the modeling issues are explained in a later section.

2.1.1 BES Performance Case Studies

Two simulation performance studies are discussed in detail to highlight the major findings from the initial literature search.

ORNL – MHEA Study (Ternes, 2007)

This study investigates the simulation performance of the Manufactured Home Energy Audit tool (MHEA), developed by Oak Ridge National Laboratory. MHEA was used to analyze a number of mobile homes in northern and mid-western states. In Figure 4 results from the study are shown. Results from the pre-retrofit analysis reveal greater discrepancy and over-prediction to the actual energy consumption than post-retrofit analysis. This also results in an over-prediction of energy savings through retrofit.

The author recognizes there could be errors from the energy audit inputs that would lead to over-prediction. Using engineering judgment, modifications in the analysis were made. Table 1 provides a description of the changes made to the envelope, infiltration, and internal load calculations to each mobile home. All the changes provided better home performance because on-site field analysis may have under-estimated the performance of the mobile homes. Figure 4 shows the reductions in simulation discrepancy as a result of the changes made to the models. The changes were able to reduce the level of discrepancy due to over-prediction, but the author still considered the discrepancy to be too high. To have good accuracy, a reduction factor of 0.6 was applied to their predicted the author resorted to applying a reduction factor of 0.6 to their predicted energy savings results in order for them to achieve a reasonable comparison. The study concludes further investigation was recommended to better address modeling discrepancy.

Table 1: Engineering-based modification for MHEA (Source: Ternes, 2007)

ORNL - MHEA Engineering-based modifications		
Building Envelope	Adjustment to envelope UA	An R-value of 1 is added to the ceiling, floor, and walls.
Infiltration loads	MHEA adjustment to blower door readings	Reduce the blower door readings by 25%.
Internal loads	Loads for appliances and occupants (two adults) were adjusted	Initial loads Day: 2400 Btu/h Night: 1000 Btu/h New loads Day: 1950 Btu/h Night: 2350 Btu/h

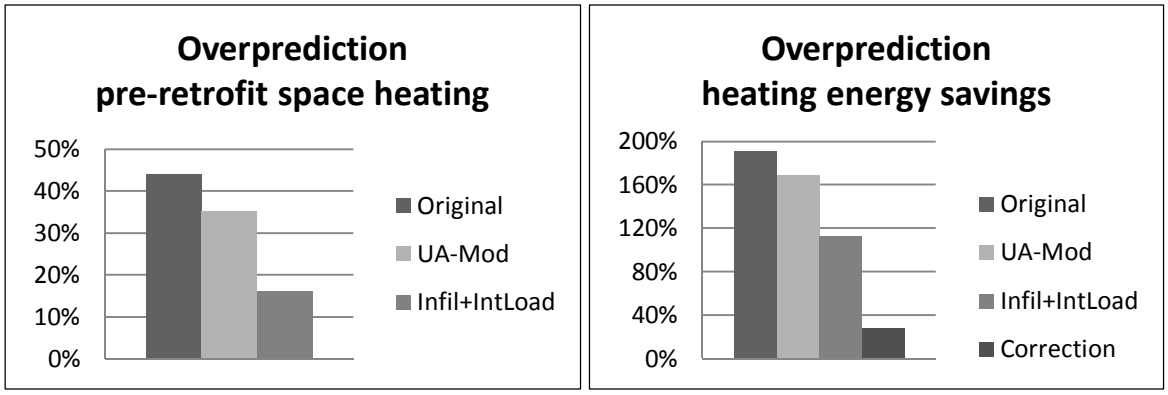

Figure 4: Reduction of discrepancy for MHEA pre-retrofit space heating and heating energy savings, Source: (Ternes, 2007)

Oregon Energy Performance Score (EPS) Report (Storm & Meredith, 2009)

The second case study tests 190 single-family Oregon homes against the annual energy predictions from four BES programs to analyze their performance for its potential implementation into the Energy Performance Score Program (EPS) in Oregon. The four tools offered varying levels of detail in their modeling capabilities, and as a result offered different levels of discrepancy, as can be seen in Figure 3. The points represent the average discrepancy found from each simulation tool when analyzing a group of homes. A detailed look is taken at the analysis done using REM/rate, a well-known home energy rating tool, to understand how each individual home prediction performs against utility data. Access to each model simulation, home building description, and measured energy consumption from utility bills was requested and provided through NREL.

Similar to the previous assessment of simulation discrepancy in Figure 3, Figure 5 shows the results from every home in the data set. As seen in the graph, an overwhelming majority of homes are being over predicted. The homes with the largest over prediction are found to be from homes built pre-1960's, indicating that more discrepancy can occur when modeling older homes.

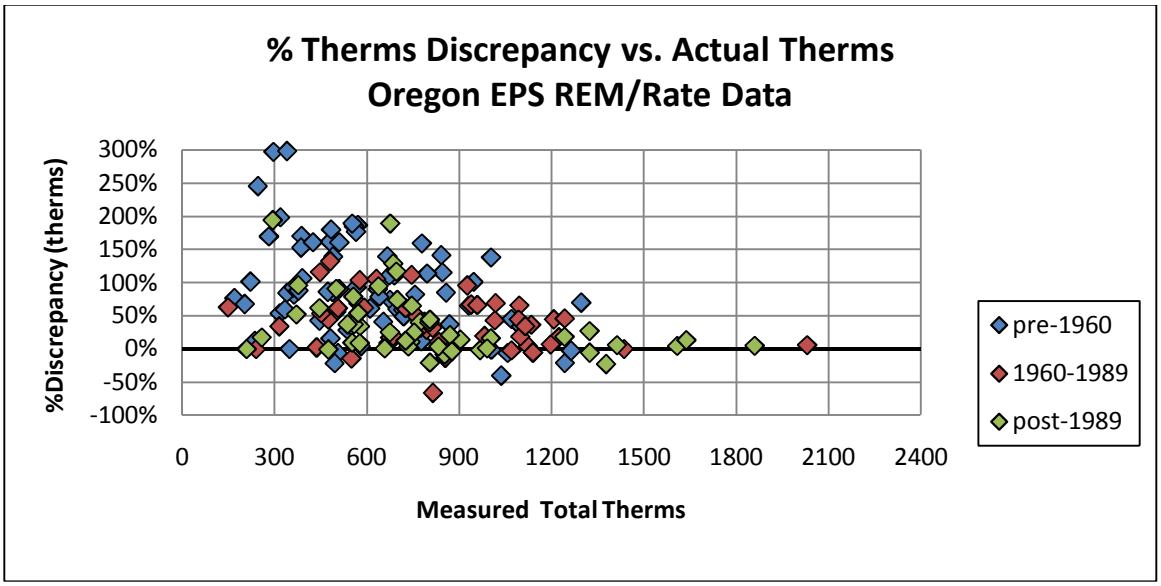

Figure 5: Energy performance score - Percent discrepancy vs. actual heating consumption

To confirm this trend, the results from each energy model prediction are reorganized by the year the home was originally built. Figure 6 provides the discrepancy when accounting for the age of the home. The homes are places into three grouped based on the year of construction. The largest discrepancy against utility bills can be found in the of pre-1960's homes, when comparing by vintage. The newer homes on average had far less discrepancy. Additional graphs from the Oregon case studies can be viewed in the Appendix.

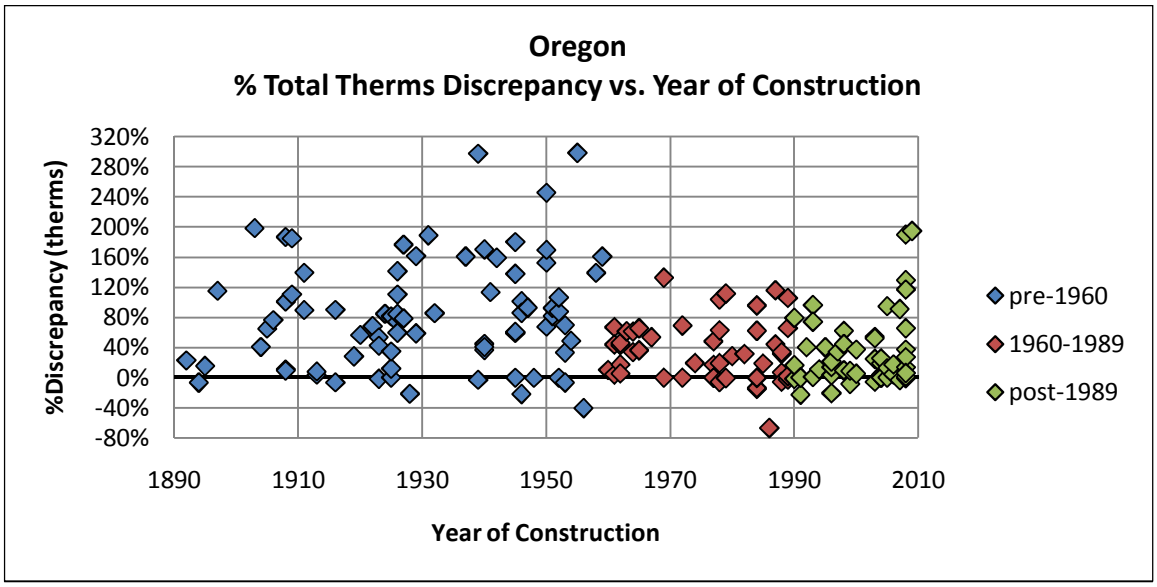

Figure 6: Energy performance score - Percent discrepancy vs. year of construction

In summary, the findings from both case studies indicate there is a need to address energy modeling discrepancy. The goal in for majority of the simulation studies is to analyze the current performance of the simulation tool, with very little focus of assessing the results. The exceptions are the authors at ORNL, where an attempt was made to correct the discrepancy found by their tool MHEA. They recognized that even though improvements could be made through the adjustment to inputs of building performance, considerable discrepancy still existed, prompting the need for further model development (Ternes, 2007). Additional literature search is needed to find specific methods that can address modeling discrepancy.

2.2 Home Energy Modeling Issues

Through sensitivity analyses of building physics modeling issues, we can evaluate the most noticeable impacts on energy predictions. A number of theories regarding home modeling issues were developed through a collaboration of experts at NREL, based on current knowledge of building physics in residential BES. A handful of topics are examined to determine which issues are important. This is done through a literature search to identify prior work from each topic. Details about each modeling issue are provided in the Appendix. The intent is to first find enough evidence in literature to determine which

issue will have an impact on energy consumption to potentially reduce modeling discrepancy. Once there is sufficient information, sensitivity studies can be built to find their impact. Table 2 provides a summary of the modeling issues chosen and key papers found.

Table 2: Summary of modeling issues

Modeling Issue	General Description	Sources
Wind Shelter Factor – Infiltration and Natural Ventilation	Load calculations for infiltration and natural ventilation models account for the effects wind speed and also the effect surroundings have on partially shielding a home from the wind. A sensitivity of this factor will show its importance is the building energy predictions.	(Parker, Fairey, & Gu, 1993) (Sherman & Modera, 1986) (U.S. DOE, 2010) (Sherman, 1990) (Walker & Wilson, 1998)
Wind Shelter Factor – Exterior Convective Surface Coefficients (DOE2)	The DOE2 exterior convective coefficient algorithm also accounts for wind speed in the model, but does not include effects from shielding. Adding this factor into EnergyPlus can provide a very large impact on the surface coefficients, impacting the building load.	See above (U.S. DOE, 2010) Add sources from E+ ref
Window Insect Screens	The majority of homes in the U.S. have insect screens installed to at least half of their windows to prevent bugs from entering. Most models do not account for the impact this can have. Insect screens shield the windows from solar gains as well as wind, providing reductions in solar gains and improvements in window performance. The impact of this can be great, especially in sunny climates.	(U.S. DOE, 2010) (Wright, Barnaby, Collins, & Kotey, 2009) (Brunger, Dubrous, & Harrison, 1999) (Kotey, Wright, & Collins, 2009)
Variable thermal conductivity of insulation	Insulation for building envelopes undergoes a standard rating procedure to provide consumers with a thermal performance rating. However, thermal conductivity is impacted by temperature, and conditions for a home are likely to be different than standard testing methods. Determining the performance of the insulation based on the weather can increase of decrease the envelope performance for a home, impacting energy consumption.	(Budaiwi, Abdou, & Al-Homoud, 2002) (Levinson, Hashem, & Gartland, 1997) (Wilkes & Childs, Thermal Performance of Fiberglass and Cellulose Attic Insulations, 1992) (Wilkes & Rucker, 1983)
Variable Air gap R-value	Air gaps in building wall envelope are common in wood frame walls, especially in older homes. These are represented in simulation through an effective R-value, derived in research, accounting effects of convection and radiation. However, air infiltration flow disrupts this heat exchange and can impact the R-value tremendously. Sensitivity of this R-value can show how important this is.	(ASHRAE, 2005) (Yarbrough, 1983)

Duct Leakage	Duct leakage can create a pressure imbalance in the conditioned space, depending on the location of the leaks. Leakage not only directly impact HVAC performance, but the induced pressure is important towards infiltration loads. Current modeling does not take this interaction into account. Research has shown infiltration in a home to increase when using a ducted air system. Accurately calculating the effects of duct leakage is important in determining energy predictions.	(ASHRAE, 2004) (Jump & Modera, 1994) (Treidler & Modera, 1994)
Infiltration Heat Recovery	Traditionally, infiltration loads are calculated independent from the wall heat transfer. Experiment has shown there to be an interaction between the infiltration and conduction heat transfer. Current methods are believed to over-predict the overall envelope performance for a house, impacting the energy predictions.	(Ackerman, Bailey, Dale, & Wilson, 2004) (Anderlind, 1985) (Buchanan & Sherman, 2000) (Krarti, 1994) (Claridge & Bhattacharyya, 1991)

3. PRELIMINARY SENSITIVITY STUDIES

The EnergyPlus simulation engine is chosen to study the impact of modeling issues in simulation. EnergyPlus (U.S. DOE, 2010) is an innovative whole building energy simulation software with a wide range of capabilities providing greater depth of analysis suited to test multiple issues surrounding residential building physics. Sensitivity analysis will address the impact of energy predictions on the algorithms in EnergyPlus. Performing each series of simulation provides information on the current capabilities and gaps existing in the simulation engine.

An interface is needed for creating and managing home energy models to run models to test each issue using parametric simulations. The Building Energy Optimization Tool, or BEopt, is a tool designed by NREL to determine the path to a net-zero energy home through a least-cost analysis method over the lifecycle of the house (Christensen & et.al., 2006). BEopt for this purpose possesses the capability to test multiple building characteristics of a home. Multiple home energy models can be managed by this program as well. This makes it an ideal tool to analyze the energy predictions of homes in multiple climates to determine the energy impact from each sensitivity study. Although the optimization capabilities in BEopt are very powerful, they were not used in the analysis of the impact on energy predictions. BEopt provides an interface to build and run simulation using EnergyPlus, and this allows better feasibility in performing multiple energy sensitivity studies.

3.1 Base Case Model

A representative base case must first be defined to analyze the impact of each modeling issue for typical homes using energy simulation. Recently, work has been done to define a set of homes across the United States that are representative of the construction practices in the time it was built. Home building characteristics are defined for 16 major cities across the United States (Albertsen, 2010). These prototypical home energy models provide a reference point which can be used to find the impact for

typical homes in a given location and climate. These base case models for each city can be created and simulated in BEopt using EnergyPlus.

To attain results of the impact found in existing homes, models representing a 1960's home construction are used, characterizing the operation and building description of the region for sixteen cities across the country (Albertsen, 2010). Characteristics of the home construction and system efficiencies have been previously calibrated to provide agreement to a typical home defined for each city in the Residential Energy Consumption Survey (RECS) (U.S. EIA, 2008). Financial and retrofit analysis is not a focus in this research; analysis is limited to understanding the impact on predicted energy consumption when addressing multiple modeling issues. It is recognized that impacts in retrofit and financial analysis will exist, but they will be considered in future analysis. Details of the building characteristics and operational descriptions are provided in a table in the Appendix. In summary, all home energy models were built and run in the following manner:

- BEopt simulation tool, v1.0
- EnergyPlus simulation engine, v6.0
- Sixteen major cities are tested, representing all climates across the Unites States.
- 3 bedrooms, 1 bathrooms, garage attached
- Building description is representative of the construction practices at the time of construction.
- Similar user operation for all locations.

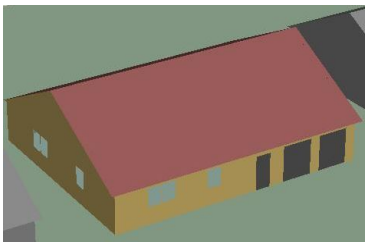

Figure 7: Example of BEopt home rendering

3.2 Preliminary Sensitivity Study Summary

The base case models provide a reference case for a prototypical home of the region's existing housing stock from the 1960's. These models will be used in sensitivity analysis of each modeling issue. This preliminary sensitivity study is a high-level analysis of the predicted energy impact on heating and cooling made to the base case model when accounting for different modeling issues. The overall assessment of energy consumption for each city provides a rough understanding of the impact in multiple climates. To compare the impact between cities, a percentage change in energy consumption relative to

the base case model is investigated. A comparison of the impacts of any two modeling issues is also possible with this analysis. A higher consideration will be given to issues showing the greatest impact on energy consumption, but this will not determine the order of the issues deemed to most improve energy simulation. For this research, the issue that proves to provide the best improvement in simulation will be implemented into EnergyPlus to capture the targeted phenomenon and determine the potential impact on energy. A summary of each sensitivity study is provided in Table 3. In the Appendix, a detailed description of each sensitivity study provides information why this issue is important. A literature search on each issue is performed to find any useful research that helps assess the potential impact. An understanding of each issue is provided and the information is used to assess how to quickly model it into EnergyPlus. Table 3 provides a summary of the findings from each modeling issue literature search and a quick description of the parametric simulation done to roughly capture the effects of each modeling issue. Sensitivity studies for each modeling issue are performed using a range of values that capture the extent of the change expected to occur. Please see the Appendix for a detailed analysis of each issue.

Table 3: Sensitivity study summary

Home Modeling Issues	Preliminary Sensitivity Study Simulation Summary
Infiltration Heat Recovery	Simulation IHR through use of air mass flow rate Reduce SLA by 20%
Duct Leakage	Parametric on leakage fraction for ducts Increase leakage fraction from 0.15 to 0.20
Air Gap R-value	Parametric on R-value of empty wall assembly Reduce air gap resistance from R-1.2 to R-1.0 (hr-ft^2-F/Btu)
Temperature Dependent Insulation Performance	Parametric on ceiling insulation R-value per inch Recalculate R-value/inch, based on the max and min outdoor temperatures
Window Insect Screens	Add window insect screen construction to window assembly Compare to this by modifying window performance Reduce U-value 10-30% Reduce SHGC 45%
Wind Shelter Factor – Exterior Surface Convection Coefficient	Add wind shelter factor to exterior film coefficient calculation Add shelter factor of 0.5
Wind Shelter Factor-Infiltration	Parametric on wind shelter factor with infiltration Increase and decrease factor by 0.1
Wind Shelter Factor – Natural Ventilation	Parametric on wind shelter factor with natural ventilation Increase and decrease factor by 0.1

To gauge the impact of each issue, criteria are set to rank each issue in terms of overall impact to simulation engines. The impact on energy alone is not enough to identify improvement in simulation. Therefore, including impact on energy, prioritization of each issue will be based on three areas:

- Energy impact of heating and cooling loads - Issues are weighed based on the magnitude impact found on heating and cooling energy consumption.
- Gaps in EnergyPlus – Issues that can be added using existing capabilities in EnergyPlus are not weighted as important as others that require additional model capabilities.
- Feasibility of model implementation– The issues that can be implemented in the easiest manner can provide the most effective impact.

Each area describes a different aspect that requires consideration in assessing the importance of each modeling issue in the energy models. Understanding the gaps in EnergyPlus, along with the changes needed, can help organize the order at which modeling issues can be prioritized.

3.3 Sensitivity Study Findings

The methodology for simulation created for each modeling issue sensitivity study is important to assess the impact found in predicted energy consumption. Described in this section is a summary of the results of each sensitivity study. As previously mentioned, sensitivity analysis was conducted in every simulation using a range of parameters representative of the effects. Several of the modeling issues from Table 3 have made a noticeable impact, while others seem to only have a minor effect. The following two graphs, Figure 8 and Figure 9, are a summary of all the sensitivity studies performed. For a detailed description of each modeling issue sensitivity study, please refer to the Appendix.

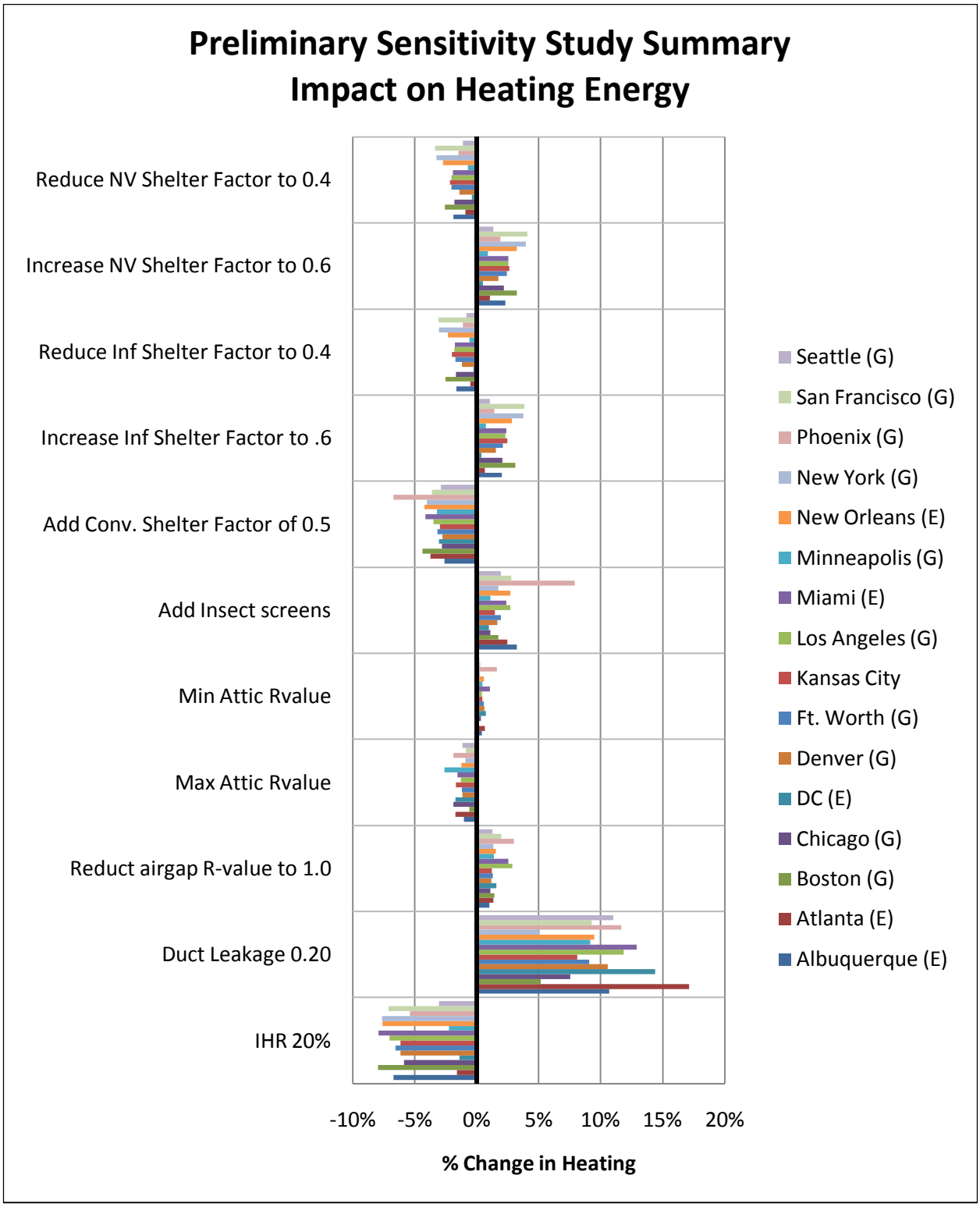

Figure 8: Modeling issue sensitivity study summary: Impact on heating energy

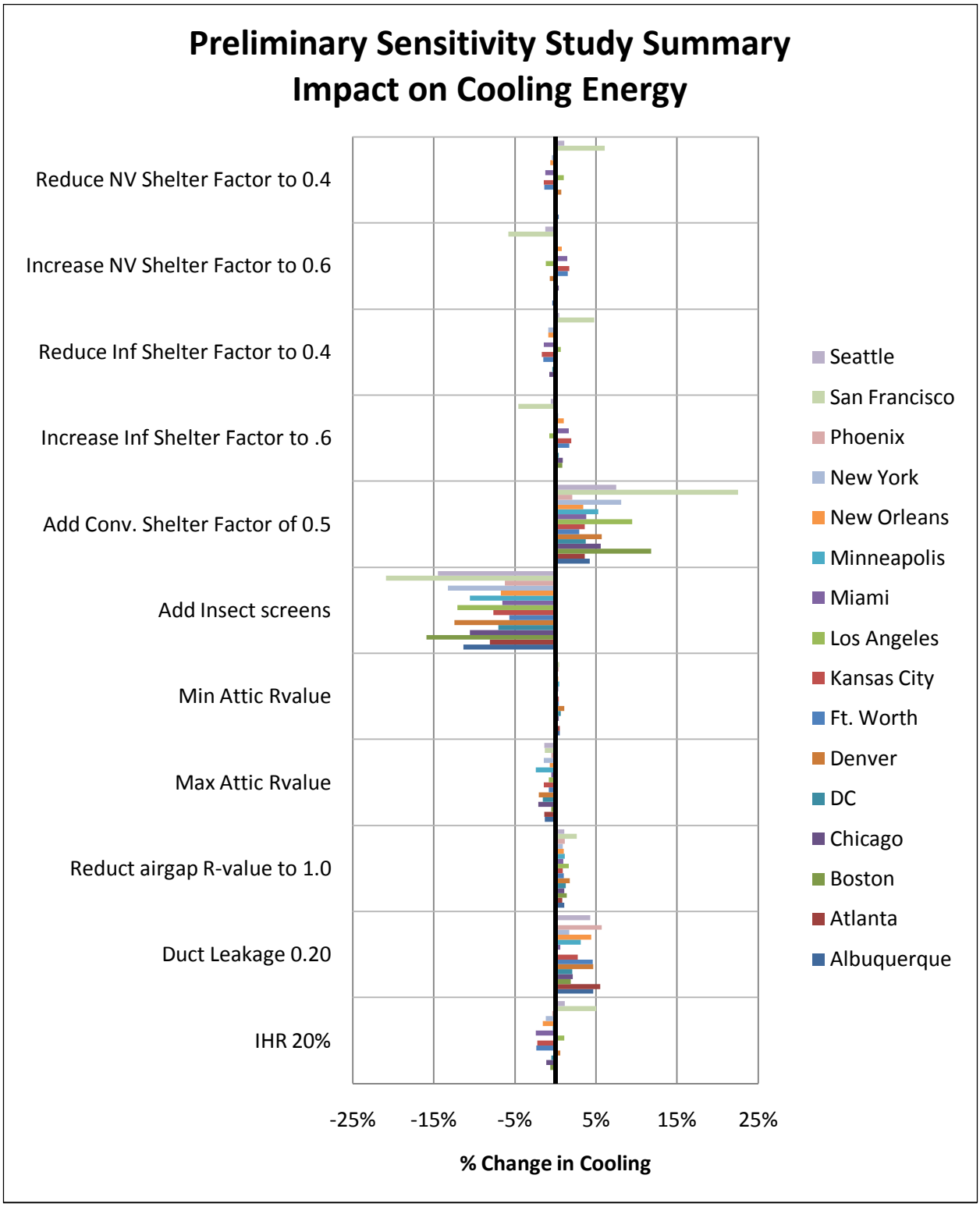

Figure 9: Modeling issue sensitivity study summary: Impact on cooling energy

The results from each sensitivity study show the predicted changes on heating and cooling for each city. The modeling issues are then prioritized from highest to lowest impact on energy consumption. When all the cities are compared, the modeling issue most often found to have the greatest impact is considered the highest priority, followed in a similar manner with the remaining modeling issues. The modeling issues are ranked by both the impact on heating and cooling energy consumption. Table 4 provides a summary of the sensitivity studies' energy impact across 16 cities. Duct leakage shows the largest overall impact on energy. However, during the time of this analysis, work at the National Renewable Energy Laboratory provided some corrections to this issue, and making it impractical to pursue further work. As a result, infiltration heat recovery was found to have the greatest impact on heating energy, while insect screens showed the greatest impact on cooling energy.

Table 4: Energy consumption impact summary

Heating Impact	
1st	*Duct Leakage*
2nd	**Infiltration Heat Recovery**
3rd	**Shelter Factor – exterior convection**
4th	Shelter Factor - Nat Vent
5th	Shelter Factor - Infiltration
6th	**Insect Screens**
7th	Air gap R-value
8th	Attic Insulation R-value
Cooling Impact	
1st	**Insect Screens**
2nd	**Shelter Factor - exterior convection**
3rd	*Duct Leakage*
4th	Attic Insulation R-value
5th	Air gap R-value
6th	**Infiltration Heat Recovery**
7th	Shelter Factor - Infiltration
8th	Shelter Factor - Nat Vent

The top three issues found based on the overall energy impact are infiltration heat recovery, insect screens, and the wind shelter factor for exterior convection coefficient algorithms. These three issues are ranked by overall impact on energy consumption in Table 5 the left-most column. The other two columns

shown order these issues again in terms of the two other criteria mentioned earlier, gaps in simulation and feasibility of model implementation. Although infiltration heat recovery does not show the biggest impact on energy consumption, it does possess the biggest modeling gap in EnergyPlus out all of the issues analyzed in this study.

Table 5: Top three modeling issues found

Criteria	Energy Consumption	Gaps in simulation engines	Feasibility in implementation
1st	Insect Screens	Infiltration Heat Recovery	Infiltration Heat Recovery
2nd	Infiltration Heat Recovery	Exterior Surface Convection Coefficient	Insect Screens
3rd	Exterior Surface Convection Coefficient	Insect Screens	Exterior Surface Convection Coefficient

Window insect screens can be modeled in EnergyPlus through the use of the envelope window construction. In addition, EnergyPlus contains a thermal model to account for the effect that insect screens or any shading device has on heat transfer through the windows. However, EnergyPlus limits the user to defining only one window shading device per window. Typically homes have drapes or blinds installed, and these are typically captured in energy models. This limitation prevents the user from modeling window insect screens, preventing EnergyPlus from accurately capturing a typical window with both screens and interior shades. Development of the simulation program source code would be needed to provide better capabilities in modeling window shading devices, outside the scope of the research.

The wind shelter factor adjusts the local wind speed to account for the nearby surroundings. Infiltration and natural ventilation algorithms already take this into account, but not the DOE-2 exterior convection coefficient algorithm. Through the use of Energy Management System (EMS) in EnergyPlus (U.S. DOE, 2010), the equations can be replicated with a wind shelter factor without opening EnergyPlus source code. However, when using EMS, the model cannot replicate the results of EnergyPlus due to the reporting functions of EMS. There is only a slight impact to the overall energy consumption, but the exterior convective coefficients were greatly impacted. Since the program could not be improved further, it was considered highly unfeasible to successfully implement the model to EnergyPlus.

The investigation of EnergyPlus revealed there are barriers to properly model window insect screens and a wind shelter factor for exterior convection. EnergyPlus contains no capability to capture infiltration heat recovery, and feasibly implementing a model provides the best potential to improve simulation. From this finding, improvements to the simulation engine can be focused on the development and implementation of a model to capture the effects of infiltration heat recovery.

4. INFILTRATION HEAT RECOVERY REVIEW AND MODEL METHODOLOGY

When determining the overall thermal performance of the building envelope, the summation of all heat transfer components is taken to find the overall performance of the envelope. Infiltration is traditionally calculated as the air leakage mass flow rate multiplied by the difference in enthalpy between the inside and outside air. This is normally calculated independent of the wall conduction heat transfer, providing no interaction with the wall transmission losses. This assumption has been found to cause over prediction in heat transfer. Past analytical and experiment work have identified an interaction between infiltration and conduction heat transfer to occur in the envelope. This phenomenon is named infiltration heat recovery (IHR), and accounting for this heat exchange can improve the predicted envelope performance and potentially beneficial in reducing the discrepancy of predicted home energy consumption in energy simulation.

A search of past steady-state infiltration heat recovery work provides a good indication of the existing knowledge quantifying infiltration heat recovery. Only the effects of sensible conduction and infiltration heat transfer are considered in the analysis. The effects from solar gains, radiation, and moisture are ignored in this particular study. The theory in the development of these models is explained to provide a comparison between different methods used to quantify infiltration heat recovery.

4.1 History

When accounting for infiltration heat recovery, the exchange in heat between the air and wall will show a decrease in overall heat transfer within the envelope, providing improved performance. This was first realized in Europe through theoretical analysis of conduction and infiltration heat transfer. Using the law of conservation of energy, the solution derived under steady-state conditions was found to provide a nonlinear temperature profile, different from the assumption of a linear wall profile in steady-state heat transfer (Anderlind, 1985). The impact of the temperature gradient depends on the direction and quantity of air flow, from warm to cold or vice versa. In a heating climate, infiltration is cold air entering a warm

space (see Figure 10). The effects of infiltration heat recovery cause the gradient to become more convex with increasing air flow. This change lowers infiltration due to a lower overall wall temperature, but increase conduction due to a steeper temperature gradient. In a cooling climate, infiltrating consists normally of warm air entering a cooler space. The impact on the temperature is opposite, creating a concave gradient with increasing air flow. The impact of heat transfer also becomes flipped, decreasing conduction but increasing infiltration. Details of this derivation are provided in the Appendix.

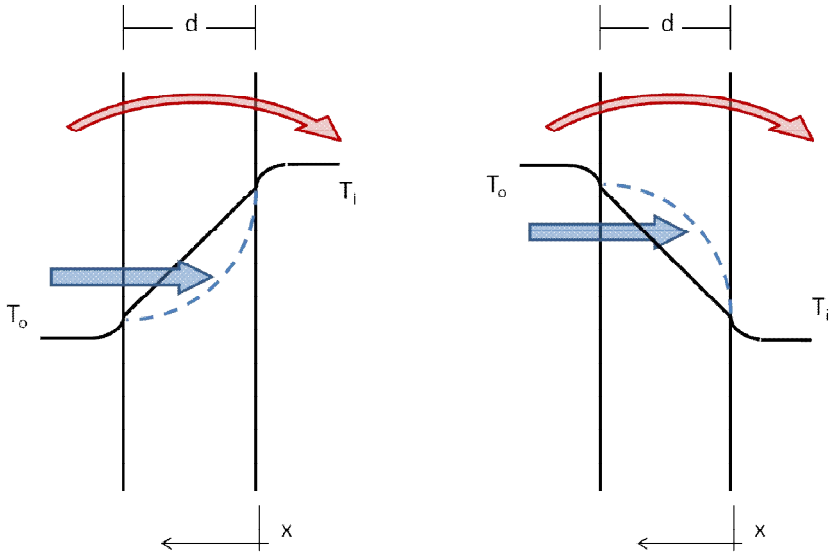

Figure 10: Impact from air flow on wall temperature distribution

This concept initially stirred interest for the development of technologies to take advantage of this effect to provide energy savings for buildings. Heat thought to be lost to the outside can be recovered by the wall and returned to the space with the use of incoming air. If the wall is compared to a heat exchanger, this is can be seen as a counter flow situation in a heating climate when air flows opposite to the direction of transmission losses. Dynamic insulation and breathing walls are examples of technologies designed to maximize the effects of infiltration heat recovery to improve building performance and have been discussed in several papers (Anderlind & Johansson, 1983) (Morrison, Karagiozis, & Kumaran, 1992) (Slowinski, 2009). However, infiltration heat recovery is a phenomenon that can also occur in typical exterior facing residential walls. The Anderlind model assumes infiltration is evenly distributed over the wall area. A wall such as this is not normally found in homes. Further development of this model

is needed to more accurately capture the impact of infiltration heat recovery in a residential building envelope.

At Texas A&M University the concept of diffuse and concentrated air flow is introduced by one author to improve upon the Anderlind model (Claridge & Bhattacharyya, 1991). Similar to an electrical current, infiltration air is expected to follow a path of least resistance. A large crack along the wall, such as a window edge or door gap, allows a fraction of air directly into the space. In the Claridge model, this is given the term concentrated air flow and is assumed to have no heat exchanged with the walls and impact from IHR as a result. The remaining fraction of air is named diffuse flow and passes through the building envelope, exchanging heat with the wall, causing infiltration heat recovery to occur. When air flow is fully concentrated, the model will show no impact from IHR. When air flow is fully diffuse, the Claridge model can be simplified to the Anderlind model. The advantage of this model is the ability to estimate IHR when a mix of diffuse and concentrated air leakage exists. This expected in a typical home, and properly accounting for these air paths is need to accurately estimate the impact of infiltration heat recovery. The lack of research to properly characterize diffuse vs. concentrated air flow in a typical wall makes this a difficult metric to apply in practice.

Lab experiments performed at Texas A&M University are able to measure infiltration heat recovery in controlled test cells with varying infiltration levels and openings. Results show IHR can be characterized based on three criteria: air flow rate, air leakage path, and crack size (Claridge & Bhattacharyya, 1991). The author finds infiltration heat recovery increases when; air flow decreases, leakage path increases, and crack size decreases. The longer the air takes to pass through a wall and the greater the surface area, the greater potential for infiltration heat recovery. The experiment, however, does not represent a full size wall construction of a home and the results provide little to quantify how much diffuse and concentrated air is expected for a wall.

In addition to the Claridge model, another student from Texas A&M University improves upon the reference model by accounting for the impact of solar radiation on envelope performance (Liu M. ,

1992). Due to solar radiation, the air temperature near the surface of a wall can be affected significantly. The effects of infiltration heat recovery up to this point was thought only to reduce the heat transfer, however solar can negate the impact and even increase the overall heat transfer. No other model accounts for solar gains in IHR, and an analysis of the model without solar gains was done for purposes of comparing to the Anderlind model. When solar is no longer considered, the model becomes identical to the Anderlind model. So although the model accounted for something unique, fundamentally the models agree under reference conditions.

One author at the University of Colorado derives an analytical solution for maximum theoretical energy savings achievable based on the performance of a dynamical wall (Krarti). The key difference between the Krarti model and the other models is the surface temperature is no longer assumed to be at the air temperature. The author recognizes the convective properties of a wall surface will cause the air temperature to change slightly before reaching the surface and entering the wall. Similar to the Liu model, this is a potentially important feature to consider for infiltration heat recovery, especially if the convective coefficient is large. In this model, in addition to the Peclet number, the dimensionless Biot number is used to characterize the resistance at each wall surface. This model is originally designed to find the total load reduction in energy; however, the format of the author's published methods is not comparable to the other models. Using the conditions defined by Krarti, an infiltration heat recovery model was derived again following the reference steady-state methodology from the Anderlind model. Details of this derivation are provided in the Appendix.

The most recent analytical work found of infiltration heat recovery was done by a group at the Lawrence Berkeley National Laboratory (LBNL). A solution was derived similar to the Anderlind model, but with two key differences. First, the definition of the Peclet number is modified slightly to include the effects of the film coefficients. Peclet defines the relation between advection and conduction for a body with air flow, in this case the walls. Using this relationship, LBNL defines what they term a "whole house" Peclet number. The actual definition of this is unclear from the paper. Second, to define how much

of the wall has infiltration, an effective area ratio is used to characterize the wall participation (Buchanan & Sherman, 2000). LBNL argues a portion of a wall that does not have air flow does not contribute towards infiltration heat recovery. This impact is shown through a modification of the Peclet number, originally calculated using the entire wall area. An effective area ratio is introduced to account for the wall with air flow involved in infiltration heat recovery. The remaining portion of the wall is considered to be air tight, therefore does not contribute in infiltration heat recovery. The concept is not analytically based, but it is a potentially effective way to characterize infiltration in a wall.

One challenge with the use of the Claridge and LBNL models is the lack of information available to explain how much diffuse air flow or wall participation occurs typically in a wall. One metric commonly used to characterize air flow through an envelope is the flow exponent from a blower door test, typically performed in a detailed home energy audit. The flow exponent is a beneficial building characteristic that can help define the infiltration paths in order to better estimate infiltration heat recovery. A higher value signifies the building air leakage has increasingly more diffuse characteristics, potentially resulting in more infiltration heat recovery. Controlled indoor and outdoor test cell experiments at Texas A&M University configured with a number of leakage paths are tested to correlate measurements of infiltration heat recovery to flow exponents measured under various leakage paths (Claridge & Bhattacharyaa, 1990) (Claridge & Liu, 1996). Although no clear correlation can yet be established, results show infiltration heat recovery tends to increase with increasing flow exponent.

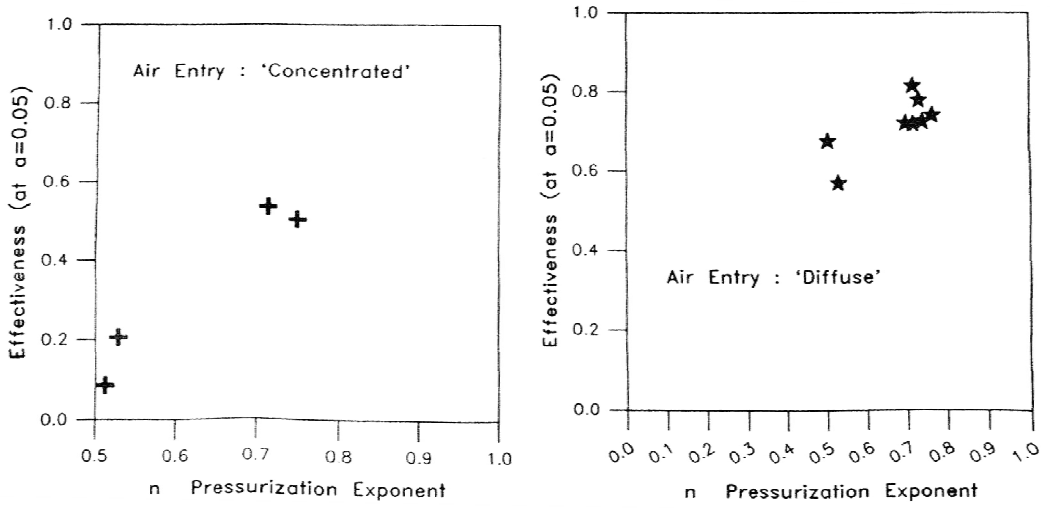

Figure 11: Infiltration heat recovery vs. flow exponent - Source: (Claridge & Bhattacharyaa)

LBNL performs a CFD simulation experiment to gauge what value of effective area ratio is appropriate when analyzing two specific wall configurations (Abadie, Finlayson, & Gadgil, 2002). By correlating the model to results from a CFD experiment, an estimation of the participation factor was found. When a direct leakage path occurs, the models find a 36% participation factor (18% per wall) provides the best correlation to CFD. Similarly, a long leakage path finds a 66% participation factor (33% per wall) works best against CFD. These factors cannot represent all possible cases for a home, but it is a good starting point to estimate IHR. In another study, a field test attempts to measure the wall participation through the use of an infrared camera test to apply the result to the LBNL model. IR photos are taken at the interior surface of a single test home before and during a blower door test of the home. Any areas of the wall found to have a difference in temperature are assumed to be wall area participating in IHR. According to their methods, they conclude very little of the wall (<5%) participates in infiltration heat recovery (Jokisalo, Kurnitski, Korpi, Kalamees, & Vinha, 2009). This method of measurement has never been performed or verified before, but results differ greatly from the previous CFD experiment analysis. The limited information available and varying results make an accurate estimation very difficult to characterize infiltration air flow.

4.2 Literature Summary

From the literature search of infiltration heat recovery, five steady-state heat transfer models have been found that provide a method to feasibly quantify infiltration heat recovery. The author's provide unique considerations in each model that provides a difference in the impact of infiltration heat recovery found. With no recognized method currently available, it is difficult to assess the models' performance. A reference methodology is needed to provide inter-model comparison using a base case infiltration heat recovery definition. This provides a fair comparison when analyzing the results from each model. Since not much is known about the influence of the parameters in each IHR models, analyzing sensitivities studies will be helpful. Previous experiments have been found that can also assess the accuracy of the infiltration heat recovery theory and to better understand each model. Further information about the experimental comparison is provided in a future section.

4.3 Derivation of Temperature within a Wall

As shown in Figure 10, when air flow is introduced, the temperature gradient in a wall deviates from the linear temperature gradient assumed in steady-state heat transfer. The impact on temperature depends largely of the amount of air flow for a given wall. This can be shown when solving for temperature in a wall with conduction and infiltration heat transfer. Under the law of conservation of energy, steady-state analysis assumes there is no energy stored or created within the wall. The temperature derived defines both the conditions of the wall and air assuming local thermal equilibrium (LTE). This allows there to be one solution for temperature. The LTE assumption has been found to make minimal impact in one dimensional analysis (Vafai & Sozen, 1990) (Krarti, 1994). When analyzing the heat flux in a wall from the law of conservation of energy, a second order differential equation is derived that can be used to solve for temperature. The following group of equations highlights how the law of conservation of energy is developed to find temperature and two solutions used by the author's. The details of this derivation and the solution for temperature can be seen in the Appendix, as well as other reports (Anderlind, 1985) (Claridge & Bhattacharyya, 1991) (Buchanan & Sherman, 2000).

$$q_{\text{wall total}} = -k\frac{dT}{dx} - \dot{m}\, C_p\, (T\,(x) - T_{ref}) \quad (1)$$

$$T(x) = T_o + (T_i - T_o)\left(\frac{e^{-Pe\frac{x}{d}} - e^{-Pe}}{1 - e^{-Pe}}\right) \quad (2)$$

$$T(x) = T_o + (T_i - T_o)\left(\frac{Bi_o Bi_i e^{-Pe} - Bi_o Bi_i e^{-Pe\frac{x}{d}} - Bi_i e^{-Pe} Pe}{Bi_o e^{-Pe} + Bi_o Bi_i e^{-Pe} - Bi_o Bi_i - Bi_i e^{-Pe} Pe}\right) \quad (3)$$

4.4 Derivation of Total Heat Transfer

To account for the effects of infiltration heat recovery when solving for the total heat transfer, the derivation for wall temperature shown can be used. This solution couples the conduction and infiltration heat transfer, otherwise typically calculated in summation. Although this interaction causes either infiltration or conduction to increase and the other to decrease through the wall, under steady-state analysis the changes are always mirrored, and any section of the wall will show a constant heat flux (Figure 12). The net impact of IHR provides a predicted total wall heat transfer less than the estimated classical heat transfer. This has the potential to reduce the predicted energy consumption. To derive the total heat load to a space using the infiltration heat recovery model, an energy balance equation for a particular space must be defined to quantify the total heating load.

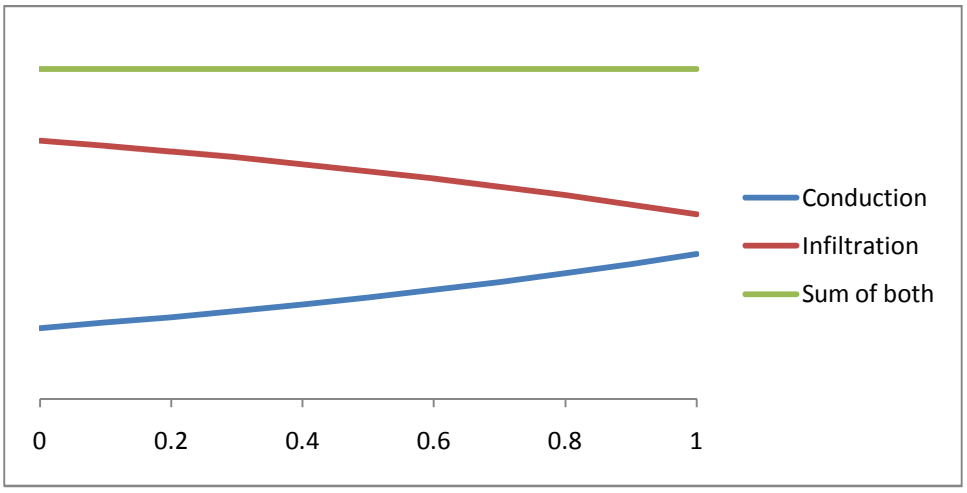

Figure 12: Infiltration heat recovery example: Impact on conduction and infiltration in a cold climate

A simple two-wall model is defined, accounting for conduction and infiltration in the energy balance. Both surfaces have no fenestration and allow one dimensional heat transfer and mass flow. The

top and bottom surfaces of the model are adiabatic. The wall temperature solution derived in the previous section is used to solve for the heat transfer. Flow from inside to outside the space designated as the positive convention. This is important to not because the derived solution assumes conduction and infiltration run in opposite directions, or counter flow. Positive mass and heat flow is assumed when flow goes from the inside to the outside. Conduction is assumed to leave the space in both walls, while air flow is assumed in one wall as infiltration and the other as exfiltration. When both air and heat flow in the same direction, the air flow in the solution must be reversed. To account for this in the heat balance, T(positive air flow) and T^* (negative air flow) is defined. In the wall with exfiltration, the Peclet number becomes negative. The model is shown in Figure 13, and details are provided in the Appendix. To quantify the load to the space, the indoor wall surface is defined as the boundary conditions of the model, where $x = 0$. Evaluating temperature at this position is used to solve for the total space heat load $Q_{recovery}$. Mass flow is assumed to be Darcy-like and of equal quantity, satisfying the mass balance criteria. When solving for the total space load, $Q_{recovery}$, the solution will be different than what is typically used. Details are provided in the Appendix.

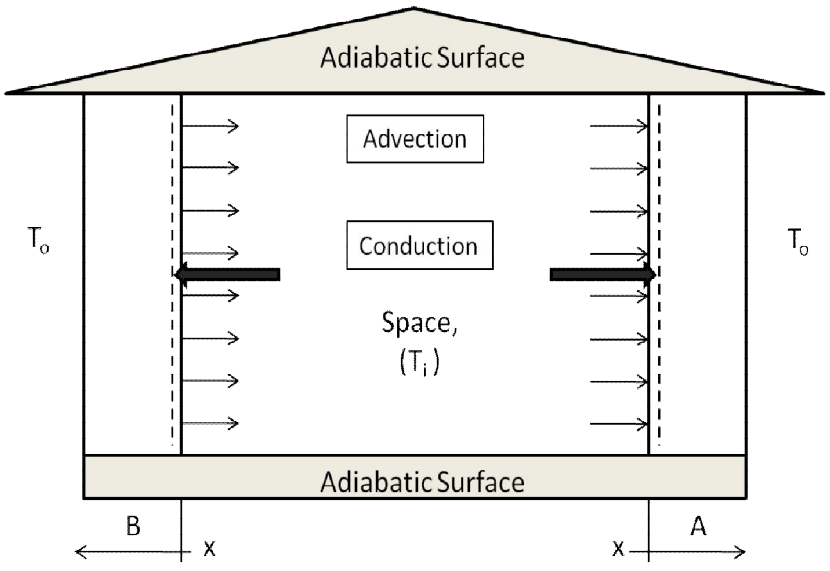

$$\mathrm{Q_{recovery}} = -\frac{\mathrm{A}}{2}\mathrm{k} * \left(\frac{\mathrm{dT}}{\mathrm{dx}_{\mathrm{x=0}}} - \frac{\mathrm{dT^*}}{\mathrm{dx}\ _{\mathrm{x=0}}}\right) + \frac{\mathrm{A\,k\,Pe}}{2\,\mathrm{d}} * (\mathrm{T_{x=0}} - \mathrm{T^*_{x=0}}) \quad (4)$$

$$\mathrm{T\ (x)} = \cdots; (+\mathrm{Pe})$$

$$\mathrm{T^*\ (x)} = \cdots; (-\mathrm{Pe})$$

Figure 13: Simple one-dimensional two-wall infiltration heat recovery model

In the analysis of the space of a simple two-wall model, each wall will be impacted equally when the surface temperature is assumed to equal the air temperature, regardless of the direction in air flow. However, when accounting for convection at the surfaces, the direction of air flow through a wall will have a varying effect on each wall. This can be proven by evaluating the solution for temperature when accounting for the film resistance. Additional derivations show this in the Appendix.

4.5 Infiltration Heat Recovery Factor

By evaluating $Q_{recovery}$, a direct comparison can be made to the classical space heat load, $Q_{classical}$, to understand the potential impact. This demonstrates the reduction in overall heat energy due to infiltration heat recovery. However, when the overall heat transfer becomes coupled, it is difficult to gauge the effect in either conduction or infiltration heat transfer. As already mentioned, conduction and infiltration have inverse effects in the wall. Several of the authors recognized this difficulty in the analysis of infiltration heat recovery, and developed an infiltration heat recovery factor applied only to the infiltration load to better characterize the. The Liu and Krarti models originally do not develop this factor, but in this paper the models are modified to match the efforts of the other authors using the methodology described in the previous sections. To derive the infiltration heat recovery factor, the conduction heat loss is assumed to remain constant. This does not assume conduction heat transfer is unaffected by infiltration heat recovery. Instead, this is used to subtract conduction from $Q_{recovery}$, and the remaining heat transfer is assumed to pertain to the infiltration heat transfer, while containing the effects of IHR in both conduction and infiltration. This allows the impact to be shown as a factor f on the infiltration load through a comparison to the traditional definition of infiltration, and the infiltration heat recovery effect can be quantified.

$$\mathrm{f} = 1 - \frac{\mathrm{Q_{recovery} - Q_{conduction}}}{\dot{\mathrm{m}}\mathrm{C_p}\Delta\mathrm{T}} \tag{5}$$

$$\mathrm{Q_{recovery}} = \mathrm{Q_{conduction}} + (1 - \mathrm{f})\dot{\mathrm{m}}\mathrm{C_p}(\mathrm{T_i} - \mathrm{T_o}) \tag{6}$$

When provided this factor, modifications can be easily made to the envelope calculations without altering the result found when calculating $Q_{recovery}$. But it is important to note conduction does change due to air leakage, as shown in the derivation, but these effects are captured by the infiltration heat recovery factor, and the overall impact is shown as a change in infiltration. A check is provided in the Appendix, highlighting how the assumption of constant conduction heat transfer does not change the impact of the total space heat load affected by infiltration heat recovery.

The infiltration heat recovery factor is the main method in this research used to determine how much recovery is found. This factor is a much easier method to use and assess infiltration heat recovery. Currently each model is derived purely from theory and utilizes ideal heat transfer conditions. Each author provides a unique interpretation of the model that accounts for a particular concept that is believed to better represent the reality of the physics in the building envelope.

4.5.1 Impact of Infiltration Heat Recovery

The potential impact of infiltration heat recovery can be defined as a function of an important dimensionless term called the Peclet number. This number describes the relationship between advection and conduction heat transfer through a body with air flow. In a building application this relation can be defined as a ratio of the infiltration loss coefficient and conduction loss coefficient for the wall area where air flow exists. This derivation can be found in the Appendix.

$$\mathrm{Pe} = \frac{\dot{m}\mathrm{C_p}}{\mathrm{UA}} \tag{7}$$

In theory, the infiltration heat recovery factor will reach a maximum of one as infiltration approaches zero. The more infiltration flows through a wall, the air has increasingly less interaction occurs between the air and wall, causing the IHR factor to drop. The infiltration heat recovery effect will approach zero when infiltration reaches an incredibly large mass flow rate, or when the Peclet approaches infinity. Figure 14 provides the relationship between IHR and Peclet, plotted using Mathematica. Each line represents a different Biot number, defining the ratio of surface convection to wall conduction losses. Details of the Peclet and Biot numbers are provided in the Appendix.

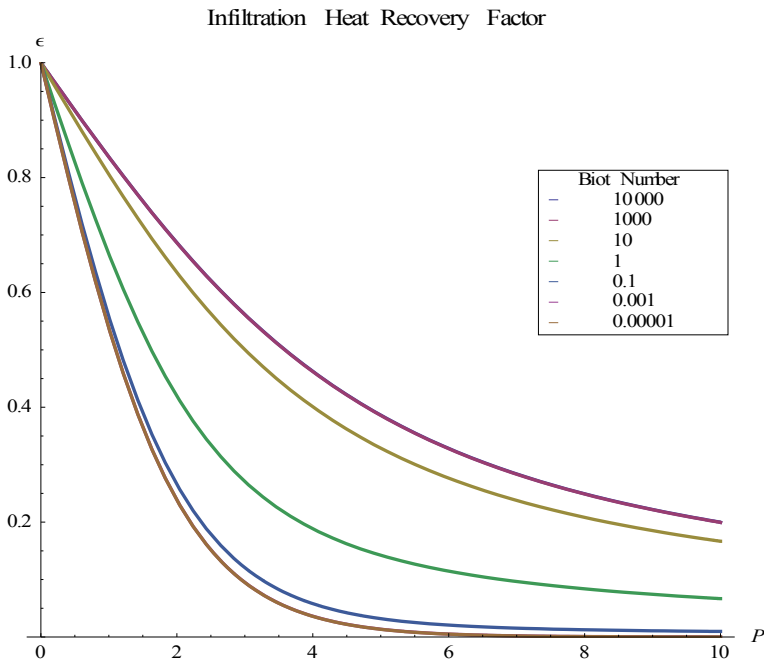

Figure 14: Infiltration heat recovery factor, function of Peclet and Biot numbers

It is important to understand, the overall impact of infiltration heat recovery is only important when a noticeable amount of heat transfer exists. When the IHR factor approaches one, the infiltration load will be very small compared to the conduction load, and the impact will be very minimal in absolute terms. Although the IHR factor will decrease at larger air flow rates, the absolute impact will be greater at higher loads. In theory, the reduction in energy due to infiltration heat recovery can increase until infiltration and conduction are of about the same magnitude load. Once infiltration largely dominates the overall heat transfer in a space, the impact of infiltration heat recovery decreases until the impact is again negligible. A theoretical example is shown in Figure 15, comparing heat transfer with and without IHR, as function of the Peclet number. The effects of heat recovery are insignificant to the overall building load when the Peclet is either very small or very large. The exception is when the wall conduction heat transfer is very small, causing infiltration heat recovery to reach the theoretical maximum of one.

The purple line along the top of Figure 15 represents conditions when the Biot number is very large, or when the surface film resistance is not contributing to the overall heat transfer, and the brown line at the bottom represents conditions when the Biot is very small, or when the film resistance high

enough the wall has very little conduction heat transfer and resembles a super insulated enclosure. The film resistance will impact the air temperature before entering and just after exiting the wall. In a practical building application, the Biot number will range between the order of 1 and 10. The other Biot numbers represent conditions not found for typical residential construction, but the limits are analyzed to test current IHR theory. Details of the analysis at the limits can be found in the Appendix.

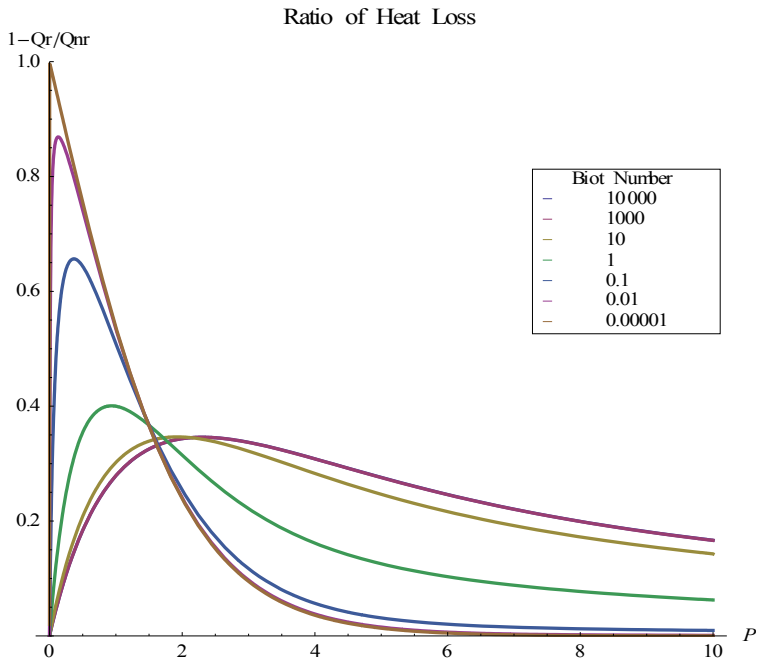

Figure 15: Overall impact of heat load from IHR, as a function of Peclet and Biot numbers

Accounting properly for the Biot number can make an impact on the range of Peclet numbers that show a significant impact of infiltration heat recovery. When the IHR factor is applied to find the overall heat transfer and compared to the traditional heat load, a peak is reached. The effect the film resistances will cause there to be a higher peak in IHR at a lower Peclet number, and eventually the peak becomes one and all heat is recovered instantly, and then afterwards recovery drops as Peclet increases. The smaller the Biot numbers are, the smaller the range of Peclet numbers can be found that define the range where significant heat recovery. Given the range of Biot numbers expected to be found for typical residential wall, the potential impact due to the Biot number is expected to be limited.

5. COMPARATIVE ANALYSIS OF INFILTRATION HEAT RECOVERY MODELS

Four steady state heat transfer models developed by different authors are compared against a fifth reference model to determine what similarities and differences exist in each model. Currently there is no accepted model, so the earliest analytical solution (Anderlind, 1985) is selected to be the reference. All other models are adjusted to ensure a fair comparison to the reference model.

Each author's research is scrutinized to understand the shortcomings and improvements that exist in relation to the reference model. In this section, the models undergo sensitivity studies of key parameters to determine their influence on infiltration heat recovery. Through this analysis, a characterization of IHR can be made to find which variables influence IHR the most. In addition, the Peclet number is a common variable found in each model; a sensitivity study of this variable will compare model trends for IHR. The common variable used in each model is the Peclet number. An additional sensitivity study of the Peclet number will compare model trends for infiltration heat recovery.

Each model is presented using the same terminology to facilitate analysis. The general methodology can be seen in the previous section. The first two sections provide a short description of the assumptions and analysis methodology that is done for each model. Afterward, a short description of each model provides the key points and assumptions, as well as results, are provided for comparison against the reference model.

5.1 Steady-State IHR Model Assumptions

For each model, steady-state heat transfer analysis is assumed for the space, with no energy storage or generation. The walls are assumed to be at local thermal equilibrium, meaning at any position in the wall at any time the temperature of air and solid are the same. This is a common assumption that allows temperature to define both wall and the air temperature for each model. Air flow is assumed to be constant through the wall section, and all air flow is assumed to follow Darcy's law.

The models all derive an infiltration heat recovery factor that is applied to the infiltration load. Conduction heat transfer is assumed to remain unchanged to simplify the analysis. Although this does not represent the building physics, mathematically this factor, named f, would account for changes for both infiltration and conduction. The infiltration heat recovery factor from each model is applied to find the new infiltration is the same manner.

$$\mathrm{Q}_{\text{new infiltration}} = (1 - f)\dot{\mathrm{m}}\mathrm{C}_{\mathrm{p}}\Delta\mathrm{T} \tag{8}$$

5.2 Comparative Model Analysis Methodology

Each model uses a similar methodology to derive the infiltration heat recovery factor. The common factor that drives each model is the Peclet number. This ratio of infiltration and conduction heat transfer is critical in understanding the potential heat recovery occurring within building walls. When conduction is assumed constant for a given home, the Peclet number becomes an indicator of how much infiltration exists. One metric used to calculate infiltration is the air changes per hour. This can be used in sensitivity analysis of each infiltration heat recovery model. As air infiltration increases, Peclet will increase, causing the infiltration heat recovery factor to reduce. This trend is expected to be present in each selected model.

In addition to the Peclet, most of the authors introduce a parameter into their model to provide improvements in how to better quantify infiltration heat recovery. The reference model derived from theory assumed air flow is ideally diffuse through the wall, meaning the entire wall area has infiltration equally distributed. However, infiltration heat recovery for a typical residential envelope rarely exhibits those conditions, and each model introduces concept to account for this. Sensitivity of the factors included in each model help understand the importance of characteristics in the building envelope.

Table 6: Summary of IHR simple test case model home

Home Test Case	Brief Description	UA (rounded)	Units
Cond. Area	1200 sq. ft., 40'x30'		
Overall Ceiling UA	Equiv. R-10 assembly	120	Btu/hr-°F
Overall Wall UA	Equiv. R-7 assembly	140.8	Btu/hr-°F
Window UA	Single Pane, 12% WWR	117	Btu/hr-°F
Foundation	Uninsulated slab	169	Btu/hr-°F
Infiltration	1 ACH	120	Btu/hr-°F
Total House UA		667	
Peclet Number	Infiltration divided by Wall+Ceiling UA	0.85	None

5.3 Reference Model - (Anderlind, 1985)

This model from Europe is the earliest published analytical work known examining the influence of air flow on the total heat transfer of insulation. In this paper, to test the effect of IHR to a space a simplified two wall model was used. First, using the law of conservation of energy, the temperature of both the air and wall must be found under steady state conditions. The temperature allows coupling to occur between conduction and infiltration, allowing for the total heat transfer to be found. The effects of the film resistance are assumed negligible. Lastly, the conduction term is subtracted and the remainder is considered to be losses due only to air infiltration. This is used to find the heat recovery factor by comparing the solution to the classical infiltration loss calculation.

$$T(x) = T_e + (T_i - T_e)\left(\frac{e^{\frac{-Pe}{d}x} - e^{-Pe}}{1 - e^{-Pe}}\right)$$

$$f = \frac{2}{Pe} - \frac{2}{e^{Pe} - 1} \tag{8}$$

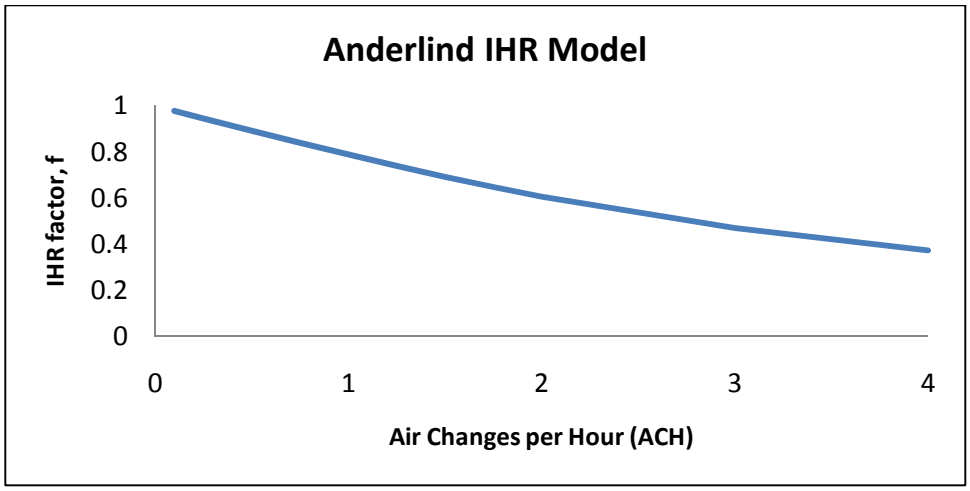

Figure 16: Sensitivity study of Anderlind model

5.4 Claridge Model - (Claridge & Bhattacharyya, 1991)

The Claridge model begins by using the same methodology as the reference model. However the key difference is the definition of the infiltration heat recovery factor. Claridge recognizes there are two main paths for air flow, diffuse and concentrated. Diffuse describes the passage of air through the walls and other porous wall components. Concentrated defines the air passing through door frames, window frames, and other edges and direct leakage paths. Concentrated air leakage is assumed to have no impact on infiltration heat recovery, and is not included when analyzing infiltration heat recovery. This model considers only the diffuse air flow to be involved in infiltration heat recovery.

$$f = \frac{2}{\mathrm{Pe}} - \frac{1-\mathrm{X}_{\mathrm{concentrated\,A}}}{\mathrm{e}^{\left(1-\mathrm{X}_{\mathrm{concentrated\,A}}\right)\mathrm{Pe}}-1} - \frac{1-\mathrm{X}_{\mathrm{concentrated\,B}}}{\mathrm{e}^{\left(1-\mathrm{X}_{\mathrm{concentrated\,B}}\right)\mathrm{Pe}}-1} \tag{9}$$

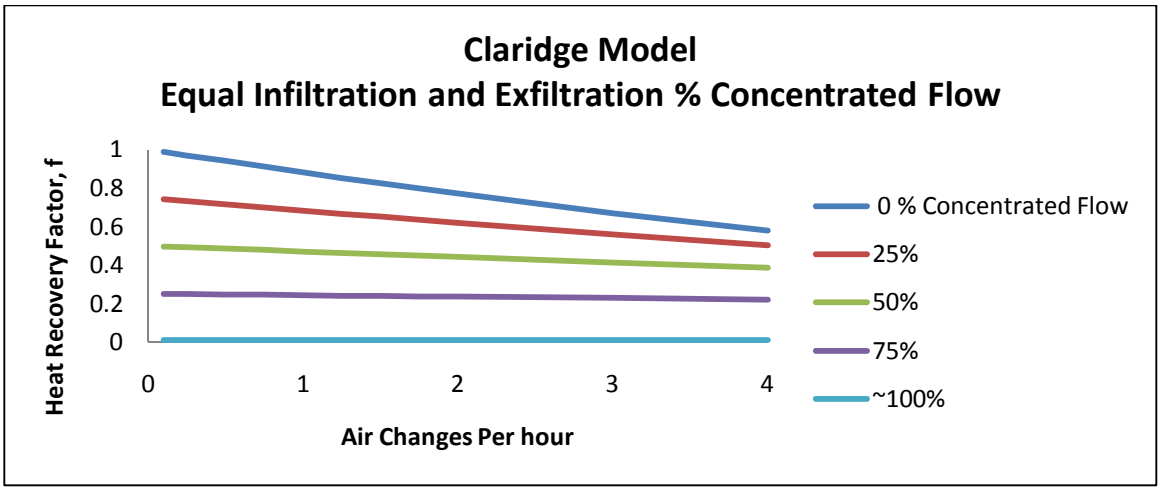

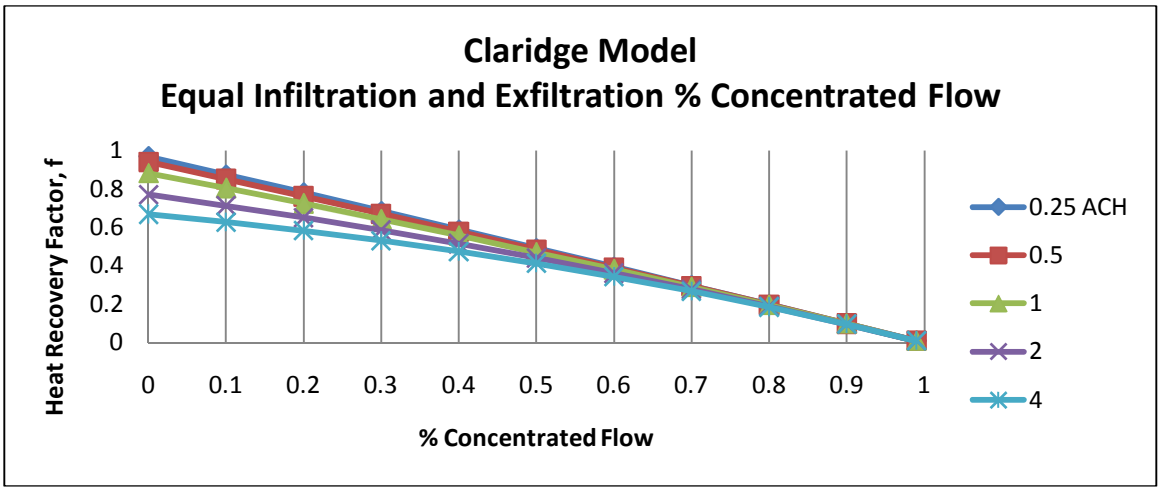

Figure 17: Sensitivity study of Claridge model

5.5 Liu Model - (Liu M. , 1992)

Liu approached this problem considering the effect of solar gains on infiltration heat recovery. Solar heat transfer is thought to amplify its effect through a change in exterior surface air temperature. In the author's model, solar gains are incorporated simply in summation of the classical load calculation. However, solar is not used in the model to derive the coupled heat transfer accounting for IHR. The classical load is used to quantify, through comparison, the effect of infiltration heat recovery. If solar gains are removed from the Liu model, the resulting solution becomes identical to the Anderlind reference model, shown in Equation 2. Liu's model originally provides analysis for a single wall, but the model is modified for analysis of a simple two wall space model for comparison against the reference model. Refer to the Anderlind derivation in the Appendix.

5.6 Krarti Model - (Krarti, 1994)

Krarti diverts from the reference model and states air infiltration enters the wall at the surface temperature, rather than the ambient temperature. This adds another important variable in determining the heat recovery factor, the convection coefficient. The temperature profile within the wall is dependent on the Biot number, in addition to the Peclet number. Originally the author's method to quantify IHR did not provide the best comparison to the reference model. Using the findings in his paper of the wall temperature profile when accounting for the surface temperature, the IHR model is derived again using the methodology previously described at the beginning of this section. The final heat recovery factor becomes a much lengthier derivation. Refer to the Appendix for details of this derivation.

$$T(x) = T_{e,a} + \left(T_{i,a} - T_{e,a}\right)\left\{\frac{Bi_i Bi_o e^{Pe} - Bi_i Bi_o e^{Pe\frac{x}{d}} + Bi_i Pe e^{Pe}}{Bi_o e^{Pe} + Bi_i Bi_o e^{Pe} - Bi_i Bi_o + Bi_i Pe e^{Pe}}\right\}$$

$$f = 1 - Bi_i Bi_o \frac{Pe\left(Bi_o\left(1+e^{2Pe}\right)+Pe\left(e^{2Pe}-1\right)\right)+Bi_i\left(Bi_o\left(e^{2Pe}-1\right)+Pe\left(e^{2Pe}+1\right)\right)}{\left(Bi_o e^{Pe}Pe+Bi_i\left(Bi_o\left(e^{Pe}-1\right)+Pe\right)\right)\left(Bi_o Pe+Bi_i\left(Bi_o\left(e^{Pe}-1\right)+e^{Pe}Pe\right)\right)} + \frac{2}{Pe\left(1+\frac{1}{Bi_i}+\frac{1}{Bi_o}\right)} \quad (10)$$

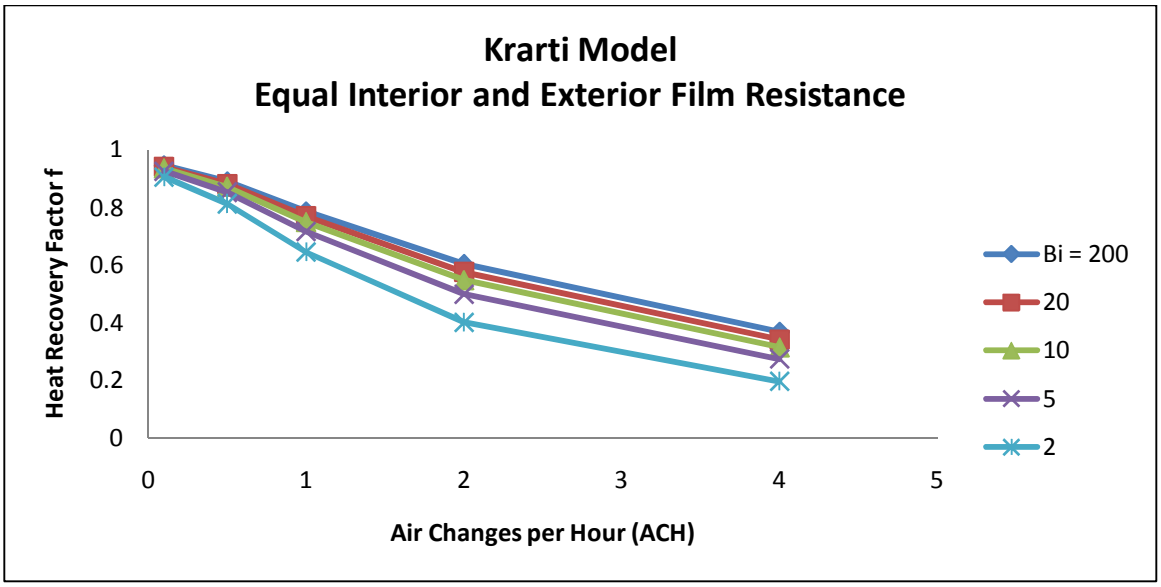

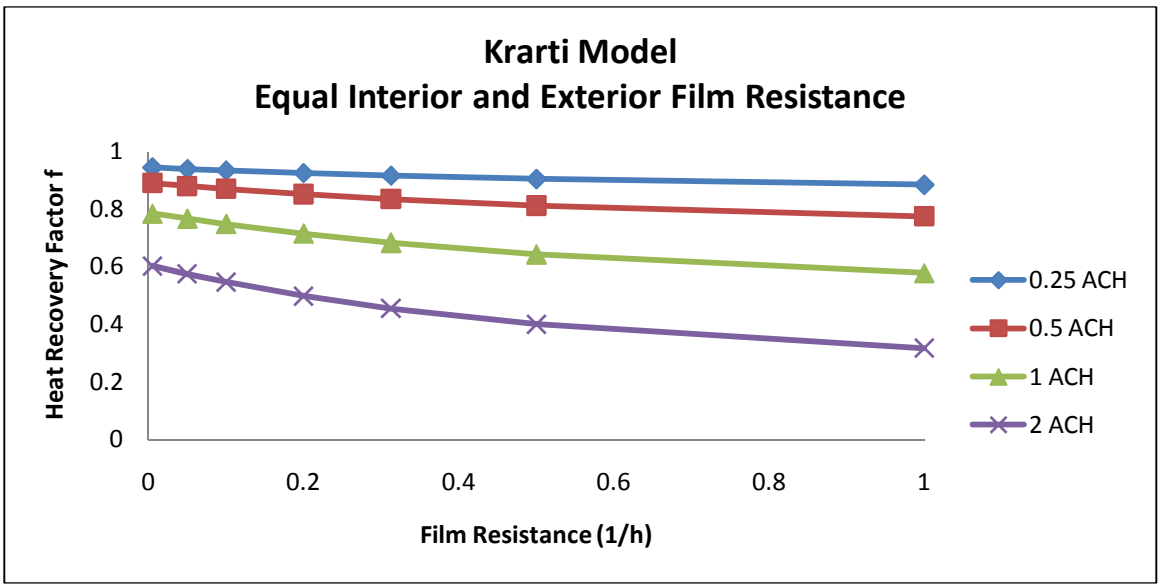

Figure 18: Sensitivity study of Krarti model

5.7 LBNL Model - (Buchanan & Sherman, 2000)

The LBNL model uses a slightly different heat balance method, yet reaches a similar model to Claridge and Anderlind. The key differences are in the definition of the Peclet number and the introduction of a wall participation factor. The author defines a Peclet for a single wall versus the entire wall area. The author argues air leakage may not occur in a portion of the wall; therefore a portion of the conduction losses are not impacted by infiltration. This causes the infiltration heat recovery effect to diminish as participation factor decreases. The effective Peclet number will increase due to decreased effective conduction loss coefficient. However, the use of a wall participation factor has not been proven analytically and has no supporting research to determine how much of the wall is interacting with air leakage. The figures show a strong dependence on this factor.

$$f = \frac{j_{inf}+j_{exf}}{Pe} - \frac{1}{\frac{Pe}{e^{j_{inf}}-1}} - \frac{1}{\frac{Pe}{e^{j_{exf}}-1}} \tag{11}$$

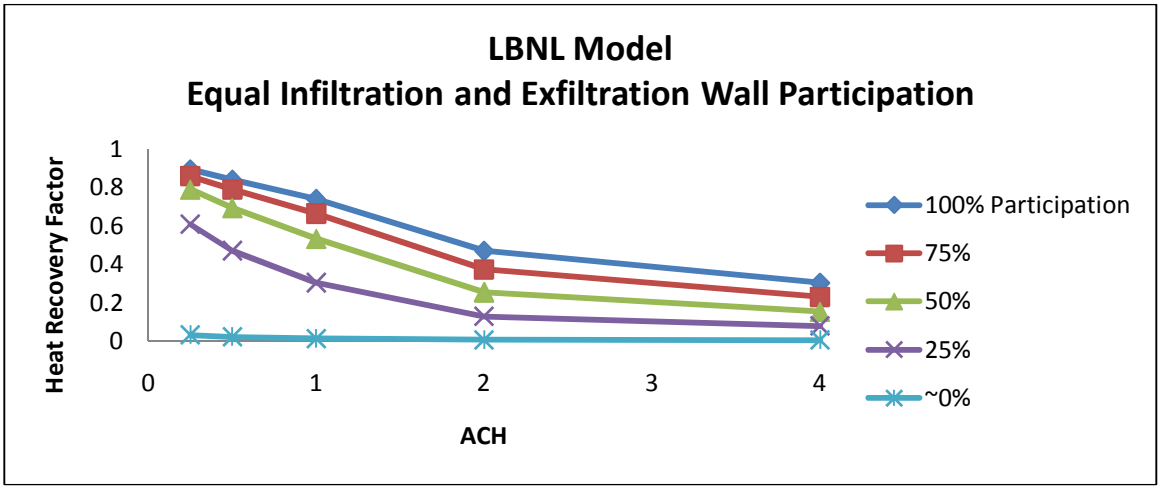

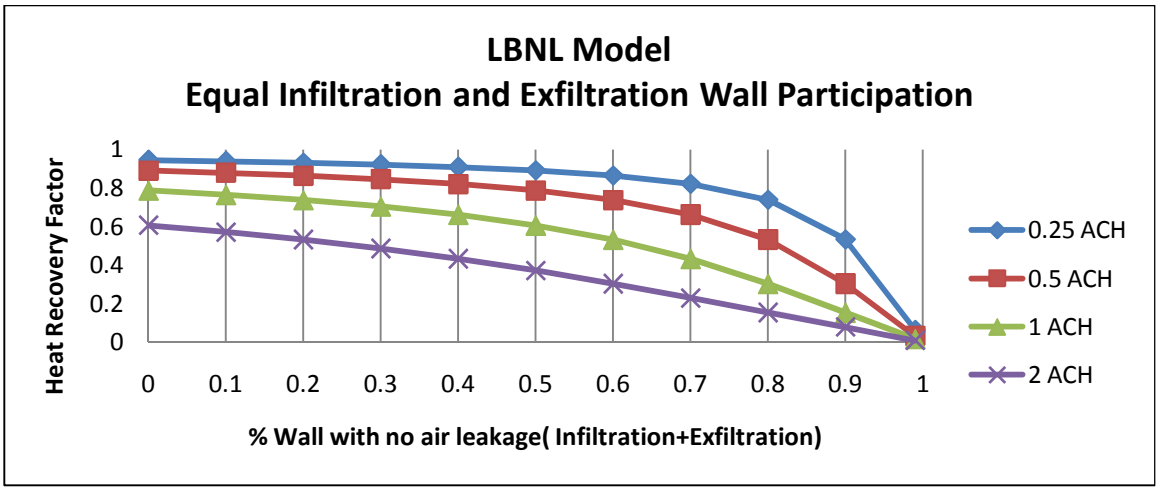

Figure 19: Sensitivity study of LBNL model

5.8 Summary

Each model contributes a unique characteristic to help calculate IHR for a typical wall. This comparison analyzes each model's performance in calculating IHR. As mentioned before, each model must be compared to find if any model is more appropriate analytically. Table 7 provides sample results at two infiltration rates for the test case home. Analysis at the original model and reference model conditions is done, and results show although each model provides different results, the models will provide the same result when assuming typical wall conditions.

Afterwards, the results from each model can be tested against experimental infiltration heat recovery data to provide an indication of which model can perform better. Finally, a set of home annual energy simulations is done with EnergyPlus with and without the IHR model implemented. After comparing the impact on energy consumption, the results from simulation are compared to energy audit data by comparing the thermal envelope performance found from using the construction details and utility data. This way of measured and simulated infiltration heat recovery can be found. Figure 20 and Figure 21 show the trends calculated from specific air flow rates, and illustrate how each model overlaps when analyzed under Anderlind conditions.

Table 7: Model results for test home, at original and reference conditions

Model	Limits applied to compare results to Anderlind model	Heat Recovery factor			
		(0.25 ACH) Peclet = 0.21		(1 ACH) Peclet = 0.85	
		Original	Corrected	Original	Corrected
Anderlind	-	0.946	-	0.859	-
Claridge	There is 100% diffuse flow, no concentrated flow.	0.716	0.946	0.668	0.859
Liu	Remove solar heat transfer from heat balance. Adjust convention	-	0.946	-	0.859
Krarti	The Biot is very large, meaning the film resistance is negligible.	0.931	0.946	0.824	0.859
LBNL	There 100% wall participation in the model. The Peclet defined is different than the other models. To correct, a factor of 0.5 is applied.	0.893	0.946	0.729	0.859

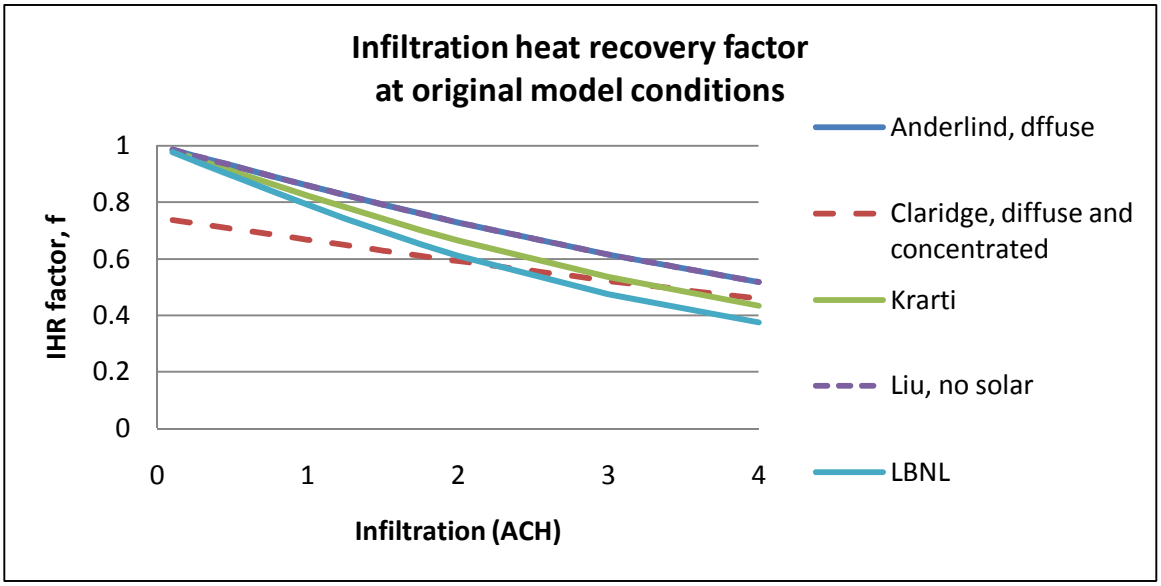

Figure 20: Infiltration heat recovery at original model conditions

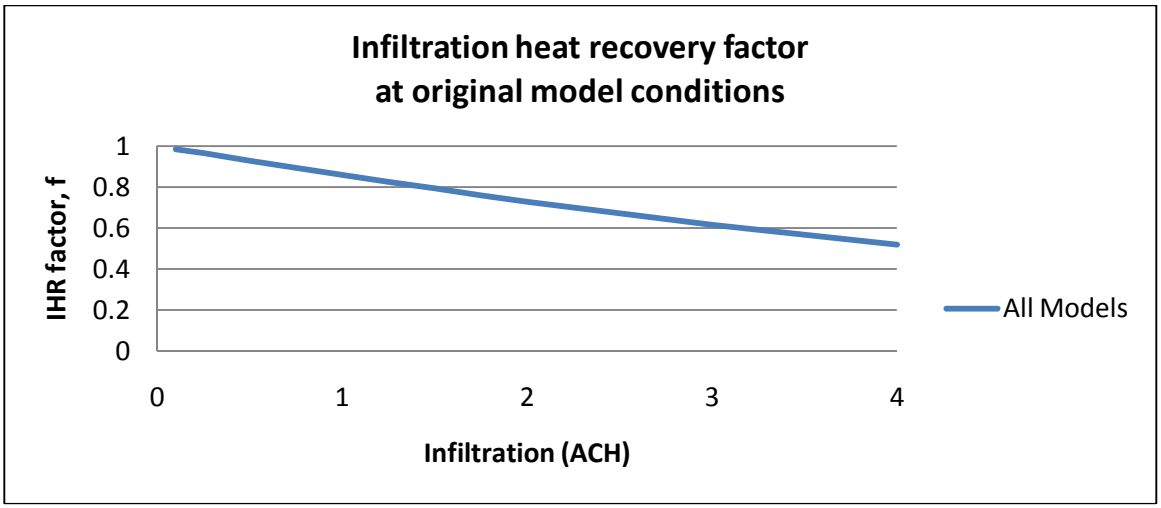

Figure 21: Infiltration heat recovery under reference conditions

Table 8 provides a draft summary of the findings used for each model. A brief description of the improvements relative to the reference is shown along with potential shortcomings and improvements of each model.

Table 8: Model conclusions

Model	Improvements to reference model	Shortcomings
Claridge	The use of diffuse and concentrated air leakage allows the models to specify the type of air flow that exists for a particular house. Currently the flow exponent from blower door testing provides that information, and it the two could be integrated.	The model assumes the surfaces have negligible effect on the heat transfer of the wall, similar to Anderlind. Also, all diffuse air flow is assumed to flow uniformly over 100% of the wall area.
Liu	The introduction of solar to the heat balance causes IHR behavior to be amplified or negated. The temperature of the air can be greatly affecting the impact of IHR.	Solar heat transfer is only an additive load; it is not coupled into simulation. Accurate solar modeling would be needed, because the effect of solar is largely influenced by the season.
Krarti	The film resistance is shown to make an impact on the air temperature not defined in other models. This allows the coupling to be more accurately portrayed for the walls of homes. Walls with little insulation are more sensitive to the effects of the surfaces films.	A similar mathematical form to portray heat recovery has not yet been achieved using this derivation. The model does not follow the same methodology as used by Anderlind. No adjustment for air flow type or participation exists.
LBNL	The model attempts to account for walls that only have portion contributing to infiltration heat recovery. This reduction in conduction loss coefficient is an important effect to consider. Also, the Peclet calculation uses film resistances of the walls.	All the air flowing through the wall is all assumed to diffuse. The use of the wall participation factor is an arbitrary factor created for the model. There is no justification in the use of this factor, either experimentally or analytically.

6. EXPERIMENTAL ANALYSIS OF IHR MODELS

Past infiltration heat recovery research has accomplished much to quantify the interaction between air flow and wall performance that impact the predictions in traditional heat load calculations. Much of this research has been pursued either analytical or experimental; however, there is very little overlap between IHR theory and experimental work. This is a beneficial and necessary bridge to gap to apply theory to reality. Never has this type of analysis been known to be performed, and findings can help indicate what developments are needed to more accurately quantify infiltration heat recovery.

The analytical models evaluated in this study are compared against experimental measurements from a past research project at the University of Alberta (Ackerman, Bailey, Dale, & Wilson, 2004). Data from the experiment is used to compare the measured heat loss to the classical method to assess the impact of infiltration heat recovery. The models are applied in a similar method by estimating $Q_{recovery}$ and $Q_{classical}$. The results of this ratio are compared to the experiment. This analysis allows the models' abilities to be tested against an experiment measuring the effects of infiltration heat recovery on the overall heat transfer found in a typical wall.

6.1 Experiment: ASHRAE RP-1169 – Infiltration Heat Recovery

In 2004, a group at the University of Alberta was given the task of investigating IHR in a research project granted by the American Society of Heating, Refrigerating, and Air-Conditioning Engineers (ASHRAE). The experiment was intended to determine the effective impact on the envelope performance when accounting for air flow through a simplified residential wood frame wall test panel. Two identical test panels were built, consisting of identical 2x4" wood frame construction with fiberglass insulation, plywood, and gypsum. Each panel is provided with a specific entry and exit point through the gypsum and plywood for air to flow through the test panel insulation. Test Panel 1 is configured with a short air leakage path directly through the center of the test panel. Test Panel 2 tests a long air leakage path, shown

in Figure 22. The gypsum board has a slit opening at the very bottom of the panel along the entire width of the panel. A similar opening is created for the plywood surface, but at the very top of the panel.

Figure 22: ASHRAE RP-1169 experiment setup. Source: (Ackerman, Bailey, Dale, & Wilson)

6.2 AHRAE RP-1169 Experimental Measurements

Using a data acquisition system, hourly air flow and temperature measurements were taken to find the overall thermal performance of the test panels (Figure 22). The tests varied in duration from one to three days. Temperature measurements of the wall were taken to find the effects of air flow when a mass flow rate was introduced into the test panels. The mass flow was maintained constant for four hours to ensure constant temperature and mass flow and simulate steady-state conditions. The measurements taken every four hours were used in the experimental comparison against steady-state models.

Each test panel is fully instrumented with thermocouples to measure temperature at the wall surface and within the insulation to find the impact of air. Thermocouple measurements capture the temperature of the air at the entry and exit points of each test panel to provide the change in the air temperature when interacting with the insulation. Air flow was controlled through the use of a mass flow meter connected to the data acquisition system. The air flow measurements were taken before entering the test panel. The quantities of air flow used in the experiment were very small, never exceeding 1 cubic foot

per minute. Provided in the report are the heat transfer calculations for total heat loss with and without accounting for IHR. Constant thermal properties for both the wall and air are assumed. This ratio is analyzed and compared against the predicted effects of the infiltration heat recovery models.

6.3 Uncertainty Analysis

Uncertainty analysis was not provided in the report, and although the report indicates the experiment was well instrumented, the possible discrepancy from measurement is needed to provide meaningful results. The report only provides general information about the thermocouples and mass flow meter in the experiment. No information on the data acquisition system was provided, but the errors for the system are considered negligible. Due to the number of temperature measurements used to calculate heat transfer, and in addition the mass flow heat transfer, it is assumed that only instrumental error will cause uncertainty in the analysis.

The objective from the measurements was to find the amount of heat recovery for a given amount of air and compare the total heat transfer found with recovery against the heat transfer typically calculated. The formula above needs to undergo uncertainty analysis using a well established method (Kline & McClintock, 1953), considering all measurements of temperature and air flow. The only uncertainty assumed to exist is the experimental instrument uncertainty. Uncertainty will be measured from every thermocouple measurement of the wall and air temperature. The thermocouple and mass flow meter are assumed to have a typical error +/- 0.5 °C and 5%, respectively. The uncertainty will be largely influenced by temperature due to the number of thermocouples used in the experiment. To find the overall uncertainty of an experiment using multiple variables, the following equations are used with respect to heat ratio analyzed (Holman, 2007). Details of the derivation and results from the uncertainty analysis are shown in the Appendix.

$$\omega = \sqrt{(\omega_{\text{random}}^2 = 0) + \omega_{\text{instrument}}^2 + (\omega_{\text{calibration}}^2 = 0)} \quad (12)$$

$$\omega_r = \sqrt{\left(\omega_{T_{g1}} \frac{dr}{dT_{g_1}}\right)^2 + \left(\omega_{T_{g2}} \frac{dr}{dT_{g2}}\right)^2 + \left(\omega_{T_{room}} \frac{dr}{dT_{room}}\right)^2 + \left(\omega_{T_{air\ exit}} \frac{dr}{dT_{air\ exit}}\right)^2 + \left(\omega_{\dot{m}} \frac{dr}{d\dot{m}}\right)^2} \quad (13)$$

6.4 Heat Loss Methodology

Hourly heat transfer was calculated in the experiments using the temperature measurements. Thermal properties of each wall material are maintained constant throughout each experiment to isolate on the influence air flow has on the temperature profile.

To understand the impact of infiltration heat recovery, a ratio of the total heat transfer is taken with and without accounting for infiltration heat recovery. The methods used in the experiment do not assess infiltration heat recovery as a factor used to modify infiltration, as has been shown in the previous models. Therefore for a fair comparison between model and experiment, the same ratio is derived using each infiltration heat recovery model to find the total coupled heat transfer. With this a ratio similar to that found in each experiment can be compared. Below both the experimental formula from the report and general model formula is shown.

Experiment

$$r = \frac{Q_{recovery}}{Q_{no\ recovery}} = \frac{\Sigma(U_{gypsum})A_{panel}\,(\Delta T_{gypsum}) + \dot{m}C_p(T_{room} - T_{air\ exit})}{U_{wall}A_{panel}\,(T_{room} - T_{ambient}) + \dot{m}C_p(T_{room} - T_{ambient})} \quad (14)$$

Model

$$\frac{Q_{recovery}}{Q_{classical}} = \frac{(U_{effective}A_{wall} + (1-f)\dot{m}C_p)(T_{room} - T_{ambient})}{(U_{effective}A_{wall} + \dot{m}C_p)(T_{room} - T_{ambient})} \quad (15)$$

$$\frac{Q_{recovery}}{Q_{classical}} = \frac{\left(1 + (1-f)\frac{\dot{m}C_p}{U_{effective}A_{wall}}\right)}{\left(1 + \frac{\dot{m}C_p}{U_{effective}A_{wall}}\right)} = \frac{(1 + (1-f)Pe)}{(1+Pe)} \quad (16)$$

6.5 Results

The two test panels tested in the experiment provide six cases analyzing the effects of infiltration heat recovery. The results from test panel 1 provided good agreement between measurement and model predictions, in both infiltration exfiltration. In order to achieve this agreement a 20% wall participation factor, j , is assumed to occur in test panel 1 when air flow occurs. To apply the wall participation factor for each model, the Peclet number is adjusted using division to adjust the effective area defining the Peclet number.

$$\frac{\mathrm{Q_{recovery}}}{\mathrm{Q_{classical}}} = \frac{\left(1+(1-f)\frac{\mathrm{Pe}}{j}\right)}{\left(1+\frac{\mathrm{Pe}}{j}\right)} \tag{17}$$

To determine the area of the test panel 1 involved in infiltration heat recovery, a look was taken at the wall temperature measurements with and without air flow. The experiment provides experimental isotherm contours of the test panel with no air flow and with varying amounts of air flow. Cold air entering the test panel will decrease wall temperature, but only in the area affected by the air flow. A clear difference would be seen in the isotherm distribution and the area affected can be measured to find the wall participation factor. Any area that sees a change of more than 1˚ C is used in the measurement. Provided by the report are isotherms measured at air flow rates of 0, 10, 20, and 30 L/min (~1 cfm). In each case, there was a 17%-23% wall participation found, so an average of 20% was chosen to modify the predictions in the models. A sensitivity study of this factor revealed a 15% change in wall participation impacts the model results by less than 1%, signifying accuracy of the factor is not critical when estimating the wall participation from isotherm graphs. Figure 23 highlights an area considered to be involved in infiltration heat recovery through the comparison of the isotherms. Table 9 shows the sensitivity of the heat recovery ratio found under different wall participation factor.

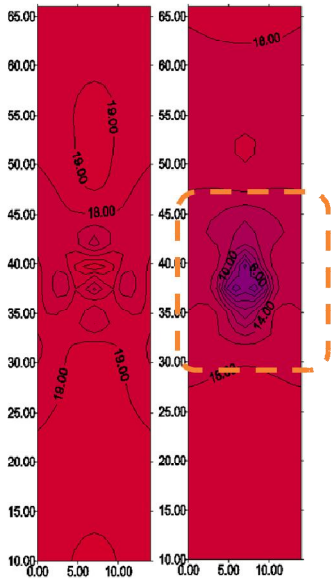

Figure 23: Test panel 1 - wall area influenced by air flow. Source: ASHRAE RP-1169

Table 9: Sensitivity of area correction - test panel 1 results

Anderlind Model			
	Wall Participation		
Peclet	**20%**	**17%**	**23%**
0.00	1.000	1.000 (0%)	1.000 (0%)
0.11	0.991	0.992 (-0.11%)	0.990 (0.11%)
0.35	0.976	0.979 (-0.31%)	0.973 (0.30%)
0.47	0.971	0.975 (-0.39%)	0.967 (0.37%)
0.88	0.956	0.962 (-0.59%)	0.951 (0.56%)
1.00	0.954	0.960 (-0.62%)	0.948 (0.59%)
1.21	0.950	0.956 (0.68%)	0.943 (0.65%)
1.33	0.948	0.954 (0.71%)	0.941 (0.67%)

Krarti Model			
	Wall Participation		
Peclet	**20%**	**17%**	**23%**
0.00	1.000	1.000 (0%)	1.000 (0%)
0.11	0.990	0.991 (-0.13%)	0.988 (0.13%)
0.35	0.973	0.976 (0.36%)	0.970 (0.34%)
0.47	0.967	0.971 (-0.44%)	0.963 (0.42%)
0.88	0.952	0.959 (-0.64%)	0.947 (0.61%)
1.00	0.950	0.956 (-0.68%)	0.944 (0.64%)
1.21	0.946	0.953 (-0.73%)	0.940 (0.69%)
1.33	0.945	0.952 (-0.75%)	0.938 (0.71%)

For the cases performed using test Panel 2 found good agreement as well, but only under infiltration air flow. The exfiltration cases provide very poor agreement to the models. The air flow in case entered the test panel warm, and results were similar regardless of the position which air entered.

Test Panel	Direction of air flow	Panel Configuration	Total tests performed
Direct path air leakage	Warm to Cold Cold to Warm	Air entry and exit at same height	2
Long path air leakage	Warm to Cold Cold to Warm	Air entry high, exit low Air entry low, exit high	4

In this section, three of the six tests are highlighted, two from test panel 1 and one from test panel 2. The comparison of the models to test panel 1 for infiltration and exfiltration cases shows good agreement between the measured experiment and models when the 20% participation factor was used. All model predictions fall within 2% of the experiment. The results from test panel 2, however, show much higher discrepancy, within 10% of the experiments. However, the model comparison to test panel 2 is not a fair comparison because the test is a 2D experiment case and 1D IHR models. However, given the limitations, only the infiltration cases provide reasonable agreement. Measurement from the exfiltration cases finds much less heat recovery. There is little guidance in the experiment to provide an explanation. Further work is needed to explain the difference in warm air infiltration versus cold air infiltration.

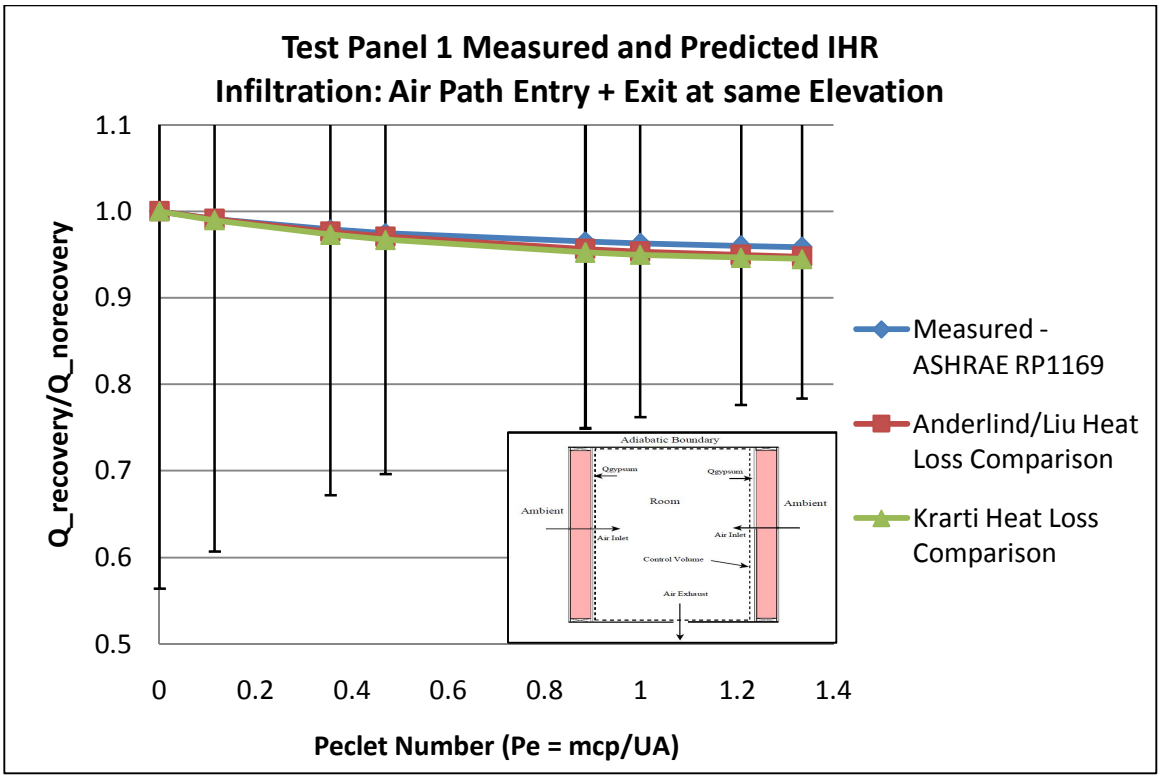

Figure 24: Test panel 1 infiltration case IHR comparison

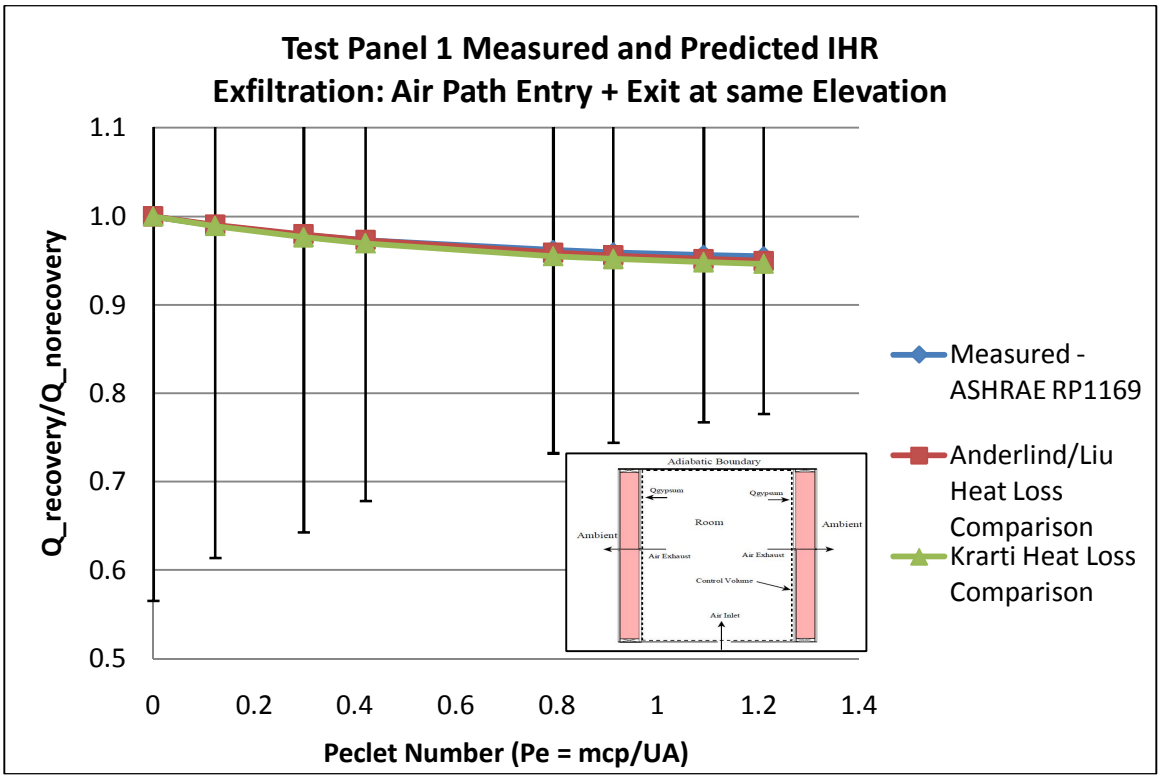

Figure 25: Test panel 1 exfiltration case IHR comparison

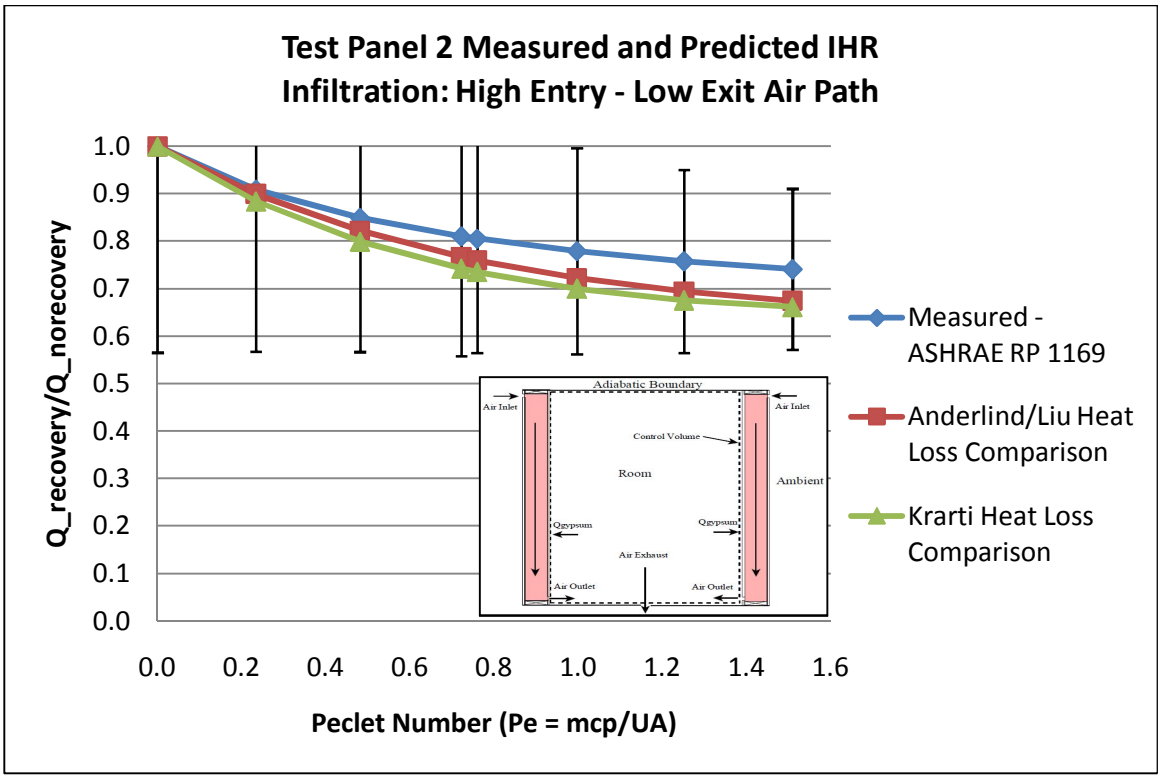

Figure 26: Test panel 2 infiltration case IHR comparison

The experimental uncertainty analysis shows potentially large discrepancy in the measurements. Although the models fall within the error bands displayed in Figure 24, the discrepancy is noticeably large. If the instrumental error was found to be smaller, then the error band would shrink significantly. More information from the experiment is needed to further examine the importance of the instruments' measurement error. Sensitivity of the error in thermocouple measurement is provided in the Appendix.

Out of the five infiltration heat recovery models available, only two models were suitable in the comparison to the experiments. The Anderlind and Krarti solution are the most feasible models to compare against experiment. The derived coupled heat transfer is a solution that can be found in each infiltration heat recovery model. Each model initially finds the total heat transfer assuming ideally diffuse infiltration and exfiltration. Since the test panels only have diffuse air flow occurring, the Claridge model is not applicable for this particular experiment. The LBNL model concept is applied in Test Panel 1 to provide the correlation seen. In general, the Anderlind and Krarti model are more general applications, therefore are the most applicable.

After comparing the two models against the experiments, the Anderlind model appears to provide slightly better correlation to results in the experiments for the cases that showed reasonable agreement. This particular experiment introduces air flow directly into the wall that is conditioned to room temperature just before entering. This relates favorably to the Anderlind model rather than Krarti, because the effects of the film resistance would not be emphasized in this particular experiment. Regardless, given the thermal properties of the wall, the effects in the Krarti model due to the film resistance did not create as great a change to the Anderlind model as anticipated. The air flows introduced to the wall are very low, never reaching more than 1 cfm. The effects on the film resistance will be very minimal in the infiltration heat recovery analysis. If much higher flow rates were tested in the experiments the effects of the film resistance would possibly be more pronounced in the model and experiment.

This experiment concludes the Anderlind model slightly more suitable to predict IHR for this specific experiment. However, the wall participation factor applied in Test Panel 1 indicates the LBNL model can also be important to consider. This reflects the findings from the sensitivity study in Figure 19. The result does not signify the reference model is the most valid solution. This experiment is the currently the best available data on infiltration heat recovery. Although it was able to show reasonable agreement for the two models analyzed, it still does not answer all the questions necessary to validate an infiltration heat recovery model. Additional scrutiny in the uncertainty analysis is needed in future experimental work to help achieve this. The results from the ASHRAE research project are highly dependent upon the accuracy of the measurements. It is possible the error from the instruments is much less than assumed, but limited information is provided by the report and author. Similar experiments in the future would benefit to improve their methods base on this experiment to provide additional answers about infiltration heat recovery.

7. IHR CASE STUDY ANALYSIS AND SIMULATION IMPLEMENTATION

In addition to the experimental comparison, a case study for a sample of home energy audits in Boulder, CO is analyzed to estimate infiltration heat recovery using data gathered at the University of Colorado. Homes in this case study undergo a screening process to minimize errors in the data. Results found from the case study are extracted using methods from previous experiments (Claridge & Bhattacharyaa) (Judkoff, Balcomb, Hancock, Barker, & Subbarao). The results from the case study and the analytical IHR models are compared to understand how close the predictions of the IHR factor are to each other. Afterwards, energy models depicting each home are tested with the IHR models implemented into the EnergyPlus engine to determine the change in energy predictions. The impact found is compared against the results from the case study to determine how close the predictions of heating energy reduction are to each other. Although the models and experimental validation work are not proven methods for infiltration heat recovery prediction, the results from this analysis indicate both possible similarities that exist and also affirm the flaws in this type of analysis. These findings can help in developing better methods to quantify infiltration heat recovery.

7.1 Infiltration Heat Recovery Case Study Sample Pre-Screening Process

The Building Energy Audits course at the University of Colorado-Boulder performed 21 detailed building energy audits as part of the coursework during the fall semester of 2010. Audits were done on a variety of building types. Table 10 provides a summary of the sample size and building types.

Table 10: IHR case study sample summary

Case Study Sampling	
Type of Building	Number of audits
Detached single family homes	10
Apartment/townhome	5
Office space	2
Mixed use building	4
Initial Sampling	21

The sampling of energy audits will be used to measure infiltration heat recovery by comparing the building loss coefficients calculated from utility bill analysis and the building construction. However, the data must be screened in a three step process to help remove energy audits from the case study with insufficient data.

7.1.1 Basic Building Type

First, each building must meet a basic building description to properly perform a detailed building energy audit. If a building is attached or has multiple uses, this will complicate the analysis and should be removed from the data sample.

1. Detached, single use building – A detached building intended for single use is ideal. A property with adjacent attached conditioned spaces causes uncertainty when performing the energy audit. Predicting heat transfer and infiltration loads is very difficult to perform when dealing an adjacent conditioned property rather than the outdoor environment. Blower door testing will only provide limited information. Pressure difference, temperature, and air leakage from the adjacent property make it very difficult to quantify the effects of air leakage.
2. Single zone – A building with a single system is ideal to properly gauge the envelope losses to the space. Multiple systems can complicate the utility bill analysis to find the BLC.
3. Uniform envelope construction – The building must have uniform wall and ceiling construction, built in the same time period. If additions were built to the house, then likely the envelope will be different than the remainder of the house. When calculating building loss coefficient, it is important for the envelope to be uniform, otherwise, the building losses can be skewed towards the area with the lowest thermal performance, and could have an impact on infiltration heat recovery calculations as well.

From the sampling provided, only the single family detached homes meet the criteria above for infiltration heat recovery testing. One property was too large to perform a blower door test, with multiple residents, multiple systems and complex construction. Many of the properties consisted of townhomes,

apartments, and office buildings that have attached adjacent properties. There are also three homes with additions, one as an office, and two as additional rooms intended for renters/visitors. For IHR testing, these properties cause unwanted variations in the building performance, and are removed from IHR testing.

Type of Building	Number of audits
Number of buildings excluded	**11**
Buildings with adjacent property	7
Large multi-story building	1
Buildings with additions	3
Number of buildings remaining	**10**

7.1.2 Quality Detailed Energy Audit Data

Second, after a building meets the basic description needed, a detailed energy audit is performed and must provide three main sources of information.

1. Utility bills - A minimum of one year of monthly utility bills must be provided, showing the energy consumption for the audited building during hot and cold weather. The utility bills must provide the number of days for each bill, along with energy consumed, for both gas and electricity. The utility bill must be solely for the property to ensure all energy is used by the same building. In addition, the number of billed days per bill is needed to determine the average daily load.
2. Blower door test data - A detailed assessment of air leakage in the building must be provided using a blower door. The test must be done at multiple pressure points to find the naturally occurring air changes per hour. The depressurization test is best to correlate the tests to infiltration, but a pressurization test is also useful to understand exfiltration as well. The pressure readings and corresponding flow rates are needed along with the flow exponent and coefficient to analyze the air leakage passing through the envelope. The final results should provide air changes per hour and estimated leakage area.

3. Detailed building envelope description - Lastly, a detailed report on the construction of the house is needed, including wall, windows, attic, and floor construction, and all associated areas. Details about the envelope area will greatly help in the analysis of building loss coefficients. Basic system efficiencies for space heating, cooling, and water use will be needed to estimate the system losses.
4. Cool down test (optional) – Thermal storage is possible in homes with heavy mass. A cool down test can be done to confirm this. Typically performed at night, the house is heated to a target temperature and once reached, the system is turned off. Indoor temperature is recorded over time. The speed at which temperature drops is used to estimate the thermal mass in the house.

Of the remaining homes, three homes provide poor quality data. One audit performs a blower door test, but the data does not provide enough confidence in the results. This is likely due to an incorrect blower door test installation and usage, therefore it the results cannot be used. Two other homes provide monthly energy consumption but fail to report the number of days measured in each bill. The number of billed days is needed to properly perform a utility bill analysis of the home.

Table 11: IHR case study sample filtered

Type of Home	Number of audits
Homes excluded from case study	**3**
Poor quality blower door data	1
Insufficient utility bill data	2
Remaining sample homes	**7**

7.1.3 Minimize Variations in Building Heat Transfer

Third, the remaining homes must meet another set of criteria that minimizes sources of error and variations in heat transfer for the infiltration heat recovery testing. The following criteria will account for system losses and help avoid homes that have high thermal mass to help minimize the impact of heat

transfer from transient loads. This allows for a more reliable BLC calculation. The final sample set possesses each of the following characteristics.

1. Lightweight buildings - To minimize transient effects from thermal storage, low mass buildings are needed. Wood frame homes are suitable. A cool down test can be used to determine the thermal mass of the building. As a rule of thumb, anything less than 40 lb/ft^2 is considered lightweight.
2. No major retrofits during time of utility bills – Retrofits for the envelope, infiltration, or systems will impact the thermal performance of a home. For the utility bills provided, there can be no retrofits done to the house during the period of time billed for energy.
3. Complete characterization of envelope components – A detailed list of all wall, window, ceiling, roof, and foundation constructions is important to calculate the correct effective thermal resistance. Accurate square footage for each surface is important as well.
4. System efficiencies – Overall system efficiency for heating, cooling, and hot water use are needed for the BLC calculations.
5. Blower door test data – A full depressurization test is preferred, but pressurization can be used as an alternative. A recommended 10 readings for pressure and air flow provide an accurate test. Using the LBNL method, the natural ACH, ELA, flow exponent, and leakage coefficient can be found to understand air flows through the envelope. The natural ACH is needed for BLC calculations.
6. Local weather (optional) – In addition to the weather files, conditions during the time of the audit are helpful, especially for the blower door test.

From the remaining homes, the sample is reduced by half. One home has hot water system retrofit during the period of utility bills provided. Two more homes cannot be used because they were found to have a large thermal mass. Four homes remain in the final sample used for the case study. While this may

not provide statistical significance to confirm any trends of infiltration heat recovery, it will provide a good indication of the potential effects that can be found.

Table 12: Final IHR case study home sample size

Type of Home	Number of audits
Homes excluded from case study	**3**
Hot water retrofit	1
High thermal mass	2
Final sample of homes	**4**

7.1.4 Remaining Sources of Discrepancy

The final sample has significantly reduced sources of error. However, there still exist sources of error that are difficult to overcome. The amount of additional work needed to minimize these errors is not practical. Results when estimating infiltration heat recovery will depend on these assumptions; quantifying their effects will require performing sensitivity studies.

1. Envelope framing factor – The envelope's thermal performance is impacted by amount of wood stud used in building structure. Assumptions are made to account for this, but in older homes the framing factor is much more variable due to less stringent building codes at the time.
2. Wall insulation levels – Over time, insulation will shift or deteriorate, affecting the thermal performance. Older homes are more likely to have this problem. The distribution and quality of the insulation, if any, is difficult to quantify when relying only on a visual inspection.
3. Thermostat schedules– Average hourly system operation is needed to estimate the BLC through utility analysis. The occupants' behavior and thermostat control can provide a good estimate. If there is no thermostat setback, the system is assumed operate close to 24 hours. A factor can be used to estimate the impact of a temperature setback. However,

schedules must be assumed. Verifying the thermostat operation time requires time intensive monitoring, not practical for an energy audit.

4. Duct distribution efficiency – For homes with air distribution systems, energy losses can occur through the duct wall by leakage or transmission. Assumptions are made to account for this; actual leakage can be tested with a duct blaster test, but this test is not typically performed in home energy audits.

7.2 Measuring Infiltration Heat Recovery

Four detailed home energy audits provide the information needed to test the effect of infiltration heat recovery on the building load, seen in Table 12. To understand the impact to the overall building performance, the building loss coefficient (BLC) is used. This metric provides an overall assessment of the home's thermal performance. The home audit screening process was designed to minimize errors and assumptions to provide the correct BLC. Similar to the models, the effects of IHR can be applied to the BLC by applying a factor to the measured infiltration load. The equation below defines the predicted BLC as the sum of the envelope losses and infiltration load.

$$\mathrm{BLC}_{\mathrm{predicted}} = \sum \mathrm{UA}_{\mathrm{envelope}} + \dot{m}\mathrm{C}_{\mathrm{p}_{\mathrm{infiltration}}} \quad (18)$$

The utility BLC must be extracted using inverse modeling analysis of the utility bills. There are various methods available to choose from, the most basic method used in this report is the three point model graph to plot the average daily heating consumption for a minimum 12 months of utility bills versus average monthly outdoor temperature (Haberl, Sreshthaputra, Claridge, & Kissock, 2003). Variable base HDD can also be used in lieu of outdoor temperature, with the highest R^2 needed to understand the how energy consumption changes with temperature. This relationship is called the heating slope, a, used to find the measured BLC.

$$\mathrm{BLC_{utility}} = -(a * \eta)/(24 * \mathrm{t}) \quad (19)$$

$$\eta = \text{Heating system efficiency}$$

$$\mathrm{t} = \frac{\mathrm{DH(T_{b,setback})}}{\mathrm{DH(T_b)}} \sim \frac{\mathrm{N_{occ}}}{24} + \left(\frac{24-\mathrm{N_{occ}}}{24} * \frac{\mathrm{T_{b,setback}} - \overline{\mathrm{T}}_{\mathrm{out,winter}}}{\mathrm{T_{b,}} - \overline{\mathrm{T}}_{\mathrm{out,winter}}}\right)$$

If the house does not have a thermostat setback, $t = 1$. If it does, $\mathrm{t} < 1$

The measured infiltration heat recovery can be estimated by using the infiltration heat recovery factor, similar to the models. The results from the case study are calculated in this manner in order to compare to the IHR model results.

$$f = 1 - \frac{\mathrm{BLC_{predicted} - BLC_{measured}}}{\mathrm{BLC_{infiltration}}} \quad (20)$$

$$\%\mathrm{ReductionBLC} = 1 - \frac{\mathrm{BLC_{New,IHR}}}{\mathrm{BLC_{predicted}}} \quad (21)$$

The measured BLC represents the load of the house estimated from inverse modeling. The predicted BLC is estimated based on the energy audit building description. The infiltration BLC is the energy load due to air infiltration based on the blower door test and LBNL infiltration model. Using these variables, the infiltration heat recovery factor is estimated, and the overall reduction of the BLC can be found. A summary of the results from the above calculations can be seen in Table 13.

Table 13: IHR case study results

Audit #	1	2	3	4
Year Built	1999	1964	1995	1960
Stories	2	1	2	2
ACH (LBL) $\frac{1}{hr}$	0.27	0.34	0.50	1.52
Flow Exponent, n	0.65	0.64	0.67	0.54
Peclet Number $\left(\frac{\dot{m}C_p}{UA_{wall}}\right)$	0.34	0.40	1.02	1.46
Measured BLC $\left(\frac{Btu}{hr-F}\right)$	462.3	455.3	520.3	575.1
Predicted BLC $\left(\frac{Btu}{hr-F}\right)$	487.1	499.3	597.7	819.8
Infiltration BLC $\left(\frac{Btu}{hr-F}\right)$	68.1	85.4	144.8	317.1
Estimated IHR factor, f	0.64	0.49	0.47	0.23
New Infiltration BLC $\left(\frac{Btu}{hr-F}\right)$	24.8	48.0	77.4	244.8
New Predicted BLC $\left(\frac{Btu}{hr-F}\right)$	443.8	457.4	530.55	747.4
BLC Reduction (%)	8.9%	8.4%	11.3%	8.8%

As previously discussed, both theory and experiment have shown infiltration heat recovery to increase when the flow rate decreases and when the wall has an increasingly diffuse distribution of air flow. From the case study a similar trend can be seen when plotting the measurements of IHR. Figure 27 and Figure 28 show the relation between the infiltration heat recovery and the Peclet number, as well as blower door leakage exponent. The leakage exponent ranges from 0.5 (concentrated) and 1.0 (diffuse). As flow exponent increases, it is expected diffuse air flow increases, causing IHR to increase (Claridge, Krarti, & Bhattacharyya, 1988). The results in the following figures provide a good indication the expected effects of IHR do occur in reality. Further analysis with additional data is needed to better understand the effects of IHR and determine if any trends exist.

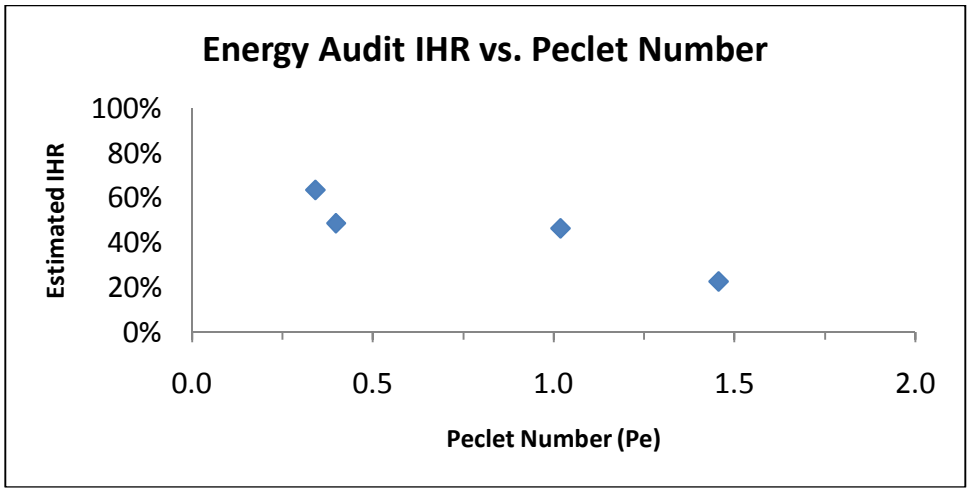

Figure 27: Case study IHR vs. Peclet

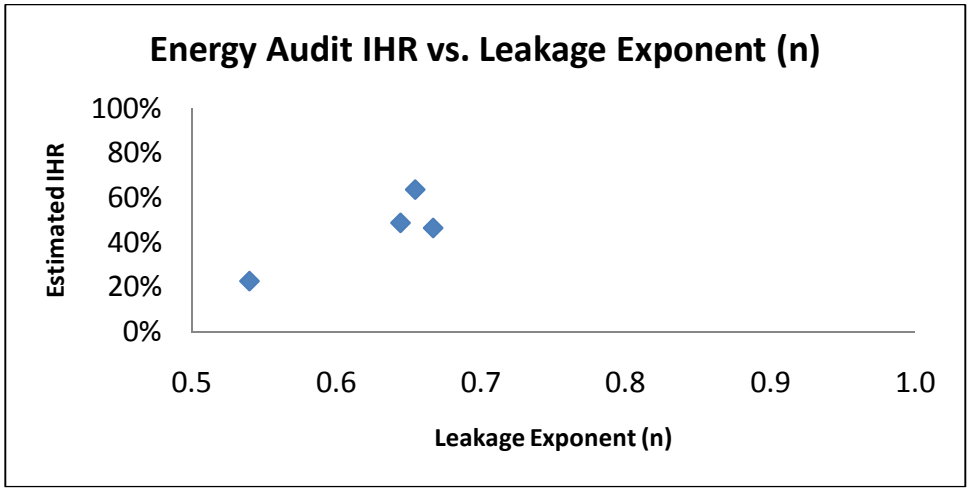

Figure 28: Case study IHR vs. Blower door flow exponent

As explained in Figure 15, despite how the effect of infiltration heat recovery is greatest as infiltration approaches zero, the absolute impact of IHR will increase with infiltration, but once infiltration dominates heat transfer, the effect will reduce. By plotting the impact on BLC with respect to the Peclet, a slight trend can be seen in Figure 29. The effect at greater infiltration rates is shown to decrease and can be seen to find the same impact as other home with lower infiltration. This range of impact found is 8-12%, within the maximum theoretical reduction of 14% (Krarti).

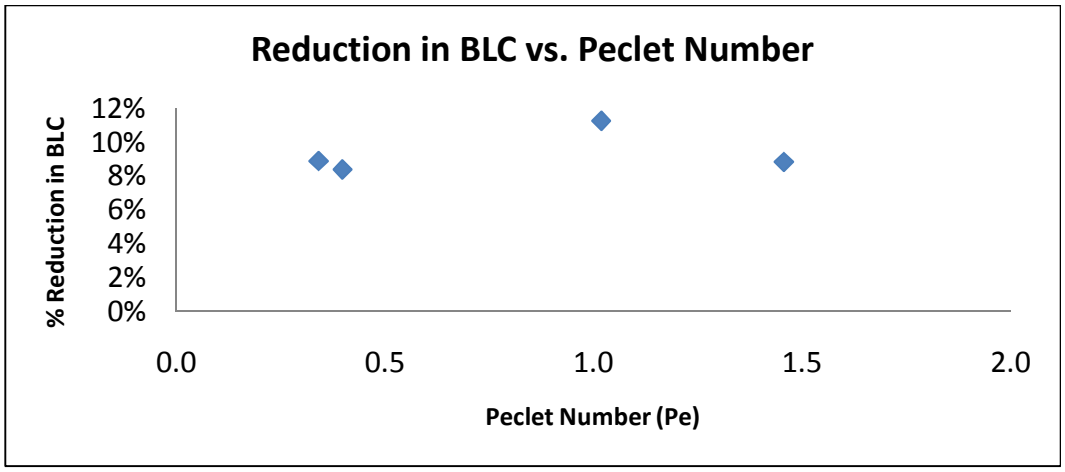

Figure 29: Reduction in BLC vs. Peclet number

7.3 Uncertainty of IHR Measurements

The measurements taken from the case study of energy audits are likely to possess error, and this creates uncertainty in the measurement of BLC and IHR. In order to test the importance of each variable, uncertainty analyses are done from the variables measured and calculated from the energy audit in order to find their importance in the calculation of IHR. All analyses are performed using the program Engineering Equation Solver (EES). The error for each input is assumed in the analysis; the results are normalized by the input error to understand how sensitive each variable is to the measured IHR.

Table 14 provides the results of the analyses. Along the left column listed are the variable(s) tested. Along each row is the input error of the variable pertaining to the measured, predicted, or infiltration BLC calculation. Results of the uncertainty for each BLC calculation is shown as well. Along the right columns is the range uncertainty found on the measured IHR for the homes tested. The uncertainty is normalized by dividing by the input error to test how important the input is in changing the IHR results. Please refer to the Appendix for the details of the calculations.

Table 14: Case study IHR uncertainty analyses

Measured BLC - Utility Bill Inverse Modeling Uncertainty Analysis			
Variable(s)	**Input Error**	**Measured BLC Error**	**Measured IHR Uncertainty:**
Heating System Efficiency	5%	*5%*	39%-54%
Heating slope	5%	*5%*	39%-54%
Combined Utility Sensitivity	**-**	*7%*	**56-79%**

Infiltration BLC Blower Door Test Uncertainty Analysis			
Variable(s)	**Input Error**	**Infiltration BLC Error**	**Measured IHR Uncertainty:**
Wind Speed	10%	*2-5%*	2-5%
Air density	5%	*7.5%*	7.5%
Natural Pressure Difference	5%	*3%*	3%
Indoor+Outdoor Temperature	5%	*4-6%*	4-6%
Blower Door Flow Coefficient and Exponent	5%	*6-7%*	6-7%
Combined Infiltration Sensitivity	**-**	***12%***	**12%**

Predicted BLC Blower Door and Building Description Uncertainty Analysis			
Variable(s)	**Input Error**	**Predicted BLC Error**	**Measured IHR Uncertainty:**
Wind Speed	10%	*0.5-1.4%*	2-5%
Air density	5%	*1-3%*	7.5%
Natural Pressure Difference	5%	*0.5-1.0%*	3%
Indoor+Outdoor Temperature	5%	*0.7-2.4%*	4-6%
Blower Door Flow Coefficient and Exponent	5%	*0.9-2.4%*	6-7%
Combined Infiltration Sensitivity	**-**	***2-5%***	**12%**
Framing factor, wall and ceiling	10%	*0.2-0.6%*	2-7%
Area of Walls, Windows, Doors, and Ceiling	5%	*0.6-1.6%*	7-20%
U-value of wall, window door, and ceiling; at cavity and stud	5%	*2-6%*	7-23%
Overall Foundation loss coefficient	5%	*0.6-1.5%*	6-18%
Combined Envelope Sensitivity	**-**	***1.5-3%***	**18-36%**

Measured IHR Uncertainty analysis of all input error associated with BLC calculations			
Variable(s)	**Input Error**	**Measured IHR Uncertainty:**	**Ratio of Uncertainty to Input Error**
Heating System Efficiency	5%	39%-54%	7.8-10.8
Heating slope	5%	39%-54%	7.8-10.8
Combined Utility Sensitivity	**-**	**56-79%**	**8-11.3**
Wind Speed	10%	2-5%	0.2-0.5
Air density	5%	7.5%	1.5
Natural Pressure Difference	5%	3%	0.6
Indoor+Outdoor Temperature	5%	4-6%	0.8-1.2
Blower Door Flow Coefficient and Exponent	5%	6-7%	1.2-1.4
Combined Infiltration Sensitivity	**-**	**12%**	**2.4 – 6.1**
Framing factor, wall and ceiling	10%	2-7%	0.2-0.7
Area of Walls, Windows, Doors, and Ceiling	5%	7-20%	1.4-4
U-value of wall, window door, and ceiling; at cavity and stud	5%	7-23%	1.4-4.6
Overall Foundation loss coefficient	5%	6-18%	1.2-3.6
Combined Envelope Sensitivity	**-**	**18-36%**	**12**

The objective is to understand how great the estimated IHR can vary in the case study.

Table 14 shows IHR to be the most sensitivity to utility bill inverse modeling, followed by the envelope inputs and blower door test. The results shown are dependent on the 5-10% input error assumed to exist in each of the variables measured. This assessment is arbitrary unless the correct input error is found for each variable. As an alternative, an analytical approach is needed to understand how uncertainty in IHR changes with respect to the variable input error. This requires additional mathematical analysis to provide a solution, outside the scope of this thesis. The analysis shown is good starting point, and further pursuit of uncertainty is recommended.

7.4 Implementing Infiltration Heat Recovery into EnergyPlus

Currently, building simulation tools do not account for IHR, and are thought to over predict heat transfer through the envelope of a building. Comparisons between typical design loads and actual loads accounting for IHR reveal a difference in the calculations. However, accounting for this using a model in EnergyPlus has not been previously documented.

To implement a model into EnergyPlus, analysis of the past IHR work was needed to establish a sound set of equations. The sensitivity analyses show the importance of the parameters in each model. The models can be feasible added into EnergyPlus. The measurements of IHR from the case study are helpful to test the performance of the model and improvement seen in predicted energy consumption. Testing and analysis will be presented with a comparison of EnergyPlus with and without the IHR models to identify any changes seen in energy predictions. The objective in this study is to find a solution that can help reduce discrepancy in energy predictions for homes using EnergyPlus.

In the Appendix, the prototype homes (Albertsen, 2010) from the preliminary sensitivity study are tested again, this time using all five IHR models. The Anderlind model requires no assumptions, other than consideration of the variables used to calculate the Peclet number. Similarly the Krarti model is assumed to use only the insulation U-value to in the calculation of the Biot number. The Claridge and LBNL require assumptions to quantify the amount of diffuse air flow and wall participation factor, respectively. A linear correlation is assumed between the flow exponent and fraction of diffuse air flow to test its effects on IHR. A flow exponent of 0.5 means 0% diffuse air flow and 1.0 represents 100% diffuse air flow. For the infiltration models, a flow exponent of 0.67 is assumed for all models, resulting in diffuse air fraction of ~34%. The LBNL model goes through CFD testing to find an optimum wall participation factor of 0.33 for the model to match (Buchanan & Sherman) the wall. The factors are used as assumptions of the Claridge and LBNL models in the results. Please see Section 3and 5 for more information about the homes and IHR models, and see the Appendix for annual simulation results.

7.5 Simulation Implementation Procedure

To account for infiltration heat recovery in EnergyPlus, the calculation of the envelope thermal performance must be taken into account. The ability of the IHR models to capture changes in energy consumption by modification of the infiltration load through an adjustment factor f, the algorithms used to calculate this factor can be feasibly implemented into the simulation infiltration model. As previously mentioned in Section 4, the adjustment factor is a simplified method that accounts for both changes in conduction and infiltration. Ideally, the effects of infiltration heat recovery directly affect the temperature profile within the wall. However, in simulation the modification of temperatures is a much less feasible task, requiring editing of the source code to modify the temperature of the wall. The factor f is a much easier method, modifying only the air mass flow rate. Although not representative of what happens physically in a wall, applying the infiltration heat recovery factor to the mass flow rate will mathematically provide the same solution under the steady state assumption. Details of this derivation can be seen in the Appendix. Currently, the infiltration models used for residential buildings assume steady-state heat transfer, making this a suitable method.

In BEopt with EnergyPlus, energy models use the Alberta Infiltration Model or AIM2 (Walker & Wilson, 1998). This model provides the mass flow rate used to calculate infiltration loads. Energy Management Systems (EMS) is used within the EnergyPlus code to implement the AIM2 model. The use of the mass flow rate calculated in this model is used solely for infiltration loads. Therefore, implementing an IHR model into the AIM2 model in EMS is feasible method that will only affect the heat transfer related to infiltration and conduction.

7.6 Results

7.6.1 Comparison between Case Study and IHR Models

Although the data set is limited, the four points in Figure 27-29 show the expected trends of infiltration heat recovery. A comparison of the measured case study results against IHR model predictions can be done to assess the capabilities of the analytical models to capture the impact found in real buildings. The results are necessary to determine if IHR models can predict the measured impact using the home descriptions.

From Section 5, each IHR model, except the Anderlind model, requires additional factors to be calculated or assumed. The Krarti model requires the envelope characteristics in order to estimate the Biot numbers. The Claridge and LBNL models, however, require assumptions for the diffuse air fraction and wall participation factor, respectively. Very little information is available to characterize the diffuse air fraction in a wall. The leakage exponent from blower door tests is one metric available that can be used to define diffuse air in the envelope. When this information is not available, a leakage exponent of 0.67 is assumed in infiltration models to calculate the loads due to air leakage (Walker & Wilson, 1998). If it is assumed a linear interpolation can be made between concentrated and diffuse air flow using this metric, a diffuse air fraction of 0.34 would be found. This will be the initial assumption used in the Claridge model for analysis. The LBNL model finds the best correlation to CFD simulation occurs when a wall participation of 0.33 is used for each wall, and this value is also assumed in the analysis (Buchanan & Sherman, 2000).

$$X_{diffuse} = \frac{n}{0.5} - 1 = \frac{0.67}{0.5} - 1 = 0.34$$

Using the assumptions from each author, in the analysis the model to initially find the best agreement is the LBNL model. The assumption used in the Claridge model appears to under predict IHR. The other models estimate IHR much greater than the impact in the case study. The initial comparison can be seen in Figure 30.

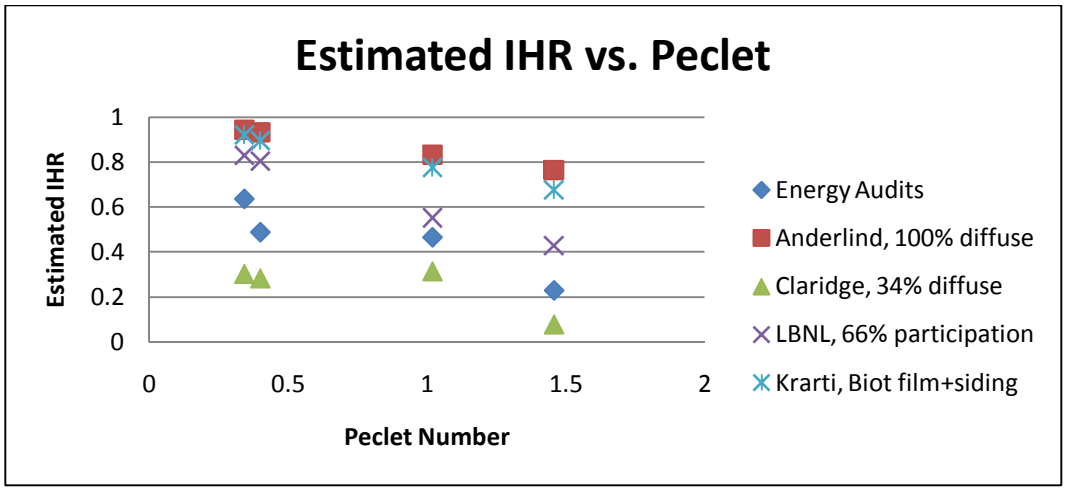

Figure 30: Comparison IHR model to case study IHR

To understand what can be done to match the case study measurements, the parameters of each model are optimized to find a way to match results from the case study. The exception is the Anderlind model, where no optimization can be made using the model defined. By adjusting the inputs, the Claridge and LBNL models are able to match each case study home. The Biot number for the Krarti model does not impact results as greatly as anticipated, even when approaching the limits of heat transfer beyond th range seen in homes. The results are shown in Figure 31, and Table 15 shows a summary of the values in each model used to match measured IHR.

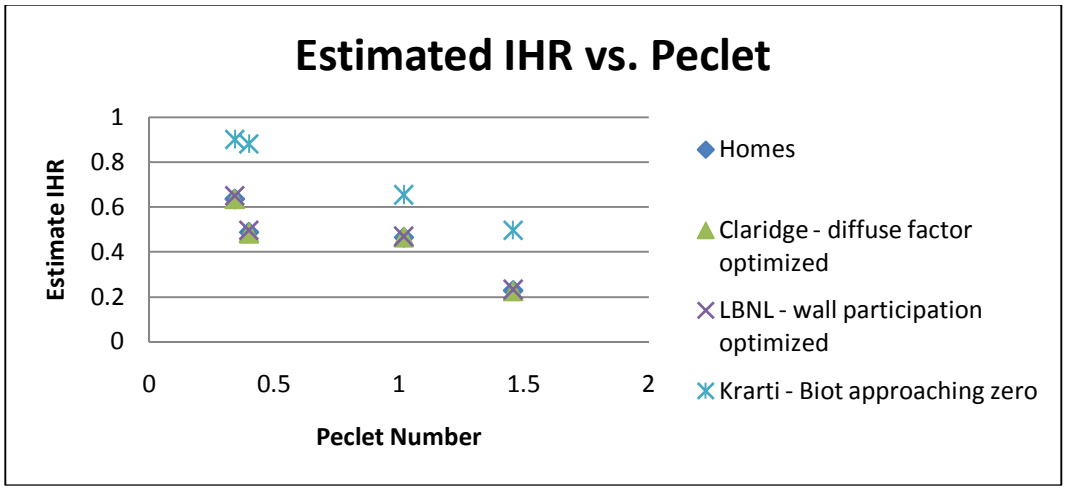

Figure 31: Optimized comparison of IHR models to measured IHR

Table 15: Optimized IHR model factors to match measurements

Optimized IHR model factors				
	Peclet Number	Claridge - Diffuse air fraction	LBNL - Wall participation factor	Krarti - Biot Number
Home #1	0.34	0.66	0.15	~0
Home #2	0.4	0.51	0.26	~0
Home #3	1.02	0.5	0.11	~0
Home #4	1.46	0.24	0.17	~0

As a result of the improved comparison between measured and predicted IHR, a similar effect will be seen analyzing the BLC reduction, shown in Figure 32 and 33.

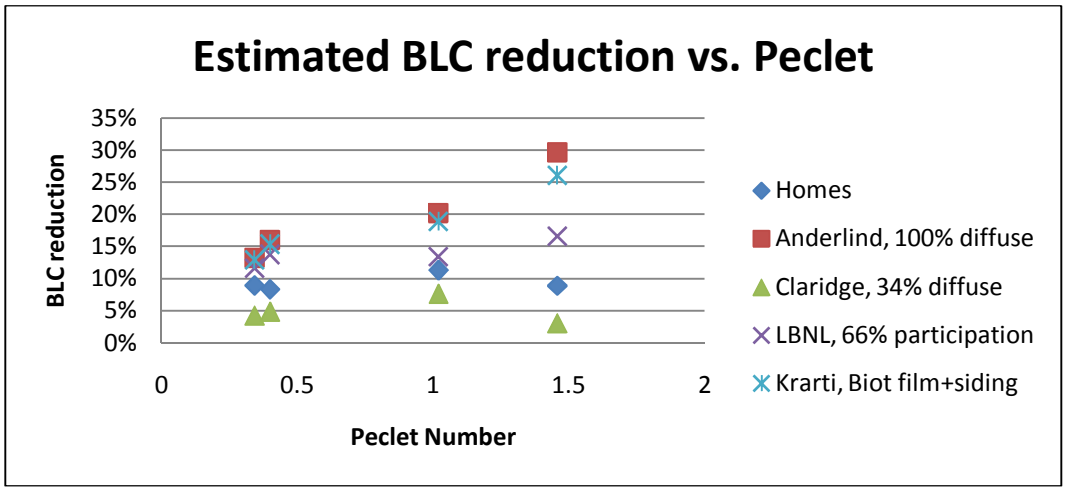

Figure 32: Comparison of measured to predicted BLC reduction

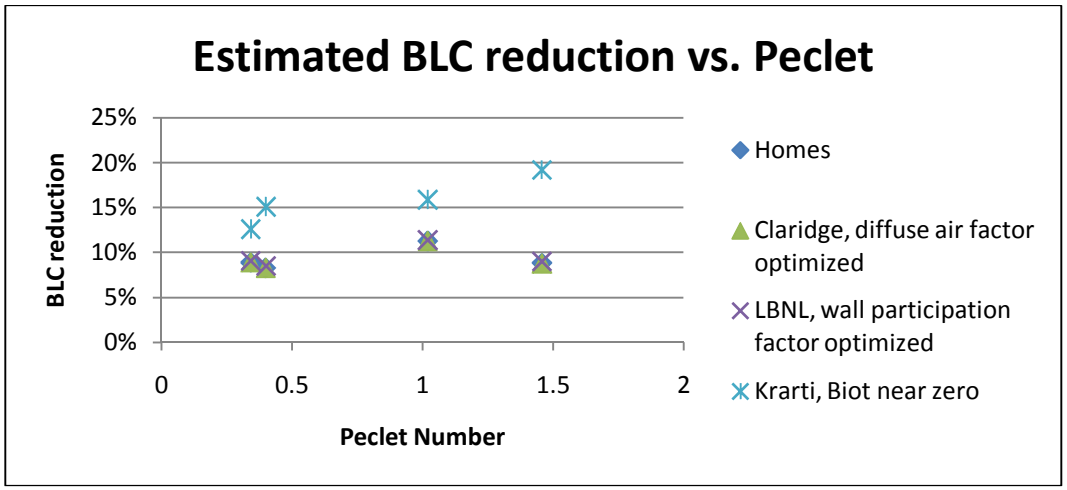

Figure 33: Optimized comparison of measured to predicted BLC reduction

From Figure 31 and 33, adjusting Biot number is shown to provide little impact to the Krarti model to match the measured IHR. The effect of the Biot number for a home has already been discussed and results have shown that is does not deviate far from the reference model, confirming the surface film resistance is not very significant for the scope of building heat transfer. To match the Krarti model to the measured data, further adjustment is needed, and this can be achieved by implementing the diffuse air fraction into the model. This is beneficial development that can provide better characterization of air flow through the envelope. To estimate the impact of diffuse air, a simple process is used to modify the results of the Krarti model when calculating IHR and applying it to infiltration. In addition, the LBNL model can also benefit from the addition of diffuse air into its equations. The Claridge model does not undergo this process because it already defines diffuse and concentrated air. The infiltration air flow that is effectively interacting with the walls should be the only portion affected by infiltration heat recovery, and is reflected below.

$$\left(\dot{m}C_p\right)_{concentrated} = \left(\dot{m}\,C_p\right) * (1 - X_{diffuse}) \tag{22}$$

$$BLC_{predicted} = UA_{envelope} + (1 - f) * \left(\dot{m}C_p\right)_{diffuse} + \left(\dot{m}C_p\right)_{concentrated} \tag{23}$$

A sensitivity study of the diffuse air fraction shows the effect diffuse air has on the Krarti model IHR predictions. The range of BLC reduction found in all homes using the Krarti model varies from 26-35%, when assuming 100% diffuse air. Overall, the sensitivity of the diffuse air fraction shows a slight curve when approaching 100%. Despite the curved appearance of the sensitivity studies, a linear best fit line places over the data points reveals a linear trend can be assumed for all these homes, confirmed by the R^2 found to be 0.96 or greater. The linear assumption simplifies the analysis, allowing the adjustment to also be performed after simulation of IHR through a linear interpolation of results using the assumed diffuse air fraction.

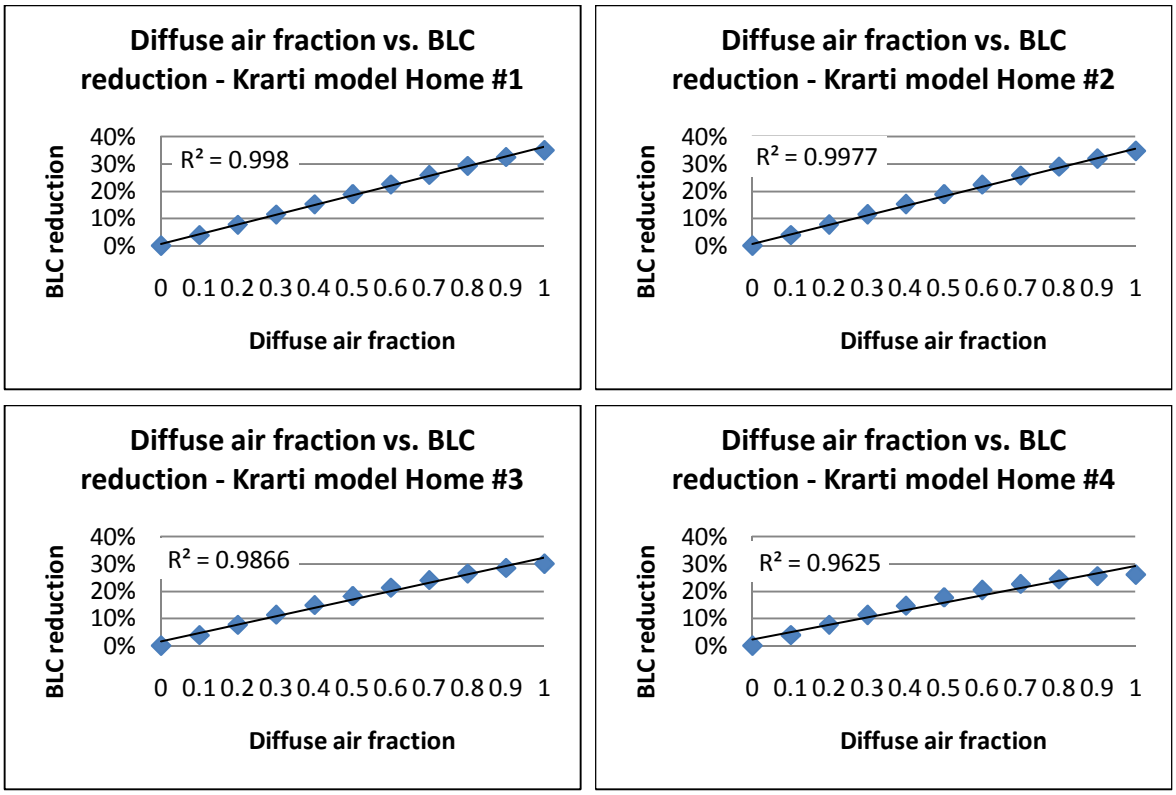

Figure 34: Sensitivity study of diffuse air fraction on Krarti model

The Krarti model is now able to match the measured by utilizing the diffuse air fraction to adjust the BLC reduction, shown in Figure 35. The factors needed in the Krarti model to match the data are provided in Table 16. The diffuse air fraction found is the same used while analyzing the Claridge model, also signifying the small impact made by the Biot number on the effects of IHR. The LBNL model can benefit from the addition of a diffuse air fraction; however, the wall participation factor already can be used to match measured IHR. The effects of diffuse air fraction on the LBNL can be seen in the Appendix.

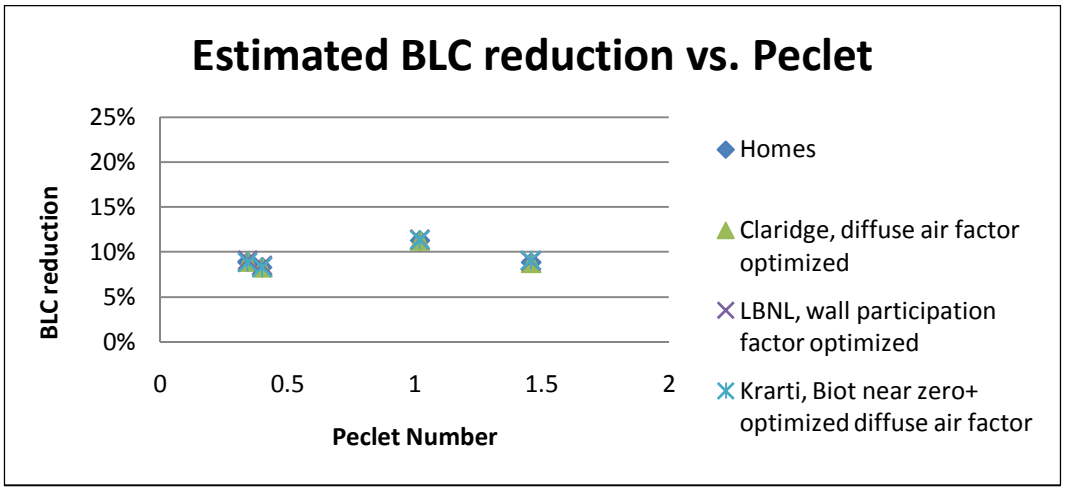

Figure 35: Optimized Krarti model with diffuse air fraction matches measured IHR

Table 16: Final optimization of IHR models

Optimized IHR model factors				
	Peclet Number	Claridge - Diffuse air fraction	LBNL - Wall participation factor	Krarti - Biot Number (+ Diffuse air fraction)
Home #1	0.34	0.66	0.15	~0 (0.66)
Home #2	0.4	0.51	0.26	~0 (0.51)
Home #3	1.02	0.5	0.11	~0 (0.5)
Home #4	1.46	0.24	0.17	~0 (0.24)

The IHR measurements reveal an improvement seen in the overall thermal performance of each home, reducing energy consumption when accounting for IHR. The theoretical models also have the ability to provide a reduction in energy consumption, but it is important for the effect to have the correct magnitude. With the results from the IHR case study, analysis of the theoretical IHR models is done to understand the current predictions and the adjustments needed for predictions to be improved.

As mentioned in Section 6, existing IHR models have never been tested against measured data. The ASHRAE experiment in the previous section revealed the models require alteration, such as the LBNL wall participation factor, in order for the IHR models to match 1D experimental data. Existing IHR models underwent testing against either experimental or field measurements of IHR in order to compare their performance. As seen in the previous section, the models appear to provide a good comparison when

applying the wall participation factor and diffuse air fraction to the IHR calculation. The same approach must be considered in the analysis of the case study homes in energy simulation.

7.6.2 Results from Case Study Energy Simulations

Using the implementation procedure described for each IHR model, the impact in heating energy consumption using EnergyPlus is found. The implementation of IHR in EnergyPlus revealed heating is greatly impacted, while the effect on cooling energy consumption is very minimal, although it has been found to increase energy consumption. The mild summers in Boulder are subject to times where the outdoor temperature may be cooler than the house, and infiltration during these times is beneficial to the space load, and energy models take this account. It is important to note infiltration heat recovery under these conditions will reduce the cooling benefit from infiltration, and cause energy consumption to increase in cooling to offset the loss of infiltration. However, the overall impact found in cooling for this climate is negligible and not shown. Further testing of IHR impacts in other cooling climates is recommended to better understand the positive and negative impacts of IHR. Figure 36-39 show the results found from the energy simulation analysis. Refer to Section 7.6.1 for information regarding the values of the factors used in each model, initially and after optimization. For more information about each case study home, refer to the Appendix for details of the energy audit, utility bills, and inputs used to build BEopt E+ energy models.

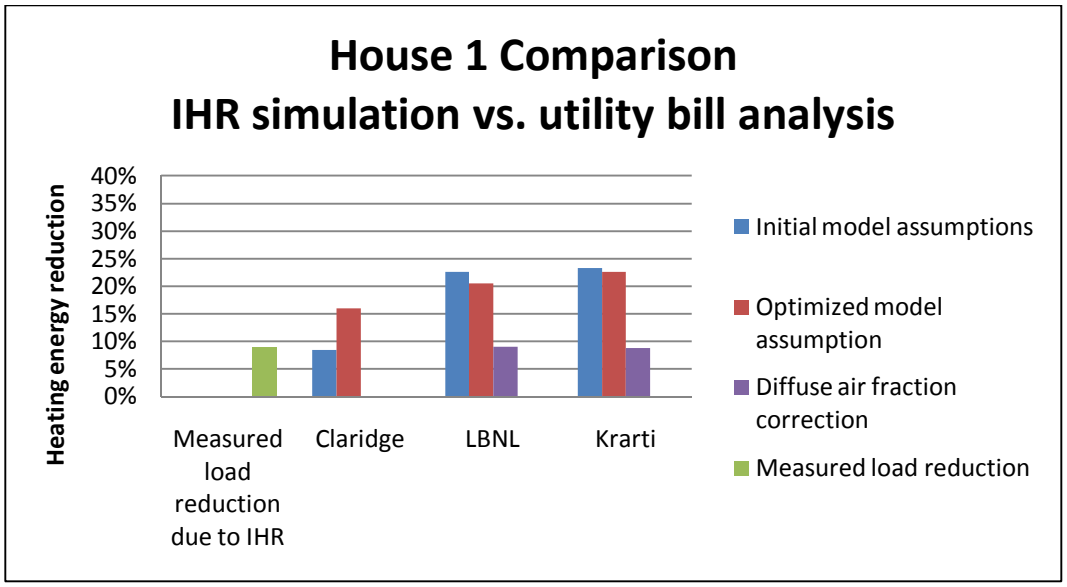

Figure 36: Predicted reduction in heating energy - Home #1

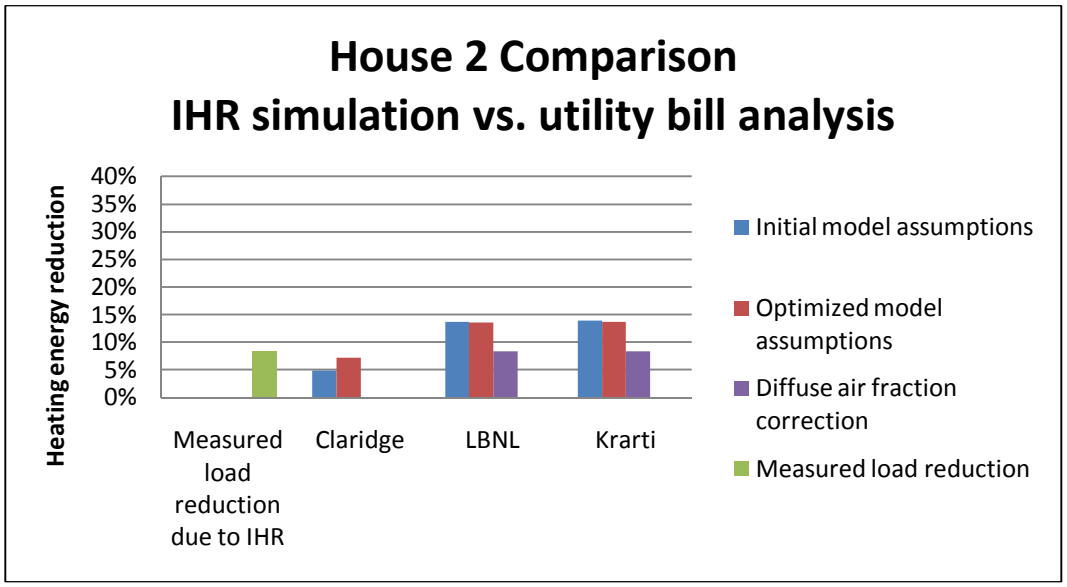

Figure 37: Predicted reduction in heating energy - Home #2

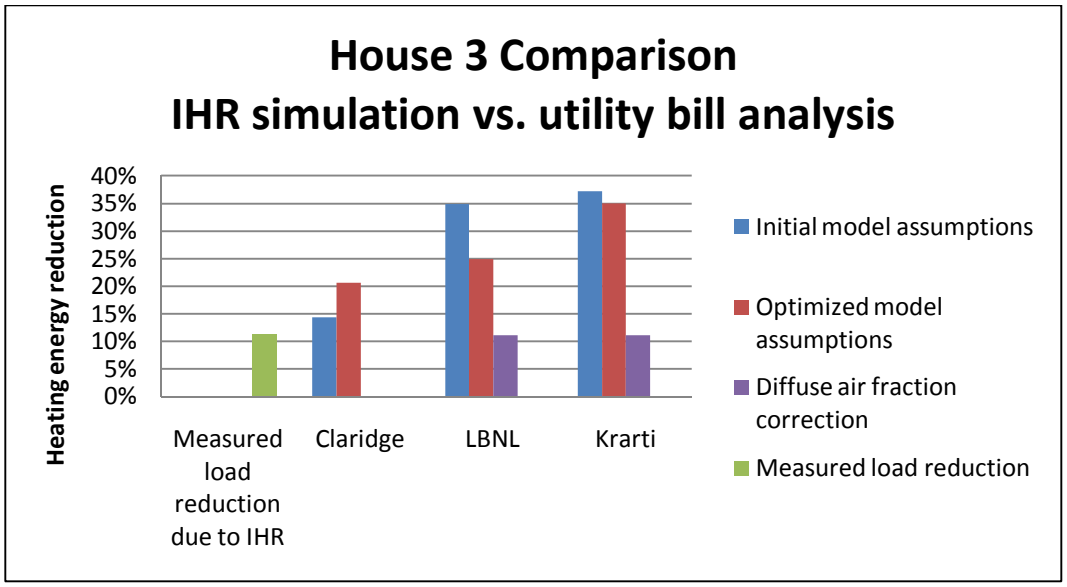

Figure 38: Predicted reduction in heating energy - Home #3

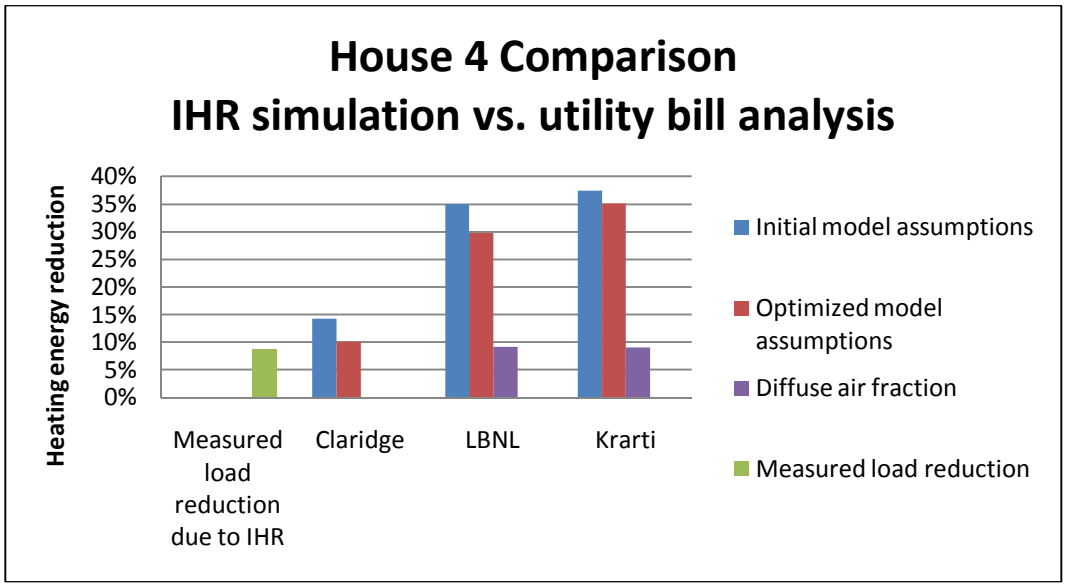

Figure 39: Predicted reduction in heating energy - Home #4

The results show there is general trend in EnergyPlus of extremely large reduction in heating energy consumption relative to the impact from the case study. From the graphs in Figure 39, the results show the Claridge model estimates a reduction is heating energy closest to the measured reduction. From the findings, the diffuse air fraction is the most effective in matching predicting to measured. However, optimizing the factors to match analytical IHR and BLC predictions does not provide the same result in simulation. In order to match reductions found in EnergyPlus to the reduction measured, a diffuse air

fraction is applied through linear interpolation of the initial model assumption results and the base case and found the diffuse air fraction needed in each home to match the homes. The diffuse air fraction found post-simulation reveals diffuse air fractions different from the analytical comparison.

$$\mathrm{Pe} = \frac{(\dot{m}C_p)_{diffuse}}{UA_{envelope}} \tag{24}$$

$$(\dot{m}C_p)_{diffuse} = (\dot{m}\,C_p) * X_{diffuse} \tag{25}$$

$$IHR_{diffuse} = (1 - f) * X_{diffuse} \tag{26}$$

$$\dot{Q}_{inf} = \sqrt{(\mathbf{c} * C_s * (\Delta T)^n)^2 + (\mathbf{c} * C_w * (s_w * V_{wind})^{2n})^2} \tag{27}$$

$$c^* = c * IHR_{diffuse} * X_{diffuse} + c * (1 - X_{diffuse}) \tag{28}$$

Table 17: Diffuse air fractions to match measured reduction in heating

Diffuse air fraction correction				
	Home #1 8.9% reduction	Home #2 8.4% reduction	Home #3 11.3% reduction	Home #4 8.8% reduction
Anderlind	0.38	0.60	0.29	0.23
LBNL	0.40	0.61	0.32	0.26
Krarti	0.38	0.60	0.30	0.24

.

8. CONCLUSION

An analysis of steady state infiltration heat recovery models is presented. A preliminary sensitivity study of multiple modeling issues revealed infiltration heat recovery can have a potentially large impact on energy predictions. Analytical, experimental, and case study comparison of IHR models are performed to provide an overall assessment of the capabilities of previously published IHR models.

A number of preliminary parametric studies have been executed for sensitivity analysis of the impact on HVAC energy consumption. The modeling issues each pertained to a building phenomenon not previously accounted in EnergyPlus during the time of this study. Infiltration heat recovery did not provide the greatest impact on energy consumption, but the existing overall gap in simulation is much greater given considerations to existing simulation and capabilities and feasibility of a model implementation.

8.1 Model Comparisons

Comparative analysis between five steady-state infiltration heat recovery models was performed to assess the capabilities and differences among previous research. After applying each model to the same methodology, the comparison revealed the models each have unique factors developed to provide a better characterization of infiltration heat recovery. However, each model is fundamentally the same when applied under ideal conditions. Many of the authors' contributions are not the development of a complete model, but rather parameters that can be used to provide a better explanation to accurately capture infiltration heat recovery. Out of the five infiltration heat recovery models tested, only two fundamental forms of the energy balance are used, with and without accounting for the surface film resistance. However, one solution does simplify to the other when the film resistance is considered negligible.

Sensitivity analysis of each model with respect to the infiltration rate reveals, for a typical home construction, each model provides a different answer, although results from the predictions are closer in magnitude than expected. Infiltration heat recovery is greatest when infiltration rates are low, but this

does not provide the largest overall impact because of small load. IHR will have the greatest impact on the building load when both infiltration and conduction heat transfer are both of the same magnitude.

8.2 Experimental Analysis

Previously published experimental work was compared against two infiltration heat recovery models to assess the abilities to predict measurements from an experimental test panel representing a typical residential wall.

Using the most applicable experiment available in research, six laboratory test cases measuring infiltration heat recovery are analyzed to compare against the models. Adjustments for both experiments and models were needed to analyze and compare the ratio of total heat transfer with and without accounting for IHR. Good agreement was found in the case when air flow is passing directly through the center of Test panel 1. When air flow enters top or bottom extremity of Test panel 2 and exits the other side on the other extremity, only the cases where cold air, or infiltration, was entering the wall did reasonable agreement occur. The remaining two cases the models found poor agreement in the tests involving warm air flowing through the test panel. In this case multiple effects are being seen, such as 2D flow and possible natural convection effects that are not accounted for in the 1D IHR models. From the other cases, overall, the Anderlind model predicted better overall against all the test cases. The Krarti model came close; however, it was not suited for this experimental comparison, because the effects at the surface were not capture. The air flow was introduced into the test panels pre-conditioned at the air temperature, and the effect from the surface film resistances would not be shown in the experiment.

8.3 Residential Case Study Analysis

A sample of 21 detailed building energy audits were evaluated to determine the most suitable audits to measure infiltration heat recovery using the field data. Using a detailed screening process, the same reduced to 4 detached single family homes picked to undergo utility bill analysis, hand calculations, and simulation analysis of building loss coefficients. Infiltration heat recovery measurements from the

field data indicate that the expected decreasing trend in infiltration heat recovery can be found with respect to the infiltration rates. The sample size and analysis must be increased substantially to for the analysis to be more meaningful, but the results thus far display all the expected trends in impact of infiltration heat recovery.

Using the results from the case study, the IHR models are first tested analytically for comparison of the estimated reduction in BLC. Claridge was found to under predict the effect while Anderlind, Krarti, and LBNL over predict, using the assumption defined for each model. The effects from the Biot number in the Krarti equation do not impact the model much, because results closely match those in the Anderlind model. The LBNL model has the closest overall match based on the initial assumption, but improvements still need to be made. Using the diffuse air fraction and wall participation factor, the Claridge and LBNL model were able match measured IHR. The Krarti model could not match the results through an adjustment of the Biot number alone. In order to match results, a diffuse air fraction adjustment was applied, and the same factors used by the Claridge model provided the Krarti model with a match. In the application of homes, the range of Biot numbers found does not impact the models greatly, but it can have an effect when larger infiltration rates exist.

8.4 EnergyPlus Analysis

Finally, the IHR models are introduced into the EnergyPlus simulation engine to analyze the impact in annual predicted energy consumption. Testing the effects in simulation across different climates confirms a reduction in heating consumption will occur, but the effects on cooling loads vary. Although mostly a reduction in cooling energy consumption is found, the opposite can occur in climates with mild summers and low cooling needs. When in cooling mode, if the outdoor temperature drops below the thermostat setpoint, outdoor air infiltration becomes beneficial to the space to offset cooling loads. In this case, the cooling benefit rather than loss is reduced when analyzing infiltration heat recovery, causing simulation to predict greater cooling energy consumption. However, for the climate where this is expected

to occur, the cooling load tends to be relatively low. Therefore the actual change in energy consumption can be minimal.

From the prototype home simulation tests, the results do not provide enough evidence to conclude what the overall impact of IHR has on annual home energy consumption. To understand if the predicted impact from the models is correctly estimated, building energy simulation of the homes in the case study is performed to assess the predictions against the results from the case study analysis. While each of the IHR models could be easily implemented into EnergyPlus, the factors used in each model are important to estimate. Similar to the case study, when the initial assumptions are used in energy simulation to predict IHR, the Claridge model under predicts while the remaining model over predict. However, using the optimized factors from the case study in the simulations only slightly improves the predictions against the case study. This means the models themselves cannot improve throughout an optimization method of the factors used in each model. Instead, each model must be corrected similar to the Krarti model in the case study and have only IHR apply to a portion of infiltration estimated to provide IHR. Using a diffuse air fraction, the models were all able to match the results in the case study. The diffuse air fraction is an important parameter to know, because the impact it has on IHR predictions is very significant. However, an understanding of the air path occurring in a residential wall is needed to properly use this factor.

9. FUTURE WORK

The abilities of existing steady-state infiltration heat recovery models have been well documented over the years. However, much of the work done has been theoretical and has undergone little performance testing. There is a need for additional experimental research on IHR. More detailed experiments will provide researchers with data to quantify the effects from IHR and can be used for future model development. Models already exist analyzing the transient effects of infiltration heat recovery. This analysis of steady-state IHR models is a starting point to provide guidance for the development of better IHR models. Other forms of heat transfer such as radiation and latent loads can be investigated to understand their impact. Transient analysis can help account for things such as energy stored in the building walls.

One of the biggest gaps in the understanding infiltration heat recovery is the passage of air through the building envelope and how it interacts physically with the walls. Current theoretical models assume ideal conditions, where air flow is evenly diffused over the wall area. This is rare to find in existing homes, vastly limiting the model's potential application. The amount of diffuse air or wall participation are key concepts needed to accurately estimate IHR, and very little characterization of this with regards to wall assemblies has been performed. The flow exponent from blower door tests has been shown to provide some correlations in the past, and is one example that can be used to help explain these issues.

As explained in this paper, the steady-state models algorithms are implemented into EnergyPlus through use of an adjustment of the infiltration load from the infiltration model written in EMS. However, to better account for IHR, implementation directly into the source code is needed. Infiltration heat recovery affects the temperature profiles of the walls, but the simulation is not impacted by the models in this way currently. Through the use of EMS in EnergyPlus, the mass flow rate can be controlled and adjusted. However, the impact this has on energy is assumed to be sensible heat. Capturing the effect on

the wall temperature profiles in simulation can impact the simulation far more that the current work, especially when analyzing transient effects. The findings in this study are dependent largely by the capabilities of the EnergyPlus simulation engine. Mirrored analysis using the DOE2 simulation engine can be done to assess if vary based on the simulation capabilities and predictions.

The case study of homes in this study only provides some indication that IHR measurements techniques can be valid in the field. An increased number of energy audits is needed provide a larger data set that can be used for more statistical significance using IHR measurement methods. As was shown in the analysis, large amounts of uncertainty in the IHR measurements can occur when errors exist in the inputs that are measured. Literature search of field studies are needed to assess what typical levels of error are associated with variables measured as a result of a home energy audit. Also, the error of propagation can be further analyzed mathematically to find the change in uncertainty that can occur with respect to a change in input error.

Further development of the existing steady-state models would be beneficial in order to determine the most effective analytical steady-state IHR model. Each model analyzes only one parameter and assumes the effect is applied to 100% of the infiltration. Using the diffuse air fraction The study concludes the parameters introduced by each model are beneficial to characterize infiltration heat recovery. It is proposed that the models be merged for an IHR model to determine the effects of each parameter.

The models presented focus on the effects when infiltration and exfiltration through in the building envelope. There could be cases, such as when whole house fan is operating, that would eliminate exfiltration through the envelope. Further derivation of the heat transfer is recommended to find how the models change and expected impact on IHR.

BIBLIOGRAPHY

1. Abadie, M. O., Finlayson, E. U., & Gadgil, A. J. (2002). *Infiltration Heat Recovery in Building Walls: Computational Fluid Dynamics Investigation Results.* Berkeley, CA: Lawrence Berkeley National Laboratory.
2. Ackerman, M. Y., Bailey, R., Dale, D., & Wilson, D. (2004). *Infiltration Heat Recovery - ASHRAE Research Project 1169 - Final Report.* University of Alberta, Department of Mechanical Engineering, Edmonton, Alberta, Canada.
3. Ackerman, M. Y., Wilson, D., Dale, D., & Bailey, R. (2006). Infiltration Heat Recovery Part I - Field Studies in an Instrumented Test Building. *ASHRAE Transaction* , 597-608.
4. Ackerman, M. Y., Wilson, D., Dale, D., & Bailey, R. (2006). Infiltration Heat Recovery Part II - Laboratory Studies of Two Test Panel Geometries. *ASHRAE Transactions* , 609-621.
5. Albertsen, S. (2010). *Estimating Energy Savings From Retrofitting Existing Housing in the United States using BEopt 0.9.* Boulder, CO: Univerisity of Colorado.
6. Anderlind, G. (1985). Energy Consumption due to Air Infiltration. *Proceedings of the 3rd ASHRAE/DOE/BTECC Conference on Thermal Performance of the Exterior Envelope of Buildings*, (pp. 201-208). Clearwater Beach, FL.
7. Anderlind, G., & Johansson, B. (1983). *Dynamic Insulation: A Theoretical Analysis of Thermal Insulation through which a Gas or Fluid Flows.* Stockholm: Swedish Council for Building Research.
8. ASHRAE. (2005). *Handbook of Fundamentals.* Atlanta, GA: American Society of Heating, Refridgerating, and Air- Conditioning Engineers.
9. ASHRAE. (2004). *Standard Method of Test for Determining the Steady-State and Seasonal Efficiencies of Residential Thermal Distribution Systems.* Atlanta, GA: American Society of Heating, Refrigeration, and Air-Conditioning Engineers.
10. Barhoun, H., & Guarracino, G. (2004). *Evaluating the Energy Impact of Air Infiltration through Walls with a Coupled Heat and Mass Transfer Method.* ENTPE, Department of Civil Engineering and Building Science, France.
11. Barhoun, H., & Guarracino, G. (2006). *Influence of Air Leakage in Building's Walls on Heat Transmission Loss through its Envelope.* ENTPE, Department of Civil Engineering and Building Science, France.
12. Berry, L. G., & Gettings, M. B. (1998). *Realization Rates of the National Energy Audit.* Oak Ridge, TN: Oak Ridge National Laboratory.
13. Bhattacharyya, S. (1999). Modeling and the Phenomenon of Infiltration Heat Exchange. *International Journal of Power and Energy Systems , 19* (1), 87-91.
14. Bhattacharyya, S., & Claridge, D. E. (1992). The Energy Impact of Air Leakage through Insulated Walls. *Proceedings of ASME Solar Energy Division Conference*, *1*, pp. 451-458. Miami.
15. Bhattacharyya, S., & Claridge, D. E. (1995). The Energy Impact of Air Leakage through Insulated Walls. *Journal of Solar Energy Engineering , 117*, 167-172.
16. Brunger, A., Dubrous, F. M., & Harrison, S. (1999). Measurement of the Solar Heat Gain Coefficient and U-value of Windows with Insect Screens. *ASHRAE Transactions , 105*, 1038-1044.

17. Buchanan, C. R., & Sherman, M. H. (2000). *A Mathematical Model for Infiltration Heat Recovery.* Berkeley, CA: Lawrence Berkeley National Laboratory.

18. Buchanan, C. R., & Sherman, M. H. (1998). Simulation of Infiltration Heat Recovery. *19th Annual AIVC Conference*, (pp. 17-26). Olso, Norway.

19. Budaiwi, I., Abdou, A., & Al-Homoud, M. (2002). Variations of Thermal Conductivity of Insulation Materials Under Different Operating Temperatures: Impact of Envelope Induce Cooling Load. *Journal of Architectural Engineering* .

20. Chebil, S., Galanis, N., & Zmeureanu, R. (2002). Computer Simulation of Air Infiltration Effects on Heat Transfer in Multilayered Walls. *eSim2002 Conference*, (pp. 97-104). Montreal, Canada.

21. Chebil, S., Galanis, N., & Zmeureanu, R. (2003). Computer Simulation of Thermal Impact of Air Infiltration Through Multilayered Exterior Walls. *Eigth International IBPSA Conference*, (pp. 155-162). Eindhoven, Netherlands.

22. Christensen, C., & et.al. (2006). *BEopt Software for Building Energy Optimization: Features and Capabilities.* Golden, Colorado: National Renewable Energy Laboratory.

23. Claesson, D. E., & Hellstrom, G. (1995). Forced Convective-Diffusive Heat Flow in Insulations: A New Analytical Technique Applied to Air Leakage Through a Slit. *Journal Thermal Insulation and Building Environment , 18*, 216-228.

24. Claridge, D. E., & Bhattacharyaa, S. (1990). The Measured Energy Impact of Infiltration in a Test Cell. *Journal of Solar Energy Engineering , 112*, 132-139.

25. Claridge, D. E., & Bhattacharyya, S. (1991). *The Measured Energy Impact of Air Leakage on Frame Wall Systems.* College Station, TX: Texas A&M University.

26. Claridge, D. E., & Liu, M. (1996). The Measured Energy Impact of Infiltration in an Outdoor Test Cell. *Transactions of the ASME , 118*, 162-167.

27. Claridge, D. E., Krarti, M., & Bhattacharyya, S. (1988). Preliminary Measurements of the Energy Impact of Infiltration in a Test Cell. *Proceedings of the 5th Symposium on Improving Building Systems in Hot and Humid Climates.* Houston, TX.

28. Claridge, D. E., Liu, M., & Bhattacharyya, S. (1995). Impact of Air Infiltration in Frame Walls on Energy Loads: Taking Advantage of the Interaction between Infiltration, Solar Radiation, and Conduction. In M. P. Modera, & A. K. Persily, *Airflow Performance of Building Envelopes, Components, and Systems* (pp. 178-196). Philadelphia: ASTM.

29. Etheridge, D. W. (1988). Modeling of Air Infiltration in Single- and Multi-cell Buildings. *Energy and Buildings , 10*, 185-192.

30. Etheridge, D. W., & Zhang, J. J. (1998). Dynamic Insulation and Natural Ventilation: Feasibility Study. *Building Services Engineering Research & Technology , 19* (4), 203-212.

31. Gettings, M. B., & al, e. (1998). *Validation of the National Energy Audit (NEAT) with Data from a Gas Utility Low- Income Residential Weatherization Program.* Oak Ridge, TN: Oak Ridge National Laboratory.

32. Haberl, J. S., & Cho, S. (2004). *Literature Review of Uncertainty of Analysis Methods (DOE-2 Program).* Energy Systems Laboratory System. College Station, TX: Texas A&M University .

33. Haberl, J. S., Sreshthaputra, A., Claridge, D. E., & Kissock, J. K. (2003). Inverse Modeling Toolkit: Application and Testing (RP-1050). *ASHRAE Transaction , 109* (2), 435-448.

34. Harris, J. (2007). *Reference Design Guide for Highly Energy Efficiency Residential Construction.* Burlington, VT: Vermont Energy Investment Corporation.

35. Hassel, S., Blasnik, M., & Hannas, B. (2009). *Houston Home Energy Efficiency Study.* Advanced Energy.

36. Holman, J. P. (2007). *Experimental Methods for Engineers.* McGraw-Hill.

37. Janssens, A. (2001). A Comparison between Analytical and Numerical Models to Estimate Infiltration Heat Recovery. *Imternational Conference on Building Envelope Systems and Technologies (ICBEST)*, (pp. 353-358). Ottawa.

38. Janssens, A. (2003). Methodology for Measuring Infiltration Heat Recovery for Concentrated Air Leakage. *Research in Building Physics* .

39. Jensen, L. (1993). Energy Impact of Ventilation and Dynamic Insulation. *Energy Impact of Ventilation and Air Infiltration 14th AIVC Conference* (pp. 251-260). Copenhagen, Denmark: Lund Institue of Technology and Building Technology.

40. Jokisalo, J., Kurnitski, J., Korpi, M., Kalamees, T., & Vinha, J. (2009). Building Leakage, Infiltration, and Energy Performance Analyses for Finnish Detached Houses. *Building and Environment , 44*, 377-387.

41. Judkoff, R., Balcomb, J. D., Hancock, C. E., Barker, G., & Subbarao, K. (2000). *Side-by-Side Thermal Tests of Modular Offices: A Validation Study of the STEM Method.* Golden, CO: NREL.

42. Jump, D., & Modera, M. (1994). *Energy Impacts of Attic Duct Retrofits in Sacramento Houses.* Berkeley, CA: Lawrence Berkeley National Laboratory.

43. Kline, S. J., & McClintock, F. A. (1953). Describing the Uncertainties in Single-Sample Experiments. *Mechanical Engineering , 75*, 3-8.

44. Kohonen, R., & Virtanen, M. (1987). Thermal Coupling of Leakage Flow and Heating Load of Buildings. *ASHRAE Transactions , 93*, 2303-2318.

45. Kohonen, R., Kokko, E., Ojanen, T., & Virtanen, M. (1985). *Thermal Effects of Air Flows in Building Structures.* Espoo: Techincal Research Centre of Finland.

46. Kotey, N. A., Wright, J. L., & Collins, M. R. (2009). Determining Off-Normal Solar Optical Properties of Insect Screens. *ASHRAE Transactions , 115*.

47. Krarti, M. (1994). Effect of Air Flow on Heat Transfer in Walls. *Journal of Solar Energy Engineering , 116*, 35-42.

48. Levinson, R., Hashem, A., & Gartland, L. (1997). *Impact of the Temperature Dependency of Fiberglass Insulation R-Value on Cooling Energy Use in Buildings.* Berkeley, CA: Lawrence Berkeley National Laboratory.

49. Liu, M. (1992). *Study of Air Infiltraion Energy Consumption.* College Station, TX: Texas A&M University.

50. Liu, M., & Claridge, D. E. (1993). *Guidelines for Measuring Air Infiltration Heat Exchange Effectiveness (IHEE).* College Station, TX: Texas A&M University .

51. Liu, M., & Claridge, D. E. (1995). Heat Flux Error of Steady-State Method for Building Components Under Dynamic Conditions. *Solar Engineering , 1*, 219-227.

52. Liu, M., & Claridge, D. E. (1992). The Energy Impact of Combined Solar Radiation/Infiltration/Conduction Effects in Walls and Attics. *Proceedings of 5th*

ASHRAE/DOE/BTECC Conference on Thermal Performance of the Exterior Envelopes of Buildings (pp. 39-47). Clearwater Beach, FL: Texas A&M University.

53. Liu, M., & Claridge, D. E. (1992). The Measured Energy Impact of Infiltration Under Dynamic Conditions. *Proceedings of the Eight Symposium on Improving Building Systems in Hot and Humid Climates* (pp. 73-78). Dallas, TX: Texas A&M University.
54. McWatters, K., Claridge, D. E., & Liu, M. (1996). A Prediction of Energy Savings Resulting from Building Infiltration Control. *Proceedings of the 10th Symposium on Improving Building Systems in Hot and Humid Climates.* Fort Worth, TX.
55. Mills, E. (2002). *Review and Comparison of Web- and Disk-based Tools for Residential Energy Analysis.* Berkeley: Lawrence Berkeley National Laboratory.
56. Morrison, I. D., Karagiozis, A. N., & Kumaran, K. (1992). Thermal Performance of a Residential Dynamic Wall. *Proceedings of Thermal Performance of the Exterior Envelopes of Buildings, 5th ASHRAE/DOE/BTECC Conference*, (pp. 229-234). Clearwater Beach, FL.
57. NYSERDA. (2005). *New York Energy Smart Program: Evaluation and Status Report, Final Report.* New York, NY: New York State Energy Research and Development Authority.
58. Parker, D., Fairey, P., & Gu, L. (1993). Simulation of the Effects of Duct Leakage and Heat Transfer on Residential Space-Cooling Energy Use. *Energy and Buildings* , 97-113.
59. Pigg, S., & Nevius, M. (2000). *Energy and Housing in Wisconsin: A Study of Single- Family Owner-Occupied Homes.* Madison, WI: Energy Center of Wisconsin.
60. Qiu, K., & Haghighat, F. (2005). Assessment of Impact of Building Envelope Porosity on Energy. *Proceedings from Ninth International IBPSA Conference* (pp. 987-994). Montreal, Canada: Concordia University.
61. Qiu, K., & Haghighat, F. (2007). Modeling the Combined Conduction - Air Infiltration through Diffusive Building Envelope. *Energy and Buildings , 39*, 1140-1150.
62. Roots, P. (1993). Skanterra: A Wall with Dynamic Insulation. *Building Physics in the Nordic Countries: Building Physics '93: Proceedings of the 3rd Symposium*, (pp. 227-233). Copenhage, Denmark.
63. Seryak, J., & Kissock, K. (2003). Occupancy and Behavioral Effects on Residential Energy Use. *Proceedings from the Solar Conference.* American Solar Energy Society.
64. Sherman, M. H. (1990). *Superposition in Infiltration Modeling.* Berkeley, CA: Lawrence Berkeley National Laboratory.
65. Sherman, M. H., & Modera, M. P. (1986). *Comparison of Measured and Predicted Infiltration Using the LBL Infiltration Model, Measured Air Leakage of Buildings.*
66. Sherman, M. H., & Walker, I. S. (2001). *Heat Recovery in Building Envelopes.* Berkeley, CA: LBNL.
67. Slowinski, R. (2009). *Thermal Performance of Ventilated Breathing Walls Under Varied Environmental Conditions.* Boulder, CO: University of Colorado.
68. Stein, J. R. (1997). *Accuracy of Home Energy Rating Systems.* Berkeley, CA: Lawrence Berkeley National Laboratory.
69. Storm, E., & Meredith, B. (2009). *Energy Performance Score 2008; Findings & Recommendations Report.* Oregon: Earth Advantage Institute, Conservation Services Group.

70. Sullivan, R. (1998). *Validation Studies of the DOE-2 Building Energy Simulation Program.* Berkeley, CA: Lawrence Berkeley National Laboratory.

71. Taylor, B. J., & Imbabi, M. S. (1997). The Effect of Air Film Resistance on the Behaviour of Dynamic Insulation. *Building and Environment , 32* (5), 397-404.

72. Taylor, B. J., Cawthorne, D. A., & Imbabi, M. S. (1996). Analytical Investigation of the Steady-State Behaviour of Dynamic and Diffusive Building Envelopes. *Building and Environment , 31* (6), 519-525.

73. Ternes, M. P. (2007). *Validation of the Manufactured Home Energy Audit (MHEA).* Oak Ridge, TN: Oak Ridge National Laboratory.

74. Ternes, M. P., & Gettings, M. B. (2008). *Analyses to Verify and Improve the Accuracy of the Manufacture Home Energy Audit (MHEA).* Oak Ridge, TN: Oak Ridge National Laboratory.

75. Treidler, B., & Modera, M. (1994). *Thermal Performance of Residential Duct Systems in Basements.* Energy and Environment Division. Berkeley, CA: Lawrence Berkeley National Laboratory.

76. U.S. DOE. (2011). *2010 Buildings Energy Data Book.* Washington, DC: U.S. Department of Energy.

77. U.S. DOE. (2010). *EnergyPlus Engineering Reference - The Reference to EnergyPlus Calculations.* Washington, D.C.: U.S. Departmentof Energy.

78. U.S. EIA. (2008). *2005 Residential Energy Consumption Survey.* Washington, D.C.: U.S. Energy Information Adminitration.

79. Vafai, K., & Sozen, M. (1990). Analysis of Momentum Transport for Fluid Flow Through a Porous Bed. *ASME Transactions , 112*, 690-699.

80. Virtanen, M., Heimonen, I., & Kohonen, R. (1992). Application for the Transfer Function Approach in the Thermal Analysis of Dynamic Wall Structures. *Proceedings of the 5th ASHRAE/DOE/BTCC Conference: Performance of the Exterior Envelopes of Buildings.* Clearwater Beach, FL.

81. Walker, I. S., & Wilson, D. J. (1998). *Field Validation of Algebraic Equations for Stack and Wind Driven Air Infiltration Calculations.* Berkeley, CA: Lawrence Berkeley National Laboratory.

82. Wang, W., Beausoleil-Morrison, I., & Reardon, J. (2009). Evaluation of the Alberta Air Infiltration Model Using Measurement and Inter-Model Comparisons. *Building and Environment , 44*, 309-318.

83. Wilkes, K. E., & Childs, P. W. (1992). *Thermal Performance of Fiberglass and Cellulose Attic Insulations.* Oak Ridge, TN: Oark Ridge National Laboratory.

84. Wilkes, K. E., & Rucker, J. L. (1983). *Thermal Performance of Residential Attic Insulation.* Technical Center, Research and Development Division. Granville, OH: Ownens-Corning Fiberglass Corportation.

85. Wright, J. L., Barnaby, C. S., Collins, M. R., & Kotey, N. A. (2009). *Improving Cooling Load Calculations for Fenestration with Shading Devices, ASHRAE RP-1311.* American Society of Heating, Refridgeration, and Air-Conditioning Engineers.

86. Yarborough, D. W., & Graves, R. S. (2006). The Effect of Air flow on Measured Heat Transport Through Wall Cavity Insulation. *ASTM Symposium on Heat, Air, and Moisture Transport in Buildings.* Toronto, Canada.

87. Yarbrough, D. W. (1983). *Assessment of Reflective Insulations for Residential and Commericial Applications.* Oak Ridge, TN: Oak Ridge National Laboratory.

APPENDIX A: BUILDING ENERGY SIMULATION PERFORMANCE LITERATURE REVIEW SUMMARY

Reference	Study Type	Location	Programs used	Home Sample Size	Simulation Size	**Findings**	Highlights	Drawbacks
Oregon, E. Storm, 2009	Validation, Program Comparison, Survey	Oregon	HES-Mid, HES-Full *REM/rate*, SIMPLE	190 (pre 1960-2008)	190*4 (four programs)	Over-prediction, except for SIMPLE. Increased accuracy for new(er) homes	Good set of representative data for homes, both geographically and of the housing stock SIMPLE performed the most accurately using less inputs Actual Occupant inputs used Absolute Error allows easy overall determination of program performance (Energy use / sqft.) metric is not recommended	Part of program selection based on LBL (Mills, 2002), see study. Another tool used spreadsheet tool, where the algorithms were unknown, but likely related to degree day Use of absolute error does not assess under, over, or reasonable prediction. Bad Accuracy = +/- 25%
Wisconsin, S. Pigg, 2002	Validation, Survey	Wisconsin	*REM/rate*	309 (1930s-1990s)	309	Over-prediction of heating energy intensity of about 20%	1950s homes are the smallest, and 1930s $\simeq$ 1990s size homes 1950s homes have largest heating energy intensity Homes are very well characterized allowing good understanding of results Poor occupant comfort leads to adjusted thermostats set points	HERS rates home, not its usage. Assumes important inputs, such as occupancy.
ORNL, M. Ternes, 2007	Validation	Missouri, North Dakota, Ohio, Virginia, Wisconsin	MHEA, HERS-BESTEST	86	86*2 (two programs)	Very low realization rates of about 33%	Lack of agreement shown between modeled and measured. Low realization rates due to over-prediction in energy savings. Problem originates in pre-retrofitted houses. Majority of modeled cases fell within defined BESTEST ranges	HERS BESTEST not designed to test manufactured homes Engineering corrections were not enough to correct error, reduction factor needed to match measured data Cases which did not match showed large deviation

Reference	Study Type	Location	Programs used	Home Sample Size	Simulation Size	Findings	Highlights	Drawbacks
LBL, E. Mills, 2002	Validation, Program Comparison	California	HES, 60+ more	2	17 Web-Based, 7 Disk-Based (1 home for each program selected)	Over-prediction for most of web-based and all of disk-based tools	Distribution of loads by end-use were shown and compared Capabilities and limitations of each program highlighted Web-based tool overall performed better than disk-based HES found best agreement	Much uncertainty in results Analysis of each tool done by separate third-party experts All models compared against a single home. Possible fortuitous results
ORNL, Gettings, 1998	Validation	New York	NEAT, DOE 2.1E, PRISM (Inverse Modeling)	49	Energy Savings: 49 DOE2 model comparison: 2*2 (pre,post-retrofit)	Over-prediction. Low realization rates of 50-70%	Detailed explanation of source errors, set-up methodology, data quality Similarities to DOE-2 suggests low realization rates not due to internal algorithms Correction of inputs did not improve over-prediction result	Study only targeted low-income, high-usage homes
NYSERDA	Validation	New York	DOE-2.1E, HomeCheck, TREAT	E-Star: Large HPwES: ~6,400 (may be post-1990)	Very Large	*Good Agreement	Energy Calculations defined Agreement of measured new home with model confirmed. Good agreement reported.	Housing sample not described or characterized HPwES audits performed using different programs. Correction factor applied
Univ. Dayton, J. Seryak, 2003	Monitoring, Verification	Ohio	ESim (Inverse Modeling)	350	350	Total Electricity usage increases with	High level of variability due to occupant behavior Natural gas usage more dependent on construction and size, while electricity is affected by occupant behavior	Unpredictable student behavior makes results hard to interpret in detail Methodology to justify annual trend changes limited Actual vs. modeled trends only

						#occupant, Total Gas does not	Min, Max, and Std. Dev. Results Useful for analysis	similar, not identical. More modifications needed.
Reference	Study Type	Location	Programs used	Home Sample Size	Simulation Size	**Findings**	Highlights	Drawbacks
VEIC, J.Harris+ M.Blasnik, 2007	Validation, Builder survey	New York	*REM/rate*, VBHDD	240	112 w/gas data, 129 w/ electric data	Good Agreement of heating and (within 10% percent)	Energy Star homes performance was examined and predicted performance is validated Homes initially screened to rule out unreliable consumption data Model to extract actual consumption data similar to PRISM Most cost effective efficiency measures determined based on projected savings Home baseline model is well defined	Regression model of *REM/rate* data contained R^2 of ~.4 Retrofit savings projected but not validated
Texas A&M, J. Harberl, 2004	Lit Review, Validation, Verification	Various	DOE-2	13	~13	Multiple Studies: Good agreement to over 20% error	Mild climate zones were mainly used in the numerous studies (Zone 3 – Zone 5) This is only a literature summary, some detailed reports will be mentioned in table	Some DOE-2 assessments done with only limited measured data versus whole building
LBL, J. Stein, 1997	Validation	Various states	REM/rate, other HERS software	185(CA) 276(CO) 30(KA+OH)	~500	Over-prediction of energy usage. HERS model error decreases with an increasing score.	Segregating CHEERS sample to just new homes showed improved accuracy. CA and CO homes showed increasing scatter of energy usage with increasing age, both predicted and actual. HERS assumptions(weather, behavior) will always create degree of natural error	No clear relation found between rating score and total energy use. Only relative comparisons of HERS's are possible. Experts have not placed enough importance on accuracy of HERS results

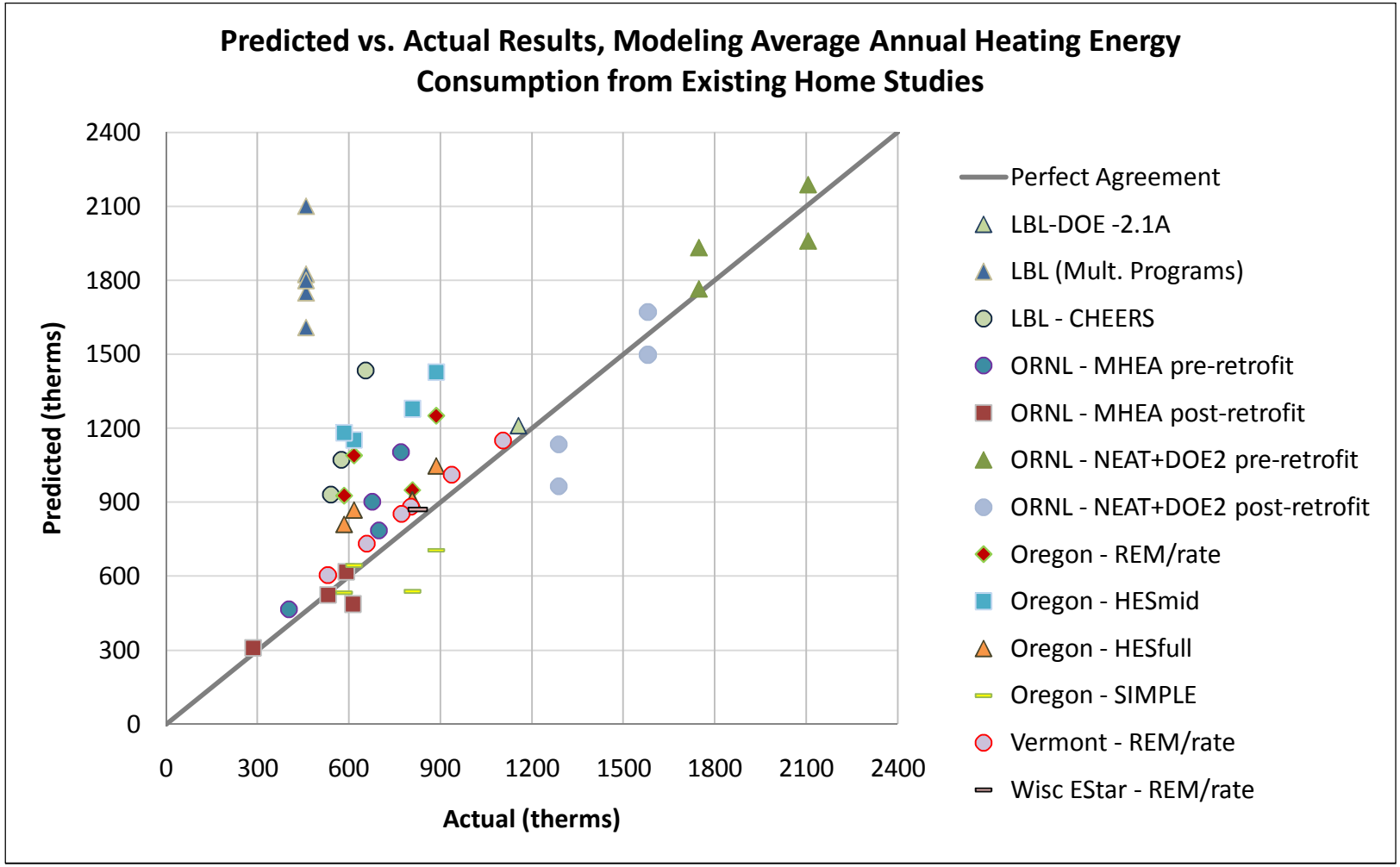
Predicted vs. Actual Results, Modeling Average Annual Heating Energy Consumption from Existing Home Studies
Predicted (therms)
Actual (therms)
0
300
600
900
1200
1500
1800
2100
2400
Perfect Agreement
LBL-DOE -2.1A
LBL (Mult. Programs)
LBL - CHEERS
ORNL - MHEA pre-retrofit
ORNL - MHEA post-retrofit
ORNL - NEAT+DOE2 pre-retrofit
ORNL - NEAT+DOE2 post-retrofit
Oregon - REM/rate
Oregon - HESmid
Oregon - HESfull
Oregon - SIMPLE
Vermont - REM/rate
Wisc EStar - REM/rate

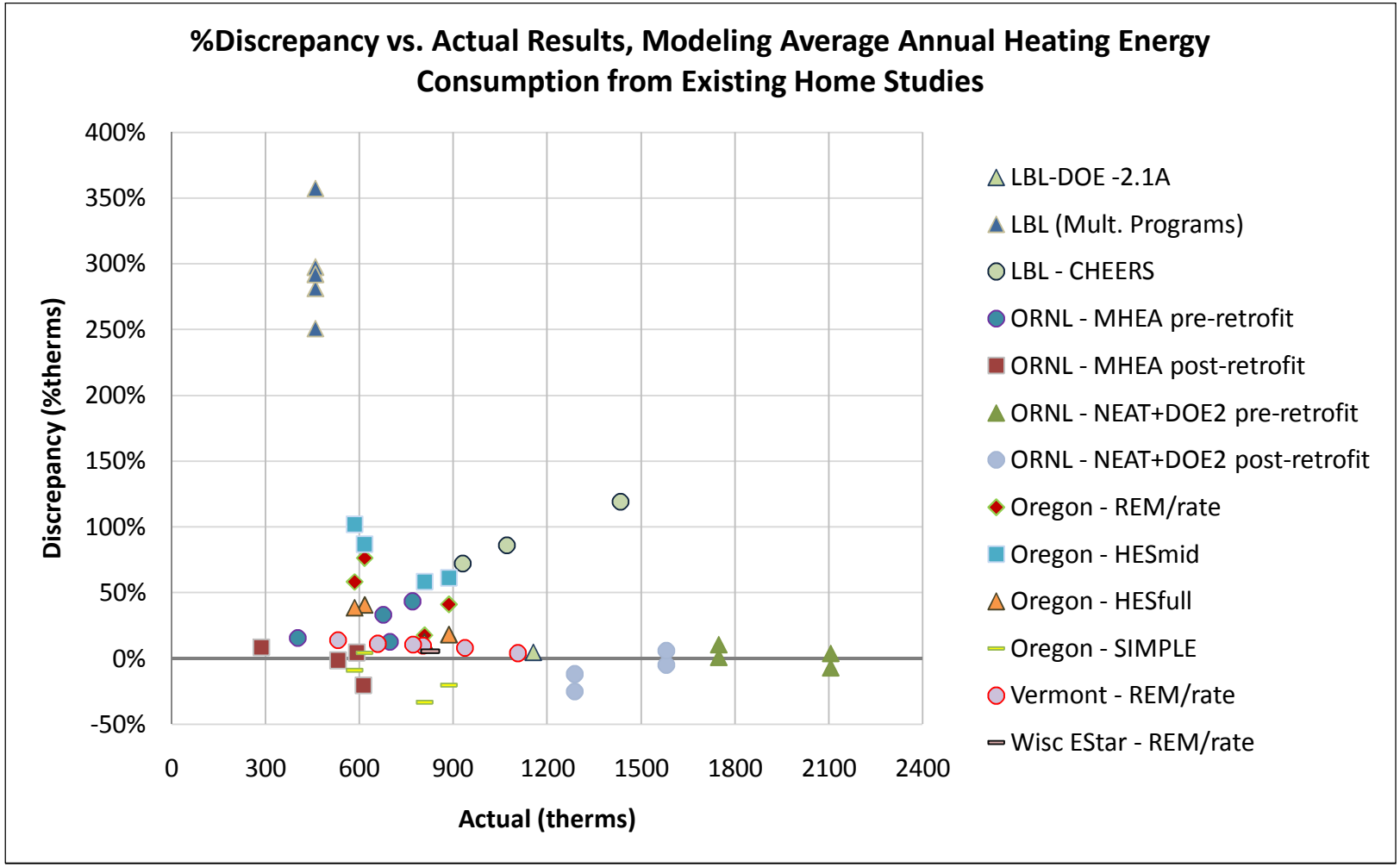
%Discrepancy vs. Actual Results, Modeling Average Annual Heating Energy Consumption from Existing Home Studies
Discrepancy (%therms)
400%
350%
300%
250%
200%
150%
100%
50%
0%
-50%
0
300
600
900
1200
1500
1800
2100
2400
Actual (therms)
LBL-DOE -2.1A
LBL (Mult. Programs)
LBL - CHEERS
ORNL - MHEA pre-retrofit
ORNL - MHEA post-retrofit
ORNL - NEAT+DOE2 pre-retrofit
ORNL - NEAT+DOE2 post-retrofit
Oregon - REM/rate
Oregon - HESmid
Oregon - HESfull
Oregon - SIMPLE
Vermont - REM/rate
Wisc EStar - REM/rate

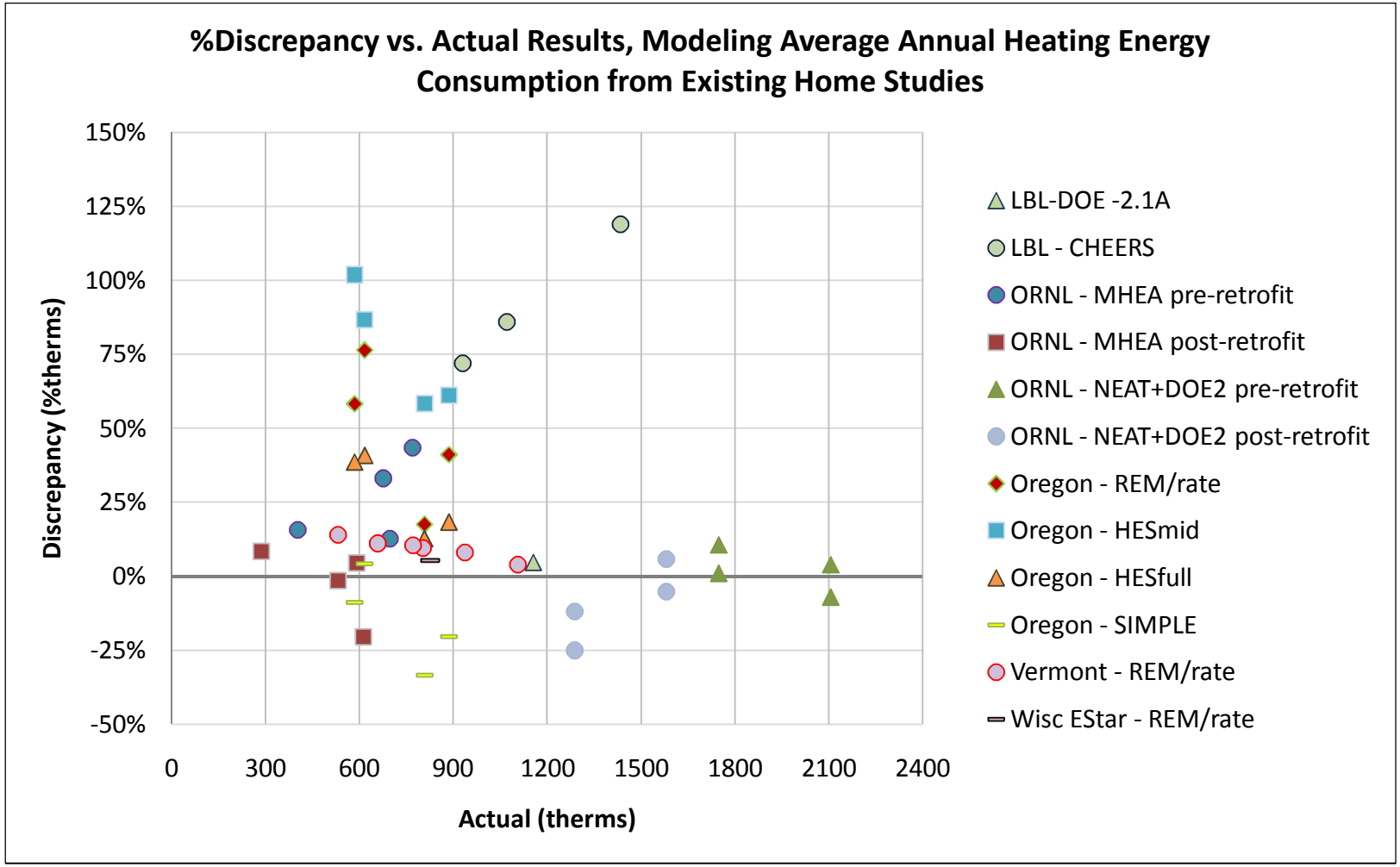
%Discrepancy vs. Actual Results, Modeling Average Annual Heating Energy Consumption from Existing Home Studies
Discrepancy (%therms)
150%
125%
100%
75%
50%
25%
0%
-25%
-50%
0
300
600
900
1200
1500
1800
2100
2400
Actual (therms)
LBL-DOE -2.1A
LBL - CHEERS
ORNL - MHEA pre-retrofit
ORNL - MHEA post-retrofit
ORNL - NEAT+DOE2 pre-retrofit
ORNL - NEAT+DOE2 post-retrofit
Oregon - REM/rate
Oregon - HESmid
Oregon - HESfull
Oregon - SIMPLE
Vermont - REM/rate
Wisc EStar - REM/rate

APPENDIX B: LITERATURE CASE STUDY - ENERGY PERFORMANCE SCORE OREGON REPORT REM/RATE MODEL DATA

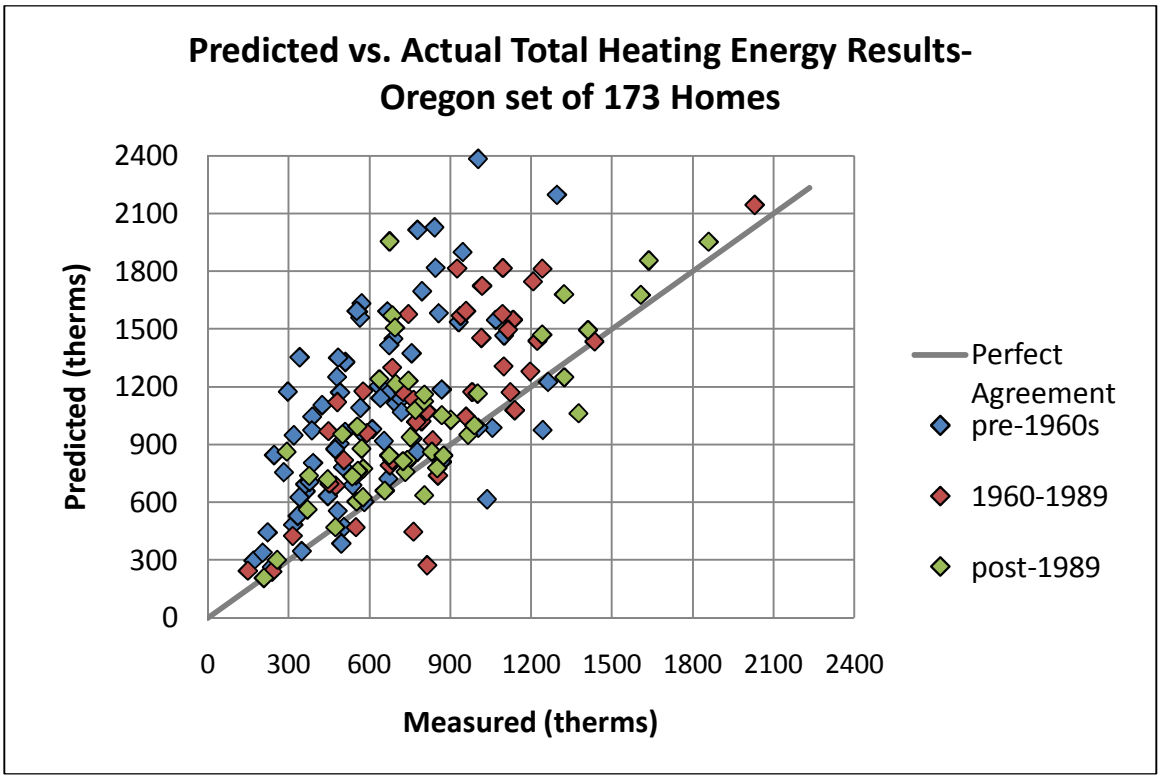

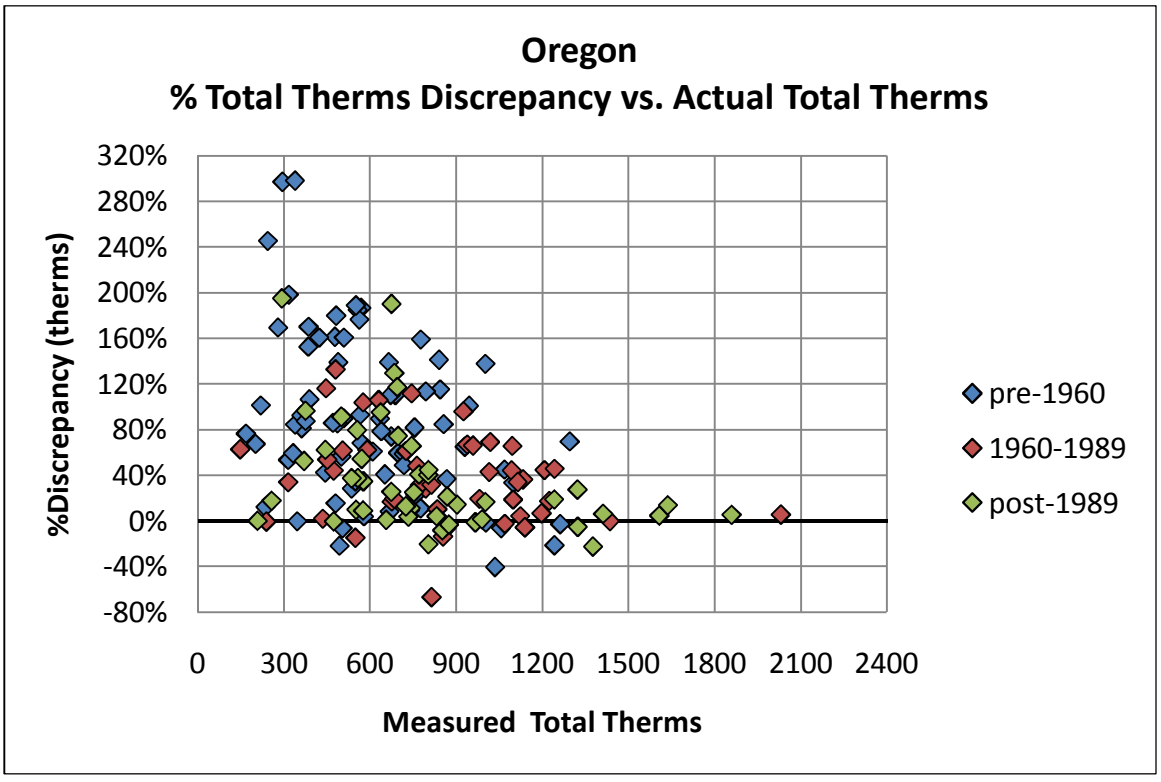

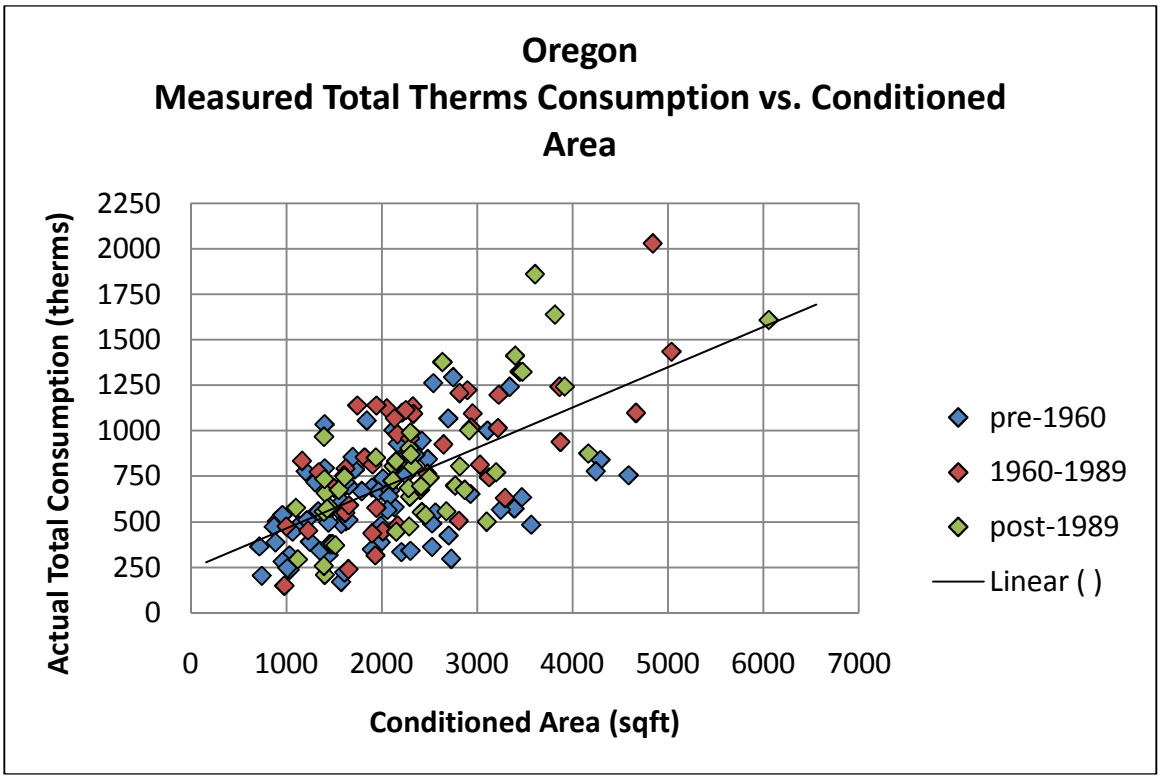
Oregon
Measured Total Therms Consumption vs. Conditioned Area
Actual Total Consumption (therms)
2250
2000
1750
1500
1250
1000
750
500
250
0
0
1000
2000
3000
4000
5000
6000
7000
Conditioned Area (sqft)
pre-1960
1960-1989
post-1989
Linear ( )

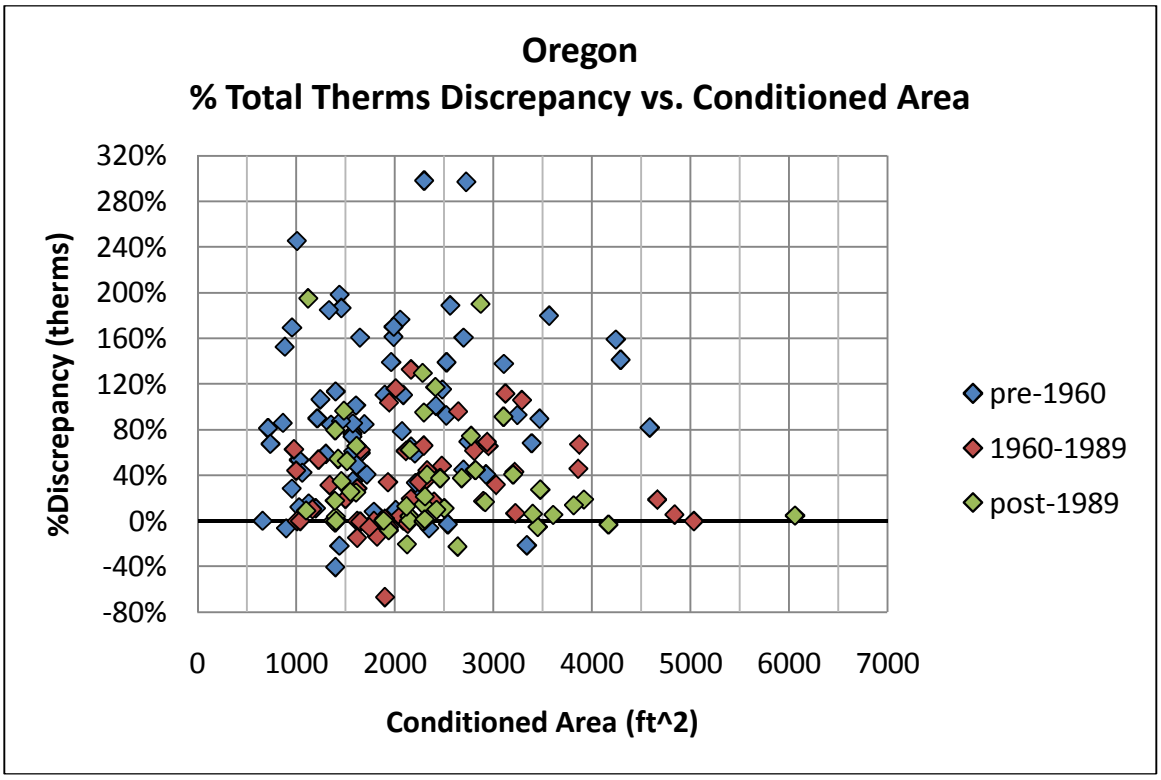
Oregon
% Total Therms Discrepancy vs. Conditioned Area
%Discrepancy (therms)
320%
280%
240%
200%
160%
120%
80%
40%
0%
-40%
-80%
0
1000
2000
3000
4000
5000
6000
7000
Conditioned Area (ft^2)
pre-1960
1960-1989
post-1989

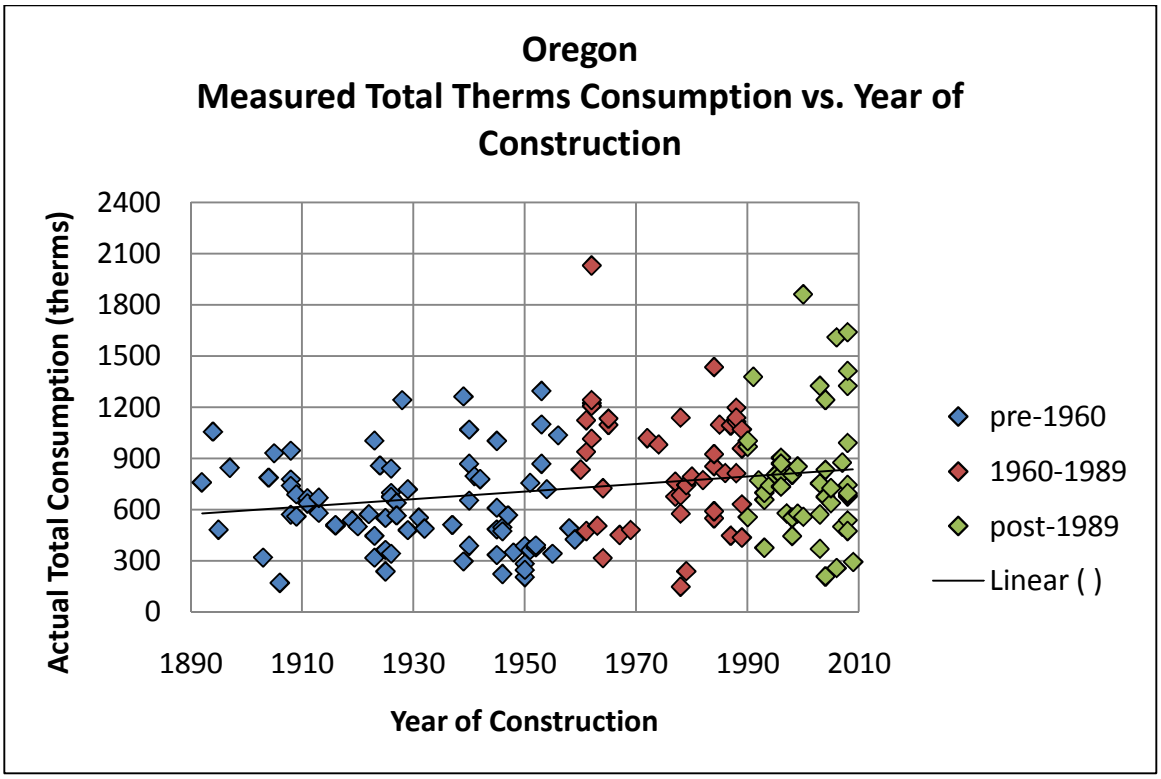
Oregon
Measured Total Therms Consumption vs. Year of Construction
Actual Total Consumption (therms)
2400
2100
1800
1500
1200
900
600
300
0
1890
1910
1930
1950
1970
1990
2010
Year of Construction
pre-1960
1960-1989
post-1989
Linear ( )

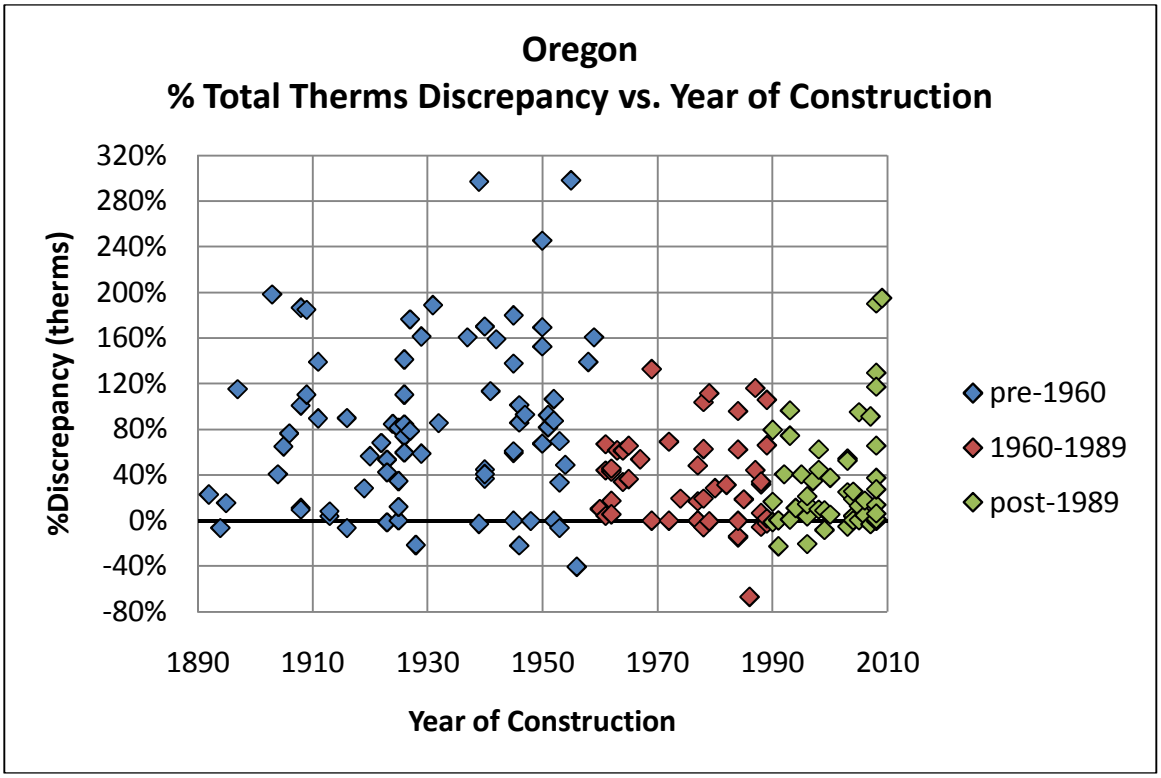
Oregon
% Total Therms Discrepancy vs. Year of Construction
%Discrepancy (therms)
320%
280%
240%
200%
160%
120%
80%
40%
0%
-40%
-80%
1890
1910
1930
1950
1970
1990
2010
Year of Construction
pre-1960
1960-1989
post-1989

APPENDIX C: HOME BASE CASE MODELS - DETAILED HOME OPERATION AND BUILDING CHARACTERISTICS

	Albuquerque	**Atlanta**	**Boston**	**Chicago**	**DC**	**Denver**	**Fort Worth**	**Kansas City**	**Los Angeles**	**Miami**	**Minneapolis**	**New Orleans**	**New York**	**Phoenix**	**San Francisco**	**Seattle**
Con. Area (ft^2)	1739	1620	1620	1557	1643	1734	1493	1487	1722	1643	1487	1493	1804	1734	1722	1722
Tot. Area (ft^2)	2058	1967	1950	1881	1967	2058	1817	1811	2046	1967	1811	1817	2128	2058	2046	2046
Stories	1	1	2	1	1	1	1	1	1	1	1	1	2	1	1	1
Garage	Attached (324 sq ft)															
Rooms	3 Bedrooms															
Bathrooms	1 Bathroom															
Orientation	West															
Neighbor	15 ft from either side															
Htng SP	70° F	75° F	67° F	61° F	75 ° F	70° F	72 ° F	62° F	70 ° F	75° F	59° F	72° F	67° F	70 ° F	70° F	70 ° F
Clng SP	77° F	77° F	76° F	74° F	77° F	77° F	78° F	72° F	73 ° F	77° F	72° F	78° F	78° F	78° F	73° F	73° F
MEL/MGL	1.00 - BA Multiplier															
Nat.Vent.	BA Benchmark															
Win.Wall Ratio	0.12 (F20 B40 L20 R20)															
Win Frame	Aluminum	Aluminum	Wood	Wood	Aluminum	Wood	Aluminum	Aluminum	Aluminum	Aluminum	Wood	Aluminum	Wood	Aluminum	Aluminum	Wood
Glazing Layers	Single Pane Clear Glass; R-value = 0.20 Btu/hr-ft^2-F , SHGC = 0.53															
Wood Stud	2x4,16”o.c. empty –Assembly R-2.2															

	Albuquerque	**Atlanta**	**Boston**	**Chicago**	**DC**	**Denver**	**Fort Worth**	**Kansas City**	**Los Angeles**	**Miami**	**Minneapolis**	**New Orleans**	**New York**	**Phoenix**	**San Francisco**	**Seattle**
Ext. Finish	Gray Wood	Gray Wood	Gray Wood	Gray Wood	Brick	Brick	Brick	Gray Wood	Stucco	Brick	Gray Wood	Brick	Gray Wood	Brick	Stucco	Gray Wood
Roof Material	Med Shingles	Dark Shingles	Dark Shingles	Dark Shingles	Dark Shingles	Dark Shingles	Med Shingles	Dark Shingles	Med Shingles	Med Shingles	Dark Shingles	Med Shingles	Dark Shingles	Med Shingles	Med Shingles	Dark Shingles
Rad. Barrier	None															
Wall Mass	½“ Drywall															
Ceiling Mass	½“ Drywall															
Foundation Type	Slab	4’ Vented Crawlspace	Unfinished Basement	Unfinished Basement	4’ Vented Crawlspace	Slab	Slab	Unfinished Basement	4’ Vented Crawlspace	4’ Vented Crawlspace	Unfinished Basement	Slab	Unfinished Basement	Slab	4’ Vented Crawlspace	4’ Vented Crawlspace
Found. Insul.	None															
Exposed Slab	20% Exposed															
	R-Values (insulation only)															
Wall	0	0	0	0	0	0	0	0	0	0	0	0	0	0	0	0
Ceiling	11	7	20	11	7	11	7	11	11	7	11	7	7	11	11	11
Floor	0	0	0	0	0	0	0	0	0	0	0	0	0	0	0	0
Glass Type	Single Pane ; U-value = 0.869 Btu/hr-ft2-°F ; SHGC = 0.619															
Interior Shade	BA Benchmark															
Eaves	1 foot offset															
Old ACH @50 Pa	1.1 (Bad2)	0.3 (Tight)	0.7 (Bad)	0.7 (Bad)	0.3 (Tight)	1.1 (Bad2)	1.1 (Bad2)	0.7 (Bad)	1.1 (Bad2)	1.1 (Bad2)	0.3 (Tight)	1.1 (Bad2)	0.7 (Bad)	0.4 (Typical)	1.1 (Bad2)	0.4 (Typical)

	Albuquerque	**Atlanta**	**Boston**	**Chicago**	**DC**	**Denver**	**Fort Worth**	**Kansas City**	**Los Angeles**	**Miami**	**Minneapolis**	**New Orleans**	**New York**	**Phoenix**	**San Francisco**	**Seattle**
Mech. Vent.	Exhaust, Spot Vent Only (avg. 6.2 cfm)															
Appliances	Non-ES; Refrigerator: 962 kWh/yr															
Hard Ltg	14% CFL															
Plug-in Ltg	10% CFL															
Heating System	Electric	Electric	Nat. Gas	Nat. Gas	Electric	Nat. Gas	Nat. Gas	Nat. Gas	Nat. Gas	Electric	Nat. Gas	Electric	Nat. Gas	Nat. Gas	Nat. Gas	Nat. Gas
AFUE	0.98	0.98	0.74	0.74	0.98	0.74	0.74	0.74	0.74	0.98	0.74	0.98	0.74	0.74	0.74	0.74
Cooling System	Central															
SEER	8															
Ducts	Typical Average Existing (0.15 Duct Leakage Fraction)															
Water Heater	Elect. Standard Existing	Elect. Standard Existing	Gas Standard Existing	Gas Standard Existing	Elect. Standard Existing	Gas Standard Existing	Gas Standard Existing	Gas Standard Existing	Gas Standard Existing	Elect. Standard Existing	Gas Standard Existing	Elect. Standard Existing	Gas Standard Existing	Gas Standard Existing	Gas Standard Existing	Gas Standard Existing
Water Heater	Standard Gas, Energy Factor 0.484 : Standard Electric , Energy Factor 0.815															

APPENDIX D: PRELIMINARY HOME MODELING ISSUE SENSITIVITY STUDY RESULTS

The modeling issues selected for sensitivity analysis in this research were selected because each one offers potential improvements for EnergyPlus simulations. This section discusses each sensitivity study performed and its findings. Included in the discussion is the purpose, past history, objective, and method to capture and quickly apply each sensitivity study.

Modeling Issue Sensitivity Study Case Summaries

As an overview, a summary of each sensitivity study describes the expected impact of each modeling issue. The sensitivity study summary shows the issues that have the greatest impact on energy consumption. Tests across 16 locations in multiple climates were made to find the overall effect any modeling issue can have, based on the reference home created, found in the previous Appendix. In each city, the impact found from each modeling issue is ranked from highest to lowest. After the ranking is completed for every cities, the modeling issue with the most first place votes is the ranked first, and the remaining topics are ranked in a similar manner.

Heating Impact	
1st	*Duct Leakage*
2nd	**Infiltration Heat Recovery**
3rd	**Shelter Factor – exterior convection**
4th	Shelter Factor - Nat Vent
5th	Shelter Factor - Infiltration
6th	**Insect Screens**
7th	Air gap R-value
8th	Attic Insulation R-value
Cooling Impact	
1st	**Insect Screens**
2nd	**Shelter Factor - exterior convection**
3rd	*Duct Leakage*
4th	Attic Insulation R-value
5th	Air gap R-value
6th	**Infiltration Heat Recovery**
7th	Shelter Factor - Infiltration
8th	Shelter Factor - Nat Vent

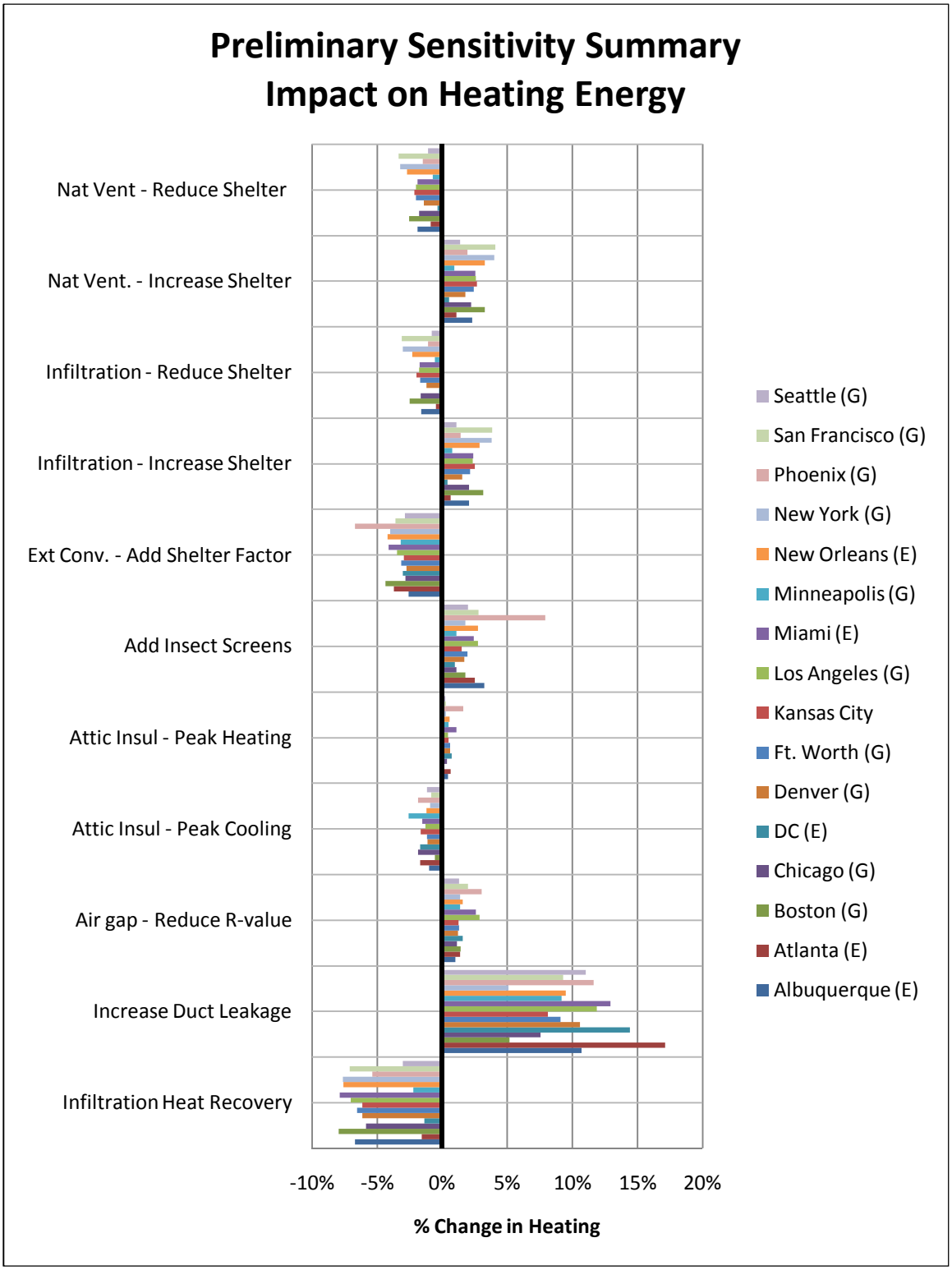
Preliminary Sensitivity Summary
Impact on Heating Energy
Nat Vent - Reduce Shelter
Nat Vent. - Increase Shelter
Infiltration - Reduce Shelter
Infiltration - Increase Shelter
Ext Conv. - Add Shelter Factor
Add Insect Screens
Attic Insul - Peak Heating
Attic Insul - Peak Cooling
Air gap - Reduce R-value
Increase Duct Leakage
Infiltration Heat Recovery
-10%
-5%
0%
5%
10%
15%
20%
% Change in Heating
Seattle (G)
San Francisco (G)
Phoenix (G)
New York (G)
New Orleans (E)
Minneapolis (G)
Miami (E)
Los Angeles (G)
Kansas City
Ft. Worth (G)
Denver (G)
DC (E)
Chicago (G)
Boston (G)
Atlanta (E)
Albuquerque (E)

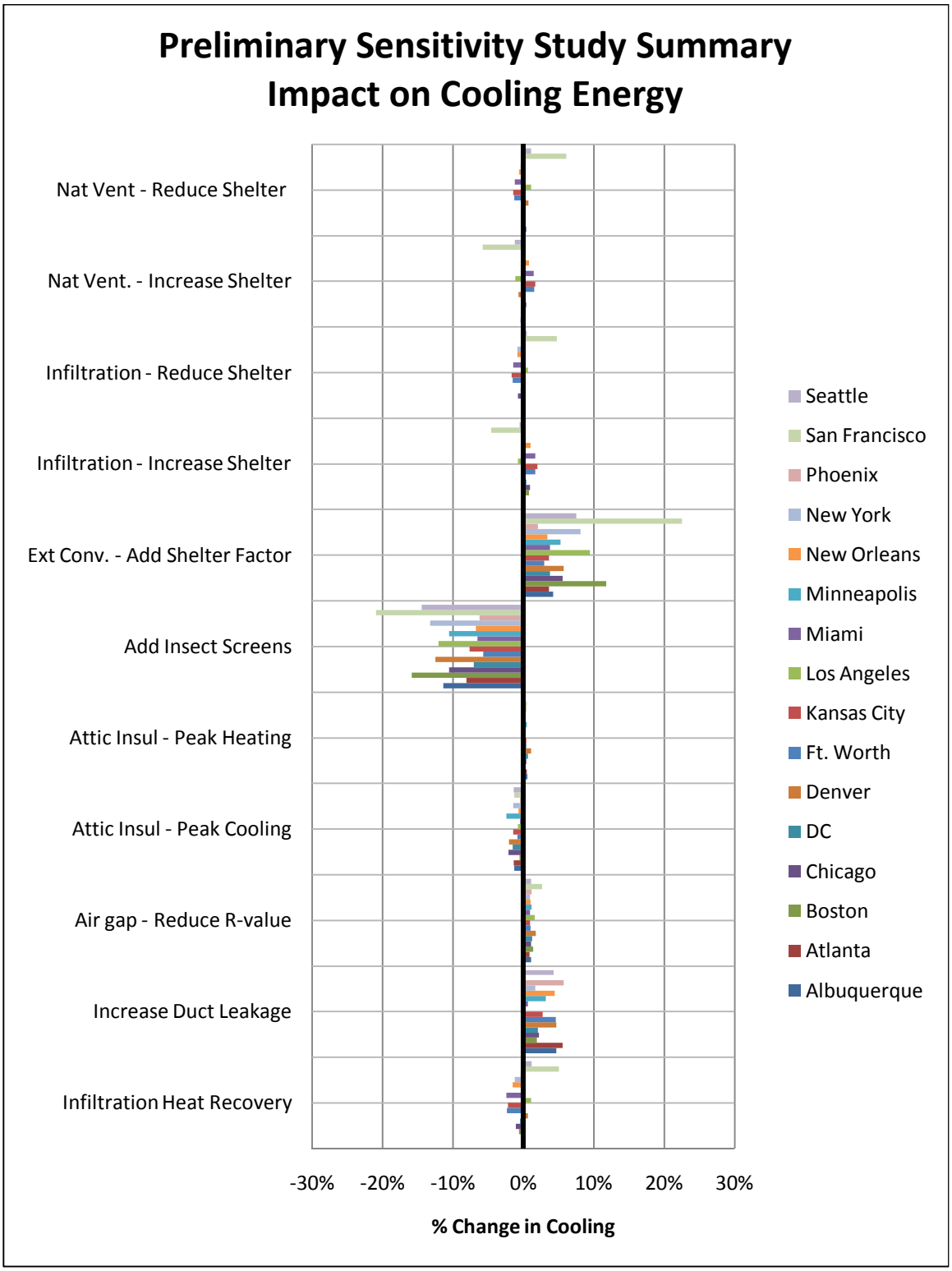
Preliminary Sensitivity Study Summary
Impact on Cooling Energy
Nat Vent - Reduce Shelter
Nat Vent. - Increase Shelter
Infiltration - Reduce Shelter
Infiltration - Increase Shelter
Ext Conv. - Add Shelter Factor
Add Insect Screens
Attic Insul - Peak Heating
Attic Insul - Peak Cooling
Air gap - Reduce R-value
Increase Duct Leakage
Infiltration Heat Recovery
-30%
-20%
-10%
0%
10%
20%
30%
% Change in Cooling
Seattle
San Francisco
Phoenix
New York
New Orleans
Minneapolis
Miami
Los Angeles
Kansas City
Ft. Worth
Denver
DC
Chicago
Boston
Atlanta
Albuquerque

Wind Shelter Factor

Study Objective:

To account for neighboring buildings and surroundings, a wind shelter factor is used to effectively reduce the wind speed based on the amount of shielding provided by the nearby surroundings. Careful selection of this factor is sometimes disregarded, resulting in an incorrect estimate of the local wind speed. Providing the appropriate wind shelter factor is important to provide more accurate wind speed for energy simulation. Wind speed is a major parameter for several key heat balance components. Infiltration and natural ventilation models already have a shelter factor integrated into the calculations. Exterior convection surface coefficients, however, do not account for wind shielding. The use of the local wind speed over predicts the impact wind will have on the surface of the building. Implementing a shelter factor can potentially make a large impact on the envelope performance.

Modeling Approach:

For infiltration calculations, energy simulation tools with an infiltration model have some form of a shelter factor incorporated within the algorithms. The AIM-2 model is well known infiltration model found to have better agreement than the LBL model (Wang, Beausoleil-Morrison, & Reardon, 2009)In EnergyPlus, the infiltration model used for load calculations is the AIM-2 model, where the shelter factor ranges from 0.10 to 0.90. Typically it is modified in increments of 0.1. For a typical home in a suburban neighborhood, the shelter factor would be 0.50. A lower shelter factor should decrease heating while increasing cooling, while a higher shelter factor should increase heating while decreasing cooling.

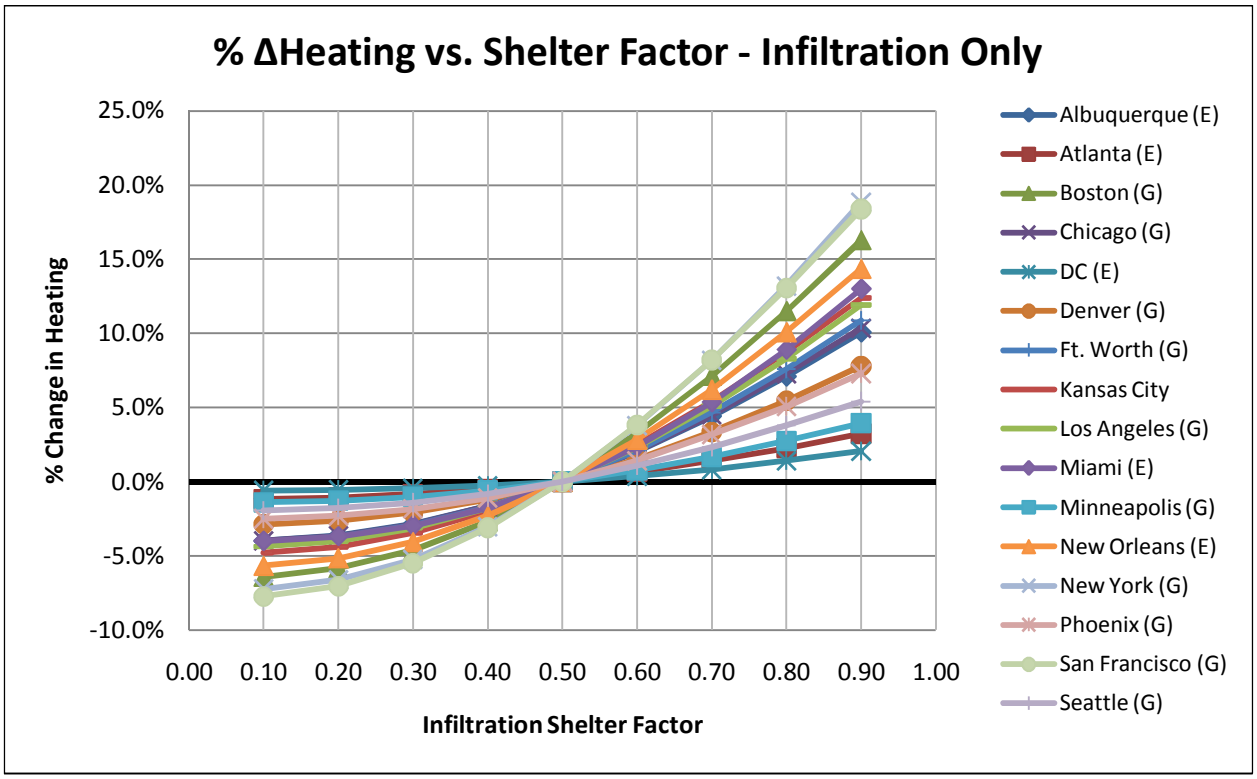
% ΔHeating vs. Shelter Factor - Infiltration Only
% Change in Heating
25.0%
20.0%
15.0%
10.0%
5.0%
0.0%
-5.0%
-10.0%
0.00
0.10
0.20
0.30
0.40
0.50
0.60
0.70
0.80
0.90
1.00
Infiltration Shelter Factor
Albuquerque (E)
Atlanta (E)
Boston (G)
Chicago (G)
DC (E)
Denver (G)
Ft. Worth (G)
Kansas City
Los Angeles (G)
Miami (E)
Minneapolis (G)
New Orleans (E)
New York (G)
Phoenix (G)
San Francisco (G)
Seattle (G)

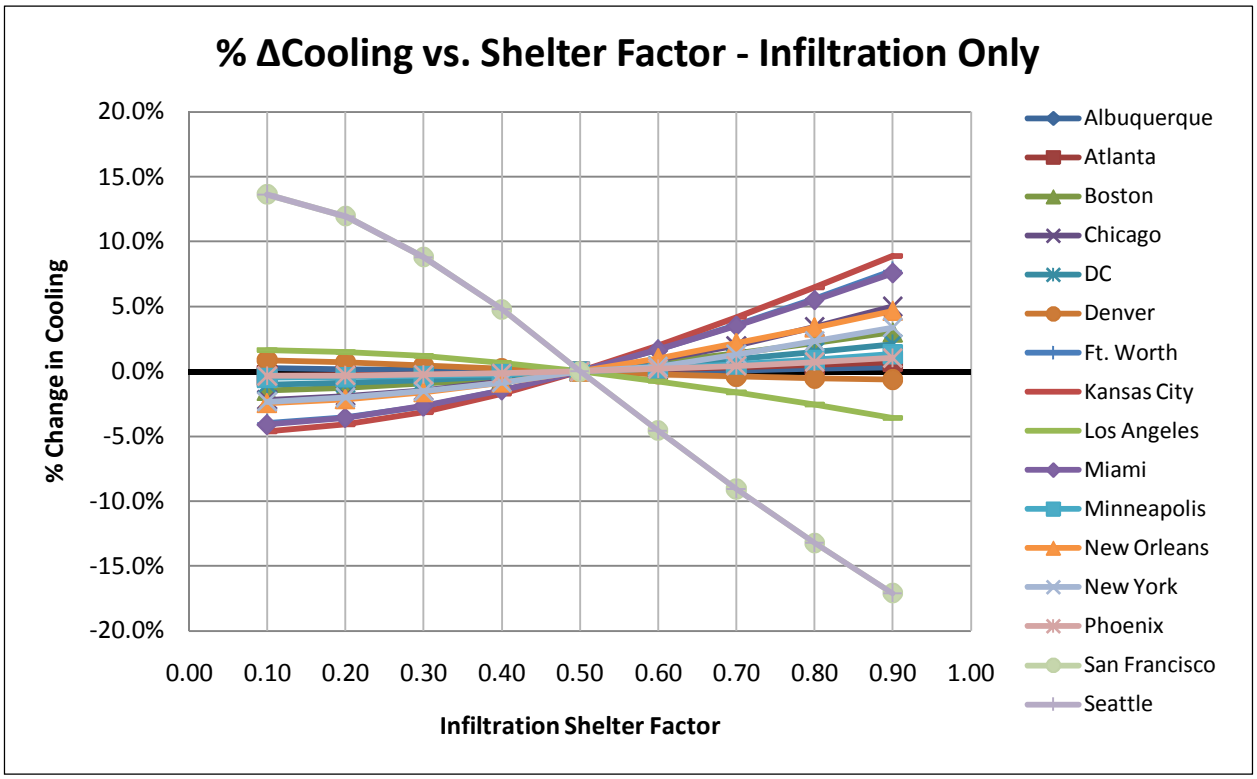
% ΔCooling vs. Shelter Factor - Infiltration Only
% Change in Cooling
20.0%
15.0%
10.0%
5.0%
0.0%
-5.0%
-10.0%
-15.0%
-20.0%
0.00
0.10
0.20
0.30
0.40
0.50
0.60
0.70
0.80
0.90
1.00
Infiltration Shelter Factor
Albuquerque
Atlanta
Boston
Chicago
DC
Denver
Ft. Worth
Kansas City
Los Angeles
Miami
Minneapolis
New Orleans
New York
Phoenix
San Francisco
Seattle

For the natural ventilation algorithm, a local wind shielding coefficient is implemented into the equations. This coefficient is derived using the LBNL infiltration model. The range of coefficient used in this model differs from the AIM2 model. The main reason for the difference in the use of slightly different wind power law equations that convert the wind speed from the weather file to the local wind speed, based on local elevation and terrain classifications. However, when comparing the two models, the coefficients used for each shielding classification differ constantly by a factor or nearly three. Therefore, the scale of the sensitivity study for infiltration can be replicated for natural ventilation load calculations, altering the shielding coefficient 0.03-0.3. The base case is 0.167 (0.5). As the shelter factor is reduced, heating should decrease and cooling increase.

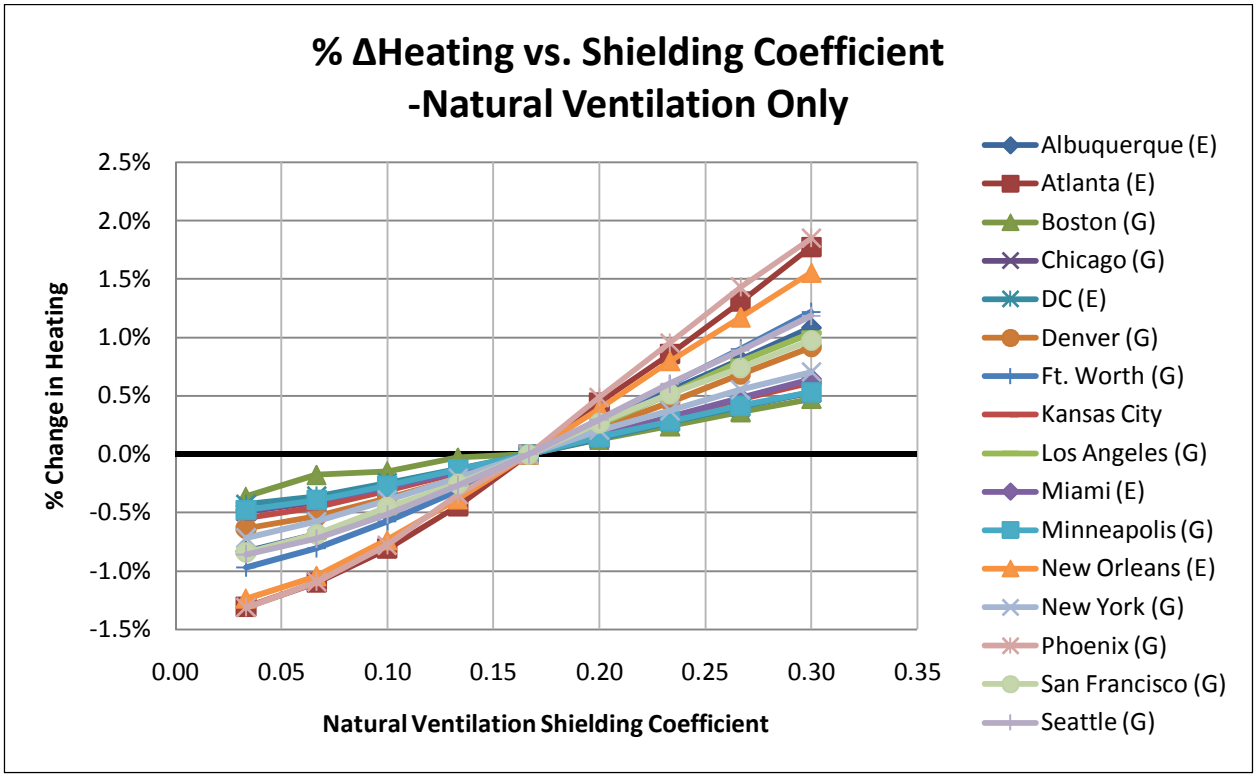

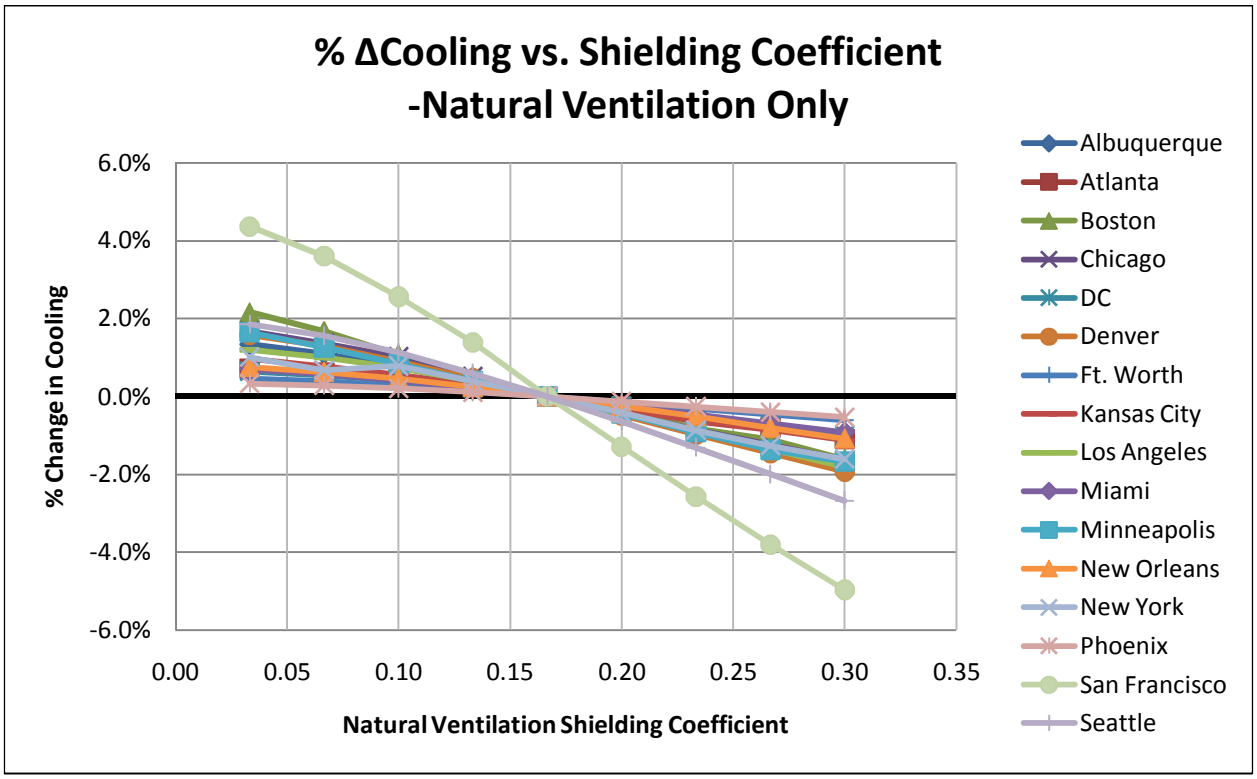

The last analysis is to test the impact of the wind shelter factor when added to into the exterior surface convection coefficients algorithms by implementing a wind shelter factor. There are a number of models available to calculate the coefficient used for the film resistance of exterior walls. For the energy models in this study, the DOE2 algorithm is selected as a common and suitable option, accounting for surface temperatures and the exterior surface roughness. A base case of one is the reference for this sensitivity study, meaning no wind shelter factor is currently implemented. To run parametric simulations, the factor must first be integrated into the simulation. This is not as feasible compared to infiltration and natural ventilation, where a modification of the mass flow rate calculation accounts for the shelter factor. The surface convection coefficient is calculation within the source code, and the adaption of the DOE2 model must be recreated using EnergyManagementSystem to account for the wind shelter factor. Internal variables, such as surface temperature, must be extracted from within the EnergyPlus source code to properly calculate for the coefficients. The sensitivity study is performed in a similar

manner to the infiltration and natural ventilation studies, impacting energy consumption in a similar manner.

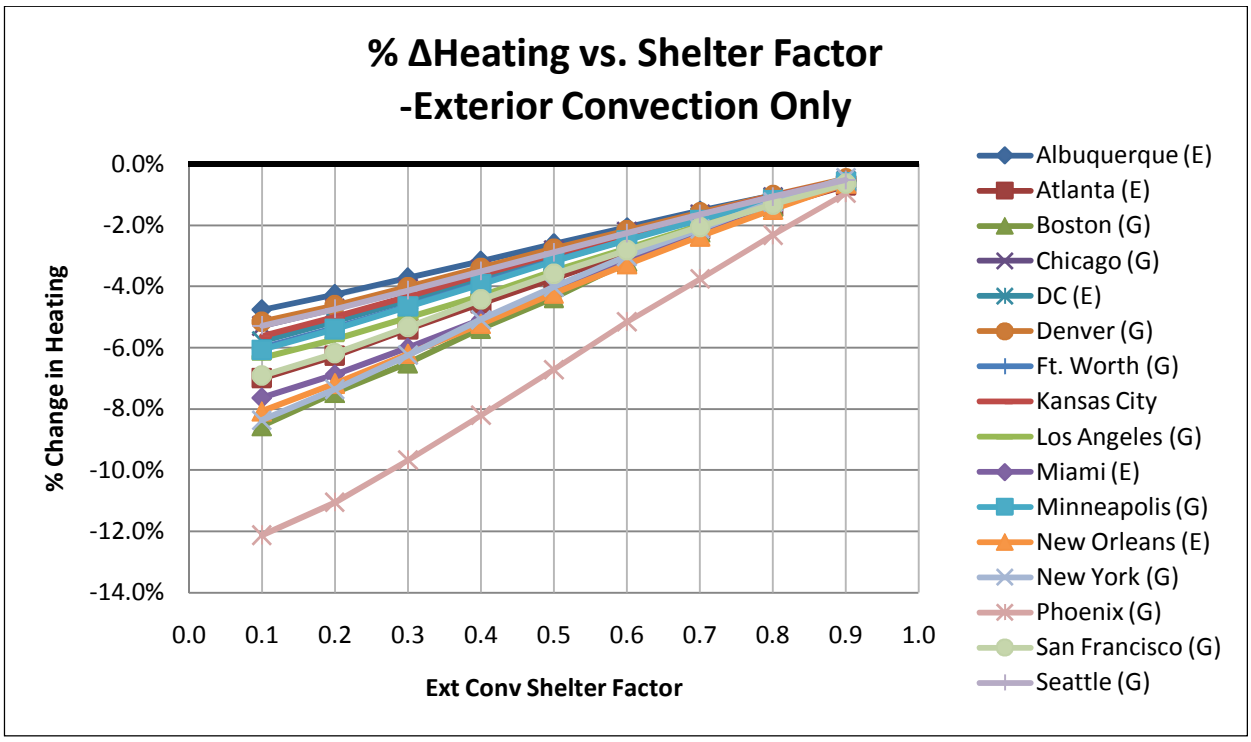

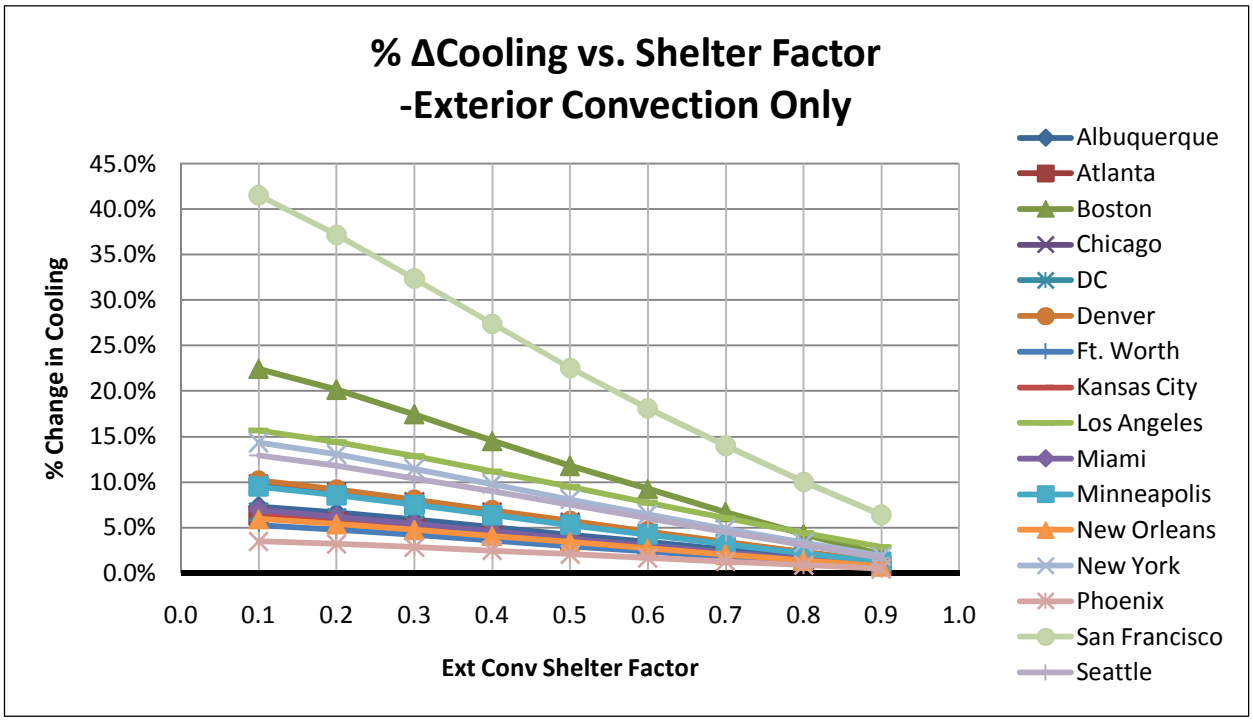

It is necessary to verify that the program written in EMS is able to reproduce the results of the original model in EnergyPlus. Otherwise, the base case energy model produces different results and this sensitivity study cannot be compared effectively to the other modeling issues. First, to verify there is no large discrepancy between the two models, an hourly comparison was done. The percentage change was calculated with respect to the original model, and a histogram was plotted in order determine the size of the discrepancy and number of occurrences throughout the year. The test was performed for the home energy model in Albuquerque. From the histogram, about three quarters of the hours throughout the year show the two models have a discrepancy between -10% to 10% change in the exterior convective coefficients from the original.

It was determined at the time that these are the best results that could be achieved using EMS in EnergyPlus 5.0. The main issue within the development of the Energy Management System relates to reporting of the outputs. Even thought the model uses inputs from one time step to calculate an output, the result is the program reports the variable into the next time step. This causes a fundamental issue each hour in simulation due to fact that the convective coefficients were calculated using weather conditions not matching the time step where the coefficient is being used to solve for the heat balance. This is a limitation in EnergyPlus that prevents that DOE2 convective coefficient algorithm to be replicated, much less with the use of a wind shelter factor. It is determined the remaining discrepancy is due to this and is reason for a change in base case energy consumption.

$$h_n = 1.31 * \Delta T^{\frac{1}{3}} \tag{D1}$$

$$h_{c,glass} = \sqrt{h_n^2 + (a * (\boldsymbol{S_{wo}} * V_{wind})^b)^2} \tag{D2}$$

$$h_t = h_n + R_f * \left(h_{c,glass} - h_n\right) \tag{D3}$$

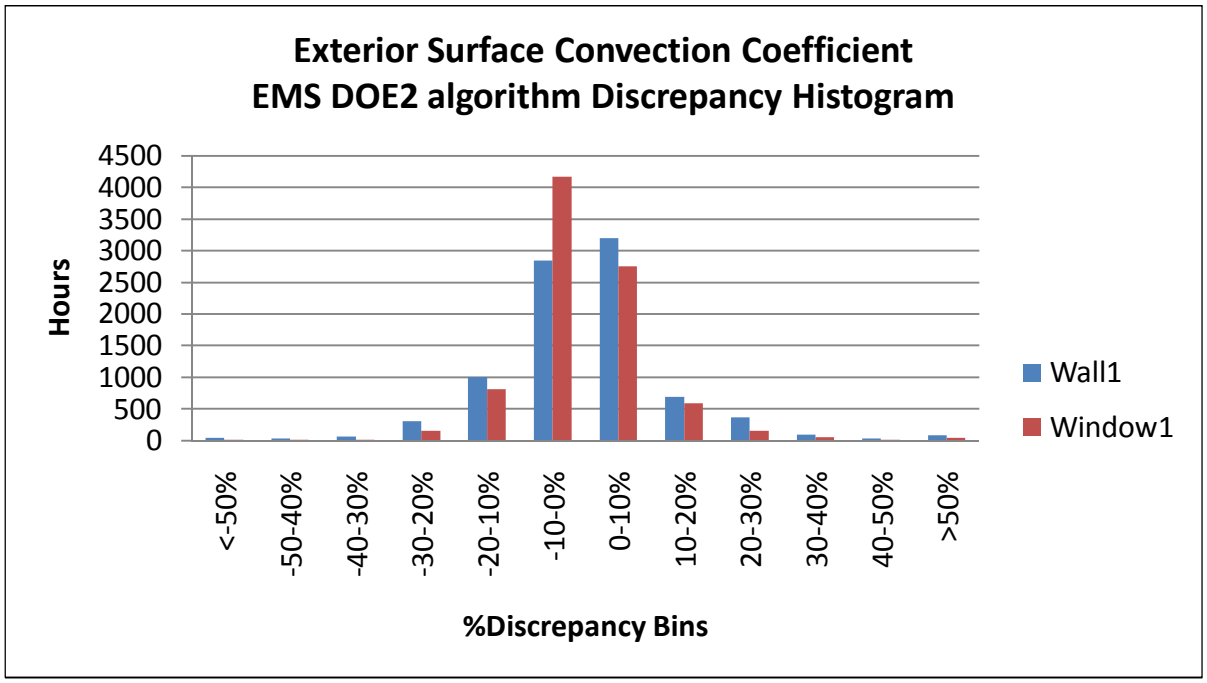
Exterior Surface Convection Coefficient
EMS DOE2 algorithm Discrepancy Histogram
Hours
4500
4000
3500
3000
2500
2000
1500
1000
500
0
<-50%
-50-40%
-40-30%
-30-20%
-20-10%
-10-0%
0-10%
10-20%
20-30%
30-40%
40-50%
>50%
%Discrepancy Bins
Wall1
Window1

Window Insect Screens

Study Objective:

Common residential window design often includes the addition of an exterior window screen designed to prevent insects from entering the homes when windows are opened. Many homes are likely to have insect screens attached to the operable section of windows. Window insect screens are often overlooked parameter in simulation of the building envelope. Research has indicated the importance of window screens when estimating heat transfer through windows. When considering screens as part of the window assembly, one experiment by a group in Ontario has shown an significant improvement in thermal performance and reduction of solar gains with the addition of exterior screens indicated that importance of accounting for insect screens in simulation (Brunger, Dubrous, & Harrison).This is due not only to the screens ability to block the sun, but also to shield the window from wind, reducing the forced convection heat loss on the window surface. The screen provides an improvement to the windows surface film resistance.

Modeling Approach:

To test the impact of windows screens, two methods are performed. EnergyPlus has the capability to account for window screens by including the geometry of the window screen as an attachment to the window assembly. However, windows can only be modeled with one shading device, either a drape, blind, or bus screen. Two or more devices cannot be modeled; this is limitation to the EnergyPlus simulation engine. Typically windows for homes also have a form of a drape or blind for privacy on the interior, also impacting the thermal and solar performance of the window. Additional adjustments are needed to account for both exterior and interior shading devices.

The experimental research in Canada determined exterior insect screens can impact the U-value of a window by 10-30% and SHGC by 45%. This is compared to the effect found when adding a window screen construction to determine both the results in sensitivity study through energy simulation.

EnergyPlus has a set of algorithm to account for the thermal effects of shading devices, both interior and exterior. First, an exterior screen is added to the window assembly by replacing the existing interior drape. Second, the window U-value is reduced by 10% and 30%, and the SHGC is reduced by 45%, to mimic the improvement in thermal performance from insect screens. The window is a single pane clear glass assembly with a base case U-value of 4.93 W/m2-K and a SHGC of 0.53. This can be seen described in the Appendix of the detailed base case energy model descriptions.

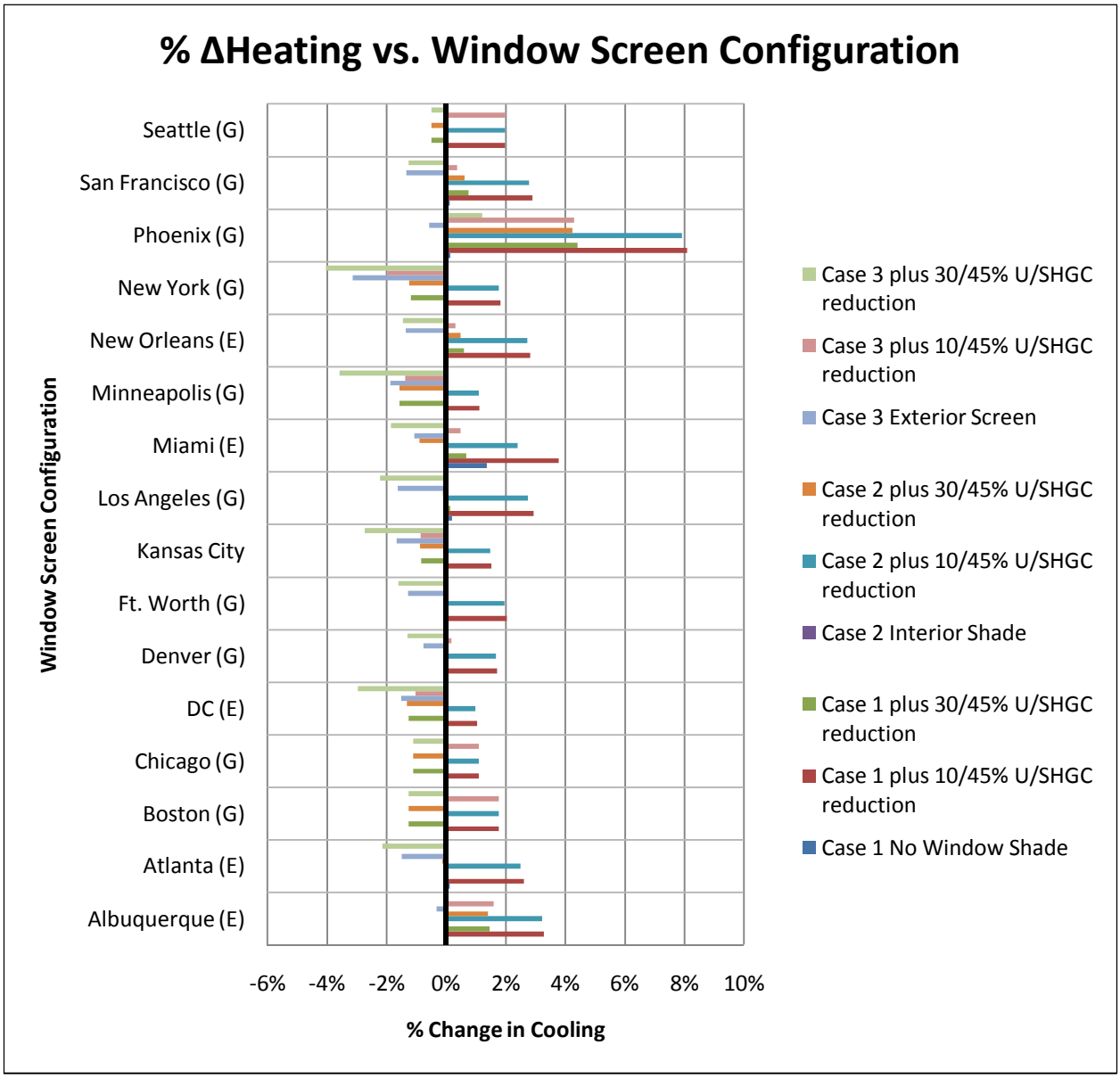

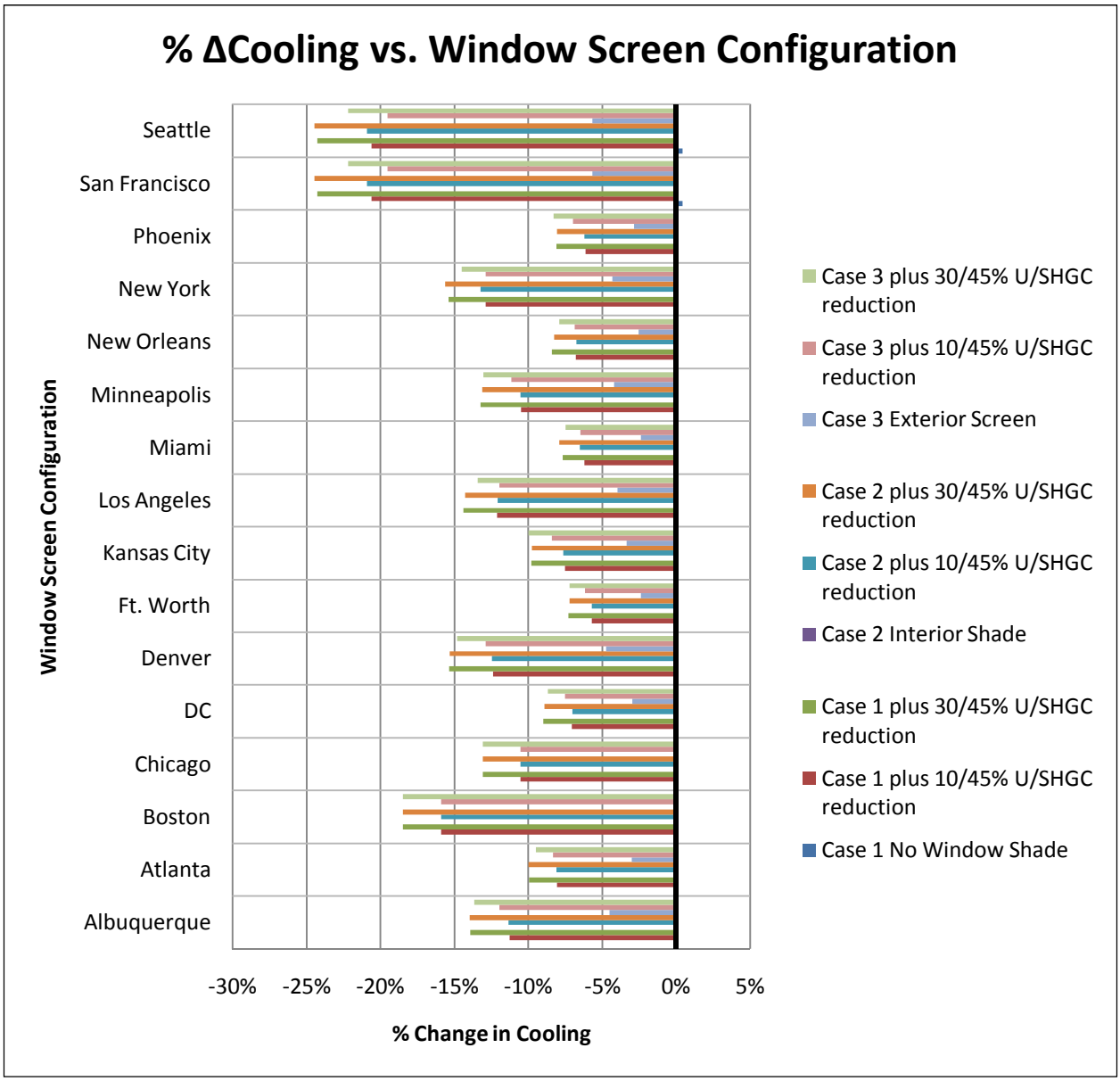
% ΔCooling vs. Window Screen Configuration
Window Screen Configuration
Seattle
San Francisco
Phoenix
New York
New Orleans
Minneapolis
Miami
Los Angeles
Kansas City
Ft. Worth
Denver
DC
Chicago
Boston
Atlanta
Albuquerque
-30%
-25%
-20%
-15%
-10%
-5%
0%
5%
% Change in Cooling
Case 3 plus 30/45% U/SHGC reduction
Case 3 plus 10/45% U/SHGC reduction
Case 3 Exterior Screen
Case 2 plus 30/45% U/SHGC reduction
Case 2 plus 10/45% U/SHGC reduction
Case 2 Interior Shade
Case 1 plus 30/45% U/SHGC reduction
Case 1 plus 10/45% U/SHGC reduction
Case 1 No Window Shade

Temperature Dependent Insulation Performance – Attic Insulation

Study Objective:

Testing for the thermal conductivity of insulation follows standardized testing conditions based on average temperature and temperature gradient (ASTM). Home insulation product ratings are based on an average temperature of 75 °F and a temperature differential of 50 °F, with a confidence interval of ± 10 °F (CFR). These test conditions do not usually mimic the conditions found for homes. Thermal conductivity is one driving force in determining R-value for insulation. However, material conductivity changes with the temperature. The rated value of residential insulation may be different than the actual installed insulation R-value due to changing temperature condition. Models currently use a single R-value insulation rating in annual simulation. What is not taken into account with this method is the change that occurs as the temperature gradient changes across the insulation. A change in temperature will affect the material's thermal performance. Relative to the rated conditions of insulations, a lower average temperature will lower the thermal conductivity, improving thermal performance, while a higher average temperature will increase its thermal conductivity, decreasing thermal performance. Since the indoor temperature of homes are always designed to be maintained around comfort conditions, the driving parameter in modifying the performance of insulation if the climate. Homes in theory would perform better in colder climates and worse in hot climates due to this.

Modeling Approach:

Ideally, the most effective way to model variable thermal conductivity is by the use of conduction finite difference (CFD) modeling method which will take into account the transient effect of the temperature of insulation and other materials in the wall or ceiling section.

Research has shown there to be increase in cooling energy in hot climates after calculating the actual thermal performance of the walls roofs. In existing homes, the attic is always subject to some level of insulation, while older homes may not have insulation within the wood frame envelope. For the

sensitivity study, cellulose insulation is assumed to be the type of insulation used. Levels of insulation are defined according to the base case energy model definition.

To feasibly and quickly find the new resistance of insulation accounting, for outdoor weather, a trend for conductivity is created based on the outdoor temperature. This trend uses a coefficient that defined the change in conductivity with change in temperature. Recalculate the thermal conductivity of the attic insulation to represent the range of R-values possible in the climate tested. Calculating the range of mean ceiling temperatures possible using the heating and cooling set points and the peak heating and cooling outdoor temperatures. Thermal conductivity can be calculated using a simple linear equation of conductivity as a function of mean ceiling temperature. Assuming the indoor temperature set points are maintained constant, then the conductivity will become a function of outdoor temperature, assuming the outdoor temperature equals the attic space temperatures.

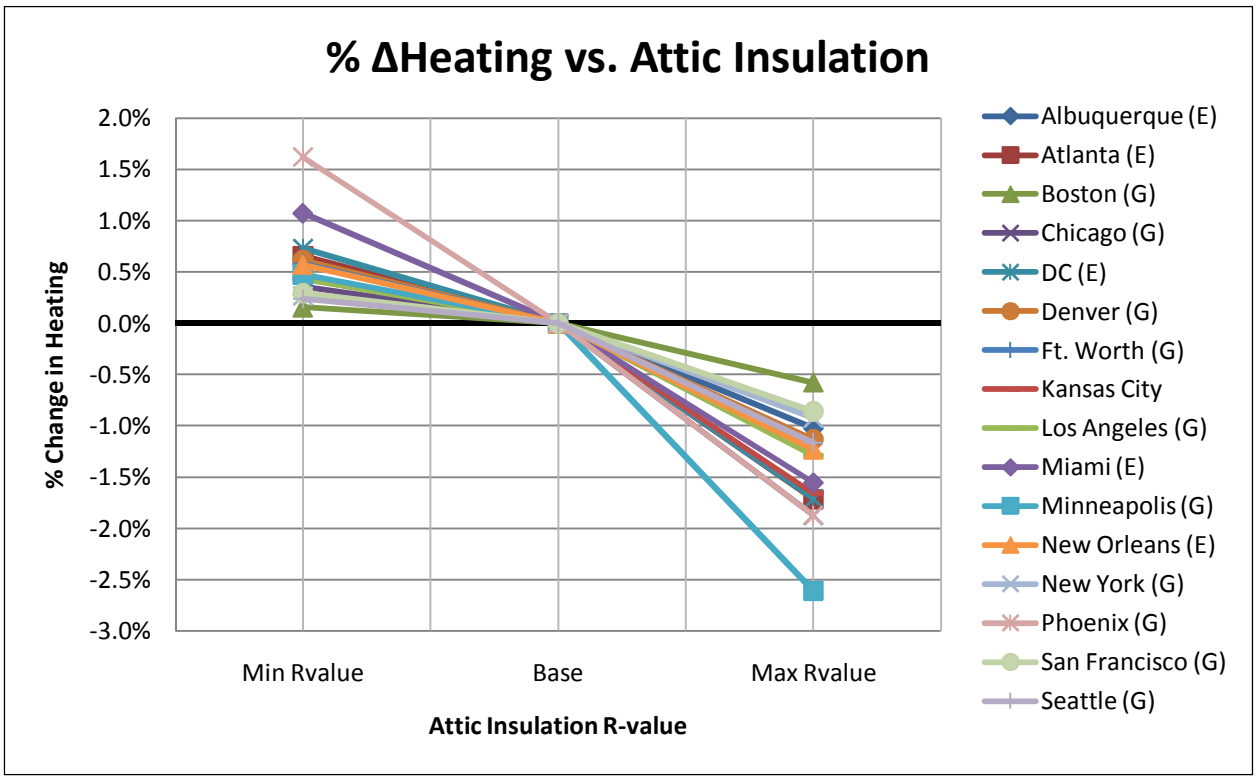

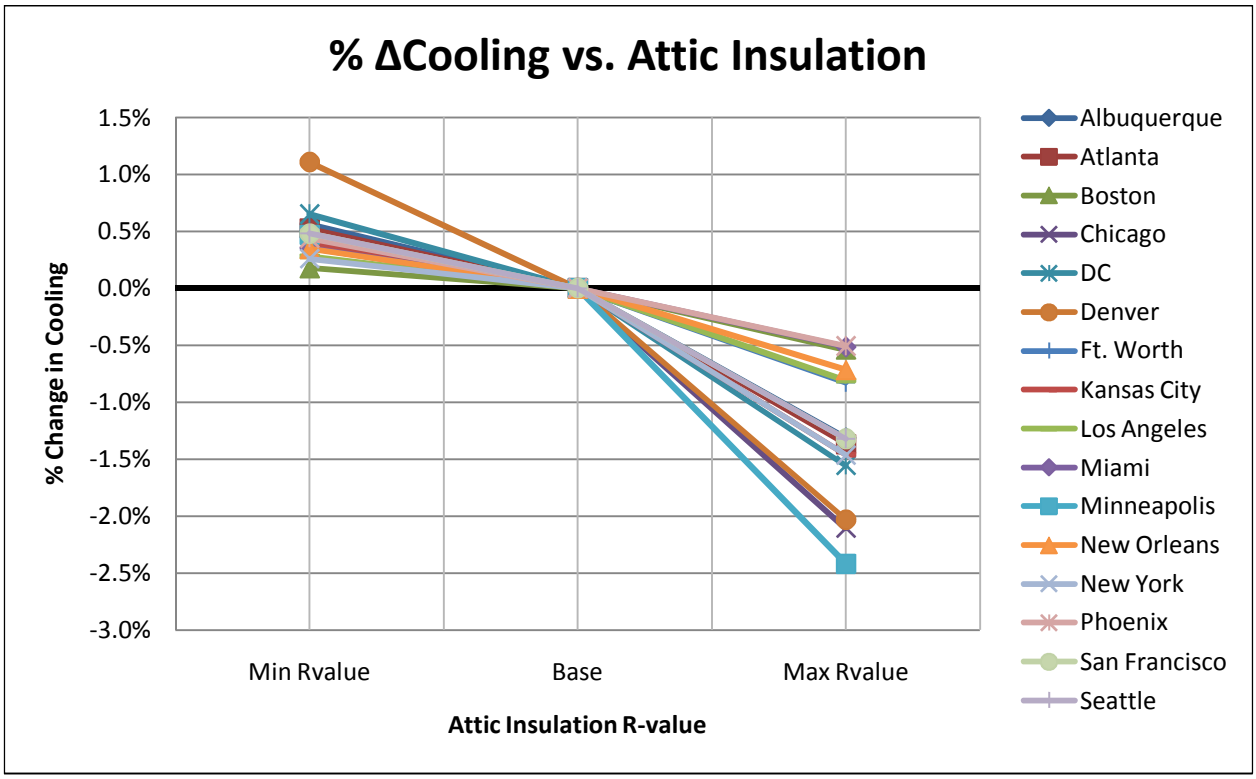
% ΔCooling vs. Attic Insulation
1.5%
1.0%
0.5%
0.0%
-0.5%
-1.0%
-1.5%
-2.0%
-2.5%
-3.0%
% Change in Cooling
Min Rvalue
Base
Max Rvalue
Attic Insulation R-value
Albuquerque
Atlanta
Boston
Chicago
DC
Denver
Ft. Worth
Kansas City
Los Angeles
Miami
Minneapolis
New Orleans
New York
Phoenix
San Francisco
Seattle

Thermal Performance of Uninsulated Wall Assembly – Air Gap R-value

Study Objective:

Older homes are more likely to have exterior walls with air gaps due to little or no existing insulation. The R-value for air is based on the indoor and outdoor temperatures. Air provides good conductive resistance as long as there is no air movement, such as infiltration. Once air is introduced, the resistance of air can reduce to increased forced convection. These conditions are unknown within existing walls, making it hard to determine the proper R-value for the air gap within an empty wall cavity.

Modeling Approach:

In the model the depth and R-value of the cavity within the wall can be defined to specify the cavity's thermal properties, based on the ASHRAE handbook. As defined in the base case energy models, the air gap depth is set to a 3.5 inch air gap with a total R-value of 1.2. In this test, the R-value is adjusted in 0.1 increments to test the impact on energy consumption. The range in R-value tested goes from 0.9-1.5 to represent the range that the air gap is thought to be able to change. ASHRAE provides a list of realistic R-values for air gaps. Based on a 3.5 in gap for a vertical wall, ASHRAE publishes a range of R-values based on the average temperature and temperature differential, ranging from 0.9 to 1.5.

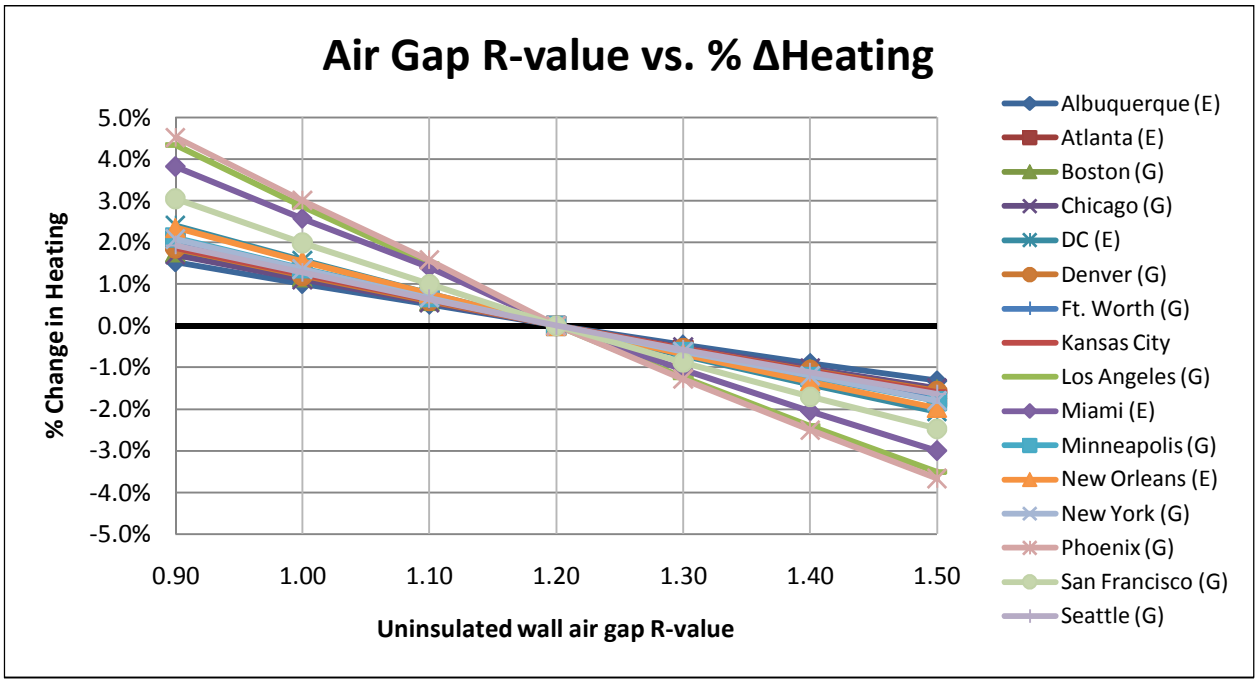
Air Gap R-value vs. % ΔHeating
% Change in Heating
5.0%
4.0%
3.0%
2.0%
1.0%
0.0%
-1.0%
-2.0%
-3.0%
-4.0%
-5.0%
0.90
1.00
1.10
1.20
1.30
1.40
1.50
Uninsulated wall air gap R-value
Albuquerque (E)
Atlanta (E)
Boston (G)
Chicago (G)
DC (E)
Denver (G)
Ft. Worth (G)
Kansas City
Los Angeles (G)
Miami (E)
Minneapolis (G)
New Orleans (E)
New York (G)
Phoenix (G)
San Francisco (G)
Seattle (G)

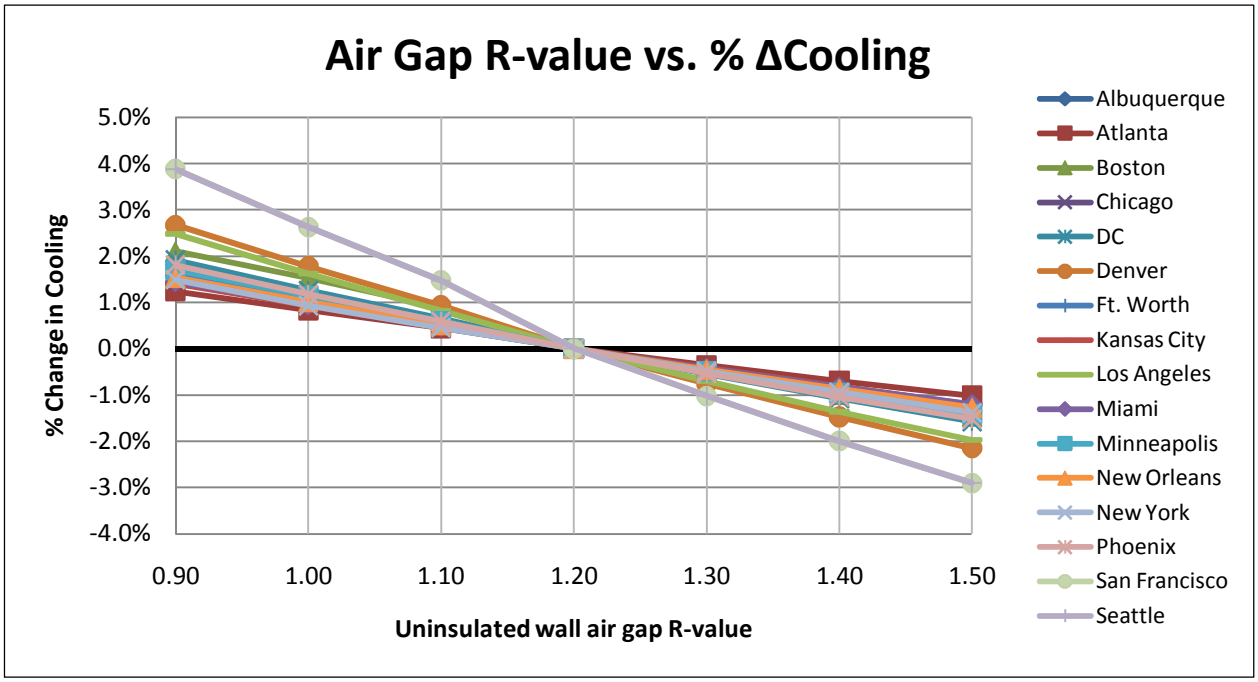
Air Gap R-value vs. % ΔCooling
% Change in Cooling
5.0%
4.0%
3.0%
2.0%
1.0%
0.0%
-1.0%
-2.0%
-3.0%
-4.0%
0.90
1.00
1.10
1.20
1.30
1.40
1.50
Uninsulated wall air gap R-value
Albuquerque
Atlanta
Boston
Chicago
DC
Denver
Ft. Worth
Kansas City
Los Angeles
Miami
Minneapolis
New Orleans
New York
Phoenix
San Francisco
Seattle

Duct Leakage

Study Objective:

Space heating and air conditioning system are a major component of home energy consumption. Duct air distribution systems are the most commonly used method in homes to distribute conditioned air. For homes with space heating, 62% of systems installed are central warm-air furnaces. For homes with space cooling, 72% of systems installed are central air-conditioners (U.S. EIA, 2008). Accurately assessing the losses that occur in ductwork are important to predict the energy consumption. Duct leakage is a common parameter used to assess energy losses to an unconditioned space.

In simulation, duct leakage does not account for the impact made on the air infiltration load. An important component to simulate, duct leakage can account for a large loss of energy in a home. Duct leakage can cause a pressure imbalance in the space between the supply and return ducts. Depending on the location of leakage, this can effectively pressurize or depressurize the conditioned space. Currently, this interaction is not taken into account. Research has shown infiltration to increase in a home operating a ducted air system. Currently, a constant pressure differential is used in infiltration calculations to account for the average pressure differential that exists under natural conditions, but that pressure change is able to increase dramatically when the HVAC system is running, increasing the infiltration load.

Modeling Approach:

In simulation there has been little development of models available to calculate the energy impact of duct leakage. Included is the lack of a correlation to account for the impact on infiltration due to the pressurization or depressurization in the conditioned space. Before any models is tested, the sensitivity of duct leakage initially to understand its impact on energy consumption. Currently, duct leakage in a home is defined with using a leakage fraction for both supply and return ducts. The base case models in the Appendix define a default of 0.15 duct leakage fraction. The leakage is tested by altering the duct leakage

fraction for ducts by 0.05 increments, maintaining the ratio of 90% supply and 10% return leakage. A duct leakage model in development at NREL is used to test the sensitivity of duct leakage in EnergyPlus.

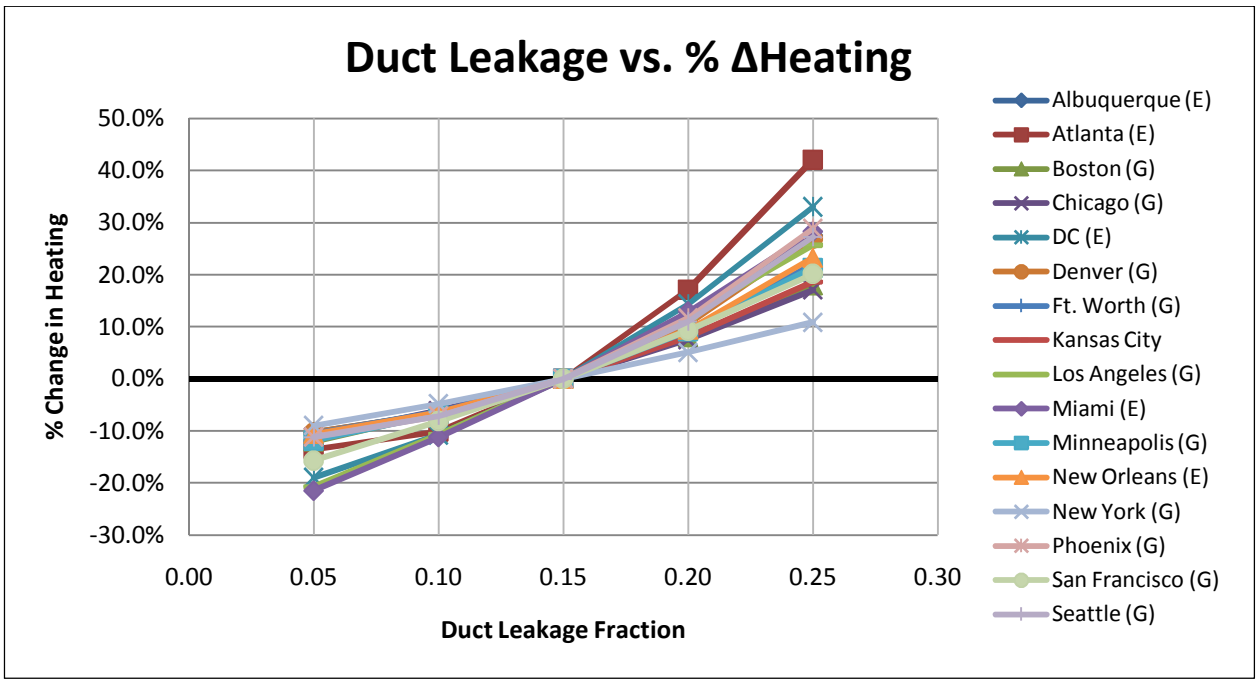

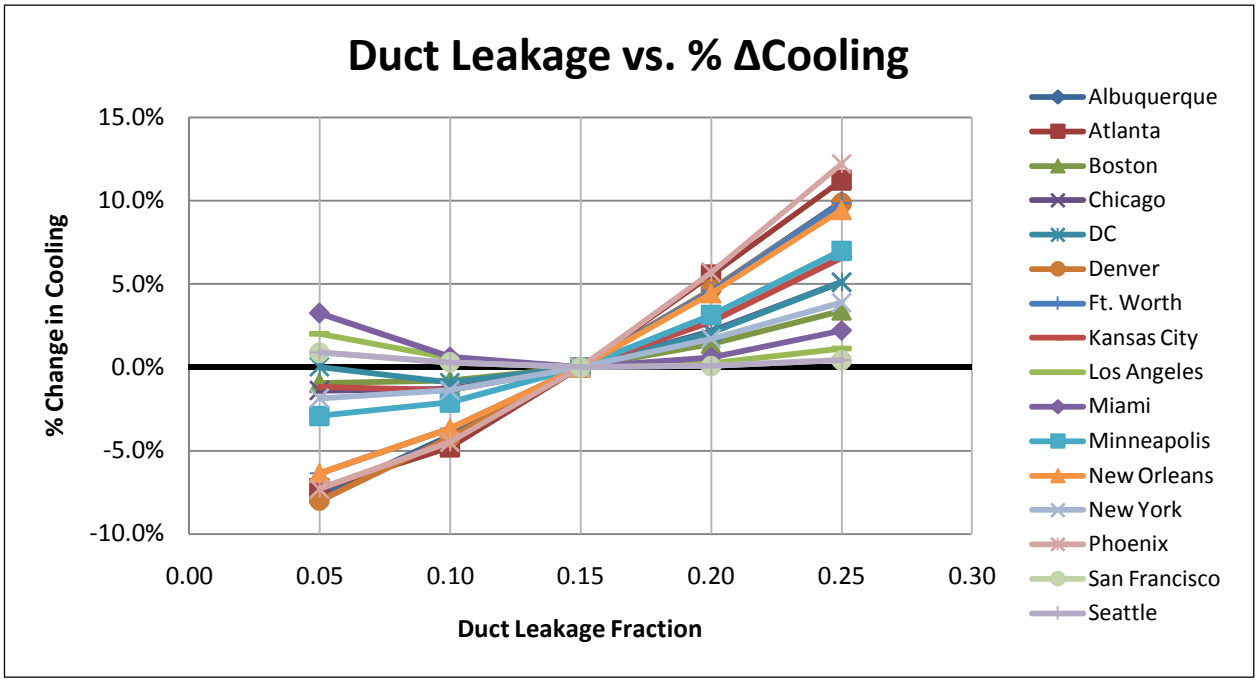

Infiltration Heat Recovery

Study Objective:

Research has found an interaction in the building physics between air infiltration and a wall the air is moving through. Infiltrating heat recovery (IHR) occurs as air exchanges heat with the wall, primarily conduction heat transfer, during infiltration. This causes not only the walls thermal profile to change, but the air to warm or cool before it enters the building. Factors such as the location, area, and length of the leaks in the walls in addition to the level of infiltration are needed determine the IHR within the walls. Current calculation methods of infiltration do not account for the heat exchange between the wall and infiltrating air. In theory, IHR would reduce the estimated energy impact from infiltration. This impact would be greater for older homes due to generally higher levels of infiltration typically found.

Modeling Approach:

Infiltration heat recovery impacts the temperature boundary of the wall, however, past models have assumed conduction heat transfer is not impacted and all changes can represented by a change in the infiltration load. As a quick and feasible method to account for IHR, the mass flow rate is reduced to account for IHR. Although this does not physically represent the impact made to heat recovery, mathematically this provides the same solution, under steady-state conditions. To accomplish in within the infiltration models, a reduction of the mass flow coefficient values in the conditioned zone garage is done to mimic the impact of IHR. For the preliminary sensitivity analysis, this is done through a reduction of the specific leakage area (SLA). In heating and cooling climates, the energy consumption is expected to reduce. However, as can be seen in the next graphs, cooling loads for certain climates increases when accounting for IHR.

The climates where this impact was found all possess very mild summers, where very little cooling is used. It is suspected for a portion of the cooling season, the indoor set point temperature is higher than the outdoor temperature. Under these conditions, the infiltration air is beneficial to the home

because it provides all or a portion of the cooling load. Accounting for IHR signifies these conditions are occurring less than thought under traditional calculations, causing an increase in cooling. Below are equations showing the changes done to mimic IHR with the AIM-2 infiltration model.

$$\dot{Q}_{inf} = \sqrt{(\mathbf{c} * C_s * (\Delta T)^n)^2 + (\mathbf{c} * C_w * (s_w * V_{wind})^{2n})^2} \quad \text{(D4)}$$

$$c = (\mathbf{SLA_{new}} * A_{floor}) * (\frac{2}{\rho_{out}})^{0.5} * \Delta\rho_{ref}^{(0.5-n)} \quad \text{(D5)}$$

$$\mathbf{SLA_{new}} = SLA * (1 - \boldsymbol{f}) \quad \text{(D6)}$$

A factor ranging from 10% - 90% is applied to the SLA of the wall and garage to test the full range of heat recovery. Research through experiments, has shown low infiltration rates and long wall leakage paths attribute to high levels of IHR, as high as 80% (Bhattacharyya & Claridge). However, for a typical existing home, the impact of infiltration heat recovery is expected to at an order of up to 20% (Claridge & Bhattacharyya) (Buchanan & Sherman).

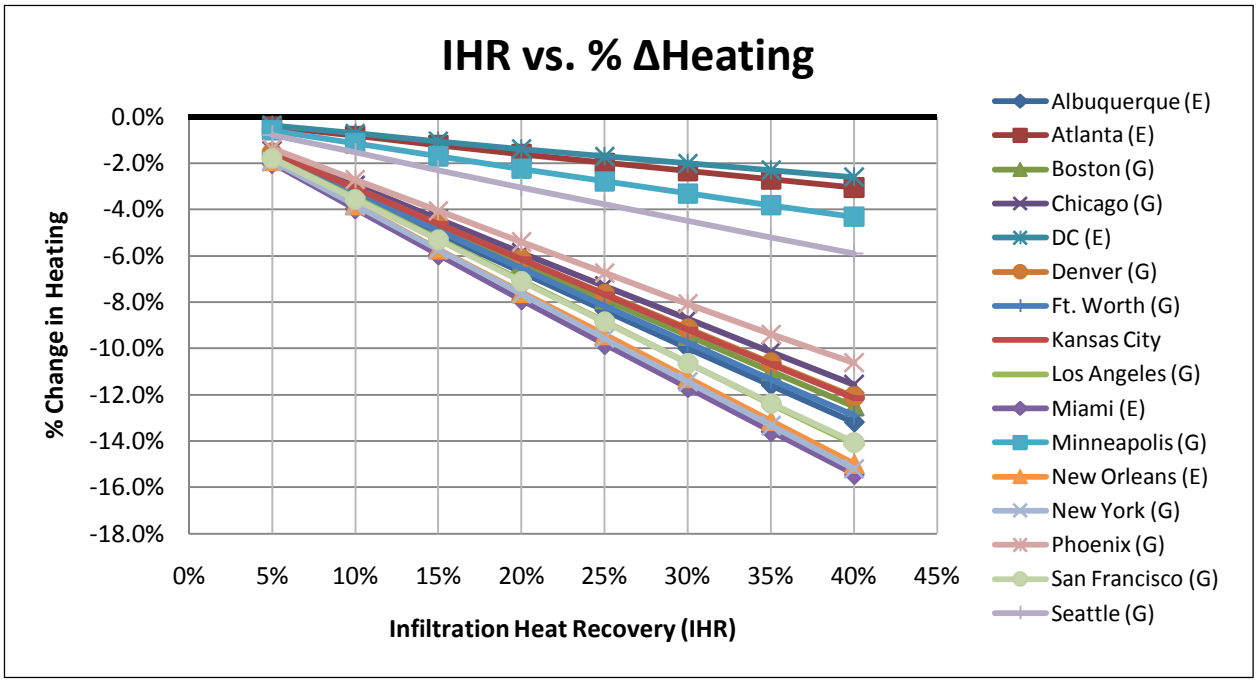

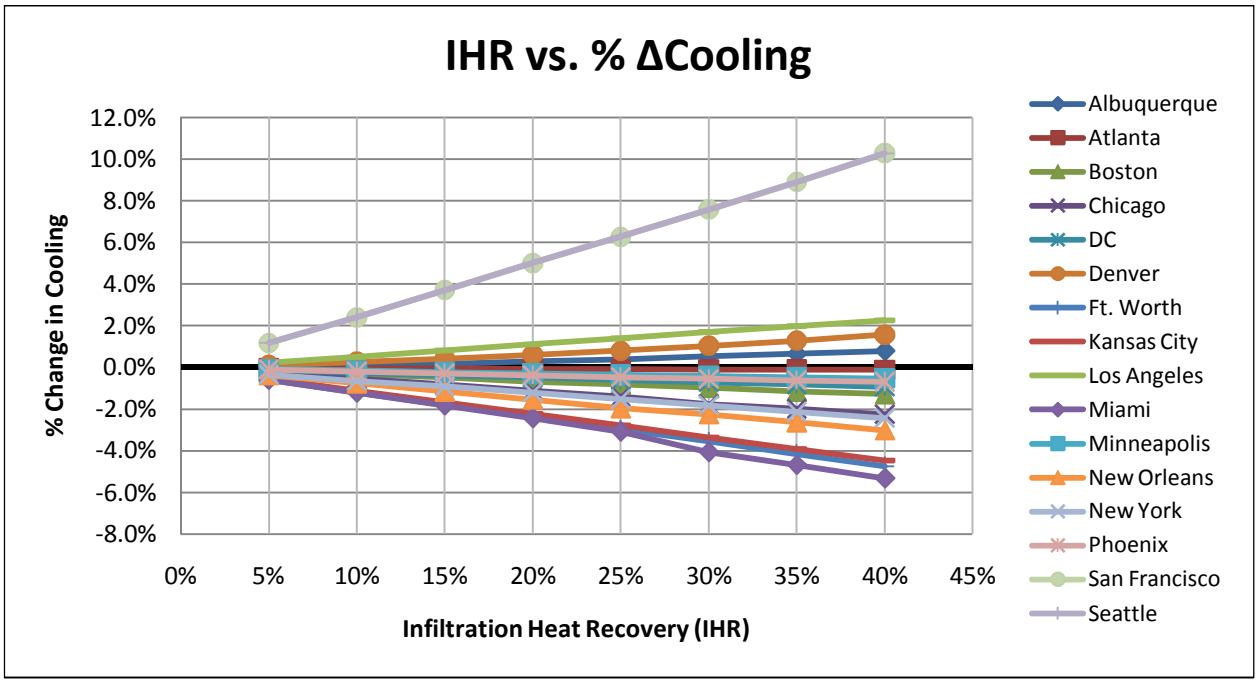
IHR vs. % ΔCooling
% Change in Cooling
12.0%
10.0%
8.0%
6.0%
4.0%
2.0%
0.0%
-2.0%
-4.0%
-6.0%
-8.0%
0%
5%
10%
15%
20%
25%
30%
35%
40%
45%
Infiltration Heat Recovery (IHR)
Albuquerque
Atlanta
Boston
Chicago
DC
Denver
Ft. Worth
Kansas City
Los Angeles
Miami
Minneapolis
New Orleans
New York
Phoenix
San Francisco
Seattle

APPENDIX E: INFILTRATION HEAT RECOVERY MODEL DERIVATION

The five steady-state models in the literature search have been adjusted to provide comparison to the reference model selected. The reference model is selected as the earliest steady state solution found in literature, and the other models will be compared for any differences in their methodologies. Shown first are the equations step by step taken to solve for infiltration heat recovery across all models. Second are the equations unique to each of the model in this study used to derive each solution. Third and final is summary of the final equations used to quantify infiltration heat recovery.

Infiltration Heat Recovery Model Methodology

For any given wall, conduction and infiltration make up total heat balance used in each model. Assuming steady-state conditions, no energy is created or stored, so the energy entering and exiting the wall must equal. The total heat balance will be constant under steady state conditions. Differentiating the energy balance equation we can solve for the temperature of the wall. To minimize the number of variables that occurs in this energy balance

$$q_{total} = q_{conduction} + q_{infiltration} \tag{E1}$$

$$q_{wall\ total} = -k\frac{dT}{dx} - \dot{m}\ C_p\ (T\ (x) - T_{ref}) \tag{E2}$$

$$T(x)\ and \frac{dT}{dx}$$

$$E_{in} - E_{out} + E_{generated} + E_{stored} = 0 \tag{E3}$$

$$q'_{walltotal} = 0; T_{ref} = Constant$$

$$0 = -k\frac{d^2T}{dx^2} - \dot{m}C_p\frac{dT}{dx} \tag{E4}$$

$$\dot{m}\ C_p = \frac{k\ Pe}{d}$$

$$\frac{d^2T}{dx^2} + \frac{Pe}{d}\frac{dT}{dx} = 0 \tag{E5}$$

To solve for the temperature using this second order differential equation, the general solution will be in form seen next. To solve for the function of temperature, the boundary conditions must be

defined. Assuming there is impact on temperature from the surface film resistance, the temperature at both the inside surface and outside surface of the wall are assumed to be at the air temperature.

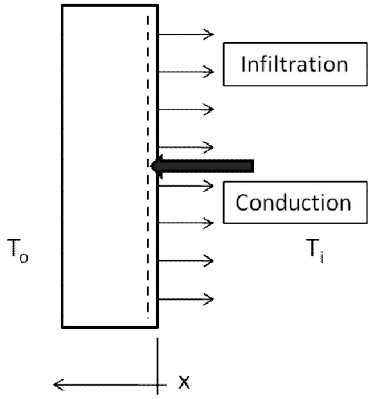

$$T(x) = Z_1 e^{-Pe\frac{x}{d}} + Z_2 \quad \text{(E6)}$$

$$T(0) = T_i = Z_1 + Z_2 \quad \text{(E7)}$$

$$T(d) = T_o = Z_1 e^{-Pe} + Z_2 \quad \text{(E8)}$$

$$\frac{dT}{dx} = -Pe\, Z_1\, e^{-Pe\frac{x}{d}} \quad \text{(E9)}$$

$$\theta(\xi) = \frac{T_x - T_o}{T_i - T_o} \quad \text{(E10)}$$

$$\xi = \frac{x}{d}$$

$$Pe = Re * Pr \quad \text{(E11)}$$

$$Pe = \frac{\rho * L * V}{\mu} * \frac{C_p * \mu}{k}$$

$$Pe = \frac{\rho * V * C_p}{\frac{k}{d}} = \frac{\frac{\dot{m}}{A} * C_p}{U} \quad \text{(E12}$$

$$Pe = \frac{\dot{m} C_p}{UA}$$

Solution for Wall Temperature

Solve for T(x) and dT/dx using the general solution defined above. The constants Z_1 and Z_2B are found by evaluating the boundary conditions of the wall. The temperature of the wall surfaces will change whether evaluating the equation at the reference conditions or when accounting for the film resistances of the wall. The solution for temperature is used to solve for the heat balance to a wall and a space. The conventions for the wall and space will be shown along with the matching heat balance solutions used to solve for infiltration heat recovery.

Infiltrating Wall

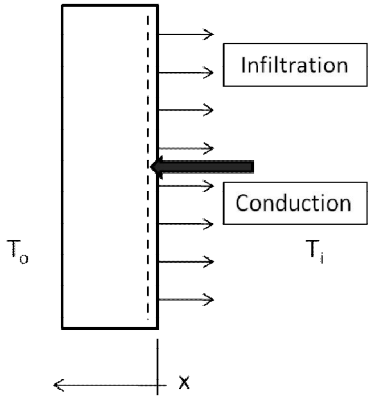

Reference Model

$$T(x) = Z_1 e^{-Pe\frac{x}{d}} + Z_2$$

$$T\,(x = 0) = T_i\,; T(x = d) = T_o$$

$$Z_2 = T_o - Ae^{-Pe} \quad ; \quad Z_1 = \frac{T_o - T_i}{1 - e^{-Pe}}$$

$$T(x) = \left(\frac{T_i - T_o}{1 - e^{-Pe}}\right) e^{\frac{-Pe}{d}x} + \left(T_o - \left(\frac{T_i - T_o}{1 - e^{-Pe}}\right) e^{-Pe}\right) \tag{E13}$$

$$T(x) = T_o + (T_i - T_o)\left(\frac{e^{\frac{-Pe}{d}x} - e^{-Pe}}{1 - e^{-Pe}}\right) \tag{E14}$$

$$\frac{dT}{dx} = -\frac{Pe}{d}(T_i - T_o)\frac{e^{-Pe\frac{x}{d}}}{1 - e^{-Pe}} \tag{E15}$$

$$\theta(\xi) = \frac{e^{-Pe\,\xi} - e^{-Pe}}{1 - e^{-Pe}} \tag{E16}$$

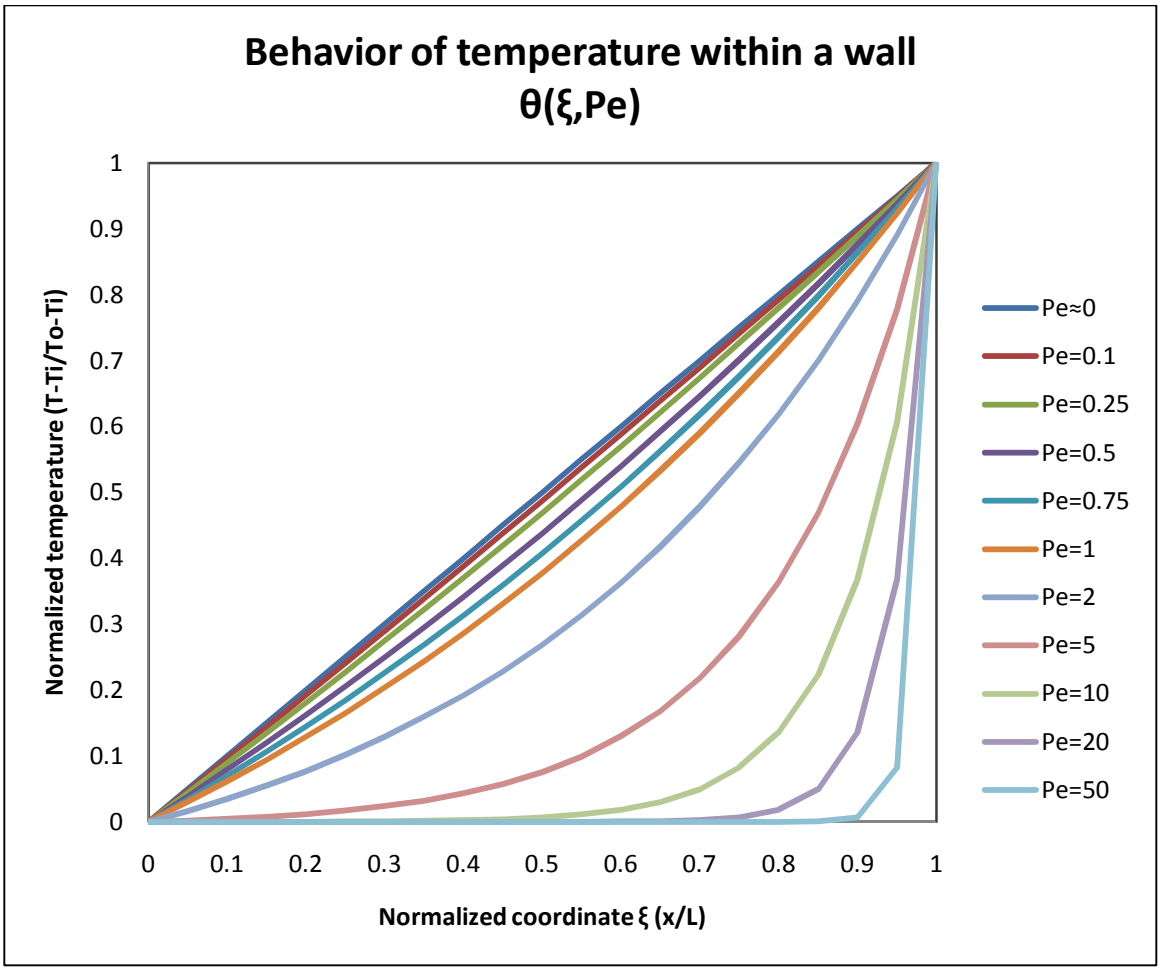

Figure 40: Normalized wall temperature, no film resistance

Model when accounting for surface film resistance

When the model includes the effects of the surface film resistance, the system must first solve for system of equations when solving for the interior and exterior surface temperature. First the energy balance must be normalized for temperature and distance. This will simplify the solution by introducing the dimensionless Biot number.

$$Bi = \frac{h * L_c}{k}$$

$$L_c = \frac{V_{wall}}{A_{wall}} = d \qquad \text{(E17)}$$

$$Bi = \frac{h * d}{k} = \frac{h}{U} \qquad \text{(E18)}$$

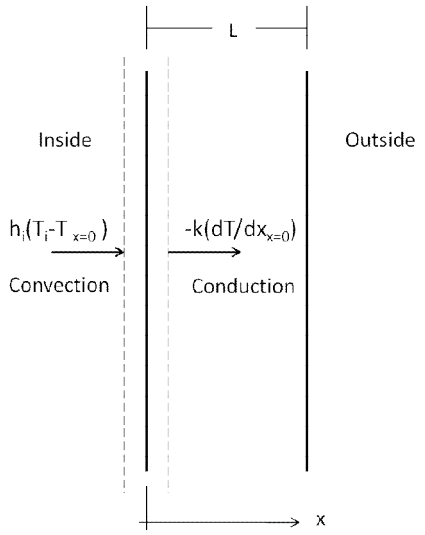

$$T\,(x=0) = T_{si}$$

$$\left(h_i\left(T_i - T_{(x=0)}\right)\right) - \left(-k\frac{dT}{dx_{(x=0)}}\right) = 0$$

$$\frac{dT}{dx_{(x=0)}} = \left(T_i - T_{(x=0)}\right) * \frac{h_i}{-k} \tag{E19}$$

$$\frac{(T_i - T_o)}{d}\,\frac{d\theta}{d\xi_{\xi=0}} = \left(T_i - T_{(x=0)}\right) * \frac{h_i}{-k}$$

$$\frac{d\theta}{d\xi_{\xi=0}} = \frac{T_i - T_{x=0}}{T_i - T_o} * \frac{h_i\,d}{-k}$$

$$\frac{d\theta}{d\xi_{\xi=0}} = \frac{T_i - T_{x=0} + T_o - T_o}{T_i - T_o} * \frac{h_i\,d}{-k}$$

$$\frac{d\theta}{d\xi_{\xi=0}} = \left(\frac{T_{x=0} - T_o}{T_i - T_o} - 1\right) * Bi_i \tag{E20}$$

$$\frac{d\theta}{d\xi_{\xi=0}} = \left(\theta_{\xi=0} - 1\right) * Bi_i \tag{E21}$$

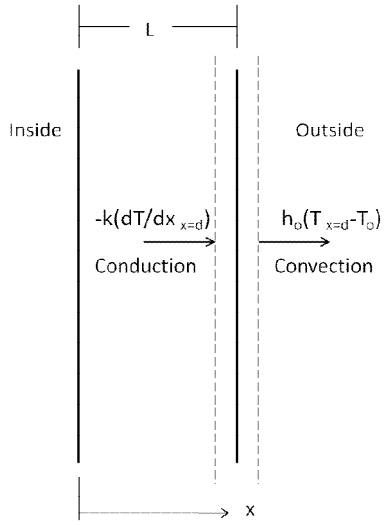

$$T(x=d) = T_{so}$$

$$h_o\left(T_{(x=d)} - T_o\right) - \left(-k\frac{dT}{dx}_{(x=d)}\right) = 0$$

$$\frac{dT}{dx}_{(x=d)} = \left(T_{(x=d)} - T_o\right) * \frac{h_o}{-k} \tag{E22}$$

$$\frac{T_i - T_o}{d}\frac{d\theta}{d\xi}_{\xi=1} = \left(T_{(x=d)} - T_o\right) * \frac{h_o}{-k}$$

$$\frac{d\theta}{d\xi}_{\xi=1} = \frac{T_{(x=d)} - T_o}{T_i - T_o} * \frac{h_o\, d}{-k}$$

$$\frac{d\theta}{d\xi}_{\xi=1} = -\theta_{\xi=1} * Bi_o \tag{E23}$$

$$(\xi = 0) \;:\; -Z_1 Pe = (Z_1 + Z_2 - 1) * Bi_i$$

$$(\xi = 1) - Z_1 e^{-Pe} Pe = \left(Z_1 e^{-Pe} + Z_2\right) * -Bi_o$$

$$Z_1 = \frac{Bi_i(Z_2 - 1)}{(Pe - Bi_i)} \tag{E24}$$

$$\frac{Bi_i(Z_2-1)}{(Pe-Bi_i)} e^{Pe} Pe = \left(\frac{Bi_i(Z_2-1)}{(Pe-Bi_i)} e^{Pe} + Z_2\right) * -Bi_o$$

$$-\frac{Bi_i}{Bi_o}(Z_2 - 1)e^{Pe} Pe = Bi_i(Z_2 - 1)e^{Pe} + Z\_2(Pe - Bi_i)$$

$$-\frac{Bi_i}{Bi_o} e^{Pe} Pe\, Z_2 + \frac{Bi_i}{Bi_o} e^{Pe} Pe = Bi_i e^{Pe} Z_2 - Bi_i e^{Pe} + Pe\, Z_2 - Bi_i Z_2$$

$$\frac{Bi_i}{Bi_o} e^{Pe} Pe + Bi_i e^{Pe} = Z_2\left(Bi_i e^{Pe} + Pe - Bi_i + \frac{Bi_i}{Bi_o} e^{Pe} Pe\right)$$

$$Z_2 = \frac{\frac{Bi_i}{Bi_o} e^{Pe} Pe + Bi_i e^{Pe}}{Bi_i e^{Pe} + Pe - Bi_i + \frac{Bi_i}{Bi_o} e^{Pe} Pe}$$

$$Z_2 = \frac{Bi_i e^{Pe} Pe + Bi_o Bi_i e^{Pe}}{Bi_o Bi_i e^{Pe} + Bi_o Pe - Bi_o Bi_i + Bi_i e^{Pe} Pe} \tag{E25}$$

$$Z_1 = \frac{Bi_i(Z_2-1)}{(Pe-Bi_i)} = \frac{Bi_i\left(\frac{Bi_i e^{Pe}Pe+Bi_o Bi_i e^{Pe}}{Bi_o Bi_i e^{Pe}+Bi_o Pe-Bi_o Bi_i+Bi_i e^{Pe}Pe}-1\right)}{(Pe-Bi_i)}$$

$$Z_1 = \frac{Bi_i(-Bi_o Pe+Bi_o Bi_i)}{(Pe-Bi_i)(Bi_o Bi_i e^{Pe}+Bi_o Pe-Bi_o Bi_i+Bi_i e^{Pe}Pe)}$$

$$Z_1 = \frac{-Bi_o Bi_i}{(Bi_o Bi_i e^{Pe}+Bi_o Pe-Bi_o Bi_i+Bi_i e^{Pe}Pe)} \quad \text{(E26)}$$

Plug Constants Z into General Solution

$$\theta(\xi) = \frac{-Bi_o Bi_i}{(Bi_o Bi_i e^{Pe}+Bi_o Pe-Bi_o Bi_i+Bi_i e^{Pe}Pe)} e^{-Pe\xi} + \frac{Bi_i e^{Pe}Pe+Bi_o Bi_i e^{Pe}}{Bi_o Bi_i e^{Pe}+Bi_o Pe-Bi_o Bi_i+Bi_i e^{Pe}Pe} \quad \text{(E27)}$$

$$T(x) = T_o + (T_i - T_o)\left(\frac{Bi_o Bi_i e^{Pe}-Bi_o Bi_i e^{Pe\frac{x}{d}}+Bi_i e^{Pe}Pe}{Bi_o e^{Pe}+Bi_o Bi_i e^{Pe}-Bi_o Bi_i+Bi_i e^{Pe}Pe}\right) \quad \text{(E28)}$$

$$\frac{dT}{dx} = \frac{(T_i-T_o)}{d}\left(\frac{-Pe\ Bi_o Bi_i\ e^{Pe\frac{x}{d}}}{Bi_o e^{Pe}+Bi_o Bi_i e^{Pe}-Bi_o Bi_i+Bi_i e^{Pe}Pe}\right) \quad \text{(E29)}$$

$$\theta(\xi) = \frac{Bi_o Bi_i e^{Pe}-Bi_o Bi_i e^{Pe\xi}+Bi_i e^{Pe}Pe}{Bi_o e^{Pe}+Bi_o Bi_i e^{Pe}-Bi_o Bi_i+Bi_i e^{Pe}Pe} \quad \text{(E30a)}$$

$$\theta(\xi) = \frac{Bi_o Bi_i e^{-Pe}-Bi_o Bi_i e^{-Pe\xi}-Bi_i e^{-Pe}Pe}{Bi_o e^{-Pe}+Bi_o Bi_i e^{-Pe}-Bi_o Bi_i-Bi_i e^{-Pe}Pe} \quad \text{(E30b)}$$

The normalized temperature solutions $\theta(\xi)$ in a wall shows the relative temperature profile within wall, give conduction and infiltration, at any difference in temperature and thickness of the wall. The influence of the Peclet and Biot numbers are understood when analyzing this solution.

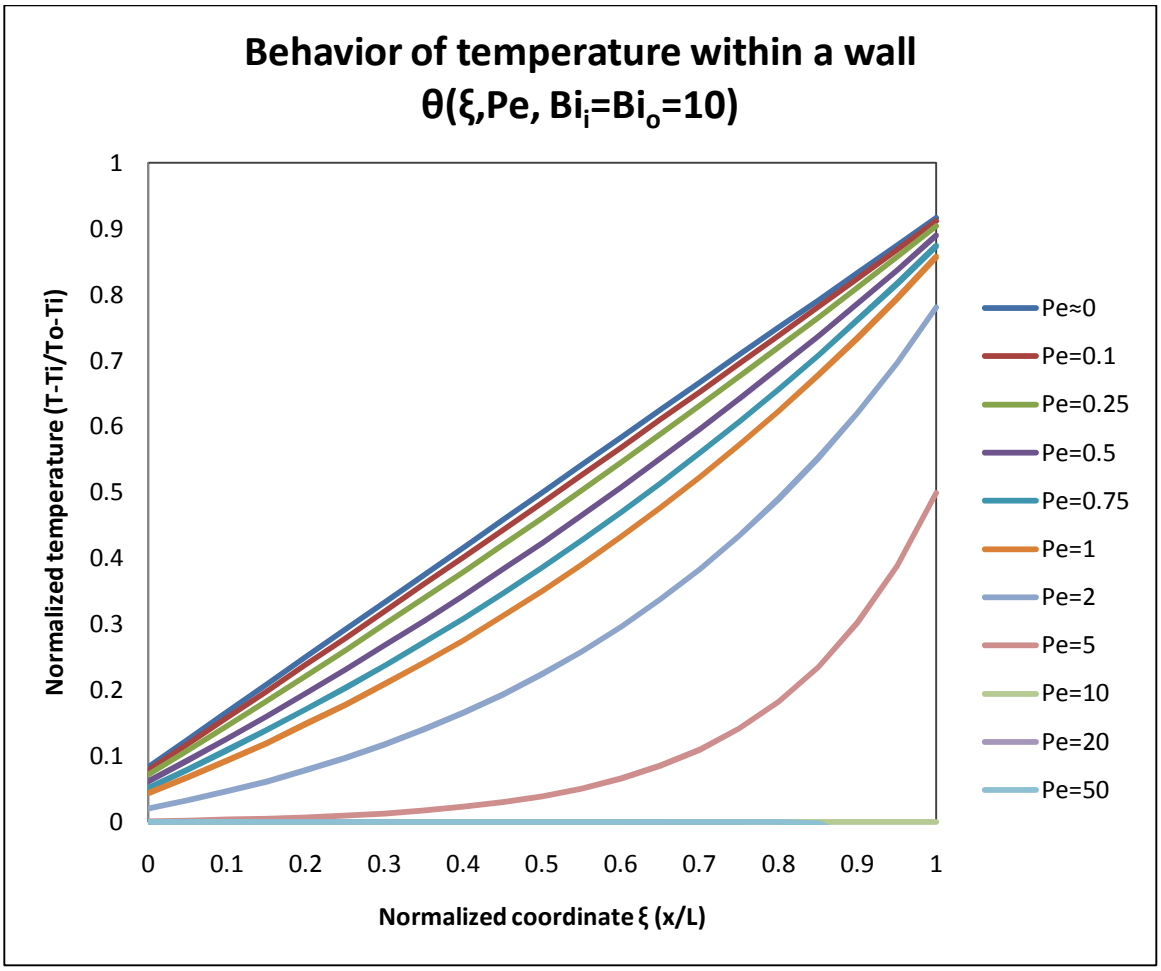

Figure 41: Normalized wall temperature, accounting for film resistance

When assuming conduction heat transfer remains constant, the Peclet number can be recognized as an indicator of the infiltration loss coefficient to the space. When Peclet is zero, infiltration is also zero, and similarly when Peclet reaches infinity. A Biot number is defined for both surfaces, and once the again assuming conduction is constant, can be an indicator of the convective properties at the surface of the wall. When Biot for either surface is zero, the wall surface film resistance goes to infinity, acting like an adiabatic layer in the wall. If the Biot is infinitely large, then the surface film resistance becomes very small and negligible in heat transfer analysis. Since the heat transfer to the space is of interest, analyzing the temperature at the inside surface, when x=0, provides a useful indication of the effect Peclet and Biot have on the temperature of the insider surface.

$$T(0) = T_o + (T_i - T_o)\left(\frac{Bi_o Bi_i e^{-Pe} - Bi_o Bi_i - Bi_i e^{-Pe} Pe}{Bi_o e^{-Pe} + Bi_o Bi_i e^{-Pe} - Bi_o Bi_i - Bi_i e^{-Pe} Pe}\right)$$

$$\lim_{Bi\to 0}\left[T_o + (T_i - T_o)\left(\frac{Bi_o Bi_i e^{-Pe} - Bi_o Bi_i - Bi_i e^{-Pe} Pe}{Bi_o e^{-Pe} + Bi_o Bi_i e^{-Pe} - Bi_o Bi_i - Bi_i e^{-Pe} Pe}\right)\right] = \frac{T_i + e^{Pe} T_o}{1 + e^{Pe}}$$

$$\lim_{Bi\to \infty}\left[T_o + (T_i - T_o)\left(\frac{Bi_o Bi_i e^{-Pe} - Bi_o Bi_i - Bi_i e^{-Pe} Pe}{Bi_o e^{-Pe} + Bi_o Bi_i e^{-Pe} - Bi_o Bi_i - Bi_i e^{-Pe} Pe}\right)\right] = T_i$$

$$\lim_{Pe\to 0}\left[T_o + (T_i - T_o)\left(\frac{Bi_o Bi_i e^{-Pe} - Bi_o Bi_i - Bi_i e^{-Pe} Pe}{Bi_o e^{-Pe} + Bi_o Bi_i e^{-Pe} - Bi_o Bi_i - Bi_i e^{-Pe} Pe}\right)\right] = \frac{Bi_i(1 + Bi_o) T_i + Bi_o T_o}{Bi_i + Bi_o + Bi_i Bi_o}$$

$$\lim_{Pe\to \infty}\left[T_o + (T_i - T_o)\left(\frac{Bi_o Bi_i e^{-Pe} - Bi_o Bi_i - Bi_i e^{-Pe} Pe}{Bi_o e^{-Pe} + Bi_o Bi_i e^{-Pe} - Bi_o Bi_i - Bi_i e^{-Pe} Pe}\right)\right] = T_o$$

$$\lim_{Bi\to 0, Pe\to 0}\left[T_o + (T_i - T_o)\left(\frac{Bi_o Bi_i e^{Pe} - Bi_o Bi_i e^{Pe\frac{x}{d}} + Bi_i e^{Pe} Pe}{Bi_o e^{Pe} + Bi_o Bi_i e^{Pe} - Bi_o Bi_i + Bi_i e^{Pe} Pe}\right)\right] = \frac{T_i + T_o}{2}$$

Reference Model Methodology

Using the derived solutions for wall temperature, the solution for infiltration heat recovery can be found for a given space. A reference methodology must be established to solve the problem for both when accounting for the surface film resistance or not. This involves naming the convention for positive and negative heat and mass flow.

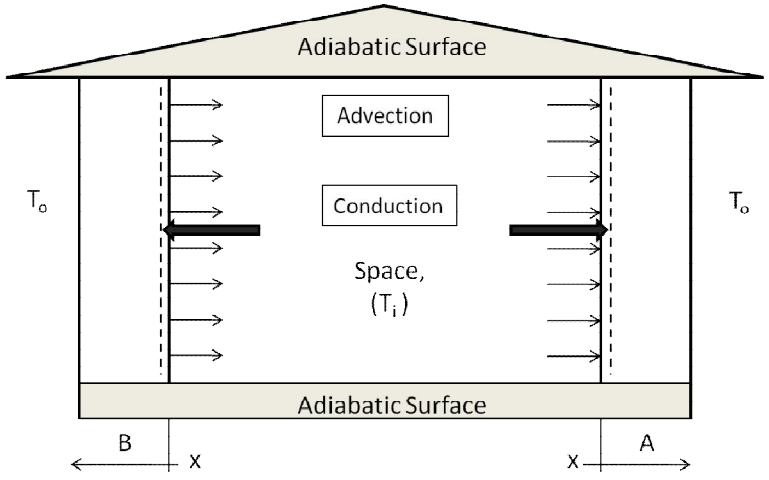

$$Q_{recovery} = -k\frac{A}{2}\left(\frac{dT}{dx_{x=0}} - \frac{dT^*}{dx}_{x=0}\right) + \frac{A}{2}\dot{m}C_p(T_{x=0} - T^*_{x=0}) \quad \text{(E31)}$$

$$Q_{conduction} = UA\,(T_i - T_o)$$

$$Q_{new\ inf} = Q_{recovery} - Q_{conduction}$$

$$f = 1 - \frac{Q_{new\ inf}}{\frac{A}{2}\dot{m}c_p(T_i - T_o)}$$

$$\frac{Q_{recovery}}{Q_{classical}} = \frac{(U_{eff}A + (1-f)\dot{m}C_p)(T_i - T_o)}{(U_{eff}A + \dot{m}C_p)(T_i - T_o)} \quad \text{(E32)}$$

The heat load is derived assuming a simple two wall model, where Wall B is assumed to provide infiltration to the space, and Wall A provides exfiltration. The star symbol on the temperature function refers to wall B, where a negative air flow creates a negative Peclet number, modifying the solution. This equation represents the heat balance needed to find the total load that will heat the space of the simplified two wall model. The boundary conditions are set to be just inside the interior surface of each wall. Both walls assume positive conduction heat flow outward from the space. Either of the solutions for temperature, with or without accounting for the film resistance, can be inserted to solve for total heat transfer. The solution must be adjusted accordingly by modifying the Peclet to become negative. The Peclet holds the mass flow rate loss coefficient and must also carry the correct convection for the derivation to provide the proper solution.

Derivation of Infiltration Heat Recovery Factor under Reference Conditions

Without accounting for the film resistance

$$Q_{recovery} = -k\frac{A}{2}\left(\frac{dT}{dx}_{x=0} + \frac{dT^*}{dx}_{x=0}\right) + \frac{A}{2}\dot{m}C_p(T_{x=0} - T^*_{x=0})$$

$$Q_{recovery} = -k\frac{A}{2}\left(\frac{Pe}{d}(T_i - T_o)\frac{1}{1-e^{Pe}} - \frac{Pe}{d}(T_i - T_o)\frac{1}{1-e^{-Pe}}\right) + \frac{A}{2}\frac{kPe}{d}\left((T_i - T_o)\left(\frac{1-e^{Pe}}{1-e^{Pe}}\right) - (T_i - T_o)\left(\frac{1-e^{-Pe}}{1-e^{-Pe}}\right)\right) \quad \text{(E33)}$$

$$Q_{recovery} = \frac{A}{2}\frac{kPe}{d}(T_i - T_o)\left(\frac{1}{1-e^{-Pe}} - \frac{1}{1-e^{Pe}}\right) + 0$$

$$Q_{new\ inf} = \frac{A}{2}\frac{kPe}{d}(T_i - T_o)\left(\frac{1}{1-e^{-Pe}} - \frac{1}{1-e^{Pe}}\right) - A\frac{k}{d}(T_i - T_o)$$

$$Q_{new\ inf} = \frac{A}{2}\frac{k}{d}(T_i - T_o)\frac{2+e^{Pe}(Pe-2)+Pe}{e^{Pe}-1} \quad \text{(E34)}$$

$$f = 1 - \frac{\frac{Ak}{2d}(T_i - T_o)\frac{2+e^{Pe}(Pe-2)+Pe}{e^{Pe}-1}}{\frac{Ak}{2}\frac{Pe}{d}(T_i - T_o)}$$

$$f = 1 - \frac{2+e^{Pe}(Pe-2)+Pe}{(e^{Pe}-1)*Pe}$$

$$f = \frac{((e^{Pe}-1)Pe-2-e^{Pe}(Pe-2)-Pe)}{(e^{Pe}-1)Pe}$$

$$f = \frac{2e^{Pe}-2-2Pe}{(e^{Pe}-1)Pe}$$

$$f = \frac{2}{Pe} - \frac{2}{e^{Pe}-1} \quad \text{(E35)}$$

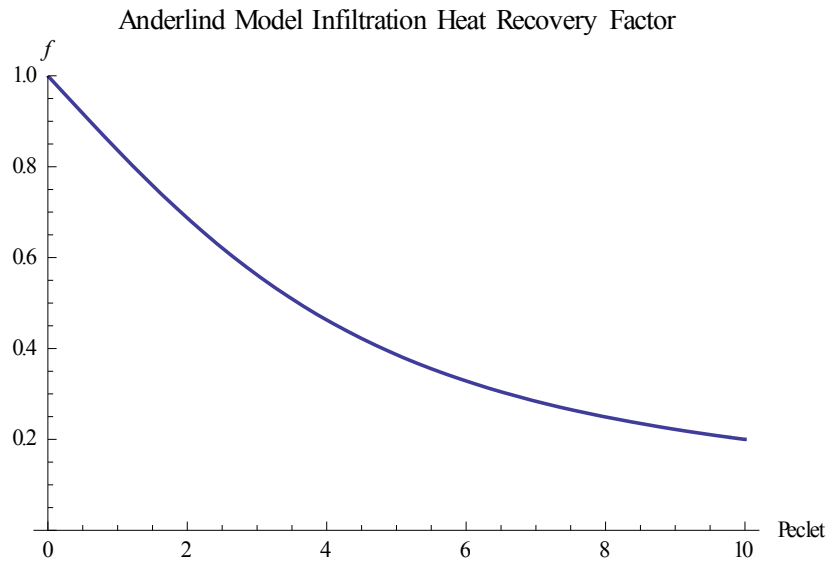

Derivation of Infiltration Heat Recovery Factor when accounting for Surface Film Resistance

Accounting for the film resistance

$$Q_{recovery} = -k\frac{A}{2}\left(\frac{dT}{dx}_{x=0} + \frac{dT^*}{dx}_{x=0}\right) + \frac{A}{2}\dot{m}C_p(T_{x=0} - T^*_{x=0})$$

$$T(0) = T_o + (T_i - T_o)\left(\frac{Bi_oBi_ie^{-Pe} - Bi_oBi_i - Bi_ie^{-Pe}Pe}{Bi_oe^{-Pe} + Bi_oBi_ie^{-Pe} - Bi_oBi_i - Bi_ie^{-Pe}Pe}\right)$$

$$\frac{dT}{dx} = \frac{(T_i - T_o)}{d}\left(\frac{-Pe\ Bi_oBi_i}{Bi_oe^{Pe} + Bi_oBi_ie^{Pe} - Bi_oBi_i + Bi_ie^{Pe}Pe}\right)$$

$$Q_{recovery} = -\frac{Ak(T_i - T_o)}{2d}\left(\left(\frac{-Pe\ Bi_oBi_i}{Bi_oe^{Pe} + Bi_oBi_ie^{Pe} - Bi_oBi_i + Bi_ie^{Pe}Pe}\right) + \left(\frac{Pe\ Bi_oBi_i}{Bi_oe^{-Pe} + Bi_oBi_ie^{-Pe} - Bi_oBi_i - Bi_ie^{-Pe}Pe}\right)\right) +$$
$$\frac{AkPe\ (T_i - T_o)}{2d}\left(\left(\frac{Bi_oBi_ie^{Pe} - Bi_oBi_i + Bi_ie^{Pe}Pe}{Bi_oe^{Pe} + Bi_oBi_ie^{Pe} - Bi_oBi_i + Bi_ie^{Pe}Pe}\right) - \left(\frac{Bi_oBi_ie^{-Pe} - Bi_oBi_i - Bi_ie^{-Pe}Pe}{Bi_oe^{-Pe} + Bi_oBi_ie^{-Pe} - Bi_oBi_i - Bi_ie^{-Pe}Pe}\right)\right)$$

$$Q_{recovery} = \frac{A}{2}\frac{kPe}{d}Bi_iBi_o\ (T_i - T_o)\frac{Pe\left(Bi_o(1+e^{2Pe}) + Pe(e^{2Pe}-1)\right) + Bi_i\left(Bi_o(e^{2Pe}-1) + Pe(e^{2Pe}+1)\right)}{\left(Bi_oe^{Pe}Pe + Bi_i(Bi_o(e^{Pe}-1) + Pe)\right)\left(Bi_oPe + Bi_i(Bi_o(e^{Pe}-1) + e^{Pe}Pe)\right)}$$

$$Q_{recovery} = \frac{A}{2}\frac{kPe}{d}Bi_iBi_o\ (T_i - T_o)\frac{Pe\left(Bi_o(1+e^{2Pe}) + Pe(e^{2Pe}-1)\right) + Bi_i\left(Bi_o(e^{2Pe}-1) + Pe(e^{2Pe}+1)\right)}{\left(Bi_oe^{Pe}Pe + Bi_i(Bi_o(e^{Pe}-1) + Pe)\right)\left(Bi_oPe + Bi_i(Bi_o(e^{Pe}-1) + e^{Pe}Pe)\right)} \quad \text{(E37)}$$

$$Q_{conduction} = U_{eff}A\ (T_i - T_o) \quad \text{(E38)}$$

$$U_{eff} = \frac{1}{\frac{1}{U} + \frac{1}{h_i} + \frac{1}{h_o}}$$

$$U_{eff} = \frac{U}{1 + \frac{1}{Bi_i} + \frac{1}{Bi_o}} \quad \text{(E39)}$$

$$Q_{new\ infiltration} = \frac{A}{2}\frac{kPe}{d}Bi_iBi_o\ (T_i - T_o)\frac{Pe\left(Bi_o(1+e^{2Pe}) + Pe(e^{2Pe}-1)\right) + Bi_i\left(Bi_o(e^{2Pe}-1) + Pe(e^{2Pe}+1)\right)}{\left(Bi_oe^{Pe}Pe + Bi_i(Bi_o(e^{Pe}-1) + Pe)\right)\left(Bi_oPe + Bi_i(Bi_o(e^{Pe}-1) + e^{Pe}Pe)\right)} -$$
$$\frac{A\frac{k}{d}(T_i - T_o)}{1 + \frac{1}{Bi_i} + \frac{1}{Bi_o}}$$

$$Q_{\text{new infiltration}} = A\dot{m}C_p(T_i - T_o)\left(Bi_iBi_o\frac{Pe\left(Bi_o(1+e^{2Pe})+Pe(e^{2Pe}-1)\right)+Bi_i\left(Bi_o(e^{2Pe}-1)+Pe(e^{2Pe}+1)\right)}{\left(Bi_oe^{Pe}Pe+Bi_i(Bi_o(e^{Pe}-1)+Pe)\right)\left(Bi_oPe+Bi_i(Bi_o(e^{Pe}-1)+e^{Pe}Pe)\right)} - \frac{2}{Pe\left(1+\frac{1}{Bi_i}+\frac{1}{Bi_o}\right)}\right) \quad \text{(E40)}$$

$$f = 1 - \frac{Q_{\text{new infiltration}}}{A\dot{m}C_p(T_i - T_o)}$$

$$f = 1 - Bi_iBi_o\frac{Pe\left(Bi_o(1+e^{2Pe})+Pe(e^{2Pe}-1)\right)+Bi_i\left(Bi_o(e^{2Pe}-1)+Pe(e^{2Pe}+1)\right)}{\left(Bi_oe^{Pe}Pe+Bi_i(Bi_o(e^{Pe}-1)+Pe)\right)\left(Bi_oPe+Bi_i(Bi_o(e^{Pe}-1)+e^{Pe}Pe)\right)} + \frac{2}{Pe\left(1+\frac{1}{Bi_i}+\frac{1}{Bi_o}\right)} \quad \text{(E41)}$$

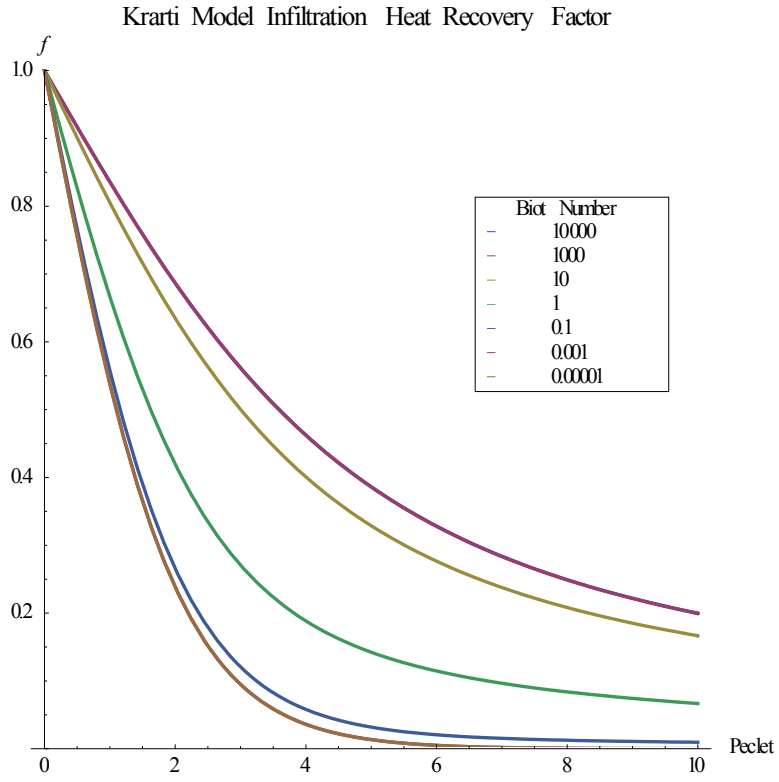

Evaluating Total Heat Transfer Ratio, with and without using Infiltration Heat Recovery Factor

The total load represents the heat transfer when accounting for infiltration heat recovery in both conduction and infiltration heat transfer. This can be compared to the traditional calculations to assess the impact. However, the impact is difficult to quantify in terms of conduction and infiltration because the two forms of heat transfer are impacted inversely. To better quantify the amount of heat recovery occurs, the assumption is made to consider conduction heat transfer as constant. This allows for all changes in

heat transfer to impact only the infiltration load. As seen in the derivation of the infiltration heat recovery factor, the removal of the traditional conduction heat transfer term allows the remaining solution to be compared to the traditional infiltration heat transfer to find the infiltration heat recovery factor. This factor, f, defines the amount of heat recovery occurring through the wall. The new infiltration and total heat transfer is calculated using the following equations. To understand the impact infiltration heat recovery has on the overall heat transfer in the model, a ratio of heat transfer with and without IHR can be made.

$$Q_{\text{new infiltration}} = (1-f)\dot{m}C_p\Delta T$$

$$Q_{\text{recovery}} = \left(U_{\text{eff}}A + (1-f)\dot{m}C_p\right)\Delta T$$

$$\frac{Q_{\text{recovery}}}{Q_{\text{classical}}} = \frac{\left(U_{\text{eff}}A+(1-f)\dot{m}C_p\right)\Delta T}{\left(U_{\text{eff}}A+\dot{m}C_p\right)\Delta T}$$

Assessing the overall impact on heat transfer can be done using two methods. Either method will achieve the same result. Each model derives a total couple heat transfer for the space accounting for infiltration heat recovery, $Q_{recovery}$. This can be plugged into the ratio for analysis, but the impact for both conduction and infiltration would be hard to quantify. Using the infiltration heat recovery factor is a much more feasible method to perform the same analysis.

Using total coupled heat loss

$$\frac{Q_{\text{recovery}}}{Q_{\text{classical}}} = \frac{\frac{AkPe}{2\ d}Bi_iBi_o\ (T_i-T_o)\frac{Pe\left(Bi_o\left(1+e^{2Pe}\right)+Pe\left(e^{2Pe}-1\right)\right)+Bi_i\left(Bi_o\left(e^{2Pe}-1\right)+Pe\left(e^{2Pe}+1\right)\right)}{\left(Bi_oe^{Pe}Pe+Bi_i(Bi_o(e^{Pe}-1)+Pe)\right)\left(Bi_oPe+Bi_i(Bi_o(e^{Pe}-1)+e^{Pe}Pe)\right)}}{\frac{A\frac{k}{d}(T_i-T_o)}{1+\frac{1}{Bi_i}+\frac{1}{Bi_o}}+\frac{AkPe(T_i-T_o)}{2d}} \tag{E42}$$

$$\frac{Q_{\text{recovery}}}{Q_{\text{classical}}} = \frac{Bi_iBi_o\frac{Pe\left(Bi_o\left(1+e^{2Pe}\right)+Pe\left(e^{2Pe}-1\right)\right)+Bi_i\left(Bi_o\left(e^{2Pe}-1\right)+Pe\left(e^{2Pe}+1\right)\right)}{\left(Bi_oe^{Pe}Pe+Bi_i(Bi_o(e^{Pe}-1)+Pe)\right)\left(Bi_oPe+Bi_i(Bi_o(e^{Pe}-1)+e^{Pe}Pe)\right)}}{\frac{1}{\frac{Pe}{2}\left(1+\frac{1}{Bi_i}+\frac{1}{Bi_o}\right)}+1} \tag{E43}$$

Using the heat recovery factor

$$\frac{\left(\mathrm{U_{eff}A}+(1-f)\dot{m}\mathrm{C_p}\right)\Delta\mathrm{T}}{\left(\mathrm{U_{eff}A}+\dot{m}\mathrm{C_p}\right)\Delta\mathrm{T}} \tag{E44}$$

$$\frac{1+\frac{(1-f)\dot{m}\mathrm{C_p}}{\mathrm{U_{eff}A}}}{1+\frac{\dot{m}\mathrm{C_p}}{\mathrm{U_{eff}A}}} \tag{E45}$$

$$\frac{1+\frac{(1-f)\dot{m}\mathrm{C_p}}{\frac{\mathrm{UA}}{1+\frac{1}{\mathrm{Bi_i}}+\frac{1}{\mathrm{Bi_o}}}}}{1+\frac{\dot{m}\mathrm{C_p}}{\frac{\mathrm{UA}}{1+\frac{1}{\mathrm{Bi_i}}+\frac{1}{\mathrm{Bi_o}}}}}$$

$$\frac{1+1+\frac{1}{\mathrm{Bi_i}}+\frac{1}{\mathrm{Bi_o}}(1-f)\mathrm{Pe}}{1+1+\frac{1}{\mathrm{Bi_i}}+\frac{1}{\mathrm{Bi_o}}\mathrm{Pe}} \tag{E46}$$

$$\frac{1+\left(1+\frac{1}{\mathrm{Bi_i}}+\frac{1}{\mathrm{Bi_o}}\right)\mathrm{Pe}-\left(1+\frac{1}{\mathrm{Bi_i}}+\frac{1}{\mathrm{Bi_o}}\right)(f)\mathrm{Pe}}{1+\left(1+\frac{1}{\mathrm{Bi_i}}+\frac{1}{\mathrm{Bi_o}}\right)\mathrm{Pe}}$$

$$1-\frac{\left(1+\frac{1}{\mathrm{Bi_i}}+\frac{1}{\mathrm{Bi_o}}\right)(f)\mathrm{Pe}}{1+\left(1+\frac{1}{\mathrm{Bi_i}}+\frac{1}{\mathrm{Bi_o}}\right)\mathrm{Pe}} \tag{E47}$$

$$f=1-\mathrm{Bi_i Bi_o}\frac{\mathrm{Pe}\left(\mathrm{Bi_o}\left(1+\mathrm{e}^{2\mathrm{Pe}}\right)+\mathrm{Pe}\left(\mathrm{e}^{2\mathrm{Pe}}-1\right)\right)+\mathrm{Bi_i}\left(\mathrm{Bi_o}\left(\mathrm{e}^{2\mathrm{Pe}}-1\right)+\mathrm{Pe}\left(\mathrm{e}^{2\mathrm{Pe}}+1\right)\right)}{\left(\mathrm{Bi_o}\mathrm{e}^{\mathrm{Pe}}\mathrm{Pe}+\mathrm{Bi_i}\left(\mathrm{Bi_o}\left(\mathrm{e}^{\mathrm{Pe}}-1\right)+\mathrm{Pe}\right)\right)\left(\mathrm{Bi_o}\mathrm{Pe}+\mathrm{Bi_i}\left(\mathrm{Bi_o}\left(\mathrm{e}^{\mathrm{Pe}}-1\right)+\mathrm{e}^{\mathrm{Pe}}\mathrm{Pe}\right)\right)}+\frac{2}{\mathrm{Pe}\left(1+\frac{1}{\mathrm{Bi_i}}+\frac{1}{\mathrm{Bi_o}}\right)}$$

$$f=1-\frac{\left(1+\frac{1}{\mathrm{Bi_i}}+\frac{1}{\mathrm{Bi_o}}\right)\left(1-\mathrm{Bi_i Bi_o}\frac{\mathrm{Pe}\left(\mathrm{Bi_o}\left(1+\mathrm{e}^{2\mathrm{Pe}}\right)+\mathrm{Pe}\left(\mathrm{e}^{2\mathrm{Pe}}-1\right)\right)+\mathrm{Bi_i}\left(\mathrm{Bi_o}\left(\mathrm{e}^{2\mathrm{Pe}}-1\right)+\mathrm{Pe}\left(\mathrm{e}^{2\mathrm{Pe}}+1\right)\right)}{\left(\mathrm{Bi_o}\mathrm{e}^{\mathrm{Pe}}\mathrm{Pe}+\mathrm{Bi_i}\left(\mathrm{Bi_o}\left(\mathrm{e}^{\mathrm{Pe}}-1\right)+\mathrm{Pe}\right)\right)\left(\mathrm{Bi_o}\mathrm{Pe}+\mathrm{Bi_i}\left(\mathrm{Bi_o}\left(\mathrm{e}^{\mathrm{Pe}}-1\right)+\mathrm{e}^{\mathrm{Pe}}\mathrm{Pe}\right)\right)}+\frac{2}{\mathrm{Pe}\left(1+\frac{1}{\mathrm{Bi_i}}+\frac{1}{\mathrm{Bi_o}}\right)}\right)\mathrm{Pe}}{1+\left(1+\frac{1}{\mathrm{Bi_i}}+\frac{1}{\mathrm{Bi_o}}\right)\mathrm{Pe}} \tag{E48}$$

$$\frac{Q_{recovery}}{Q_{classical}}=1-\frac{2+\left(1+\frac{1}{\mathrm{Bi_i}}+\frac{1}{\mathrm{Bi_o}}\right)\left(1-\mathrm{Bi_i Bi_o}\frac{\mathrm{Pe}\left(\mathrm{Bi_o}\left(1+\mathrm{e}^{2\mathrm{Pe}}\right)+\mathrm{Pe}\left(\mathrm{e}^{2\mathrm{Pe}}-1\right)\right)+\mathrm{Bi_i}\left(\mathrm{Bi_o}\left(\mathrm{e}^{2\mathrm{Pe}}-1\right)+\mathrm{Pe}\left(\mathrm{e}^{2\mathrm{Pe}}+1\right)\right)}{\left(\mathrm{Bi_o}\mathrm{e}^{\mathrm{Pe}}\mathrm{Pe}+\mathrm{Bi_i}\left(\mathrm{Bi_o}\left(\mathrm{e}^{\mathrm{Pe}}-1\right)+\mathrm{Pe}\right)\right)\left(\mathrm{Bi_o}\mathrm{Pe}+\mathrm{Bi_i}\left(\mathrm{Bi_o}\left(\mathrm{e}^{\mathrm{Pe}}-1\right)+\mathrm{e}^{\mathrm{Pe}}\mathrm{Pe}\right)\right)}\right)\mathrm{Pe}}{1+\left(1+\frac{1}{\mathrm{Bi_i}}+\frac{1}{\mathrm{Bi_o}}\right)\mathrm{Pe}}$$

$$\frac{\mathrm{Q_{recovery}}}{\mathrm{Q_{classical}}}=1-\frac{2+\left(1+\frac{1}{\mathrm{Bi_i}}+\frac{1}{\mathrm{Bi_o}}\right)\left(1-\mathrm{Bi_i Bi_o}\frac{\mathrm{Pe}\left(\mathrm{Bi_o}\left(1+\mathrm{e}^{2\mathrm{Pe}}\right)+\mathrm{Pe}\left(\mathrm{e}^{2\mathrm{Pe}}-1\right)\right)+\mathrm{Bi_i}\left(\mathrm{Bi_o}\left(\mathrm{e}^{2\mathrm{Pe}}-1\right)+\mathrm{Pe}\left(\mathrm{e}^{2\mathrm{Pe}}+1\right)\right)}{\left(\mathrm{Bi_o}\mathrm{e}^{\mathrm{Pe}}\mathrm{Pe}+\mathrm{Bi_i}\left(\mathrm{Bi_o}\left(\mathrm{e}^{\mathrm{Pe}}-1\right)+\mathrm{Pe}\right)\right)\left(\mathrm{Bi_o}\mathrm{Pe}+\mathrm{Bi_i}\left(\mathrm{Bi_o}\left(\mathrm{e}^{\mathrm{Pe}}-1\right)+\mathrm{e}^{\mathrm{Pe}}\mathrm{Pe}\right)\right)}\right)\mathrm{Pe}}{1+\left(1+\frac{1}{\mathrm{Bi_i}}+\frac{1}{\mathrm{Bi_o}}\right)\mathrm{Pe}} \tag{E49}$$

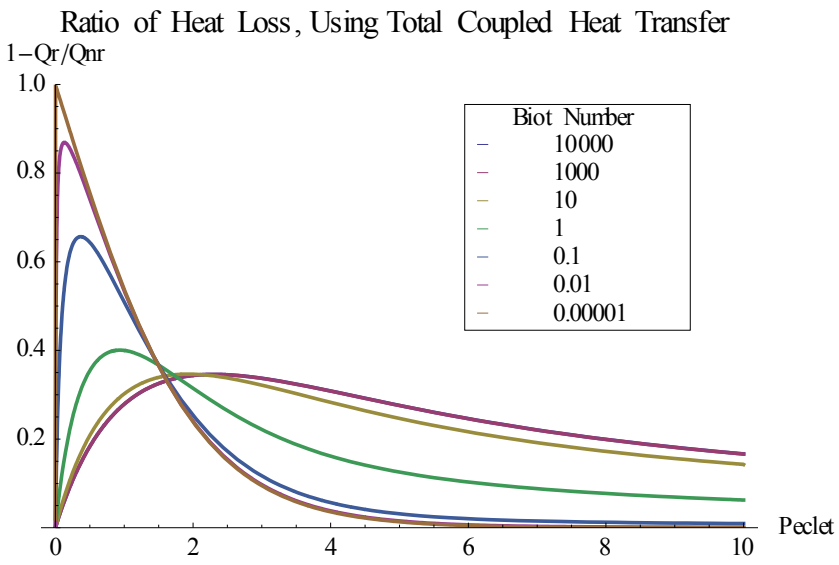

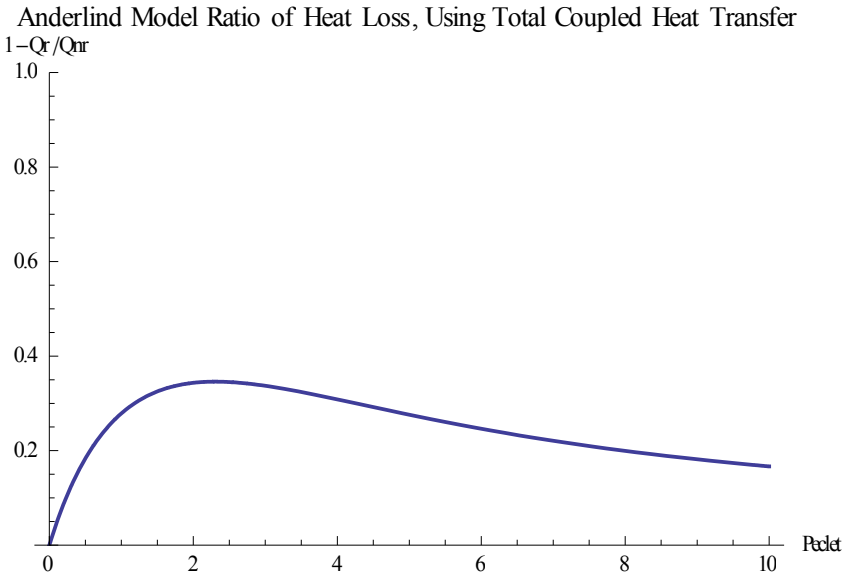

According to the figure above, infiltration heat recovery reaches a peak in reduction of heat transfer. The peak will shift based on the effects of wall surface film resistance. Under typical conditions, the Biot number is between the order of one and ten, and causes a peak in infiltration heat recovery to be reached at a Peclet number between one and two. Despite the effects of the wall surface film resistance, the effects on the building load due to IHR always approaches zero when Peclet approaches zero and infinity. At this range of Peclet, the impact of IHR can be considered insignificant to the predicted space heat transfer. It is important to understand the conditions where significant infiltration heat recovery occurs in typical homes. A Peclet of two signifies the infiltration heat loss coefficient accounts for two

thirds of the BLC under its simple definition. For a typical home, it is unlikely Infiltration in homes typically accounts for about a third of the home's energy consumption, signifying a Peclet number of around one half. In homes, it is unlikely the Peclet number will reach an order much greater than one, therefore the impact of infiltration heat recovery should always be considered for homes with large amounts of infiltration. When infiltration levels are very small, the impact on heat transfer may become insignificant. It is beneficial to characterize the lower range where IHR is no longer considered important to gauge air tight homes that could potential small IHR effects.

APPENDIX F: EXPERIMENTAL COMPARISON RESULTS

In total there were six experiments that were tested against two derivations of coupled heat transfer that account for infiltration heat recovery with and without accounting for the effects from the film resistance at both the interior and exterior wall surfaces. In both the experiment and models, the ratio is measured between total coupled heat transfer and decoupled heat transfer.

The theoretical models are 1D sensible heat transfer assuming diffuse air flow ideally throughout the entire wall area. Out of the two test panels, one is configured with a direct air leakage path, preventing 100% of the wall from participating in heat recovery. Through analysis of the isotherms gathered from each test, it can be seen roughly 20% of the area of the wall was involves in heat recovery. The couple heat transfer analysis was adjusted accordingly to allow for comparison. The second test panels measures the effects from an air leakage path that allows almost 100% of the wall to participate in heat recovery. The models do not need to be adjusted to compare to this case.

$$r = \frac{Q_{recovery}}{Q_{no\ recovery}} = \frac{\Sigma(U_{gypsum})A_{panel}\,(\Delta T_{gypsum}) + \dot{m}C_p(T_{room} - T_{air\ exit})}{U_{wall}A_{panel}\,(T_{room} - T_{ambient}) + \dot{m}C_p(T_{room} - T_{ambient})} \quad \text{(F1)}$$

$$\omega = \sqrt{(\omega_{random}^2 = 0)\ + \omega_{instrument}^2 + (\omega_{calibration}^2 = 0)} \quad \text{(F2)}$$

$$\omega_r = \sqrt{\left(\omega_{T_{g1}}\frac{dr}{dT_{g_1}}\right)^2 + \left(\omega_{T_{g2}}\frac{dr}{dT_{g2}}\right)^2 + \left(\omega_{T_{room}}\frac{dr}{dT_{room}}\right)^2 + \left(\omega_{T_{air\ exit}}\frac{dr}{dT_{air\ exit}}\right)^2 + \left(\omega_{\dot{m}}\frac{dr}{d\dot{m}}\right)^2} \quad \text{(F3)}$$

$$\frac{dr}{dT_{g1}} = \frac{U_{gypsum}A_{panel}}{(U_{panel}A_{panel} + \dot{m}C_p)\,(T_{room} - T_{ambient})} \quad \text{(F4)}$$

$$\frac{dr}{dT_{g2}} = -\frac{dr}{dT_{g1}}$$

$$\frac{dr}{dT_{room}} = \frac{\dot{m}C_p\left((U_{panel}A_{panel} + \dot{m}C_p)\,(T_{room} - T_{ambient}) - \left(U_{gypsum}A_{panel}\Delta T_{gypsum} + \dot{m}C_p(T_{room} - T_{air\ exit})\right)\right)}{\left(U_{panel}A_{panel}(T_{room} - T_{ambient})\right)^2} \quad \text{(F5)}$$

$$\frac{dr}{dT_{ambient}} = \frac{\left(U_{gypsum}A_{panel}\Delta T_{gypsum} + \dot{m}C_p(T_{room} - T_{air\ exit})\right)}{(U_{panel}A_{panel} + \dot{m}C_p)\,((T_{room} - T_{ambient})^2)} \quad \text{(F6)}$$

$$\frac{dr}{dT_{air\ exit}} = -\frac{\dot{m}C_p}{(U_{panel}A_{panel} + \dot{m}C_p)(T_{room} - T_{ambient})} \quad \text{(F7)}$$

$$\frac{dr}{d\dot{m}} = \frac{C_p * \left(\left((U_{panel}A_{panel} + \dot{m}C_p)(T_{room} - T_{air\ exit})\right) - \left(U_{gypsum}A_{panel}\Delta T_{gpysum} + \dot{m}C_p(T_{room} - T_{air\ exit})\right)\right)}{(U_{panel}A_{panel} + \dot{m}C_p)^2(T_{room} - T_{ambient})} \quad \text{(F8)}$$

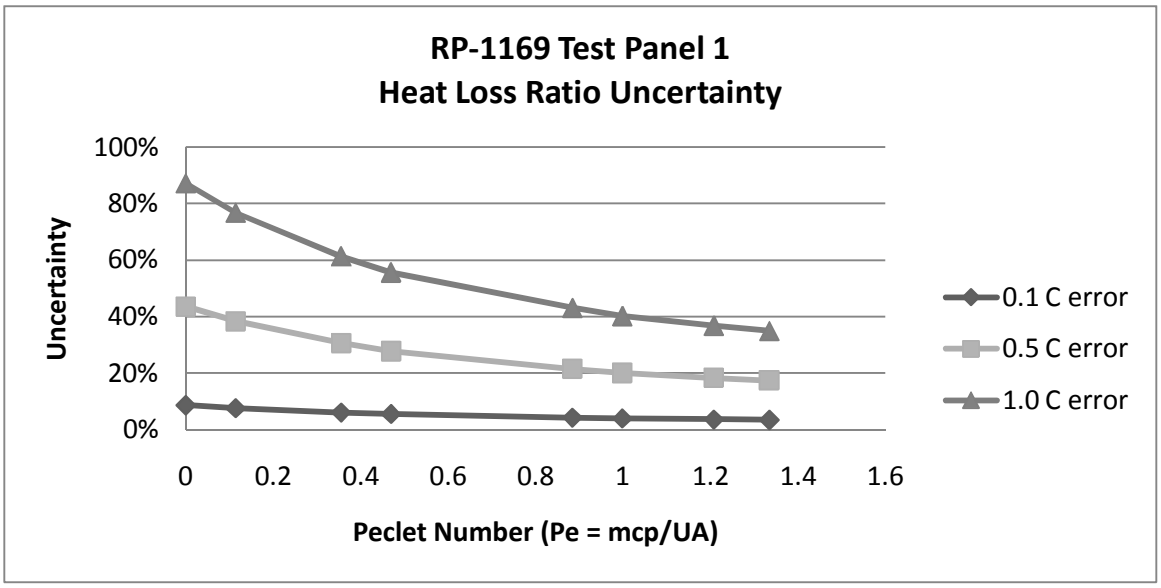
RP-1169 Test Panel 1
Heat Loss Ratio Uncertainty
Uncertainty
100%
80%
60%
40%
20%
0%
0
0.2
0.4
0.6
0.8
1
1.2
1.4
1.6
Peclet Number (Pe = mcp/UA)
0.1 C error
0.5 C error
1.0 C error

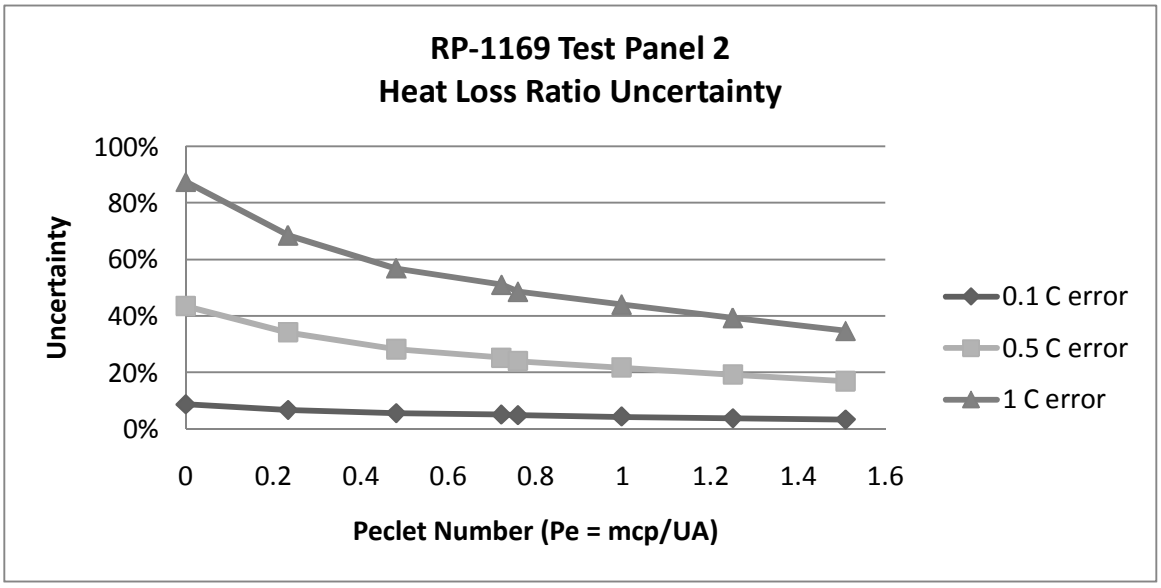
RP-1169 Test Panel 2
Heat Loss Ratio Uncertainty
Uncertainty
100%
80%
60%
40%
20%
0%
0
0.2
0.4
0.6
0.8
1
1.2
1.4
1.6
Peclet Number (Pe = mcp/UA)
0.1 C error
0.5 C error
1 C error

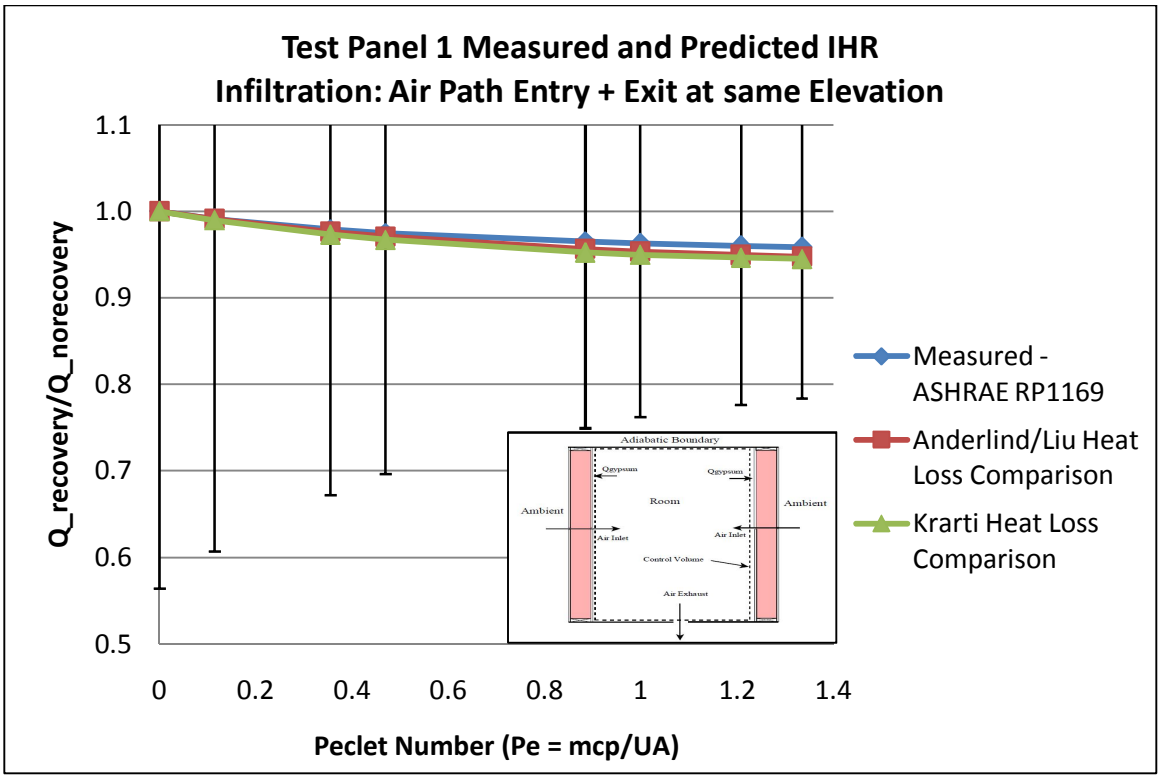
Test Panel 1 Measured and Predicted IHR
Infiltration: Air Path Entry + Exit at same Elevation
Q_recovery/Q_norecovery
1.1
1.0
0.9
0.8
0.7
0.6
0.5
0
0.2
0.4
0.6
0.8
1
1.2
1.4
Peclet Number (Pe = mcp/UA)
Measured - ASHRAE RP1169
Anderlind/Liu Heat Loss Comparison
Krarti Heat Loss Comparison
Adiabatic Boundary
Qgypsum
Qgypsum
Room
Ambient
Ambient
Air Inlet
Air Inlet
Control Volume
Air Exhaust

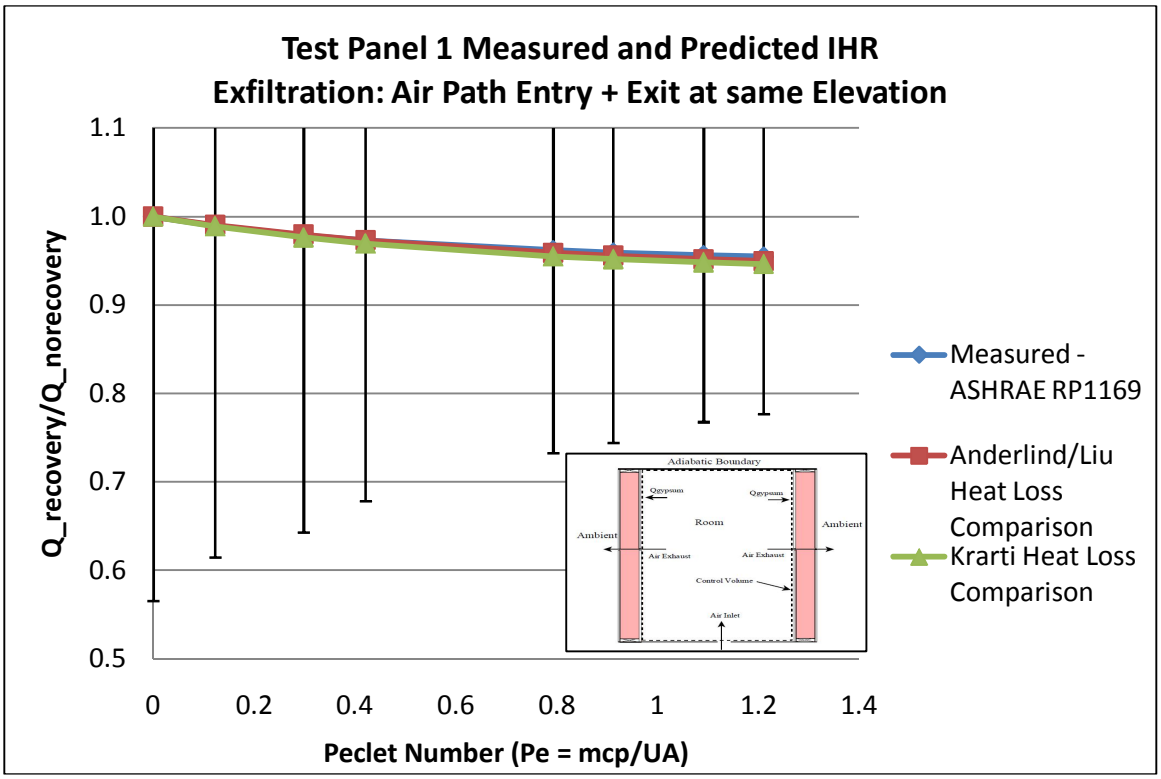
Test Panel 1 Measured and Predicted IHR
Exfiltration: Air Path Entry + Exit at same Elevation
Q_recovery/Q_norecovery
1.1
1.0
0.9
0.8
0.7
0.6
0.5
0
0.2
0.4
0.6
0.8
1
1.2
1.4
Peclet Number (Pe = mcp/UA)
Measured - ASHRAE RP1169
Anderlind/Liu Heat Loss Comparison
Krarti Heat Loss Comparison
Adiabatic Boundary
Qgypsum
Qgypsum
Room
Ambient
Ambient
Air Exhaust
Air Exhaust
Control Volume
Air Inlet

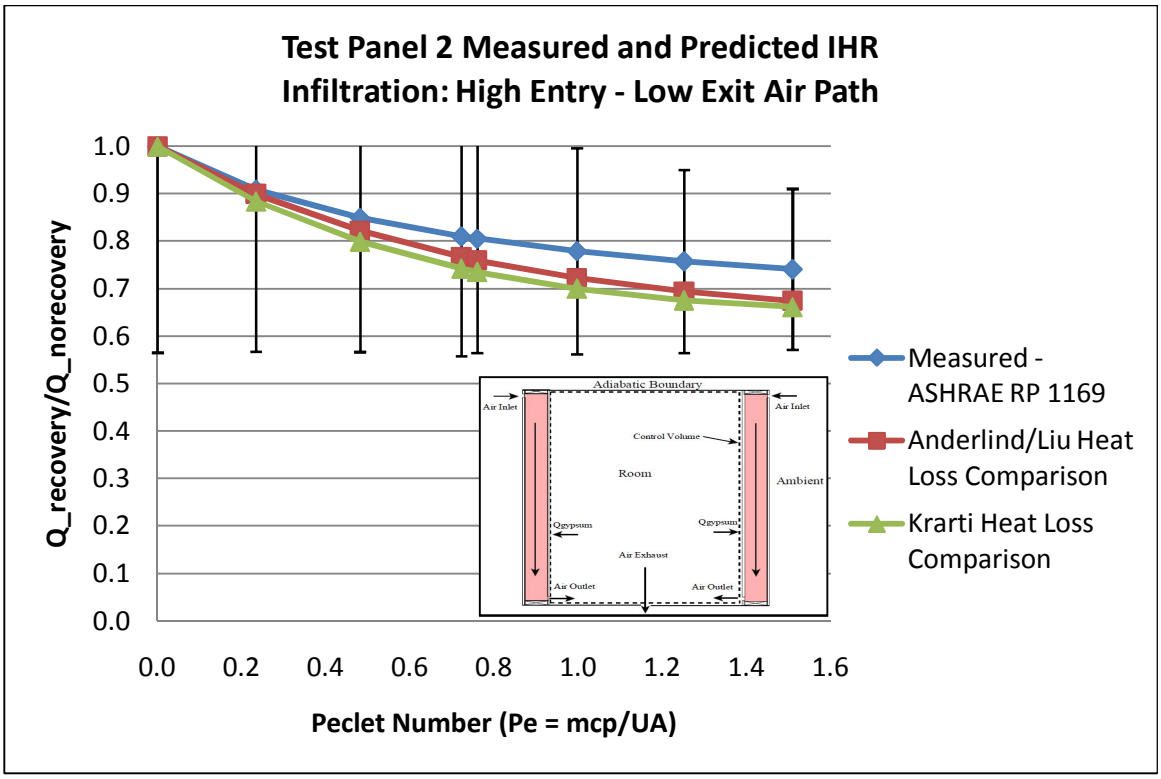
Test Panel 2 Measured and Predicted IHR
Infiltration: High Entry - Low Exit Air Path
Q_recovery/Q_norecovery
1.0
0.9
0.8
0.7
0.6
0.5
0.4
0.3
0.2
0.1
0.0
0.0
0.2
0.4
0.6
0.8
1.0
1.2
1.4
1.6
Peclet Number (Pe = mcp/UA)
Adiabatic Boundary
Air Inlet
Air Inlet
Control Volume
Room
Ambient
Qgypsum
Qgypsum
Air Exhaust
Air Outlet
Air Outlet
Measured - ASHRAE RP 1169
Anderlind/Liu Heat Loss Comparison
Krarti Heat Loss Comparison

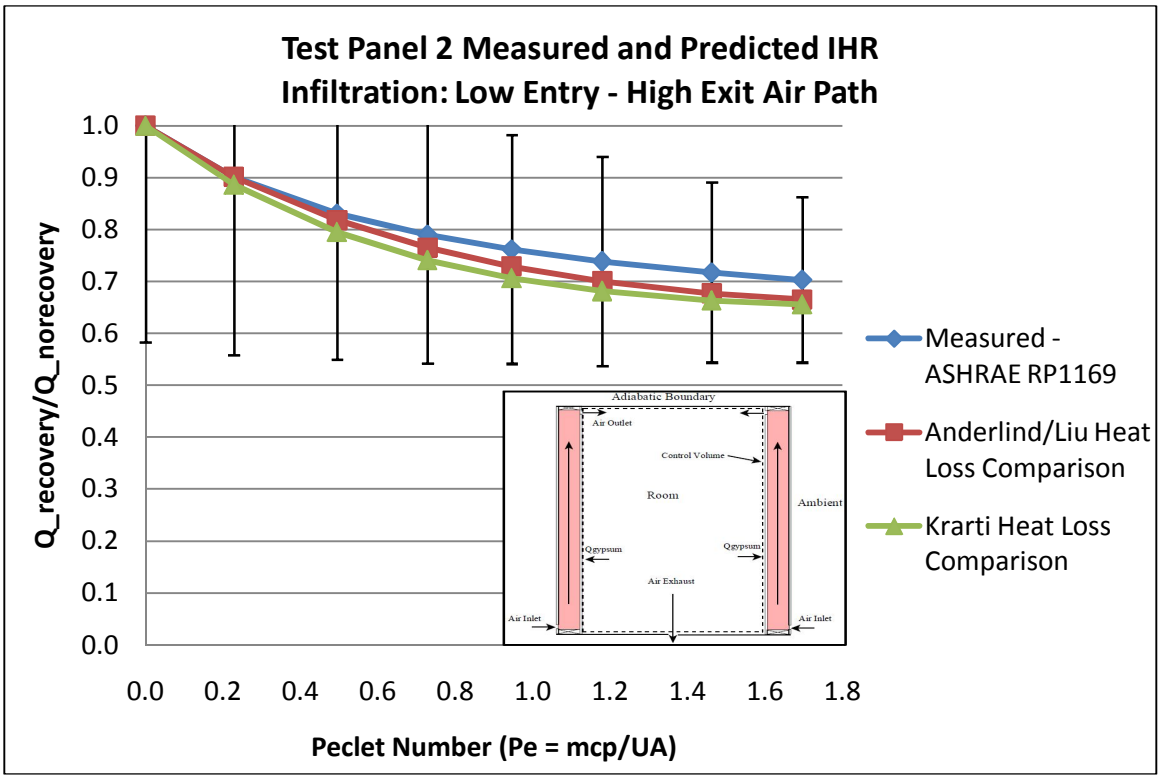
Test Panel 2 Measured and Predicted IHR
Infiltration: Low Entry - High Exit Air Path
Q_recovery/Q_norecovery
1.0
0.9
0.8
0.7
0.6
0.5
0.4
0.3
0.2
0.1
0.0
0.0
0.2
0.4
0.6
0.8
1.0
1.2
1.4
1.6
1.8
Peclet Number (Pe = mcp/UA)
Adiabatic Boundary
Air Outlet
Control Volume
Room
Ambient
Qgypsum
Qgypsum
Air Exhaust
Air Inlet
Air Inlet
Measured - ASHRAE RP1169
Anderlind/Liu Heat Loss Comparison
Krarti Heat Loss Comparison

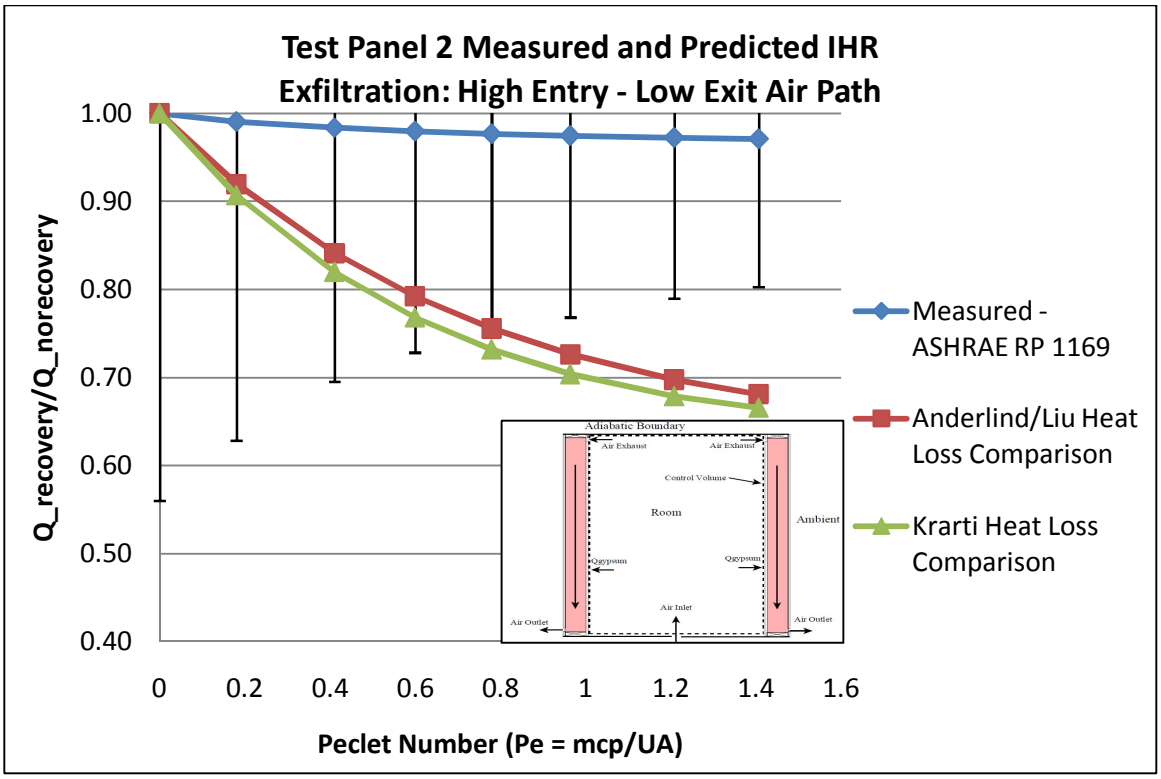
Test Panel 2 Measured and Predicted IHR
Exfiltration: High Entry - Low Exit Air Path
Q_recovery/Q_norecovery
1.00
0.90
0.80
0.70
0.60
0.50
0.40
0
0.2
0.4
0.6
0.8
1
1.2
1.4
1.6
Peclet Number (Pe = mcp/UA)
Measured - ASHRAE RP 1169
Anderlind/Liu Heat Loss Comparison
Krarti Heat Loss Comparison
Adiabatic Boundary
Air Exhaust
Air Exhaust
Control Volume
Room
Ambient
Qgypsum
Qgypsum
Air Inlet
Air Outlet
Air Outlet

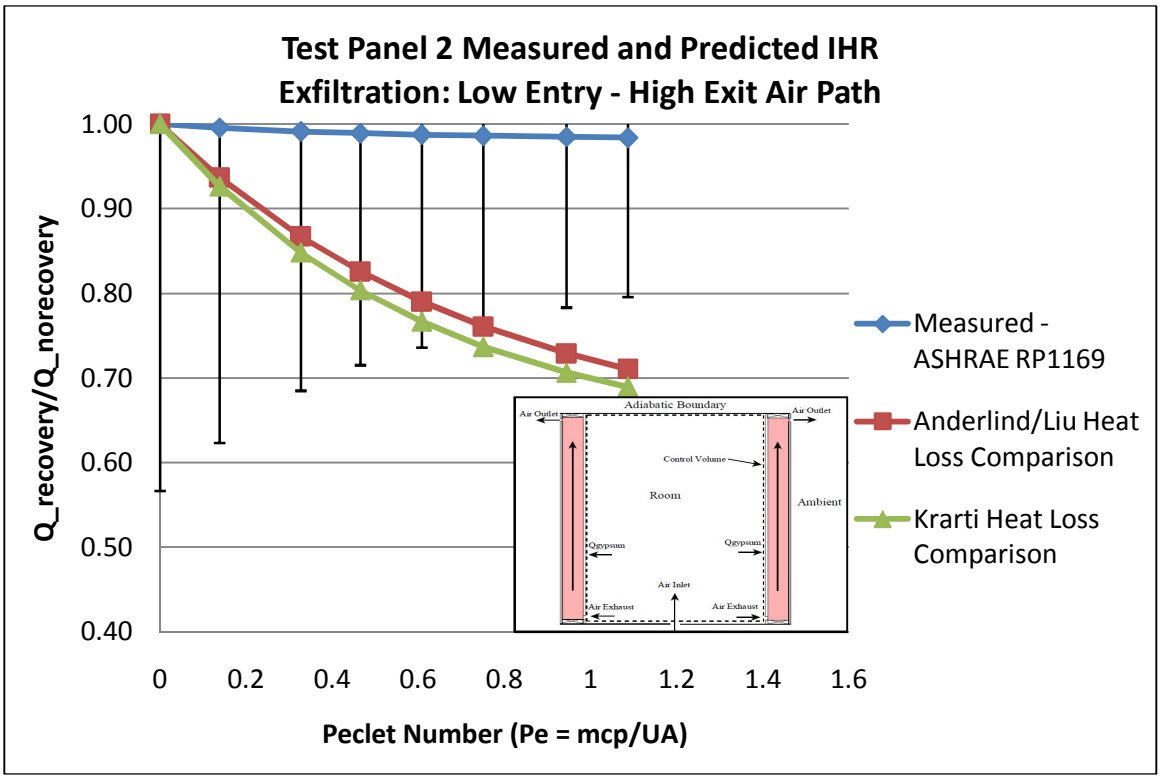
Test Panel 2 Measured and Predicted IHR
Exfiltration: Low Entry - High Exit Air Path
Q_recovery/Q_norecovery
1.00
0.90
0.80
0.70
0.60
0.50
0.40
0
0.2
0.4
0.6
0.8
1
1.2
1.4
1.6
Peclet Number (Pe = mcp/UA)
Measured - ASHRAE RP1169
Anderlind/Liu Heat Loss Comparison
Krarti Heat Loss Comparison
Adiabatic Boundary
Air Outlet
Air Outlet
Control Volume
Room
Ambient
Qgypsum
Qgypsum
Air Inlet
Air Exhaust
Air Exhaust

APPENDIX G: INFILTRATION HEAT RECOVERY MODEL TEST RESULTS ON PROTOTYPICAL HOMES

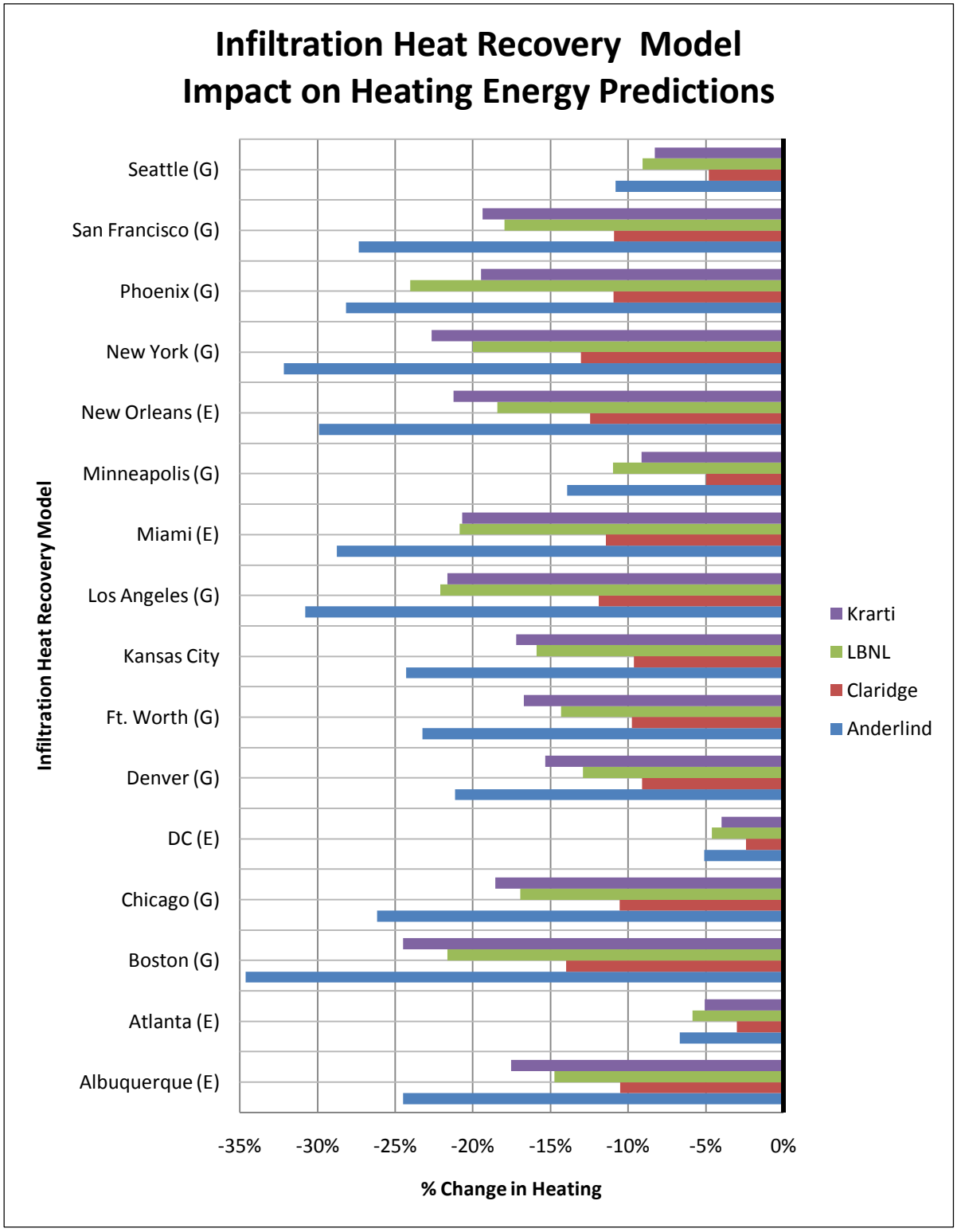

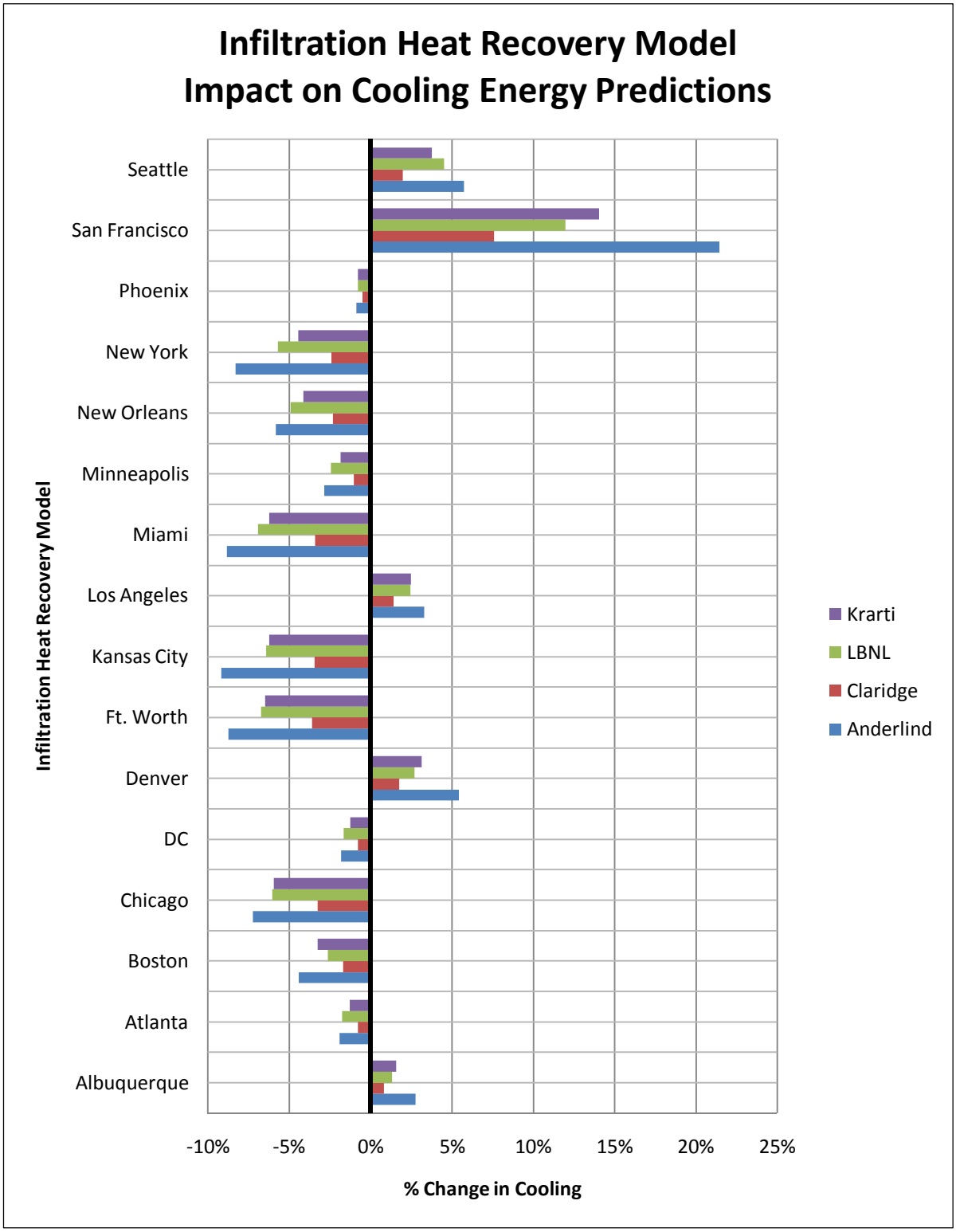
Infiltration Heat Recovery Model
Impact on Cooling Energy Predictions
Infiltration Heat Recovery Model
Seattle
San Francisco
Phoenix
New York
New Orleans
Minneapolis
Miami
Los Angeles
Kansas City
Ft. Worth
Denver
DC
Chicago
Boston
Atlanta
Albuquerque
-10%
-5%
0%
5%
10%
15%
20%
25%
% Change in Cooling
Krarti
LBNL
Claridge
Anderlind

APPENDIX H: HOME ENERGY AUDIT INFILTRATION HEAT RECOVERY CASE STUDY

Case Study General Information and Energy Model Inputs Table

	Home #1	Home #2	Home #3	Home #4
Location	Superior, CO	Boulder, CO	Superior, CO	Boulder, CO
Year Built	1999	1964	1995	1960
Con. Area (ft^2)	*1948*	1800	2200	*1452*
Tot. Area (ft^2)	*3112*	2000	2515	1716
Stories	2	1	2	1 (split-level home)
Garage	Attached (380 sqft)	Attached (200 sqft)	Attached (315 sqft)	*Attached (264 sqft) assumed to be crawlspace*
Rooms	5	5	4	3
Bathrooms	3	2	3	2
Orientation	East	North	South	East
Neighbor	*15 ft on either side*	*10 ft on either side*	*15 ft on either side*	*15 ft on either side*
Htng SP	62 º F 12am-7am, 67 º F 7am-8am, 62 º F 8am-3pm, 67 º F 3pm-9pm, 62 º F 9pm-12am	70 º F -24 hrs	*70 º F -24 hrs*	*69 º F -24 hrs*
Clng SP	Off 12am-9am, 78 º F 9am-3pm, 73 º F 3pm-9pm, Off 9pm-12am	N/A	78 º F -24 hrs	N/A
MEL/MGL	*0.50/1.00* *BA Multiplier*	*1.00/1.00* *BA Multiplier*	*1.00/1.00* *BA Multiplier*	*1.00/1.00* *BA Multiplier*
Nat.Vent.	*BA Benchmark*	*BA Benchmark*	*BA Benchmark*	*BA Benchmark*
Exterior Walls	Wood Stud R15 2x4 16”o.c.	Two layer brick wall R8 equivalent	Wood Stud R19 2x6 24” 0.c.	Wood Stud R7 2x4 16”o.c.
Exterior Finish	Gray Vinyl	Red Brick	Red Brick	Red Brick
Interzonal Walls	R15 2x4 16”o.c.	Uninsulated 2x4 16”o.c.	Uninsulated 2x4 16”o.c.	Uninsulated 2x4 16”o.c.
Unfinished Attic	*R30 Blown-in Cellulose*	R7 Blown-in Cellulose	R30 Blown in Cellulose	*R7 Blown-in Cellulose*
Roofing Material	Medium Shingles	Light Shingles	Dark Shingles	Medium Shingles
Radiant Barrier	*None*	*None*	*None*	*None*

Foundation	Unfinished Basement	Finished Basement	Finished Basement	*Finished Basement+Slab*
Foundation Insulation	*8ft R10 rigid*	*None*	*None*	*4ft R5 rigid*
Win.Wall Ratio	*0.15 (F20 B40 L20 R20)*	0.134 (F47 B51 L0 R 02)	0.134 (F31 B54 L11 R 03)	*0.15 (F20 B40 L20 R20)*
Window Type	*Clear Double Pane ; U-value = 0.447 Btu/hr-ft^2-° F, SHGC = 0.547*	*Clear Single Pane; U-value = 0.869 Btu/hr-ft^2-° F, SHGC = 0.619*	*Low-e, very high SHGC Double Pane U-value = 0.352 Btu/hr-ft^2-° F, SHGC = 0.511*	*Clear Single Pane; U-value = 0.869 Btu/hr-ft^2-° F, SHGC = 0.619*
Interior Shading	*Benchmark*	*Benchmark*	*Benchmark*	*Benchmark*
Eaves	*2 foot offset*	*2 foot offset*	*2 foot offset*	*2 foot offset*
SLA	0.00027	0.00044	0.00059	0.00184
ACH@50	5.6	9.1	9.7	38.1
Annual Avg ACH	0.27	0.44	.59	1.5
Mech. Vent.	*Spot Vent*	*Spot Vent*	*Spot Vent*	*Spot Vent*
Refrigerator	*Standard, Side-by-Side Freezer*	*Standard, Side-by-Side Freezer*	*Standard, Side-by-Side Freezer*	*Standard, Top Mount Freezer*
Range	*Electric, Conventional*	*Electric, Conventional*	*Electric, Conventional*	*Electric, Conventional*
Dishwasher	EnergyStar	*Standard*	*Standard*	*Standard*
Clothes Washer	*Standard*	*Standard*	*Standard*	*Standard*
Clothes Dryer	Electric	Electric	Electric	Electric
Hardwired Lighting	*14%*	*14%*	*14%*	*14%*
Plug-in Lighting	*10%*	*10%*	*10%*	*10%*
Air Conditioner	*SEER 10*	None	*SEER 10*	None
Furnace	*Gas, AFUE 80%*	*Gas, AFUE 75%*	*Gas, AFUE 80%*	Gas, AFUE 95%
Ducts	*Typical, R6 Insulation*	*Typical, R6 Insulation*	*Typical, R6 Insulation*	*Typical, R6 Insulation*
Ceiling Fans	None	*Benchmark*	*Benchmark*	*Benchmark*
Water Heater	*Gas, 50 gal EF 0.72*	Gas 40 gal, EF 0.52	*Gas, 50 gal EF 0.52*	*Gas, 40 gal EF 0.59*

*Note: Fields written in italics indicate inputs that are assumed for use in the home energy models.

Case Study Home Energy Audit Summary and Utility Data

Home #1

The home located in Superior, CO was built in 1999 as a two-story single family home with attached two car garage. The unconditioned basement houses the water heater, furnace, clothes washer and dryer. Features include an overhang at the main entrance facing east, vaulted ceiling over a portion of the first floor. Insulation has been added to the garage and basement walls. The construction of the walls is wood frame with asphalt shingles, vinyl siding, and double pane windows. Heating and cooling is provided through a central system with ducts distribution in the floors; system efficiency typical of the time of construction. Appliances are less than 10 years old. The dishwasher is an EnergyStar rated appliance. The home is occupied only by one person during most of the year.

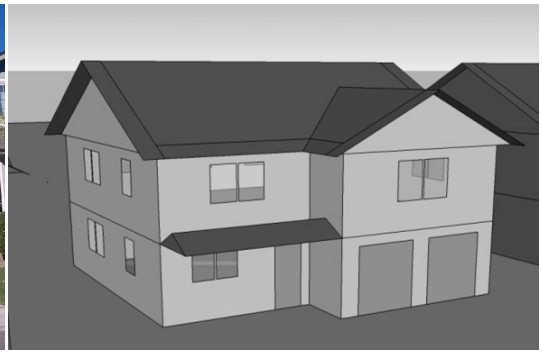

Home #1		
Field	**Information**	**Comments**
Location	Superior, CO	
Basic building description	2500 sq. ft. two-story home built in 1999 with attached garage. Home entrance oriented East.	Actual conditioned area is approx. 2000 sq ft. Total area including basement is around 3000 sq. ft.
Exterior Walls	2x4” wood frame construction with green painted vinyl siding. R-15 fiberglass in wall cavities.	No assessment of building conditions. Insulation assumed, typical of construction type.
Windows/Doors	All windows and sliding glass doors are double-pane clear glass windows. Front door is typical wood core type. Approx. 314 sq. ft. of windows measured.	No window performance info provided by energy audit.
Attic/Roof	Unconditioned attic and vaulted ceiling construction found. 13” fiberglass blown insulation found throughout attic. Roof is covered with dark asphalt shingles.	Conditions of attic, attic door hatch, or roof were not provided.
Foundation	Unconditioned basement construction found. Basement windows are along one wall. Walls partially covered with insulation and vapor barrier. Noticeable air leakage occurring	

	through a hole between basement wall and wood floor. Hot water heater, furnace, washer and dryer are located in the basement.	
Heating System	Central natural gas furnace with duct located in the floor. AFUE 80%	Information about ducts not provided in report. System efficiency is assumed.
Cooling System	Central electric A/C unit. Same distribution system as heating system. SEER 10	Information about ducts not provided in report. System efficiency is assumed.
Thermostat	Programmable thermostat. Winter schedule: 62 º F 12am-7am, 67 º F 7am-8am, 62 º F 8am-3pm, 67 º F 3pm-9pm, 62 º F 9pm-12am Summer Schedule: Off 12am-9am, 78 º F 9am-3pm, 73 º F 3pm-9pm, Off 9pm-12am	Thermostat schedules provided by home occupant
Water Heating System	Natural gas water heater with 40 gallon tank. There is no insulation on the tank or distribution.	Energy audit photos show lack of insulation. No information about water use provided.
Lighting	Only 6 of 63 light bulbs were found to be CFL's in conditioned space. Linear T8 fluorescent bulbs in the garage.	
Appliances	EnergyStar dishwasher found. All appliances are electric.	No appliance performance information was provided in the energy audit.
Blower Door	Full blower door test performed. Data from analysis: Coefficients C=106.61 n=0.65 ELA= 69.33 in^2 ACH=0.27	Depressurization test is used. The LBNL method is used to calculate air leakage levels. Average seasonal temperatures and wind speed for Superior were used.

Month	Billed Days	Electricity Use(kWh)	Gas Use (therms)	kWh/day	Therms/day
Jan-10	30	247	107	8.23	3.57
Feb-10	29	293	105	10.10	3.62
Mar-10	31	219	66	7.06	2.13
Apr-10	29	175	35	6.03	1.21
May-10	29	168	26	5.79	0.90
Jun-10	30	230	9	7.67	0.30
Jul-10-	32	385	7	12.03	0.22
Aug-10	29	465	7	16.03	0.24
Sep-10	30	364	7	12.13	0.23
Oct-10	31	226	11	7.29	0.35
Nov-10	28	235	50	8.39	1.78
Dec-10	35	258	102	7.37	2.91

Home #2

The home located in Boulder, CO is ranch style one-story single family home built in 1964. A single car garage and conditioned basement house the water heater, furnace, clothes washer and dryer. Features include a north facing entrance with bay window, and window all along the basement walls. The construction of the house consists of double brick layer wall with air gap, wood roof with asphalt shingles, brick siding, and retrofitted double pane argon filled windows. No cooling system exists. Heating is provided through a central furnace system with ducts in the floors with 75% efficiency. A hot water heater was installed in 2006. No EnergyStar appliances were installed. The home is occupied only by four adults throughout most of the year.

Home #2		
Field	**Information**	**Comments**
Location	Boulder, CO	
Basic building description	1800 sq. ft. one-story Ranch style home built in 1964 with attached garage. Home entrance oriented North.	Attached garage provides an additional 200 sq. ft.
Exterior Walls	Full brick wall construction. Exterior finish of red colored brick. No insulation exists in the walls (R-8).	Typical brick construction consists of two brick layers with air gap in between.
Windows/Doors	All windows and sliding glass doors are double-pane argon-filled glass windows. Front door is made of wood. Window to wall ratio is calculated to be 0.25.	No window performance info provided by energy audit. Double pane windows are a retrofit performed by the landlord.
Attic/Roof	Unconditioned attic construction. One half of the attic is insulated with 3" of blown cellulose (R-7), the other half has 6" fiberglass batt insulation (R-10). Overall insulation levels estimated to be R-10. Roof is covered with light colored asphalt shingles.	Conditions of attic, attic door hatch, or roof were not provided.
Foundation	Conditioned basement found. Basement windows exist along north and south wall. Walls are uninsulated. Hot water heater, and furnace located in the basement.	Vapor barrier unknown. Condition of basement walls unknown.
Heating System	Central natural gas forced air furnace with	Information about ducts not

	efficiency of 75%	provided in report. System efficiency assumed.
Cooling System	No cooling system exists in the house.	
Thermostat	Heating only 70 º F -24 hrs	Setpoints are assumed in energy audit.
Water Heating System	Natural gas water heater with 50 gallon tank and reported EF of 0.52. The tank is covered with 2-in of fiberglass insulation.	No information about distribution system or water use. Hot water heater recently replaced.
Lighting	Lighting is reported to consist of 90% CFL light bulbs. LPD estimated to be 0.5 W/ sqft	
Appliances	No information about the appliances was provided.	
Blower Door	Full blower door test performed. Data from analysis: Coefficients C=177.03 n=0.64 ELA= 114.63 in^2 ACH=0.34	Depressurization test is used. The LBNL method is used to calculate air leakage levels. Average seasonal temperatures and wind speed for Boulder were used.

Month	Billed Days	Electricity Use(kWh)	Gas Use (therms)	kWh/day	Therms/day
Aug-09	29	443	17	15.28	0.59
Oct-09	32	717	34	22.41	1.06
Nov-09	29	796	77	27.45	2.66
Dec-09	33	715	118	21.67	3.58
Jan-10	35	522	165	14.91	4.71
Feb-10	29	891	118	30.72	4.07
Apr-10	30	782	81	26.07	2.70
May-10	30	685	31	22.83	1.03
Jun-10	32	750	32	23.44	1.00
Jul-10	32	598	27	18.69	0.84
Aug-10	31	568	21	18.32	0.68
Sep-10	29	596	21	20.55	0.72

Home #3

The home located in Superior, CO was built in 1995 as a two-story single family home with attached two car garage. An unconditioned basement underneath only a portion of the first floor houses the water heater, furnace, and A/C. Features include a south facing entrance with casement window, and window all along the basement walls. Insulation has been added to the garage and basement walls. The construction of the walls is wood frame with asphalt shingles, brick siding, and double pane windows. Heating and cooling is provided through central system with duct distribution; system efficiency typical of the time of construction. No EnergyStar appliances were installed. The home is occupied only by four residents for most of the year.

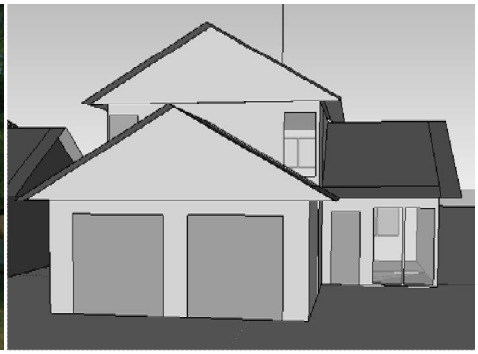

Home #3		
Field	**Information**	**Comments**
Location	Superior, CO	
Basic building description	2200 sq. ft. two-story home built in 1995 with attached garage. Home entrance oriented South.	Conditioned area is approx. 2200 sq ft. Total area including basement is around 2500 sq. ft.
Exterior Walls	2x6" wood frame construction with red brick exterior finish. R-19 assumed fiberglass in wall cavities.	No assessment of building conditions. Insulation assumed, typical of construction type.
Windows/Doors	All windows and sliding glass doors are double-pane clear glass windows. Front door is typical wood core type. Approx. 270 sq. ft. of windows measured.	No window performance info provided by energy audit
Attic/Roof	Vaulted ceiling construction found above the second floor master bedroom and a portion of the first floor. An unconditioned attic occupies the remaining ceiling space. Approx. R-30 fiberglass insulation found in the attic. Roof is covered with moderate colored asphalt shingles.	Insulation levels not explicitly described, instead they were extracted from attic UA calculations. Conditions of attic, attic door hatch, or roof were not provided
Foundation	Unconditioned basement construction found. Basement windows are along one wall. Hot water heater, furnace, and A/C are located in the basement.	Conditions of walls, insulation levels, or possible vapor barrier reported in energy audit.
Heating System	Central natural gas forced air furnace with duct	Information about ducts not

	located inside the conditioned area. AFUE 80%	provided in report
Cooling System	Central electric A/C unit. Same distribution system as heating system. SEER 9.7	Information about ducts not provided in report
Thermostat	Heating: 68 º F -24 hrs Cooling: 78 º F -24 hrs	Setpoints found during the energy audit. Programmable thermostat is installed, but is not utilized.
Water Heating System	Natural gas water heater with 40 gallon tank. There is no insulation on the tank or in distribution system.	Energy audit photos show lack of insulation. No information about water use.
Lighting	Incandescent light bulbs light 100% of the conditioned area of the home. Garage is mostly incandescent as well.	
Appliances	All appliances are electric, non-EnergyStar appliances.	No appliance performance information was provided in the energy audit
Blower Door	Full blower door test performed. Data from analysis: Coefficients C=185.86 n=0.67 ELA= 124.16 in^2 ACH=0.59	Depressurization test is used. The LBNL method is used to calculate air leakage levels. Average seasonal temperatures and wind speed for Superior were used.

Month	Billed Days	Electricity Use(kWh)	Gas Use (therms)	kWh/day	Therms/day
Jan-08	32	609	184	19.03	5.75
Feb-08	29	615	157	21.21	5.41
Mar-08	30	601	116	20.03	3.87
Apr-08	29	556	96	19.17	3.31
May-08	32	542	54	16.94	1.69
Jun-08	29	493	29	17.00	1.00
Jul-08	30	720	24	24.00	0.80
Aug-08	31	950	29	30.65	0.94
Sep-08	31	656	30	21.16	0.97
Oct-08	29	601	53	20.72	1.83
Nov-08	31	673	86	21.71	2.77
Dec-08	35	1401	192	40.03	5.48

Home #4

The home located in Boulder, CO was built in 1960 as a split level one-story single family home with attached two car garage. A conditioned basement underneath only a portion of the first floor houses the water heater and furnace. Features include a east facing entrance, and window all along the basement walls. Insulation has been added to the garage and basement walls. The construction of the walls is wood frame with asphalt shingles, brick siding, and single pane casement windows. No cooling system exists. Heating is provided through central furnace system with ducts in the floors with 95% system efficiency. No EnergyStar appliances were installed. The home is occupied only by four residents for most of the year.

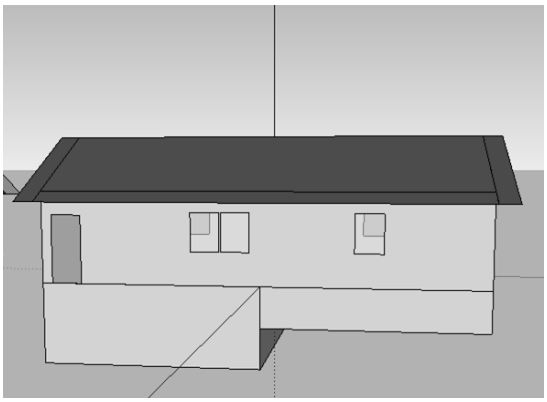

Home #4		
Field	Information	Comments
Location	Boulder, CO	
Basic building description	1188 sq. ft. one-story split level home built in 1960 with attached garage. Home entrance oriented East.	From basic floor plan layout, square footage reported is possibly smaller than in reality. Attached garage provides an additional 264 sq. ft.
Exterior Walls	2x4" wood frame construction with green painted vinyl siding. R-13 fiberglass in wall cavities.	No assessment of building conditions. Insulation assumed due to age of house.
Windows/Doors	All windows and sliding glass doors are single-pane clear glass windows. Front door is made of wood. Window to wall ratio is calculated to be 0.12.	No window performance info provided by energy audit. Double pane windows are a retrofit performed by the landlord.
Attic/Roof	Unconditioned attic construction. 7" of blown fiberglass was found throughout the attic (R-22). No insulation on attic hatch. Roof is covered with light colored asphalt shingles.	Conditions of attic and roof were not provided.
Foundation	Conditioned basement found. Basement windows exist along north and south wall. Walls are uninsulated. Hot water heater, and	Vapor barrier unknown. Condition of basement walls unknown.

	furnace located in the basement.	
Heating System	Central natural gas forced air furnace was recently replaced, rated with an AFUE of 95%	Information about ducts not provided in report.
Cooling System	No cooling system exists in the house.	
Thermostat	Heating setpoint only 69 º F -24 hrs	Setpoint based on interview with landlord.
Water Heating System	Natural gas hot water system is used. No information about the system is provided.	No information about distribution system or water use. Hot water heater recently replaced.
Lighting	No information regarding the lighting in the house is mentioned in energy audit.	
Appliances	No information about the appliances was provided.	
Blower Door	Full blower door test performed. Data from analysis: Coefficients C=177.03 n=0.64 ELA= 114.63 in^2 ACH=0.34	Depressurization test is used. The LBNL method is used to calculate air leakage levels. Average seasonal temperatures and wind speed for Boulder were used.

Month	Billed Days	Electricity Use(kWh)	Gas Use (therms)	kWh/day	Therms/day
Jan	31	N/A	126	N/A	4.06
Feb	29		108		3.72
Mar	29		66		2.28
Apr	29		33		1.14
May	32		25		0.78
Jun	30		16		0.53
Jul	30		15		0.50
Aug	32		11		0.34
Sep	32		26		0.81
Oct	29		79		2.72
Nov	33		106		3.21
Dec	31		153		4.94

Case Study IHR Measurement Equations

$$f = 1 - \frac{(BLC_{predicted} - BLC_{measured})}{\dot{m}C_p} \quad \text{(H1)}$$

$$f = 1 - \frac{\left[(UA_{walls} + UA_{ceiling} + UA_{foundation} + UA_{windows} + UA_{door} + \dot{m}C_p) - \frac{-a*10^5*\eta}{24}\right]}{\dot{m}C_p} \quad \text{(H2)}$$

$$U_{wall\ \text{or}\ ceiling} = U_{cavity}(1 - \%frame) + U_{stud} * \%frame \quad \text{(H3)}$$

$$\dot{m} = ACH * Volume * \rho_{air} \quad \text{(H4)}$$

APPENDIX I: SENSITIVITY OF DIFFUSE AIR FRACTION ON IHR MODELS

Analytical IHR Models Adjustment

$$\mathrm{Pe} = \frac{(\dot{m}C_p)_{diffuse}}{UA_{envelope}} \quad (I1)$$

$$(\dot{m}C_p)_{diffuse} = (\dot{m}\,C_p) * X_{diffuse} \quad (I2)$$

$$(\dot{m}C_p)_{concentrated} = (\dot{m}\,C_p) * (1 - X_{diffuse}) \quad (I3)$$

$$BLC_{predicted} = UA_{envelope} + (1 - f) * (\dot{m}C_p)_{diffuse} + (\dot{m}C_p)_{concentrated} \quad (I4)$$

Impact of diffuse air LBNL Model

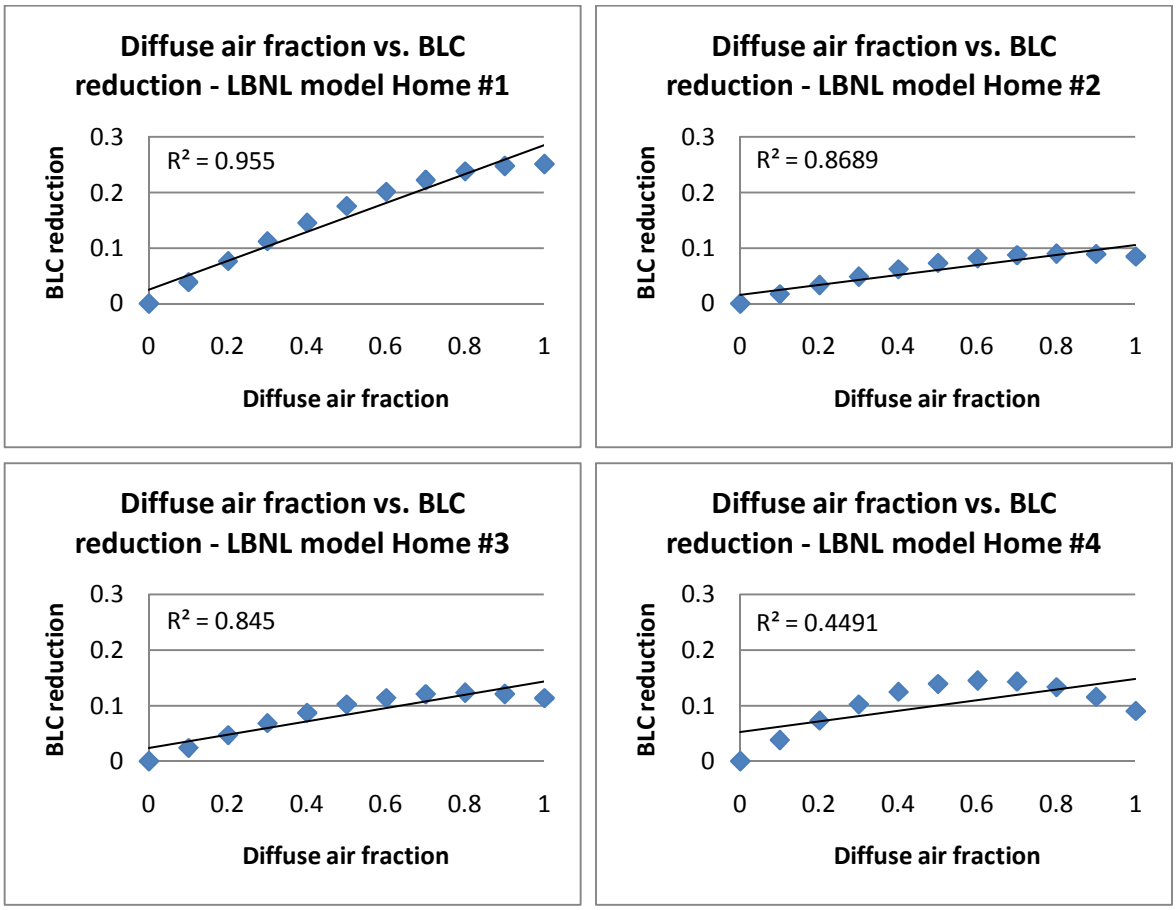

Impact of diffuse air on Krarti Model

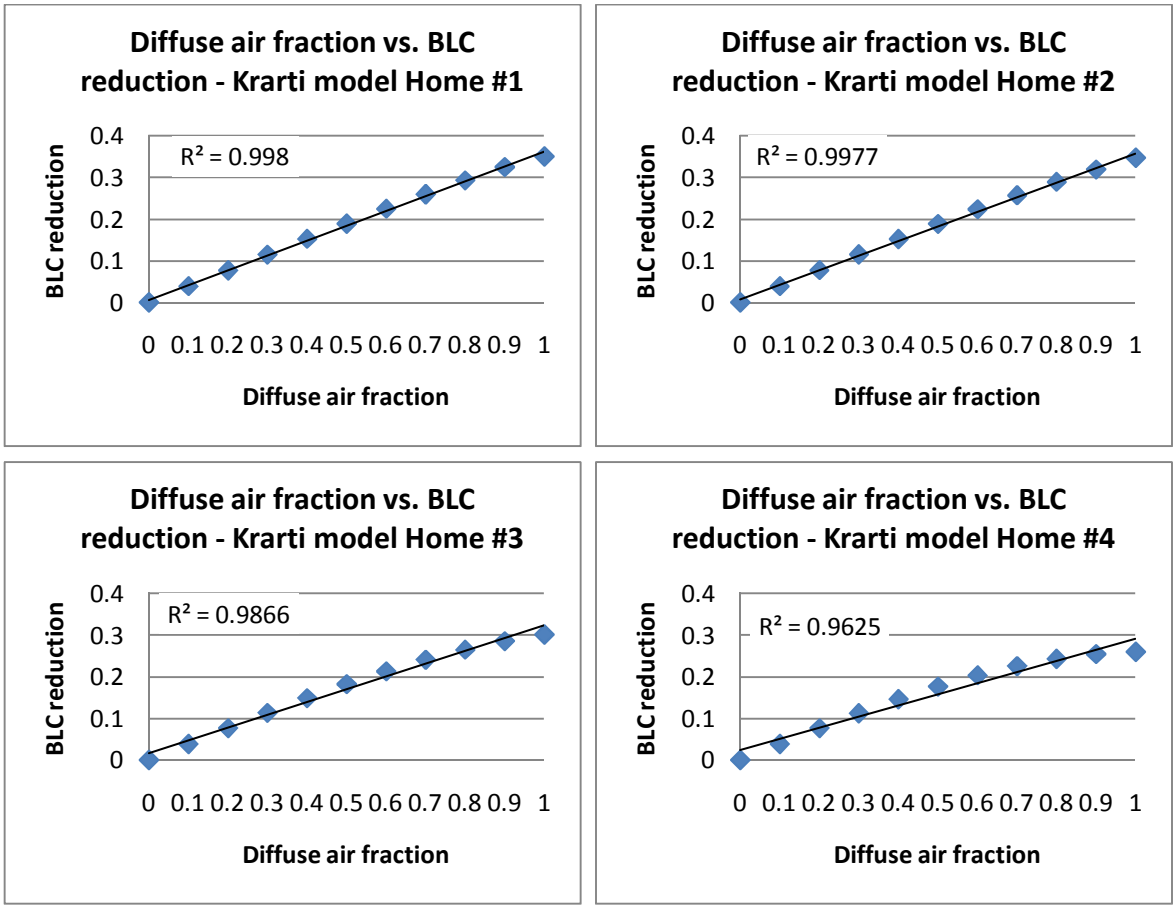

Impact on EnergyPlus Simulation

$$Pe = \frac{(\dot{m}C_p)_{diffuse}}{UA_{envelope}} \quad \text{(I5)}$$

$$(\dot{m}C_p)_{diffuse} = (\dot{m}\ C_p) * X_{diffuse} \quad \text{(I6)}$$

$$(\dot{m}C_p)_{concentrated} = 1 - (\dot{m}C_p)_{diffuse} \quad \text{(I7)}$$

$$IHR_{diffuse} = (1 - f(Pe)) * X_{diffuse} \quad \text{(I8)}$$

$$IHR_{concentrated} = (1 - 0) * (1 - X_{diffuse}) \quad \text{(I9)}$$

$$\dot{Q}_{inf} = \sqrt{(\boldsymbol{c}^* * C_s * (\Delta T)^n)^2 + (\boldsymbol{c}^* * C_w * (s_w * V_{wind})^{2n})^2} \quad \text{(I10)}$$

$$c^* = c * IHR_{diffuse} * X_{diffuse} + c * (1 - X_{diffuse}) \quad \text{(I11)}$$

Anderlind Model Impact of diffuse air (i.e. Claridge model)

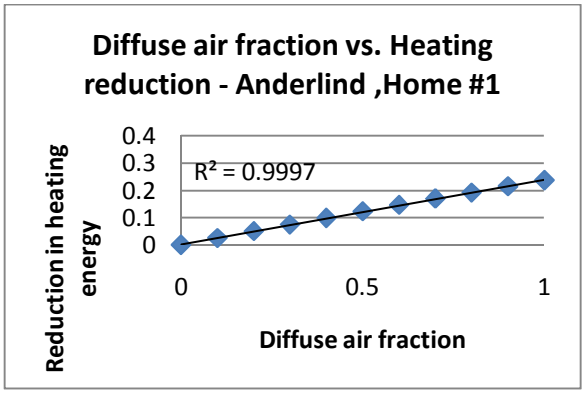

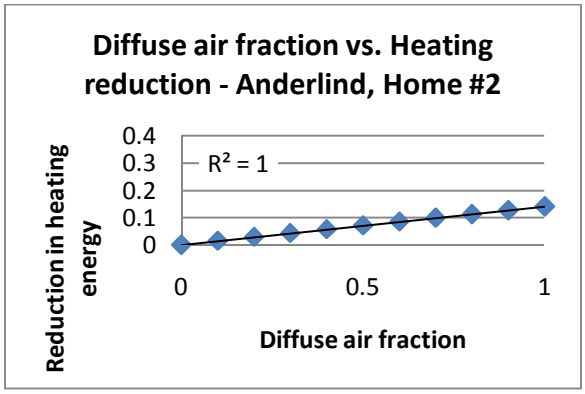

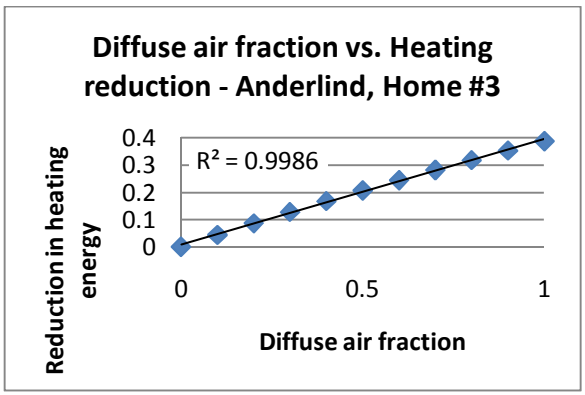

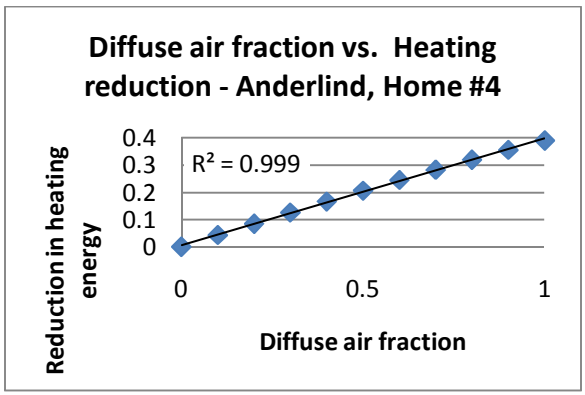

LBNL Model Impact

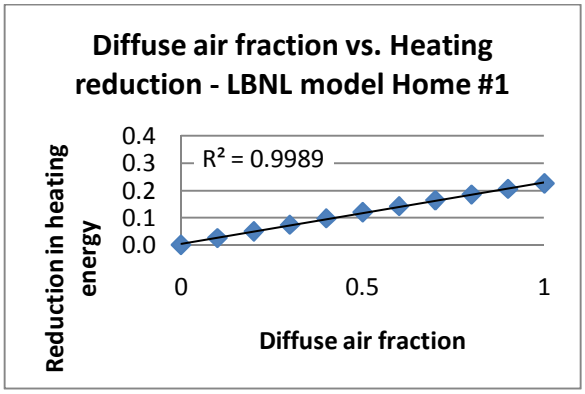

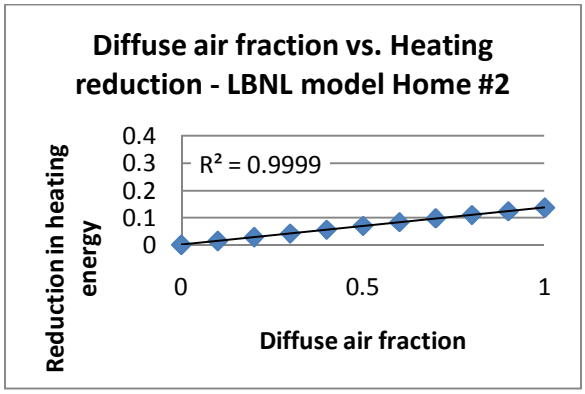

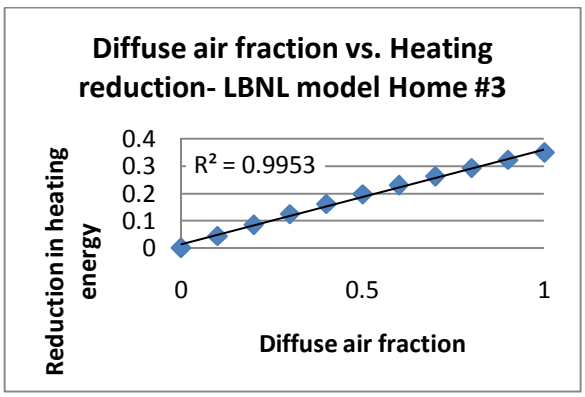

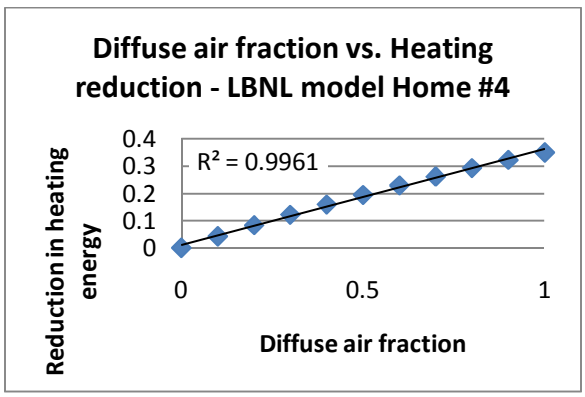

Krarti Model Impact